2217 /ᴗᴛᴗ

THESIS

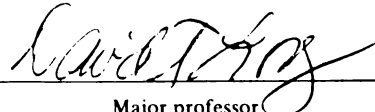This is to certify that the

thesis entitled

The Oxidation of Chromium by Manganese Oxide:
the Nature and Controls of the Reaction

presented by

Michael James Takacs

has been accepted towards fulfillment
of the requirements for

___Masters___ degree in __Geology__

Major professor

Date _5/20/88_

THE OXIDATION OF CHROMIUM BY MANGANESE OXIDE: THE NATURE AND CONTROLS OF THE REACTION

By

Michael James Takacs

A THESIS

Submitted to
Michigan State University
in partial fulfillment of the requirements
for the degree of

MASTER OF SCIENCE

Department of Geological Sciences

1988

ABSTRACT

THE OXIDATION OF CHROMIUM BY MANGANESE OXIDE: THE NATURE AND CONTROLS OF THE REACTION

By

Michael James Takacs

The trace metal chromium (Cr) occurs in aqueous systems in two oxidation states; the non-toxic trivalent species and the toxic, mobile hexavalent species. One mechanism by which Cr may be oxidized from the trivalent to the hexavalent state is through an oxidation-reduction reaction with manganese oxides. This research explored the general nature and chemical controls of Cr oxidation by a synthetic manganese oxide. The results of laboratory experiments conducted at pH 4.5 show the oxidation occurs through the reduction of surficial tetravalent manganese (Mn) ions. The reaction appears to be preceded by the adsorption of Cr onto the oxide surface and new surface sites for the reaction are generated by the reduction/dissolution of the Mn oxide surface. The reaction is inhibited at neutral pH's by the formation of Cr hydroxide but is otherwise unaffected by changing solution chemistry. The reaction also proceeded in mixed manganese-iron oxide systems.

To my wife Audrey and to my parents, without whose support and patience I could not have maintained the will to see this project to its conclusion.

TABLE OF CONTENTS

SUMMARY AND CONCLUSIONS

v

LIST OF TABLES

LIST OF FIGURES

INTRODUCTION

The following section of this report provides an introduction to the topic addressed by this research. After a general discussion of the historical development and relevance of this field of research, a brief summary of the aqueous geochemistry of chromium (Cr) is provided. A detailed summary of past research which is pertinent to the present project is presented as Appendix I. The introduction is concluded with a discussion of the specific goals of this research.

1.0 GENERAL INTRODUCTION

The realization of the importance of trace metals to human health, in both a detrimental and essential role, has generated immense interest in the chemical behavior of these elements in man's environment. As aqueous systems are a major point of interaction between man and his environment, both directly, and through the food chain, much effort has been expended to define the sources, sinks and pathways of these trace metals in the oceans, atmosphere, streams, lakes and ground waters. It is essential to understand the geochemical and biochemical processes which control the mobility and bioavailability of these elements in order to predict the fate of the increasing anthropogenic sources to our environment. In general, the environmental fate of trace metals is influenced by a variety of

processes; chemical, physical and biological. The important processes are known to include the weathering of rocks and sediments, mineral precipitation and dissolution, complexation by both inorganic and organic ligands, adsorption onto mineral and solid organic surfaces and the uptake by organisms and consequent cycling through the food chain. These processes are in turn controlled by external variables such as pH, the redox state of the system, the partial pressure of gas phase components, temperature and any other condition which affects the chemical speciation or bioavailability of the metal ion in the environment.

The trace metal Cr is an element that has been shown to be both toxic and a dietary essential. In general, trivalent Cr is considered to be essential for animal and human health. There is also some evidence for essentiality to plant life (Mertz, 1971), although this point has not been entirely resolved. In high levels, there is evidence for toxic effects of the trivalent form to aquatic life (McKee and Wolf, 1963), although in general, this form is not considered highly toxic to animals or plants (Mertz, 1971). The hexavalent form of Cr is considered to be highly toxic to both animals and plants, and is a suspected carcinogen (Beliles, 1979).

Chromium is used in a variety of industries including tannery, plating, metallurgic, and chemical. Wastes from these industries, as well as municipal waste, are commonly landfilled, applied to agricultural land or released to

rivers or other water bodies. The natural source of Cr to the environment occurs primarily through the weathering of ultramafic rocks. The mineral chromite is the most important commercial source of this metal. Garrels et al., (1974) estimated that the interference index for man's effects on the natural exogenic cycle for Cr was 71%, which suggests that it is important to evaluate the fate of this increasing anthropogenic source.

Much of the recent research on the environmental fate of metals such as Cr has focused on the role of adsorption onto sediment or suspended particles for controlling trace metal concentrations in aqueous systems. Studies of metal partitioning in sediments, soils and suspended particulate materials have shown that hydrous oxides of iron (Fe) and manganese (Mn), organic materials and clays are the most important adsorbing phases. The idea that adsorption by hydrous oxides is an important process for controlling the distribution of trace metals in sea water was first suggested by Krauskopf (1956). Jenne (1968) proposed that adsorption by these species is a principle control of trace element mobility in soil and fresh water environments. Iron and Mn oxides have been shown to scavenge metals more effectively than other co-existing mineral species (Chao and Theobald, 1976). Reasons for this include, 1) the occurrence of these oxides as coatings on clays or other mineral grains, which allows greater chemical reactivity than their concentrations would suggest (Jenne, 1968), 2) the large

surface areas of these oxides, which can exceed 100 m^2/g, and 3) the high amount of available surface binding sites capable of forming strong covelant bonds with trace metals (Stumm and Morgan, 1981). Besides adsorption, reactions at solid surfaces may also include redox reactions which can further influence the behavior of metal species (Hem, 1978). At the present time, adsorption by hydrous oxides is widely recognized as an important process, but the quantitative role in geochemical cycles is poorly understood.

It has become apparent, that any attempt to model trace metal behavior in the aqueous environment, will have to include both the solution chemistry, in order to predict the speciation and solubility controls, and some way of assessing the role of adsorption and co-precipitation reactions. One approach to assess the role of adsorption has been to determine the thermodynamic data for the reactions between metals and model adsorbents, such as synthetic Mn and Fe oxides, in the laboratory. The ultimate goal of this approach is to use the experimentally determined binding constants in a predictive equilibrium model, such as those currently used to model solution chemistry. This approach is hindered by the difficulty in characterizing the adsorbents present in the complex natural environment, and by the limitations of the experimental data itself over a wide range of environmental conditions. Still, this approach holds some promise for predicting trace metal behavior in at least a semi-quantitative sense.

In the case of Cr, the interaction with solid surfaces, such as those of Mn and Fe oxides, is more complex than for most other metals. Chromium occurs in two oxidation states which exhibit very different chemical characteristics, including very different adsorptive behaviors. Furthermore, the controls on the valence state transformations in the environment are poorly understood. The adsorptive behavior of this metal is also complicated by redox reactions which are catalyzed by adsorption onto Mn oxides and possibly other solid species. A model to describe the environmental behavior of Cr will thus be more complex than those for other metals. In order to predict the oxidation state of this element it is likely that the model will involve kinetic considerations, as well as thermodynamic data, if a semi-quantitative approach is to be attained.

The research presented in this report is an attempt to provide data that will contribute to an overall model of Cr geochemistry. The focus of this research is on the interaction of Cr with a hydrous Mn oxide similar to those found naturally occurring. Specifically, this research will attempt to 1) provide a fundamental description of the oxidation of Cr by Mn oxide, 2) determine the effect of solution chemistry on this reaction, and 3) study the oxidation of Cr by Mn oxide in the presence of an additional solid species, Fe oxide, which is often associated with Mn oxide in the environment.

2.0 AQUEOUS GEOCHEMISTRY OF CHROMIUM

The element Cr (atomic number 24), is a VI-B group transition metal. The ground state electron configuration is [argon] $3d^5 4s^1$ (Douglas et al., 1983), thus all orbitals are half-filled. Chromium can lose any number of these six electrons. The two oxidation states which are stable in natural aqueous systems are Cr^{3+} and Cr^{6+}. Trivalent Cr has three 3d electrons, which are in the high spin state when in octahedral coordination, and the resulting octahedral site preference energy is the largest of the transition metals (Murray et al., 1983). In the aqueous environment, Cr^{3+} is amphoteric, and is usually a positively charged or neutral aquo-species, unless the pH is very high. The hexavalent form is very acidic, and is an anionic aquo-species under most conditions. This form is also a strong oxidizing agent.

In the aqueous environment the trivalent form, Cr^{3+}, is octahedrally coordinated with hydration water, which in a kinetic sense is "permanent" (Elderfield, 1970). These water molecules are hydrolyzed to various extents, dependent on pH. A recent study by Rai et al., (1986) experimentally evaluated the hydrolysis and solubility constants for Cr^{3+}. It was shown that the thermodynamic data previously reported in the literature were both inadequate and inaccurate. Their research demonstrated that $CrOH^{2+}$, $Cr(OH)_3^0$ and $Cr(OH)_4^-$ are the dominant hydroxy species, and that polynuclear species are not important, which is in contrast to some previously

reported data. These authors also evaluated the solubility of $Cr(OH)_3$-solid and $(Cr,Fe)(OH)_3$-solid solution, which probably control Cr^{3+} solubility in most systems. It was shown that the kinetics of precipitation-dissolution of these compounds is very fast, and that when sufficient Fe is present, $(Cr,Fe)(OH)_3$-ss should control Cr solubility. It is apparent that over the pH range of most natural waters, the solubility of Cr^{3+} is very low; even lower than previously reported. Several studies have demonstrated that Cr^{3+}-complexes are unimportant compared to the hydroxy species, even in sea water conditions (Rai et al., 1986; Elderfield, 1970; Van Der Weijden and Reith, 1982). The importance of Cr^{3+}-organic complexes has not been satisfactorily evaluated.

Hexavalent chromium, Cr^{6+}, is present in natural aqueous systems primarily as the tetrahedrally coordinated chromate ion, CrO_4^{2-}, with minor amounts of $HCrO_4^-$, H_2CrO_4, and $Cr_2O_7^{2-}$ (Elderfield, 1970; Leckie et al., 1983). This species is very soluble and is generally considered to be very mobile under many environmental conditions.

Based on the available thermodynamic data, Cr^{6+} should be the dominant species for most oxygenated systems. Under sea water conditions (pH=8.1 and pe=12.5) the calculated ratio of Cr^{6+} to Cr^{3+} is about 10^{21} (Elderfield, 1970; Nakayama et al., 1981). Reducing the pe to 8.5 only changes this ratio to 10^9 (Nakayama et al., 1981). Cr^{6+} has also been shown to be stable in oxic, alkaline ground waters (Robertson, 1975).

In contrast to the calculated predictions, many investigators have found considerable Cr^{3+} in analyses of fresh water and sea water (Pankow et al., 1977; Nakayama et al., 1981; Elderfield, 1970; Fukai, 1967). Potential reasons for this discrepancy include; 1) analytical techniques do not adequately distinguish between Cr^{3+} and Cr^{6+}, 2) published stability constants are in error, 3) estimates of the redox conditions in environments such as sea water are incorrect, 4) the oxidation state of Cr is kinetically controlled, and 5) there have been important stable species of Cr^{3+} that have been overlooked (Elderfield, 1970). Although analytical techniques may be responsible for some inaccurate data, 4) and 5) above seem likely to be responsible for this observation.

The slow kinetics of oxidation of Cr^{3+} to Cr^{6+} by O_2 have been demonstrated in several studies. Schroeder and Lee, (1975) found only 3% of an initial 0.125 mg/L Cr^{3+} spike was oxidized by O_2 in 30 days, in a solution buffered at pH=8.6. Nakayama et al., (1981) did not find any detectable oxidation in sea water over 300 hours. Similarly, Van Der Weijden and Reith, (1982) could not detect any oxidation of 0.100 mg/L Cr^{3+} in either fresh water or sea water (pH 5.5-8.0) over a six week period. The reaction is thought to be very slow, due in part, to the change in coordination number upon change in oxidation state (Elderfield, 1970). The ability of thermodynamic equilibrium to describe the oxidation state of Cr will depend on the

residence time of the dissolved species in the particular environment of interest, and the competition from other reactions. Cranston and Murray (1978) have shown that the oxidation state of Cr does seem to respond to redox conditions in the environment. Rate data for the reduction of Cr^{6+} in a reducing environment is apparently scarce.

Oxidation and reduction reactions between Cr and a variety of other species, which may influence the behavior of this element in the environment, have been demonstrated to occur in the laboratory. Oxidation of Cr^{3+} has been shown to occur via adsorption onto Mn oxides, apparently by the reduction of surface Mn^{4+} (Schroeder and Lee, 1975; and others). Reduction of the highly oxidizing Cr^{6+} has been shown to occur with a variety of substances, including reducible organics, such as ascorbic, humic and gallic acids (Nakayama et al., 1981; James and Bartlett, 1983), organic compounds containing sulfhydryl groups (Schroeder and Lee, 1975), hydrogen sulfide (Smillie et al., 1981) and ferrous iron (Schroeder and Lee, 1975). It is difficult to predict the environmental importance of these reactions as the rate of these processes are not well known.

Another generally unresolved component of the overall geochemical behavior of Cr is the possible formation of "inert" complexes of Cr^{3+} with organic ligands. Nakayama et al. (1981) have shown that the Cr^{3+}-citric acid complex does not coprecipitate with Fe oxide and is not oxidized by Mn oxides. James and Bartlett (1983) have shown that under

certain conditions in soils, citric acid will increase the solubility of Cr^{3+} by the formation of soluble Cr complexes.

The geochemical behavior of Cr, as with any trace metal, is also influenced by adsorption. The speciation of a dissolved metal species must be considered in adsorption reactions, and this is especially true for Cr, with its two valence states. Cr^{3+} would be expected to adsorb strongly over the pH range of natural waters on many solid surfaces (see Appendix I). As an anion, Cr^{6+} adsorption on many common adsorptive substrates would be limited (see also Appendix I.). For instance, adsorption on Fe oxides would be important only at pH's in the lower range for natural waters, and adsorption of this species by most Mn oxides would not be expected to occur at all (see Appendix I).

Assembling the data from these previous investigations into a qualitative description of Cr geochemistry results in a complicated model. Figure 1 is a schematic of the geochemical processes which are thought to control the behavior of Cr in oxygenated aqueous systems. In solution, Cr^{3+} (as a kinetically stable hydroxy species) can exist only in very low concentrations, possibly unless complexed with organic ligands. Some Cr^{3+} may become oxidized by O_2 by this kinetically slow reaction, but the tendency will probably be for this species to precipitate as $Cr(OH)_3$ or $(Fe,Cr)(OH)_3$, or to adsorb on particulate Fe oxide, organics, or clays. Thus Cr^{3+} species will tend to accumulate in sediments. The potential of these sediment
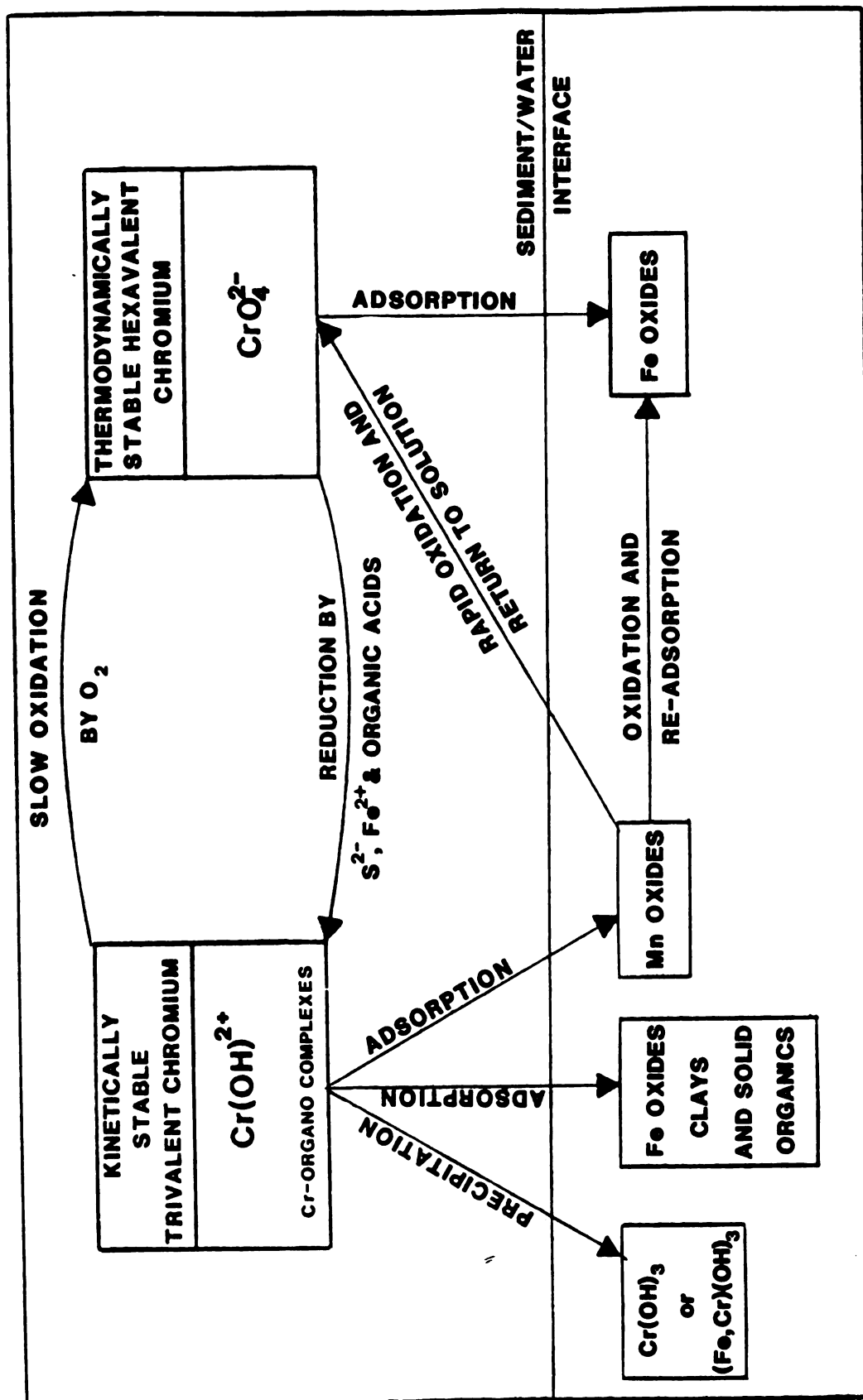
FIGURE 1. CONCEPTUAL MODEL OF CHROMIUM GEOCHEMISTRY IN OXIC AQUEOUS SYSTEMS

forms of Cr^{3+} to become oxidized by the Mn oxides which tend to accumulate in oxic sediments and other oxic-anoxic boundaries, is not known. Assuming some oxidation does occur in the sediment environment, the resulting Cr^{6+} will be highly mobile, as its adsorption potential will be limited at most pH's. This Cr^{6+} may be remobilized into the solution phase. Cr^{6+} in the solution phase (CrO_4^{2-}) is thermodynamically stable but may be subject to reduction by organics and possibly the uptake by organisms. This species apparently can also be reduced in reducing environments, although the mechanisms and kinetics in aqueous systems have not been well demonstrated.

Field studies seem to verify at least some parts of the qualitative model of Cr geochemistry presented above. As previously stated, many studies report the occurrence of significant amounts of Cr^{3+} in water analyses, suggesting Cr^{3+} is kinetically stable. The tendency of Cr^{3+} to be associated with particulate matter (i.e. be adsorbed) has also been demonstrated for both fresh water (Benes and Steinnes, 1975) and marine systems (Loring, 1979; Cranston and Murray, 1980). The role of organic matter in the reduction of Cr^{6+} has been demonstrated in flocculation experiments (Cranston and Murray, 1980) where the organic rich particles were believed to cause reduction. Furthermore, Benes and Steinnes (1975) found the Cr^{3+} to Cr^{6+} ratio increased with increasing organic content of the water. Campbell and Yeats (1981) found that the levels of Cr

in Atlantic Ocean waters followed the nutrient cycle, suggesting biochemical influence on Cr behavior.

Several studies have also demonstrated the response of the valence state of Cr to the redox conditions of the water column. Dissolved Cr^{6+} was shown to decrease or disappear at the O_2 minimum in the Pacific Ocean (Murray, et al., 1983). These authors suggested the existence of microenvironments of highly reducing conditions, as O_2 was still measurable in samples where Cr^{6+} was depleted. Hexavalent Cr was also shown to be present above, but became depleted at, the oxic-anoxic boundary in a fiord (Emerson, et al., 1979), although Cr^{3+} was found to some extent in the oxic layer. This redox boundary was described as a O_2/H_2S boundary, but the authors did not discuss whether the sulfide was responsible for Cr^{6+} reduction, as was shown by Smillie et al. (1981) for Cr^{6+} in waters overlying sediments producing H_2S.

Direct evidence for the oxidation of Cr^{3+} by Mn oxides in the environment has not yet been provided. Indirect evidence includes the widespread observation of Cr depletion in marine Mn nodules compared to low Mn marine sediments (Turekian, 1978 and others). Interestingly, the low concentrations of dissolved Cr^{3+} above the oxic/anoxic boundary (i.e. in oxic waters) in the study of fiord waters by Emerson et al., 1979, was attributed to adsorption onto the abundant particulate matter at this boundary, although these authors did not rule out oxidation. This particulate matter, however, was described as "manganese oxide

particulates", suggesting oxidation could have been responsible for at least part of the disappearance of Cr^{3+}. A study by Gephart (1982) can be interpreted to provide indirect evidence for the oxidation of Cr by Mn oxides in fluvial sediments. In this study the partitioning of Cr and a variety of other trace metals between the various sediment components was measured by using a series of selective chemical extractions. The data were then normalized to the weight of each hypothesized adsorbing phase. The normalized data revealed that on a weight basis, most metals correlated very highly with the Mn oxide fraction of the sediment. Cr however, showed a relatively higher affinity for the Fe oxide and organic phases. One explanation of these results is that the apparent low affinity of Cr for the Mn oxide phase is due to its oxidation and desorption by this oxide. These conclusions are speculative, however, and at best provide only indirect evidence for the importance of this process in nature.

From this discussion of Cr geochemistry it is obvious that there is a need for further research in many areas. One such area for further research is the role of Mn oxides in controlling the environmental fate of this metal. Mn oxides are a sink for most trace metals, but in the case of Cr, these species may promote oxidation to the mobile and toxic form of this metal.

3.0 STATEMENT OF PURPOSE

3.1 Approach to the Problem

As the previous discussion has illustrated, the geochemical behavior of Cr is very complex, and its fate in the environment is not well understood. It is evident that much needs to be done to develop a more complete understanding of the exogenic cycle of this element. Both field studies and laboratory research are needed to accomplish this goal. Research in the controlled laboratory environment is necessary to gain fundamental knowledge of the processes which may be operating in natural systems, as these processes are difficult to isolate in the study of natural systems. By measuring the characteristics of all components and controlling all variables, an unambiguous interpretation of rates and mechanisms of individual processes can be attained. This research will apply this experimental approach to study a portion of the overall model of Cr geochemistry. The part of the model to be studied, focusing on the oxidation of Cr^{3+} by Mn oxide, is portrayed in Figure 2. The results of this research may be valuable for interpreting data from natural systems and will assist in the development of a predictive geochemical model for chromium.
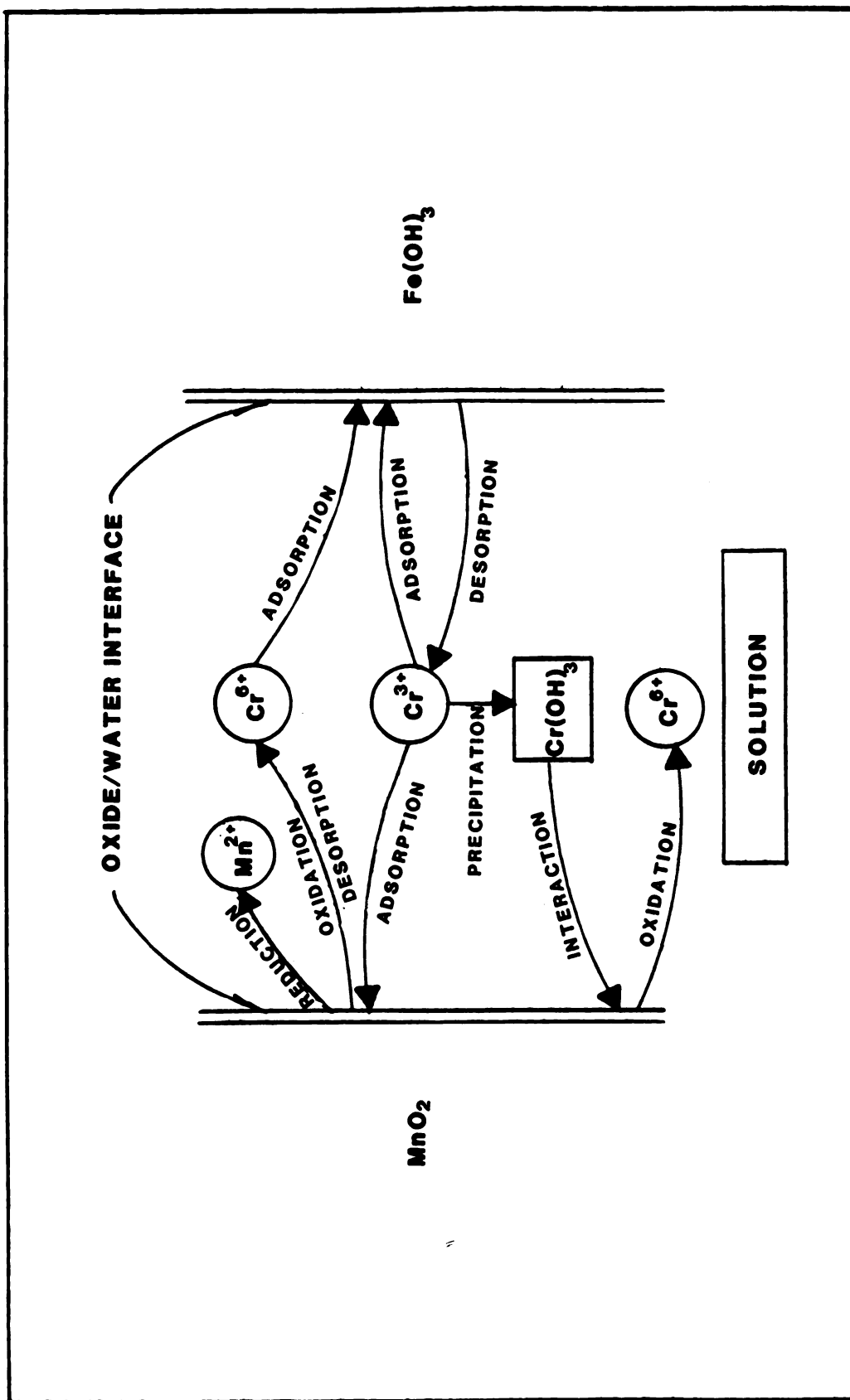
FIGURE 2. SCHEMATIC OF CHROMIUM/Mn-Fe OXIDE INTERACTIONS ADDRESSED IN PRESENT STUDY

3.2 The Goals of this Research

This research results from the need for a clear understanding of the fundamental nature of the oxidation of Cr by Mn oxides. This hydrous oxide has been found to be important in controlling the behavior of other metals but has not been adequately considered in geochemical studies of Cr. The available laboratory studies of Cr-Mn oxide interactions have either neglected the influence of solubility controls on Cr, or have used forms of Mn oxide that are vastly different to those occurring in nature (see Appendix I). No previous study has adequately demonstrated the influence of solution chemistry or the ability of the reaction to proceed in the presence of other solid phases. The purpose of this research is to attempt to define, in a controlled laboratory environment, the nature and controls of the oxidation of Cr^{3+}, by a form of MnO_2 that is similar to the oxide minerals identified in natural systems. The "nature" of the reaction includes the mechanism, stoichiometry and rate dependence, and the "controls" include the influence of solution chemistry, the formation of insoluble Cr species, and the presence of a "competing" adsorbent, amorphous Fe oxide. The specific areas to be explored by experimentation include:

1. The stoichiometry of the oxidation-reduction reaction between Cr^{3+} and MnO_2 throughout the duration of the reaction.

2. The kinetics of the oxidation reaction and insight into the reaction mechanism from a kinetic interpretation.

3. The effects on the oxidation rate of varying reactant concentrations.

4. The effects on the oxidation rate of solution chemistry including pH, ionic strength, nature of the swamping electrolyte, and the presence of another adsorbed trace metal.

5. The effect of the presence or absence of dissolved O_2 on the oxidation reaction.

6. The extent of oxidation of solid $Cr(OH)_3$ in the presence of a large excess of MnO_2.

7. The competition of $Fe(OH)_3$ with MnO_2 for the adsorption of Cr^{3+}, and the ability of MnO_2 to oxidize Cr that is adsorbed to $Fe(OH)_3$.

The results of these experiments will be interpreted in light of current surface chemistry theories to provide a description of the nature and chemical controls of the interaction of Cr with Mn oxides. This research will also have implications for assessing the potential importance of this reaction in the natural environment. Furthermore, the experiments using both Fe and Mn oxide will provide insight into the nature of the competition of two adsorbents for one adsorbate, which has not been previously demonstrated

experimentally. In particular, this phase of the study will demonstrate whether an equilibrium distribution of adsorbed Cr will be attained between these two solid phases, or whether a Cr ion adsorbed onto one oxide surface is, in a kinetic sense, removed from the solution permanently, and thus not reactive with respect to the other oxide surface.

METHODS

This section of the report describes the materials and analytical procedures employed in this research. Included in this section is a description of; 1) the methods used to prepare and characterize the synthetic Fe and Mn oxides used in the experiments, 2) the general procedures used in the experiments, 3) the reaction vessel designed and constructed for this research, and 4) the analytical method designed to determine the concentration of both oxidation states of Cr in solution. Quality control data are also presented in this section.

1.0 GENERAL APPROACH AND LIMITATIONS

The general procedural approach for studying the oxidation of Cr by Mn oxide was to add known amounts of aqueous Cr^{3+} (as the nitrate salt) to a reaction vessel containing a known amount of well characterized MnO_2 slurry, at a fixed pH and solution composition. As the reaction proceeded, representative samples were withdrawn at time intervals and quickly filtered to stop the sorbent-sorbate interactions. The supernatant was then analyzed for changes in the pertinent reactants and products.

The general lack of research on Cr geochemistry, as compared to many other metals, may be due in part to the complex behavior of this element which causes difficulties

in experimental design and analytical procedures. Because of the low solubility of $Cr(OH)_3$, it was necessary to conduct many of the experiments at low pH (less than 5.0). This allowed the use of Cr concentrations high enough to ensure good analytical precision for both Cr^{6+} and Cr_{total} determinations by flame atomic absorption spectrophotometry. The use of low pH's, of course, limits the application of the resulting data to most natural aqueous systems, however, this was the only way to assess the fundamental nature of the reaction, which may or may not change in higher pH regions. Experiments at higher pH's were also conducted to determine the reactivity of the hydroxide species.

Considerable effort was expended in the development of experimental and analytical techniques for the rapid sampling and accurate analysis of all pertinent parameters throughout an experimental procedure. The following section of this report describes the synthesis and characterization of the Mn and Fe oxides, the equipment and materials, general methodologies and quality control used in the experimental procedures of this research. Some of the experimental methods and background experimental data are presented in the results section, as they are a necessary part of the discussion.

2.0 PREPARATION AND CHARACTERIZATION OF Mn OXIDE

2.1 Introduction

There have been over twenty different naturally occurring tetravalent oxides of manganese identified in a variety of exogenic systems (Burns and Burns, 1979). The fundamental structural unit of these oxides is the $[Mn^{4+}O_6]$ octahedron. Like Cr^{3+}, the electron configuration of the central Mn ion is $[Argon]3d^3$, which in octahedral coordination has a very high crystal field stabilization energy (Burns and Burns, 1979). The octahedra are linked by corner-sharing or edge-sharing, resulting in a variety of structures. The close proximity of neighboring Mn^{4+} ions causes structural instability, which along with random and periodic vacancies and extensive solid solution, results in non-stoichiometric, cryptocrystalline minerals which are often difficult to characterize (Burns and Burns, 1979).

In the marine environment, the minerals todorokite, birnessite and δ-MnO_2 have been identified as the primary Mn oxides (Bricker, 1965; Burns and Burns 1979; Crerar et al., 1980). Birnessite has also been identified as the primary Mn oxide in stream sediments (Potter and Rossman, 1979) and in soils (Ross et al., 1976). There is some apparent confusion over the nomenclature of Mn oxides, especially in naming synthetic products. The mineral name birnessite has been used interchangeably with δ-MnO_2, manganous-manganite,

and manganate IV (Murray, 1974). Burns and Burns (1979) have suggested that the mineral birnessite is distinctly different from δ-MnO$_2$, and vernadite has been proposed as the proper name for δ-MnO$_2$.

2.2 Preparation of MnO$_2$

Because of the widespread occurrence of the minerals birnessite and vernadite, a synthetic form similar to these minerals was selected for use in this research. Various methods of preparing birnessite have been reported (McKenzie, 1971). The MnO$_2$ used in this study was prepared by the method of Murray (1974), which involves the oxidation of the manganous ion with permanganate by the reaction:

$$3 \text{ MnCl}_2 + 2 \text{ KMnO}_4 + 2 \text{ H}_2\text{O} = 5 \text{ MnO}_2 + 4 \text{ H}^+ + 6 \text{ Cl}^-$$
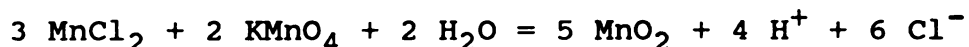
This method was chosen because of the exhaustive characterization of the oxide formed in this manner in a series of papers describing its adsorptive behavior (Murray, 1974; Murray, 1975; Balistrieri and Murray, 1982; and others). The exact procedures followed for preparation of the oxide used in this research are as follows:

1. A 500ml stock solution of 0.2 M KMnO$_4$ was prepared by dissolving 15.804 grams of reagent grade KMnO$_4$ in double distilled water.

2. A 500ml stock solution of 0.3 M MnCl$_2$ was prepared by dissolving 29.687 grams of MnCl$_2 \cdot 4$H$_2$O in double distilled water.

3. 3.20 grams of NaOH was dissolved in 10ml double distilled water.

4. The $MnCl_2$ stock solution was standardized by the method of Lingane and Karplus (1946).

5. 200ml of the $KMnO_4$ stock solution and the 10ml of 8.0 N NaOH was placed in a 1000ml Pyrex beaker and titrated with an equivalent amount of $MnCl_2$ solution (approximately 200ml) as the solution was briskly stirred with a magnetic stirring device.

6. To ensure complete reduction of the MnO_4^-, approximately 1.0 extra ml of $MnCl_2$ solution above the calculated equivalent was added. This was done because residual permanganate would greatly affect the oxidizing characteristics of the resulting Mn oxide.

7. The precipitate was transferred to glass centrifuge bottles and washed five times with double distilled water, by shaking the precipitate in the water, centrifuging, decanting and adding fresh distilled water.

8. The precipitate was then suspended in approximately 1 liter of double distilled water in a stoppered glass jar and stored at room temperature on a slowly stirring magnetic stirring device.

The oxide produced in this manner was used over the next two years in oxidation experiments.

2.3 Characterization of MnO_2

2.31 X-Ray Diffraction

Mn oxide prepared in the above manner is poorly crystalline and has a high oxidation state. The normal x-ray peaks found are broad, diffuse and indistinct (Burns and Burns, 1979). The peaks, when seen, are commonly at 1.4 and 2.4 A and sometimes at 7.3 A (Crerar et al.,1980). To prepare the oxide suspension for x-ray diffraction, a small amount of slurry was allowed to air dry on a glass slide.

The sample was x-rayed using Cu radiation at a scan speed of .5°/min. This x-ray analysis revealed no distinguishable peaks, even after the oxide had aged for over two years. This result is similar to those of Van den Berg and Kramer (1979), whose oxide prepared in a similar manner was x-ray amorphous for over two years.

2.32 Oxidation State

The average oxidation state of the Mn in the MnO_2 stock suspension was measured by iodometric titration. This method involves the reduction of Mn^{4+} and Mn^{3+} by the oxidation of iodide to iodine, essentially a modified Winkler Titration. The iodine is then titrated with standardized thiosulphate to obtain the total oxidized equivalents. By convention, the resulting oxidation state of the oxide is expressed as MnO_x, where:

$$x = \frac{[\text{ total oxidized equivalents}]}{[\text{total Mn}]} \times 0.5 + 1.0$$

The methods used were similar to that of Murray et al., (1984) and are summarized as follows:

Standardization of thiosulfate

1. A stock KIO_3 solution was prepared by dissolving 0.3567 gram of desiccated KIO_3 in 1 liter double distilled water. Then for each replicate of standardization, 25ml of this solution was transferred to a 250ml flask, followed by the addition of 75ml distilled water and 0.50 gram KI crystals.

2. To each 250ml flask was added 10ml 3.6N H_2SO_4 and the solution stored in the dark for 5 minutes.

3. Each solution was then titrated with freshly prepared 0.01N $Na_2S_2O_3$, with 2ml starch indicator added after the appearance of the straw yellow color.

4. The normality of the standardized $Na_2S_2O_3$ was then computed by: N $(Na_2S_2O_3)$ = .25 / ml titrated. This was repeated three times and the average value used.

<u>Titratible equivalents of oxide</u>

1. 50 ml of a solution consisting of 4M KI (33.2g) and 8M KOH (22.4g) was prepared, as well as a 6N H_2SO_4 solution.

2. For each replicate, to a 250ml flask was added 47 ml double distilled water, 1 ml KOH-KI solution, 1 ml MnO_2 stock solution, and 1 ml H_2SO_4. The mixture was allowed to react for 5 minutes, after which there was no visible MnO_2 remaining.

3. After the addition of 1 ml starch indicator the solution was then titrated with the standardized thiosulphate, the volume of titrant recorded.

4. The titrated solutions were then analyzed for total Mn by flame atomic absorption spectrophotometry.

The average stoichiometry of the MnO_x was x = 1.95 with a standard deviation of 0.005 for seven replicates. This is consistent with other synthetic Mn oxides prepared in this manner, particularly with that used by Balistrieri and Murray (1982) which was referred to as δ-MnO_2.

2.33 Binding Capacity of MnO_2

The binding capacity of the oxide stock suspension used in this research was not measured. Methods currently used for determining the binding capacity of oxide surfaces include; 1) experimental determination of a metal adsorption isotherm, 2) calculation by knowing the specific surface area and the estimated surface area covered by an adsorbed

species, and 3) determination of the amount of hydrogen
exchangeable sites by rapid tritium exchange. There are
problems with all of these methods, especially with Mn
oxides (Louma and Davis, 1983). Since the binding capacity
for Cr^{3+} can not be determined directly from adsorption
isotherms, 2) and 3) were the only options for this study.
Since both of these methods are very general and surface
area determinations for MnO_2 are tenuous at best, it did not
appear that this information would be useful.

A survey of reported binding capacities of $\delta-MnO_2$ from
other studies shows that most are on the order of 1.0-7.0
mmole of adsorbed metal per gram of Mn oxide. On a molar
basis for Cr this represents 0.1-0.5 mole of adsorbed metal
per mole of oxide. The binding capacity however, is metal
dependent and also pH dependent. The above range will be
used as a guideline in discussions of the present
experimental results.

2.4 Stability of the MnO_2 Stock Suspension

2.41 Stability with Time

There are advantages and disadvantages in preparing fresh
oxide stock suspensions for each experiment or group of
experiments. The main advantage to preparing fresh oxide is
that "aging" effects do not influence the properties of the
oxide over time, which may effect experimental results. The
main disadvantage is the possibility that each batch of

oxide may be slightly different. In this study, one Mn-oxide stock suspension was used over the entire period of research. Reasons for this decision included, 1) the large amount of time required to synthesize and characterize each batch of oxide, and 2) the ambiguity over what is a reasonable time period to use an oxide as "fresh" as opposed to "aged". The stock suspension used in this research was used unaged only in preliminary, method development experiments. No experimental data was collected until the oxide was more than 6 months old. Hence all of the data reported in this study are from experiments with MnO_2 that was "aged" to some extent.

Changes in the MnO_2 expected to occur over time include increasing crystallinity and increasing particle size due to coagulation. Changes in crystallinity were not evaluated, in part, due to the difficulty in attaining x-ray diffraction patterns, even after two years of aging. A change in particle size upon aging, although not measured directly, was evident from visual observation as small particles were visible when aliquots of the aged oxide were added to distilled water. These particles were not visible when the oxide was fresh.

The change in particle size was also evaluated indirectly in the way most important to this research; by the effect on the oxidation rate of Cr. It would be expected that the increased grain size due to aging would cause a slower reaction rate, at least if the oxidation

reaction is surface area controlled. The results of identical experiments conducted shortly after the oxide was synthesized and then 5 months later are shown on Figure 3. There was a relatively small but definite decrease in the oxidation rate due to the aging of the oxide over this time period. Also shown in this figure is a second experiment conducted on the later date after the oxide suspension had been placed in a sonic vibration water bath for twenty minutes before use in the experiment. The resulting oxidation rate increased to almost exactly that of the initial experiment. It appears that much of the coagulation effect can be reduced by sonic vibration. Thus the vibration step became part of the experimental procedure, and experimental results could be reproduced with good accuracy over fairly long time periods.

Even with the use of sonic vibration, the reactivity of the oxide (in terms of the oxidation rate) did decline with age, possibly due to changes other than just coagulation. Anderson, et al., (1973) found that adsorption kinetics (but not capacity) was strongly related to the crystallinity of Mn oxides. For this reason sets of experiments to be used to compare the resulting data were all done consecutively on one day, or over several days. This ensured that the effects on the reaction rate due to solution conditions, etc., were clearly separate from those caused by the gradual aging of the oxide. No conclusions were drawn from
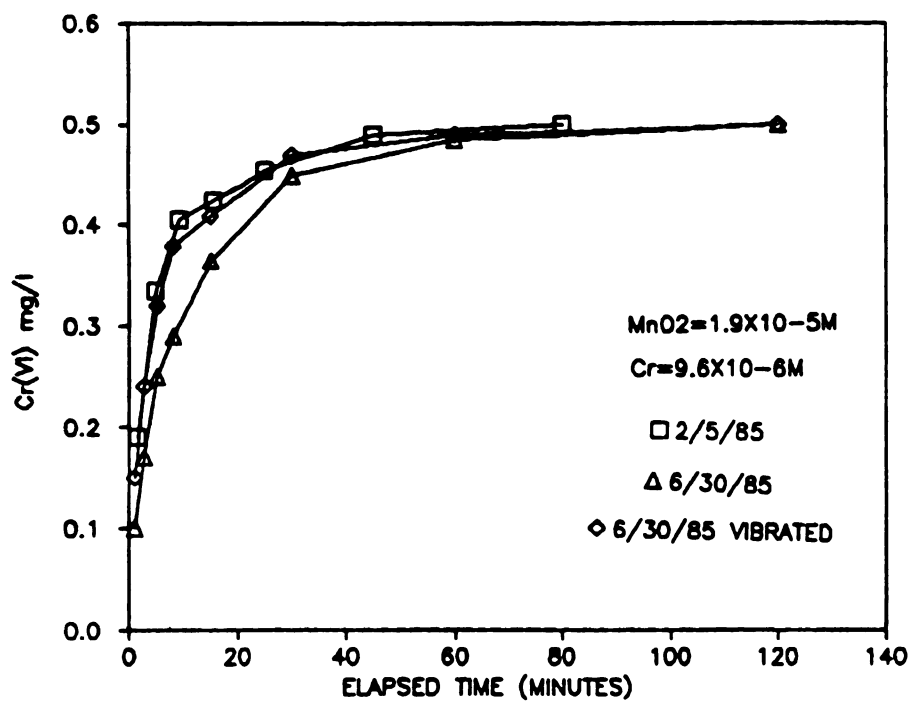
Figure 3. Effect of Oxide Aging and Sonic Vibration Pretreatment on the Oxidation Rate of Cr by MnO_2

comparing experimental data from distinctly different time periods.

Because of the possibility of significant alteration of the surface properties of hydrous oxides upon dehydration (Parks, 1965), the MnO_2 stock suspension was never dried out before use. This meant that the MnO_2 was added to experimental systems as an aliquot, primarily by eppendorf pipette. To assess the amount of variation that this procedure caused in the experimental MnO_2 concentrations, a replicate analysis was performed. Ten $200\mu l$ aliquots were removed from the stirring stock suspension, placed in a 250ml volumetric and dissolved with 0.1M hydroxylamine monohydrochloride in 25% v/v acetic acid. After addition of double distilled water to volume, the replicates were analyzed for Mn by AAS. The results, which take into account all of the relative errors in this procedure, gave an average molarity of Mn (based on dilution to 500ml) of 1.85 ($^+/_-$ 0.02) X 10^{-5}, where 0.02 is one standard deviation. One standard deviation represents a 1.1% variation in the average molar value of MnO_2 in an aliquot. This variability between aliquots is well within the total experimental error and thus should not have influenced the reproducibility or reliability of the experimental data.

The stock suspension was also checked at time intervals to make sure the concentration to volume relationship remained constant. It was found that periodic adjustments were required, and double distilled water was added as

necessary to make the proper dilutions. The concentration vs. volume relationship, as derived from the periodic measurements, is shown graphically on Figure 4. The small variations over time should be of little consequence, as again, comparisons between experimental results were only made if the experiments were all done over a short time period.

2.42 pH Dependent Stability

Because it was necessary to conduct the oxidation experiments at relatively low pH's, the stability of the MnO_2 stock suspension at these pH's was explored. To determine the stability of MnO_2, aliquots of the oxide suspension were added to 0.10M $NaNO_3$ solutions adjusted to various pH's with HNO_3. The solutions were then sampled over time, filtered and the supernatant analyzed for total Mn by AAS. The results (Figure 5) show that at pH 4.5, where most of the experiments were conducted, the oxide did not dissolve over four hours time, which demonstrates that oxide dissolution is unimportant over the time interval required to complete most of the oxidation experiments. As is shown on Figure 5 dissolution does occur at pH 3.0 and below. These results are consistent with those of Murray (1974) who found MnO_2 to be stable to pH 3.5, as predicted from equilibrium Eh-pH relationships. At pH's lower than 3.5 it is predicted that MnO_2 will be unstable in water. For any experiments conducted at a pH below 3.5 a blank was
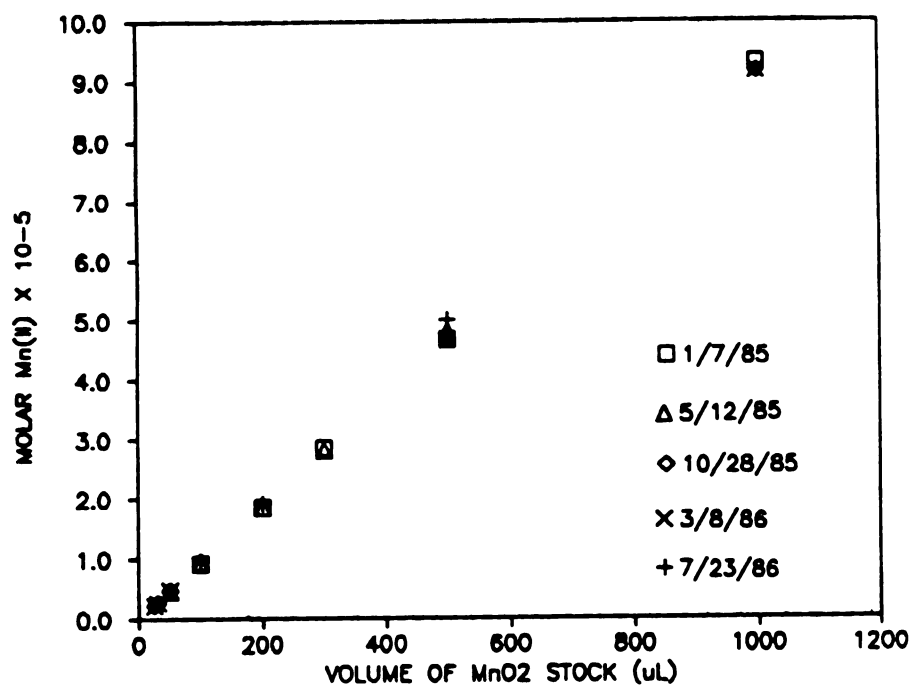
Figure 4. Concentration of Mn in Aliquots of MnO_2 Stock
Solution Sampled Over Time
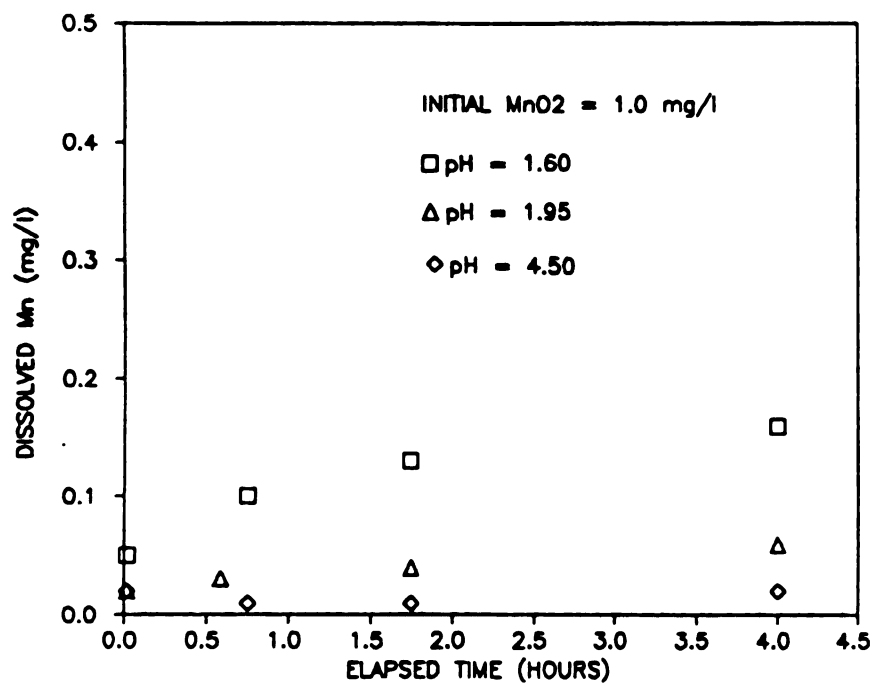
Figure 5. Stability of MnO$_2$ Suspension at Various pH's

prepared and simultaneously sampled for Mn^{2+}, so that a correction of the experimental data could be made in terms of the Mn^{2+} released.

The stability of the MnO_2 stock suspension was also explored at pH 4.5 in an N_2 purged (i.e. no O_2) system. One liter of 0.10 M $NaNO_3$ was purged with N_2 until the O_2 concentration as measured by a dissolved O_2 electrode (Orion model 97-00-99) was less than 0.10 ppm. Then 600 μL of stock suspension was added and the system continuously purged for four hours. Samples were periodically withdrawn, filtered, and measured for dissolved Mn by flame AAS. Only the initial sample (elapsed time 2:00 minutes) showed Mn levels above detection (0.01 ppm), suggesting that the oxide did not undergo any significant dissolution over four hours time.

3.0 PREPARATION AND CHARACTERIZATION OF Fe OXIDE

3.1 Introduction

Iron oxides occurring as particulates or sediment coatings are found in a range of crystalline states, from entirely amorphous to crystalline. The initial precipitate is usually amorphous or microcrystalline, and becomes more crystalline with age (Louma and Davis, 1983). At atmospheric temperature and pressure the amorphous oxide is stable for months (Swallow et al., 1980). The amorphous forms of iron oxide generally exhibit higher surface areas and adsorption

capacities than crystalline forms. Although Fe oxides are very often associated with Mn oxides, apparently, Fe and Mn coexist as distinctly separate phases (Carpenter and Hayes, 1980).

3.2 Preparation of Hydrous Ferric Oxide

The hydrous ferric oxide (also called amorphous ferric oxyhydroxide) that was used for the mixed sorbent experiments (i.e. both Mn and Fe oxides present in the system) was prepared by the hydrolysis of ferric nitrate at room temperature, by a method similar to that of Leckie et al., (1980). Although generally represented as $Fe(OH)_3$-am, the chemical composition of the oxide prepared in this manner was measured thermogravimetrically and determined to be $Fe_2O_3 \cdot H_2O$ (Leckie et al., 1980). The method used in this study is summarized as follows:

1. One liter of 10^{-3} M $Fe(NO_3)_3$ in 0.10 M $NaNO_3$ was placed in the reaction vessel on top of the magnetic stirring device; the whole apparatus enclosed in the MSU Geochemical Laboratory glove-box. The sealed glove-box was then flushed with N_2 gas.

2. The solution itself was then bubbled with N_2 gas for approximately 20 minutes, which was long enough to reduce the dissolved O_2 content to less than 0.10 mg/l.

3. The solution was then titrated to pH 7.5 with N_2 purged 1.0 N reagent grade NaOH. As the hydroxide formed and the pH dropped, 0.10 N NaOH was added to keep the pH at 7.5 $^+/_-$ 0.2.

4. The precipitate was allowed to age under N_2 conditions for four hours, with the pH maintained at 7.5, after which time the pH was adjusted to the desired pH with dilute HNO_3 and the desired experiment was conducted.

The concentration of the resulting amorphous ferric oxyhydroxide was assumed to be approximately 10^{-3} M, or equal to the initial Fe_T. Consequent experiments were conducted by adding the desired reagents to the reaction vessel, thus the Fe oxide was used as formed in situ.

3.3 Characterization of Fe Oxide

3.31 X-Ray Diffraction

The amorphous nature of the freshly precipitated Fe oxide was confirmed by x-ray diffraction. Due to the inability to air dry the oxide on a glass slide, the oxide suspension was drawn through a porous ceramic tile by a vacuum driven device, which left an oxide coating on the outside of the tile. The x-ray analysis was done with Cu radiation and the amorphous nature of the oxide was confirmed.

3.32 pH_{zpc}

The pH_{zpc} of the Fe oxide was estimated using the salt addition method. A batch of freshly prepared Fe oxide (as above except in distilled water, not $NaNO_3$ solution) was divided into eight 100 ml portions. Each was set at a desired pH from 7 to 9 and allowed to stabilize for one hour. Then, a small amount of solid $NaNO_3$ (0.1 gram) was added to each sample and the resulting pH change was monitored. Below the pH_{zpc} the addition of the salt causes

a rise in pH, with the opposite occurring above the pH_{zpc}. The pH at which no change is observed is an estimate of the pH_{zpc}. This procedure resulted in a pH_{zpc} at about pH 7.8 for this oxide. This value is consistent with the values found by other investigators.

3.33 Stability at pH 4.5

Because most of the experiments were conducted at pH 4.5, it was necessary to confirm the stability of the Fe oxide suspension at this pH over time. An oxide suspension prepared as above was adjusted to pH 4.5 and sampled over time. The samples were filtered and measured for dissolved Fe by flame AAS. There were no iron levels found above the detection limit (0.05 ppm) over four hours time.

4.0 GENERAL EXPERIMENTAL PROCEDURES

4.1 Clean Techniques

Many precautions were taken to ensure that the experiments in this research were not affected by contamination or the occurrence of undesired chemical reactions. Of major importance was to ensuring that potential contamination by any heavy metal species, especially Cr, was minimized. The potential sources for contamination included airborne particles, contaminated glassware and impure reagents, including the distilled water

supply. The potential undesired chemical reactions included adsorption by and dissolution of glassware or other apparatus in contact with the experimental system.

To minimize potential contamination various protective measures were taken. First of all, the experiments of this research were all undertaken in the MSU Geochemical Laboratory clean-room, which is designed to minimize air-flow from the outside except through filtered air vents. Secondly, all standard preparation was done inside a plexiglas positive pressure hood, pressurized with filtered air. Finally, all glassware used in these experiments were subjected to a rigorous multi-step cleaning procedure. The first step in this procedure was an alconox/hot water scrub, followed by rinsing in single distilled or deionized water. The glassware was then soaked in 1:3 concentrated HCl/double distilled water for at least 24 hours. After rinsing three times with double distilled or distilled-deionized water, the glassware was then allowed to air dry in the positive pressure hood or other protected areas.

To reduce the potential for chemical reaction between the experimental system and laboratory apparatus only resistant materials were used. All lab ware in contact with the experimental system was composed of Pyrex, Teflon, or polypropylene. Blanks were run to ensure that adsorption of metals to glassware was not significant during the time period of the experimental procedures. All reagents used were reagent grade or better. The distilled water supply

used as the solvent in these experiments was either double distilled (house distilled, followed by lab distillation) or distilled-deionized (house cartridge deionized followed by lab distillation).

4.2 Reaction Vessel

A specially designed reaction vessel was constructed for use in many of the experimental procedures (Figure 6). This vessel is similar to that described by Zasoski and Burau (1979). The vessel was constructed from a thick-walled Pyrex beaker which was cut to have a flat, smooth surface along the top rim. The beaker was then sandwiched between two plexiglas squares which could be tightened together via six threaded metal rods, with wing-nuts, around the outside of the beaker. The top plexiglas sheet had holes machined at various locations for contact with the experimental system. These holes were of the proper dimensions for 2 pH/Eh electrodes, an O_2 electrode, a Teflon tube for gas addition, a Teflon tube for sample extraction, and two extra holes for reagent addition by glass or eppendorf pipette and for gas escape. All of these ports could be sealed by glass stoppers if necessary. The entire set-up could be used on top of a magnetic stirring device, and the experimental system was isolated from the heat given off by this device by approximately 1/2 inch of air and plexiglas. With this design, the experiments could be run free of dust input, free from loss of solvent by evaporation, in an O_2 free
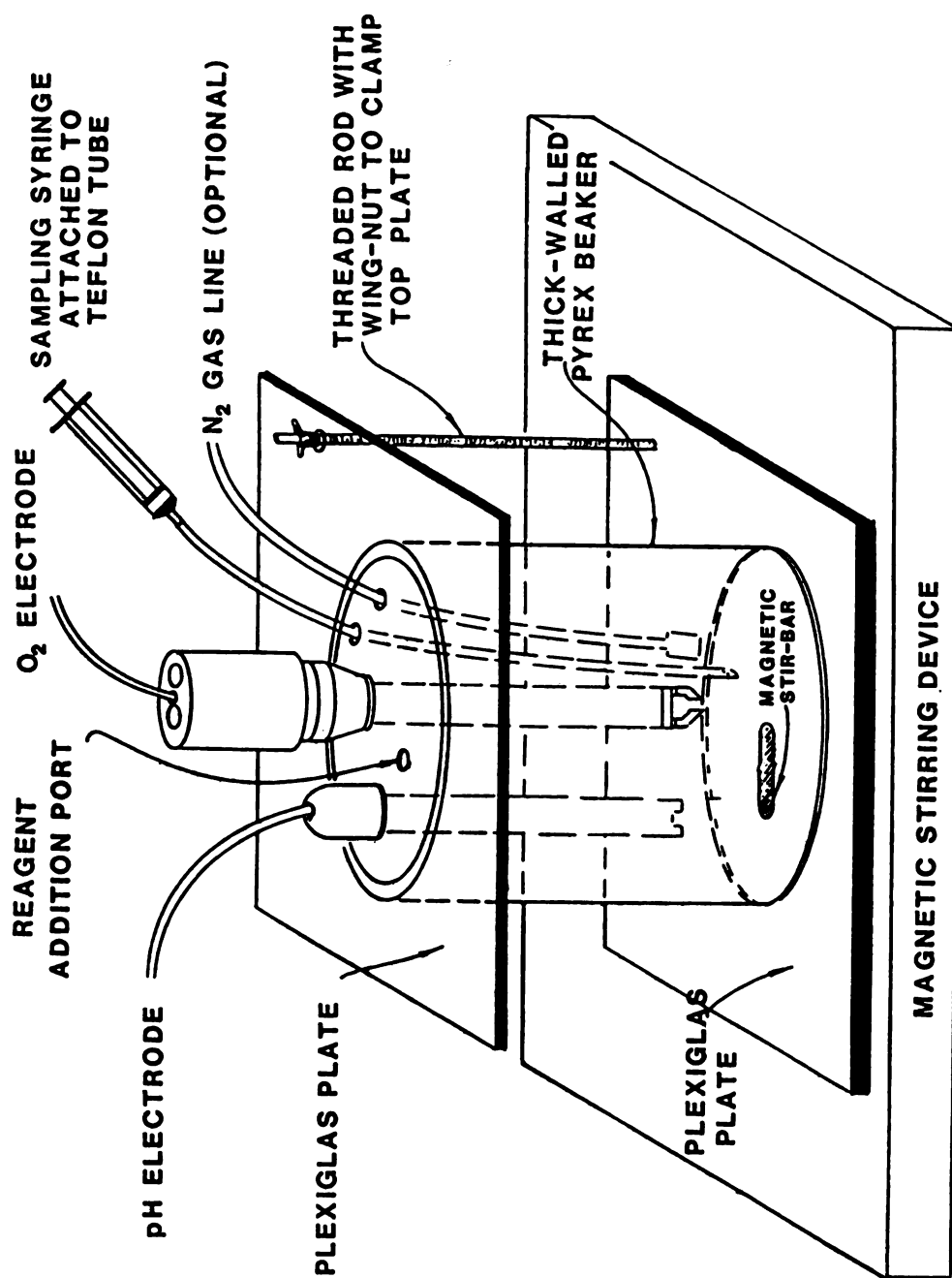
FIGURE 6. EXPERIMENTAL REACTION VESSEL

atmosphere (by bubbling N_2 through the system), and with ease of reagent addition and sampling. For some of the experiments of this project, this entire system, including the magnetic stirring device, was also used inside a glove-box so that the atmosphere outside the reaction vessel could also be purged with N_2.

4.3 General Experimental Procedures

The following procedures are a general description of the methods used for most of the short-term (0.25-4 hrs.) experiments used to study the oxidation of Cr^{3+} by MnO_2. Special procedures used in mixed Fe-Mn oxide systems, kinetic studies, long term experiments, etc. are described in the appropriate results sections of this report. A typical oxidation experiment was conducted as follows:

1. The proper volume (usually 500 or 1000 ml) of double-distilled water containing the desired background electrolyte was added to the reaction vessel and adjusted to a pH near that desired for the experiment with the appropriate acid or base (i.e. HNO_3 and NaOH for an $NaNO_3$ background solution).

2. The MnO_2 stock solution was placed in the sonic vibration water bath for 20 minutes and then returned to the magnetic stirring device so that any suspension that had settled during vibration would be resuspended.

3. An aliquot of MnO_2 suspension, containing the desired amount of MnO_2, was removed from the stock solution by glass or eppendorf pipette while the suspension was stirring briskly on the magnetic stirrer.

4. The aliquot of MnO_2 suspension was added to the reaction vessel and the pH adjusted to that desired for the reaction.

5. The system was allowed to equilibrate for at least 1 hour at this pH and the pH was re-adjusted to the desired level if drift occurred.

6. Cr^{3+} was added to the reaction vessel as a small aliquot of 1000 mg/l $Cr(NO_3)_3$ stock solution to obtain the desired initial concentration of Cr^{3+}. The Cr was added via an eppendorf pipette to ensure that the addition was essentially instantaneous. The pH was re-adjusted to the desired level if drift occurred.

7. The system was then sampled over time by removing an aliquot (15-20 ml) by either pipette or sampling syringe connected to a Teflon tube.

8. The samples were then immediately filtered through a $0.22\mu m$ millipore filter (see below).

9. The resulting supernatant was used for analysis of the desired parameters, usually Cr (total), Cr^{6+}, and Mn^{2+} by atomic absorption spectrophotometry (AAS).

4.4 Sample Filtration

The filtering of aliquots of the experimental system to separate the solution (and solutes) from the oxide(s) (and hence terminate the reaction between the two phases) was an important step in the experimental procedure. This procedure had to meet the following requirements: 1) there had to be no measurable uptake or release of chemical species that would effect the analytical results, 2) there had to be essentially complete removal of the solid phases from the sample, and 3) the process had to be fast with respect to the rate of reaction.

Two different filtration techniques were used in this study. The first, used only in early experiments, was the removal of an aliquot by glass pipette followed by delivery

to a vacuum driven Millipore glass filtering device, where the sample was collected in a glass test tube connected to the end of the filter stem. This method worked well but was much too slow (approximately 30-45 seconds) for the early part of the oxidation reaction and inadequate for the kinetic studies.

Since a faster process was necessary, a second technique was developed. This consisted of sampling the system with a plastic syringe connected to a Teflon tube and then injecting the sample through a Millipore Swinnex polypropylene filter holder. The sample was forced through the filter by pressure rather than drawn through by a vacuum. This whole process took only about 10 seconds which is relatively fast with respect to the reaction rate for most of the experiments performed in this study. For consistency, the time of the sample with respect to the start of the experiment was always recorded as the end of the filtering process.

The use of Millipore mixed cellulose acetate and nitrate filters did not appear to affect the sample chemistry by retention or release of chemical species. This determination was made by analyzing filter blanks and metal standards that were filtered. For a solution with pH 4.5 and 0.10M $NaNO_3$ the filtering process did not effect levels of Cr, Mn, Cu, or Zn as measured by flame AAS.

Both $0.45 \mu m$ and $0.22 \mu m$ filters were tested for the ability to remove iron and manganese oxides from solution.

Both filter sizes appeared to be adequate for removal of freshly precipitated amorphous iron oxide as the resulting supernatants were below detection for Fe by flame AAS methods. However, the $0.45\mu m$ filter did not appear to remove as much MnO_2 from solution as the $0.22\mu m$ filter. In four $0.45\mu m$ filtered sample replicates, detectable Mn was measured in all four replicates with an average value of 0.03 mg/l. In four replicates filtered by a $0.22\mu m$ filter the Mn levels were at or below detection level (0.01 mg/l). Furthermore, the Mn levels of samples passed through the $0.45\mu m$ filter could be reduced to detection by re-filtering through the $0.22\mu m$ filter, suggesting that small MnO_2 particles do pass through the $0.45\mu m$ filter. It is not known whether the $0.22\mu m$ filters allow passage of a small quantity of finely particulate MnO_2 or whether the detection limit values (if real) were due to dissolved Mn^{2+} in the system. At these levels the Mn does not effect the experimental results. The $0.22\mu m$ filters were used for all experimental data presented in this report.

4.5 Analysis of Cr^{3+} and Cr^{6+} in Solution

The success of this research, in part, depended on the ability to accurately determine the oxidation state of Cr in solution. The method to be employed had to be effective for small sample sizes, relatively simple due to the large number of samples, and accurate through the necessary concentration ranges of the experiments.

There have been various analytical methods of Cr^{3+}/Cr^{6+} determination reported in the literature. These include: cation/anion exchange resins (Pankow et.al.,1977 and Smillie et.al., 1981), the diphenylcarbazide colorimetric method for Cr^{6+} described in Standard Methods (APHA et.al.,1975) and used by Schroeder and Lee (1975) and Bartlett and James (1979), the coprecipitation of Cr^{3+} (and exclusion of Cr^{6+}) with amorphous iron hydroxide (Fukai, 1967; Nakayama et.al., 1981; Cranston and Murray, 1978), and the precipitation of the Pb-Cr^{6+} complex with SO_4^{2-} (Martin and Riley, 1982).

Because of the reported accuracy, working concentration range, and equipment requirements, the method of Martin and Riley (1982) was investigated for use in this research. The rationale for this method is based on the strong complex formed between Pb and hexavalent Cr in solution at low pH's. After this complex forms, it can be coprecipitated with lead-sulfate. Hence after centrifugation, the precipitate will contain all of the Cr^{6+} and the Cr^{3+} will remain in solution. After separation from the solution, the precipitate can then be resolubilized, diluted to the original sample volume and measured for Cr by AAS.

Most of the experiments in this study required accurate Cr^{6+} determinations over the range of 0.01 to 0.50 mg/l. Hence the Pb-SO_4 method of Martin and Riley (1982) was tested over this range for the efficiency of Cr^{6+} recovery and Cr^{3+} exclusion. Figure 7 shows the efficiency of Cr^{6+} recovery for six standards, all with 0.50 mg/l total Cr,

with various amounts of the two oxidation states, using the unmodified Martin-Riley method. The 45° line represents 100% recovery and points plotting below the line represent incomplete recovery. As the data demonstrate, this method was not able to recover all of the Cr^{6+}, with the recovery rate getting worse with increasing Cr^{6+} concentration.

Before abandoning this method, however, an attempt was made to modify it by adding more lead and more sulfate, as following the exact method resulted in only very small amounts of precipitate. Figure 8 shows the efficiency of recovery using twice the amount of $Pb(NO_3)_2$ and $(NH_4)_2SO_4$ (i.e. $200\mu l$ vs. $100\mu l$). This resulted in a much better recovery rate as only the samples containing 0.40 and 0.50 mg/l Cr^{6+} were slightly depleted with respect to the standard. The use of three times the amount of these reagents resulted in a very good recovery rate in all standards as shown on Figure 9. Thus, this modification of the Martin-Riley method resulted in a potentially useful procedure. The points on these graphs are the average of four measurements, with two replicates taken of each standard and each replicate measured twice by AAS. There was very little variation between measurements suggesting good accuracy as well as good precision.

This modified method was studied further for recovery efficiency in a variety of background electrolytes and trace metals, for optimization of the amount of reagents necessary to resolubilize the precipitate, and for the best method for

UNMODIFIED Cr(VI) EXTRACTION
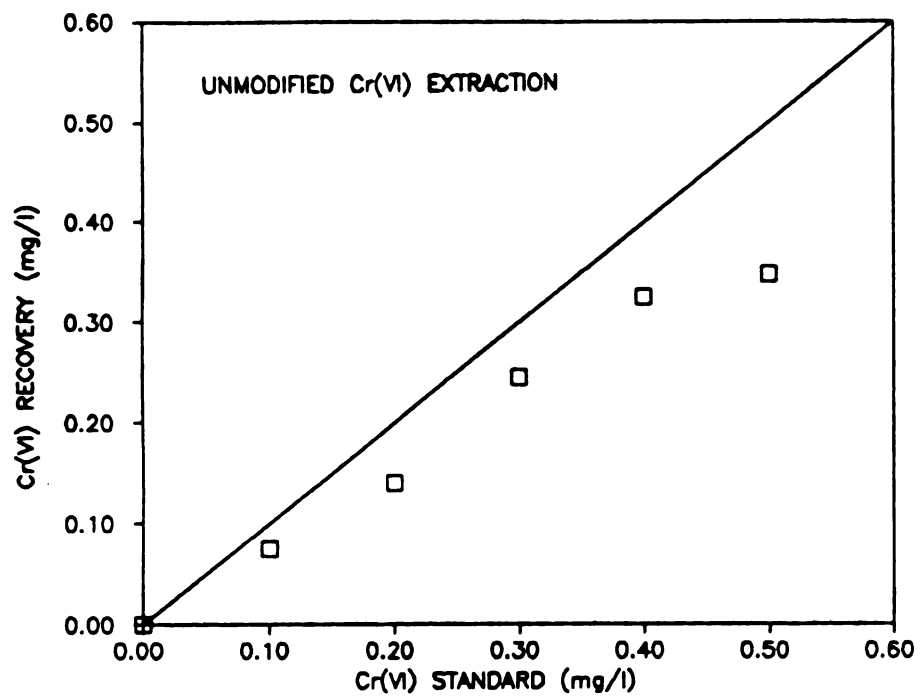
Figure 7.   Efficiency of Unmodified Cr^{6+} Extraction
            Procedure from Martin and Riley (1982)
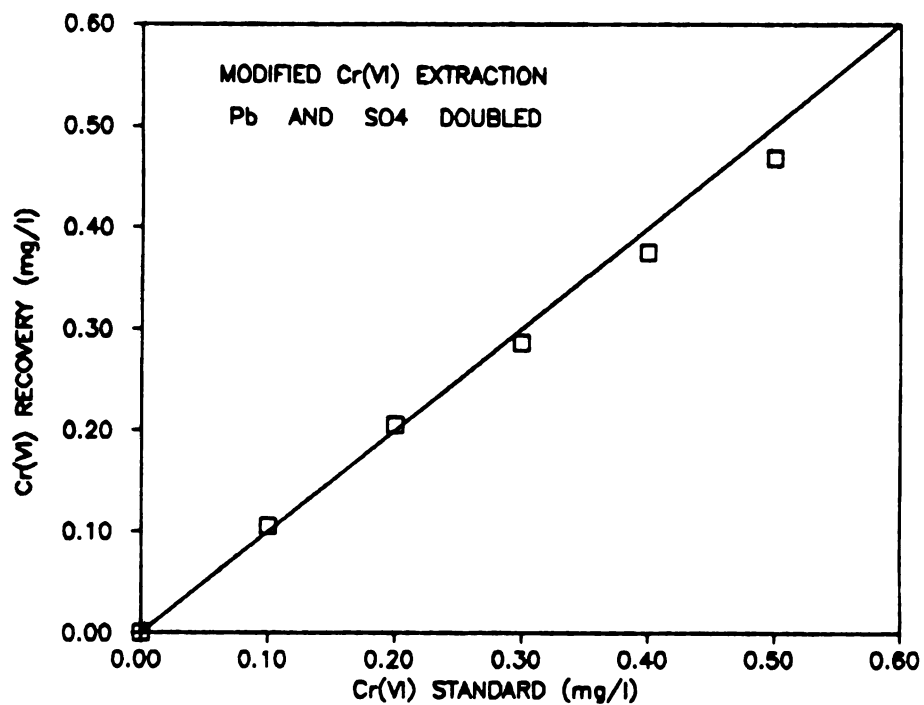
Figure 8. Efficiency of Modified (2 X) Cr^{6+} Extraction Procedure from Martin and Riley (1982)
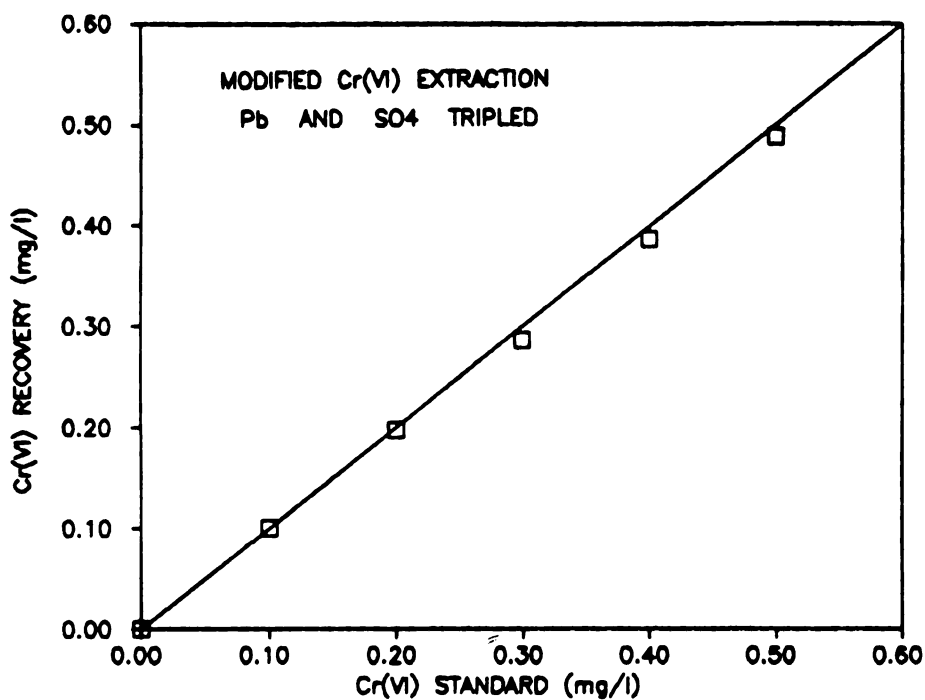
Figure 9. Efficiency of Modified (3 X) Cr^{6+} Extraction Procedure from Martin and Riley (1982)

the preparation of AAS standards. Since some of the adsorption/oxidation experiments were designed to explore the effects of different electrolytes and ionic strengths, it had to be shown that this modified method of Martin and Riley (1982) (hereafter referred to as MMR) would work in a variety of experimental matrices. To address this concern, 0.50 mg/l Cr^{6+} and Cr^{3+} standards were made in various matrices and the MMR extraction was used to test for complete recovery of Cr^{6+} and complete exclusion of Cr^{3+}. The results for the 0.50 mg/l Cr^{3+} standards showed that there was no removal of Cr^{3+} by the Pb-SO_4 precipitate in any of the matrices tested. The results for Cr^{6+} recovery from 0.50 mg/l standards showed there was complete recovery, or near complete recovery, in all of the matrices tested except two. The only potential problems occurred with the 0.10 M Na_2SO_4 matrix and 0.5 M NaCl, both of which resulted in a low recovery rate. In the first case, the presence of a high amount of SO_4^{2-} in the matrix caused a precipitate to form upon addition of the $Pb(NO_3)_2$. The $PbSO_4$ precipitate thus forms at an earlier step in the procedure than required. This may explain the low recovery and suggests that this method may not be useful for solutions containing high levels of sulfate. Similarly, a precipitate also formed upon Pb addition in matrices with a high level of Cl. The formation of this precipitate (probably $PbCl_2$) also caused a low recovery rate. Lower levels of Cl salts did not affect the reliability of this method.

To ensure that the presence of other trace metals did not effect the MMR technique, 0.50 mg/l Cr^{6+} solutions containing 1.00 mg/l Mn^{2+}, Cu^{2+}, or Zn^{2+} in 0.10 M $NaNO_3$ were also tested for interference with the recovery of Cr. The results showed that there was no interference by these trace metals, and thus the MMR method was suitable for experiments designed to explore the effects of competing trace metals on the oxidation rate of Cr by MnO_2.

The modification of the method of Martin and Riley (1982) by increasing the amount of $Pb-SO_4$ precipitate resulted in a fairly concentrated solution matrix to be analyzed by AAS. To minimize any error due to matrix effects when comparing samples to standards and blanks, the standards and blanks were prepared exactly like the samples, except all solution and reagent volumes were increased by a factor of 10, and the Cr was added to the standard after the $Pb-SO_4$ precipitate was resolubilized. Thus the standard preparation was not actually an extraction procedure but the resulting matrix was very similar to that of the samples. The exact procedure of standard preparation is listed in detail below.

With the modifications and careful standard/blank preparations this method for determining the concentration of Cr^{6+} was found to be adequate for use in this research. An error analysis of 10 replicates showed that over the range of 0.02 to 0.50 mg/l that the precision (standard

error) was approximately +/- 0.02 mg/l. The exact MMR method as used in this research is listed as follows:

1. A 10ml aliquot of filtered sampled was placed into a 50 ml Pyrex centrifuge tube.

2. The pH of the sample was adjusted to 3.5 +/- 0.2 by the addition of 10% v/v acetic acid, usually about 10μl for samples starting at a pH of 4.5. If the sample pH was lower than 3.5 or inadvertently lowered below 3.3, it was raised to the proper range by 10% v/v NH_4OH.

3. 300μl of 1.0 M $Pb(NO_3)_2$ was added to the sample by eppendorf pipette and the solution mixed on a vortex stirrer for about 15 seconds. This was allowed to set for 3 minutes to allow the Pb-Cr complex to form.

4. 500μl of concentrated acetic acid was added to the sample and the solution mixed on the vortex stirrer. This was done to make sure all Cr^{3+} is solubilized.

5. 300μl of 0.20 M $(NH_4)_2SO_4$ was added to the sample by eppendorf pipette and the solution stirred for 15 seconds on the vortex stirrer. The Pb-Cr-SO_4 precipitate begins to form.

6. The centrifuge tubes were capped and placed in the centrifuge. The rpms were increased slowly over the first 5 minutes to a speed of 10,000 rpm. The samples were spun at this rate for 10 minutes.

7. The samples were removed from the centrifuge and the solution was removed from the precipitate by a vacuum driven suction device.

8. To the precipitate was added 1.0 ml of concentrated nitric acid, 100μl of 30% hydrogen peroxide, and 100 μl of 0.5 M $Ca(NO_3)_2$.

9. The volume of the sample was then returned to its original 10 ml with double-distilled water and stirred on the vortex stirrer until all of the precipitate was resolubilized.

10. The sample was then analyzed for Cr by AAS. The left over sample from which the initial 10 ml aliquot was taken was analyzed for total Cr (and Mn or any other species) and thus Cr^{3+} was determined by [Cr] total - [Cr^{6+}].

The preparation of blanks and standards was conducted as follows:

1. Two flasks of 100 ml of double-distilled water containing the same background electrolytes as the experimental system were poured into 200 ml glass centrifuge tubes.

2. The pH of each was adjusted to 3.5 with 10% v/v acetic acid.

3. 3 ml of 1.0 M $Pb(NO_3)_2$ was added and the solutions stirred.

4. 5 ml of concentrated acetic acid was added to each followed by stirring.

5. 3 ml of 0.20 M $(NH_4)_2SO_4$ was added and the solutions stirred and then centrifuged at 10,000 rpm for 15 minutes.

6. The solution was removed from the precipitate as described above and then to both was added 10 ml concentrated nitric acid, 1 ml 30% hydrogen peroxide, and 1 ml 0.50 M $Ca(NO_3)_2$.

7. One of these was then returned to the original volume of 100 ml with double-distilled water and stirred until all of the precipitate dissolved. This was the blank matrix for the AAS analysis.

8. To the other was added 5 ml of freshly prepared 10 mg/l Cr standard. The volume was then returned to its original 100 ml with double distilled water. This resulted in a 0.50 mg/l Cr standard.

4.6 Atomic Absorption Spectrophotometry

The samples were analyzed for Cr_T, Cr^{6+}, Mn_T or any other metal parameter by flame atomic absorption spectrophotometry with a Perkin Elmer 560 atomic absorption unit. The flame was an air/acetylene mix. The wavelength used for Cr analysis was 357.9 nm with a slit width of 0.7. For Mn analysis the wavelength was 279.5 nm with a slit width of 0.2.

4.7 Experimental Reproducibility

Several experiments were repeated to determine whether the data were reproducible. This was done over a period of several weeks to avoid the possibility of changing oxide reactivity due to an increase in particle size. Figure 10 shows the results of two identical oxidation experiments performed about two weeks apart. Some of the samples were collected at slightly different time intervals, such that the data points should fall along the same curve. The data show the reproducibility is very good, especially for the measured Cr^{6+}. The amount of solution Mn was slightly higher for one experiment, however the agreement is within analytical error. Comparisons of other experimental data from duplicate experiments, presented in the results section also show good reproducibility.
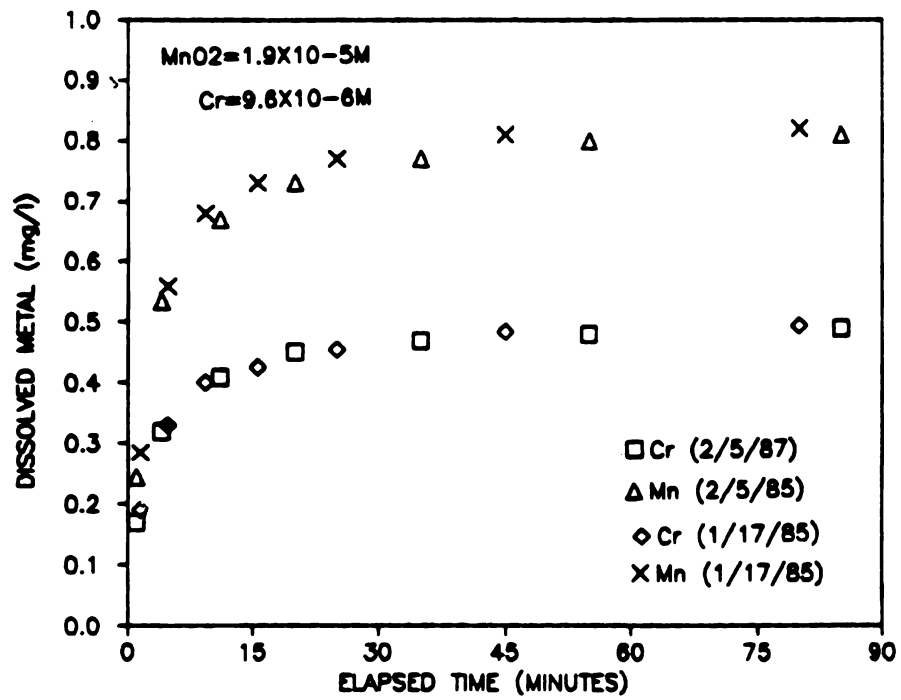
Figure 10. Reproducibility of Oxidation/Reduction
Experiment

RESULTS AND DISCUSSION

In this section of the report, the results of the experiments conducted to investigate reaction between Cr and MnO_2 are presented, discussed and interpreted. The results are presented in three main parts: 1) the general nature, stoichiometry and kinetics of the reaction, 2) the effect of solution chemistry on this reaction, and 3) the competition between Fe and Mn oxides for dissolved Cr. In each part, the results are discussed and interpreted in light of current adsorption theories in an attempt to describe the interaction between Cr and hydrous oxide surfaces in some detail. The experimental data presented on each figure are listed in Appendix II.

PART 1.0 THE OXIDATION OF Cr(III) BY MnO_2

1.1 THE GENERAL NATURE OF THE REACTION

1.10 Introduction

Preliminary experiments were conducted to optimize the experimental parameters so that the reaction between Cr^{3+} and the MnO_2 surface could be most effectively studied with the analytical techniques developed. In particular, these experiments determined the reactant concentrations and solution parameters necessary to obtain reliable rate data and to ensure that all reaction products remained in solution so that reaction stoichiometry could be determined.

Quality control and repeatability analyses were also done at this time. Data from these experiments were used to describe the general reaction characteristics.

The adsorption experiments described in this section of the report were all conducted at pH 4.5 in a solution matrix of 0.10 M $NaNO_3$, in an open to the atmosphere environment at room temperature. At this pH, there was no precipitation of Cr hydroxides and the adsorption of reaction products was minimal. The concentration of reactants was varied, however initial reactant concentrations of 9.6 X 10^{-6} M Cr^{3+} and 1.9 X 10^{-5} M MnO_2 were used as a control, or base-line experiment for describing the reaction, for comparing rates under different solution conditions and for repeatability analyses. Experiments conducted with these reactant concentrations, for convenience, are referred to as the "standard" oxidation experiment in the following text.

1.12 Results and Discussion

The addition of Cr^{3+} to an MnO_2 suspension resulted in visual changes to the system within minutes. The suspension became lighter and took on a yellowish brown tint. Measurement of solution Cr^{6+} and total dissolved Mn typically yielded a pattern of rapid increase of these parameters over the first several minutes, followed by a decreasing rate of increase as these reaction products approached a constant level. For the standard oxidation experiment, the reaction was usually nearly complete within

30 minutes. Total solution Cr_T (i.e. dissolved Cr^{3+} plus Cr^{6+}) remained very nearly constant at the initial concentration of Cr^{3+}, except for a very small depletion at the very beginning of the reaction. A graph of solution Mn, Cr^{6+} and Cr_T versus time for the "standard" oxidation experiment is shown in Figure 11. As shown on the figure, the concentrations of solution Mn and Cr^{6+} increase together as the reaction proceeds and, except for a slight depletion at the beginning of the experiment, Cr_T remains nearly constant throughout the reaction.

The most surprising result of these initial experiments was the high rate and completeness of the reaction, even at this relatively low initial MnO_2 concentration. Under the conditions of the "standard" oxidation experiment, it took only 30 minutes to oxidize more than 90% of the Cr^{3+} in solution, with over half of the Cr oxidized within the first 5 minutes. The initial molar ratio of MnO_2 to Cr^{3+} in this experiment is only about 2 to 1. Based on past research, the adsorption of other trace metals such as Cu, Ni and Zn at pH 4.5 with this metal to oxide ratio ions would be minimal. The quantity of Cr oxidized even at this low MnO_2 loading would seem to indicate that Cr^{3+} has an unusually high affinity for the MnO_2 surface.

When the initial MnO_2 loading was less than the initial Cr^{3+} concentration the reaction proceeded until nearly all of the MnO_2 was depleted, and may have gone to completion if given enough time. Figure 12 shows the results of an
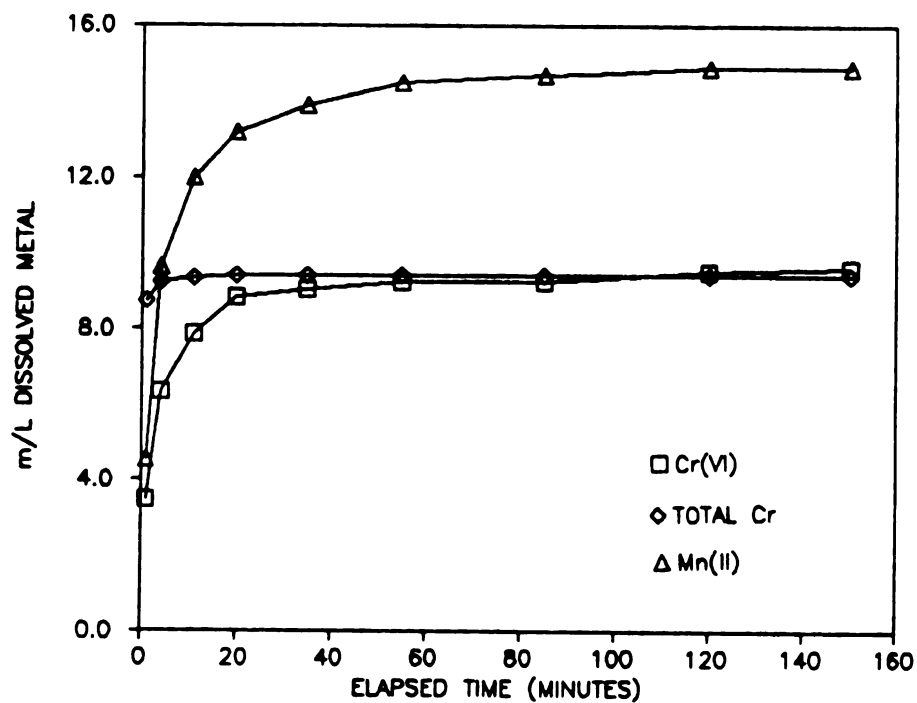
Figure 11.   Oxidation of Cr^{3+} by MnO_2 Under the Conditions
of the Standard Oxidation Experiment
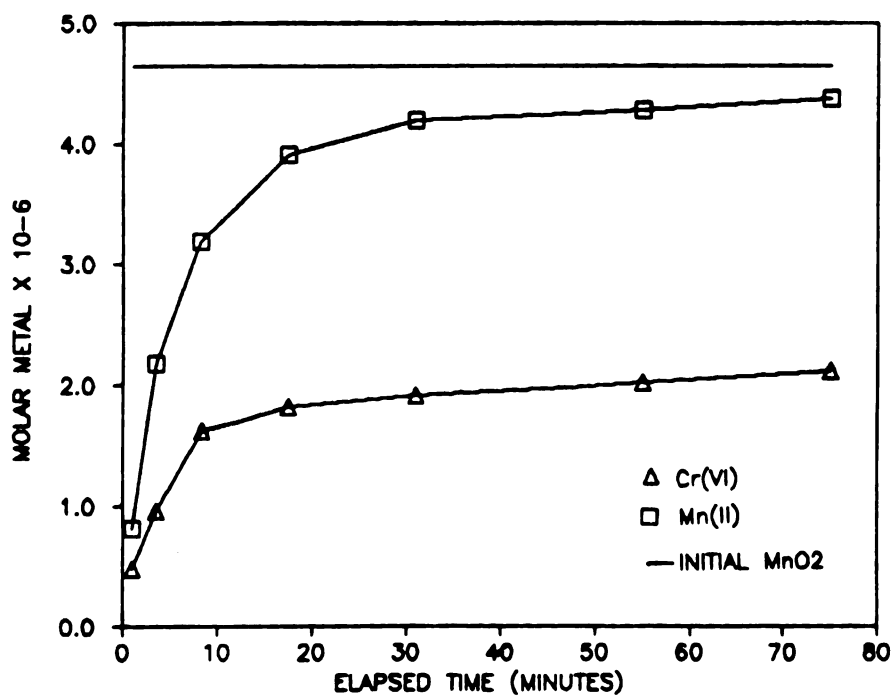
Figure 12.   Oxidation of Cr^{3+} in Molar Excess by MnO_2

experiment with the initial MnO_2 concentration less than the initial Cr^{3+} concentration. After several hours all but a small fraction of the initial MnO_2 was reduced.

In addition to an apparent high affinity of Cr^{3+} for the MnO_2 surface, these results suggest that the oxidation-reduction process cannot be explained with an adsorption model which assumes a fixed quantity of adsorption sites. The reaction is obviously not limited by the adsorption capacity of the initial oxide suspension, which on a molar basis usually represents only a relatively small fraction of initial oxide concentration. Rather, it appears that there are nearly unlimited sites for adsorption of Cr, up to the predicted molar stoichiometric ratio of the reaction. This behavior is not "adsorption-like" in the sense that similar concentrations of other trace metals would not even adsorb to any significant extent under these conditions.

Based on these initial observations, two working hypotheses were formulated at this point. The first was that the redox reaction is not adsorption controlled, at least in the sense of the formation of covelant bonds between the oxide surface and Cr^{3+}. Possibly, the Cr ion need only to enter the electrical double layer (EDL) of the oxide, with oxidation taking place without direct coordination with surface oxygens. In this case the interaction between Cr^{3+} and oxidized Mn would exhibit characteristics of a solute-solute type interaction. This could explain the oxidation of Cr under conditions where

adsorption reactions should not occur. The second working hypothesis was that the reaction is adsorption controlled, with the reaction driven by a high affinity of Cr^{3+} for surface sites on MnO_2, and that the oxidation-reduction reaction is autocatalytic, generating new surface sites for adsorption as the reaction proceeds. The idea of autocatalysis is suggested because the reduction of Mn^{4+} to Mn^{2+}, which would be unstable in the MnO_6 octahedron, must cause partial dissolution of the MnO_2 structure. As the MnO_2 particulates dissolve it is feasible that new surface sites are created. If it is assumed that the reduction and desorption of an Mn ion produces one new surface site, the total number of surface sites would not begin to decrease until the reduction and release of Mn to solution no longer produced a new site (or sites). This would probably occur only as the MnO_2 particles reached a critical size or dissolved completely. It would also be possible for the oxidation-reduction reaction to cause an increase in the surface area of the remaining oxide or to otherwise influence its reactivity. In other words, as the concentration of the oxide decreases it is possible that the specific surface area (and number of surface sites) of the remaining oxide may remain constant or even increase. The results of subsequent experimentation were used to test these working hypotheses.

Even if adsorption is a required reaction step, the constant concentration of Cr_T in solution shows that Cr^{3+} is

not removed from solution for very long before it is oxidized and returned to solution. As described above, only a small depletion of total solution Cr is measured at the very beginning of the reaction (see Figure 11). This depletion (4-8% of an initial 0.50 mg/l) however, was seen in all standard experiments and, although barely outside of the expected analytical variation, does appear to be real. If this depletion is real, it may indicate that Cr^{3+} is removed from solution (adsorbed) for a very short time prior to oxidation. As there is no evidence for the adsorption of Cr by MnO_2 without consequent oxidation, the rate of oxidation appears to be dependent on the ability of Cr to come in contact with the oxidizing agent.

As demonstrated on Figure 11, the kinetics of the reaction are somewhat parabolic, with the initial rate nearly linear and the rate quickly slowing down with time. Since the Cr^{3+} does not adsorb without being oxidized, the decreasing reaction rate must reflect an increasing amount of time necessary for the remaining Cr^{3+} in solution to come in contact with the oxidizing agent. Experimentally induced parabolic kinetics in heterophase reactions have been caused by grinding up the solid phase to decrease the grain size. Unless pre-treated, solids prepared in this manner may contain fine particles which are highly reactive as compared to the bulk solid (Holdren and Berner, 1979). Although this particular situation is not applicable to the present research, it is possible that the fast part of the reaction

between Cr^{3+} and MnO_2 occurs with small, highly reactive MnO_2 particulates (high surface area) and the slower part occurs with the remaining larger particulates which have lower surface area. Without a study of grain size distribution this possibility can not be evaluated.

The decreasing reaction rate with time could also be caused by several properties of adsorption reactions. The sorbent/sorbate ratio is continuously decreasing during the reaction, as three moles of MnO_2 are dissolved for every two moles of Cr oxidized (see next section). This decreasing ratio may cause a lower fractional adsorption over time thus reducing the oxidation rate. If the reaction is adsorption controlled the reaction rate would also decrease as the particulates become very small or dissolve, as the rate of production of new sites would not be proportional to amount of Mn dissolved. In this case there would simply be less adsorption sites as the reaction proceeds.

The kinetics of adsorption reactions on hydrous oxides typically exhibit a very rapid uptake of the metal ion, followed by a period of very slow uptake. This slow part of the reaction is thought to be due to the diffusion of the metal ions to binding sites within the oxide structure. However, if the oxidation reaction is generating new sites on the oxide surface, it seems unlikely that diffusion would become rate limiting.

1.2 THE STOICHIOMETRY OF THE REACTION

1.21 Introduction

The general hypothesized reaction between Cr^{3+} and MnO_2 is given by the equation:

$$3MnO_2 + 2Cr^{3+} + 12H^+ = 3Mn^{2+} + 2Cr^{6+} + 6H_2O$$
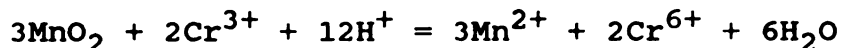
At pH 4.5 the predominant Cr species are $Cr(OH)^{2+}$ and $HCrO_4^-$ (Leckie et al., 1983). Using these species and the unhydrolyzed Mn^{2+} ion would result in a reaction that is proton neutral:

$$3MnO_2 + 2Cr(OH)^{2+} = 3Mn^{2+} + 2HCrO_4^-$$
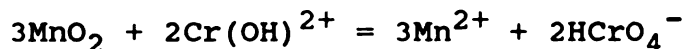
From this reaction the predicted ratio of products would be 3:2 Mn^{2+} to Cr^{6+} with no change in pH. This does not include the stoichiometry of any adsorption reactions in terms of balancing the hydrogen ions.

The stoichiometry of the reaction was evaluated by calculating the molar ratio of total dissolved Mn to Cr^{6+} from the experimental data. Thus Mn/Cr^{6+} could be plotted over time for each experiment. The experimental conditions were designed to assure that re-adsorption of products did not affect the stoichiometry, at least after the reaction had neared completion (see below). The value of total dissolved Mn represents the Mn that passed through the $0.22\mu m$ filter. It is assumed that this is primarily dissolved Mn^{2+} as filtration studies (see Methods) showed

that only very small amounts of MnO_2 pass through the filters, and other oxidation states of Mn are unstable in water as free ions (Hem, 1978).

1.22 Results and Discussion

The measured molar Mn/Cr^{6+} values, in general, confirm the predicted stoichiometry. Although there was some variation, most of the experimental data exhibit the pattern of Mn/Cr^{6+} ratios with time shown in Figure 13. The ratio in the first several minutes of the reaction (when the reaction is fastest) was typically well below the predicted ratio. The ratio then quickly increased to a value very near the predicted 1.5. By the time the reaction was essentially complete, the Mn/Cr^{6+} ratio was almost always between 1.5 and 1.6. This would appear to confirm that the surface Mn^{4+} is reduced to Mn^{2+} during the oxidation of Cr, rather than to Mn^{3+} as was shown to occur during the oxidation of Co^{2+} by MnO_2 (Crowther et al., 1983). Reduction to Mn^{3+} might result in the disproportionation to Mn^{2+} and MnO_2, however this would not produce the present Mn/Cr ratio unless exactly one half of the Mn^{3+} became Mn^{2+}. This does not fit the stoichiometry of the probable disproportionation reactions described by Hem (1978). However, this possibility can not be entirely ruled out based on the data from this study.

Assuming the hypothesized reaction stoichiometry is indeed correct, the possible causes for deviation of the
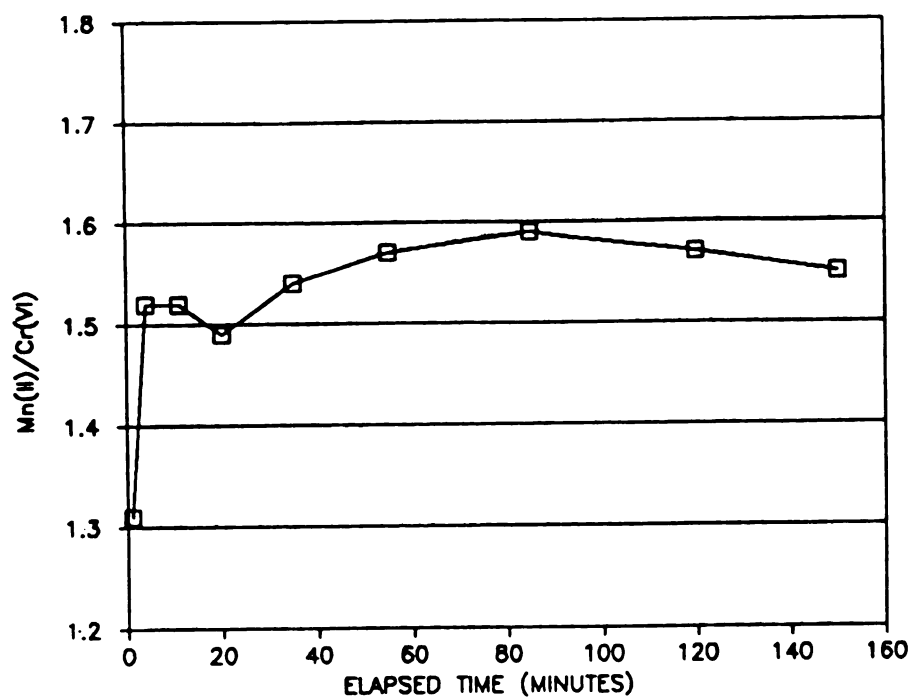
Figure 13. Stoichiometric Ratio of Reaction Products

Mn/Cr ratio from the predicted 1.5 include; 1) analytical error, 2) adsorption of reaction products, 3) different rates of release to solution of the reaction products, 4) desorption of any adsorbed Mn^{2+} (residual from oxide preparation) upon the adsorption of Cr^{3+} or dissolution of the oxide structure, and 5) an average oxidation state of Mn in the oxide of less than or greater than four (i.e. the presence of Mn^{3+}, etc.).

The reason for the low Mn/Cr ratio at the beginning of the reaction is not clear. The analytical data from this part of the experiment has a large relative error due to the low levels of both Cr and Mn. However it seems unlikely that the error would be systematic, always resulting in a low ratio. If the low ratios in the early part of the reaction are not caused by analytical procedures, they could be caused either by adsorption of the Mn produced, or by the slow release (as compared to Cr^{6+}) of Mn to solution.

If adsorption of Mn^{2+} does occur in the early stages of the reaction, it may become desorbed as the sorbent/sorbate ratio decreases as the reaction proceeds. This would explain the increase of the ratio with time. To address this possibility, experiments were conducted to determine the extent of Mn^{2+} adsorption at MnO_2 and Mn^{2+} concentrations similar to those encountered over time during the "standard" oxidation experiment. In these experiments, the concentrations of solution Mn and MnO_2 were chosen to represent the quantities that should be present in the
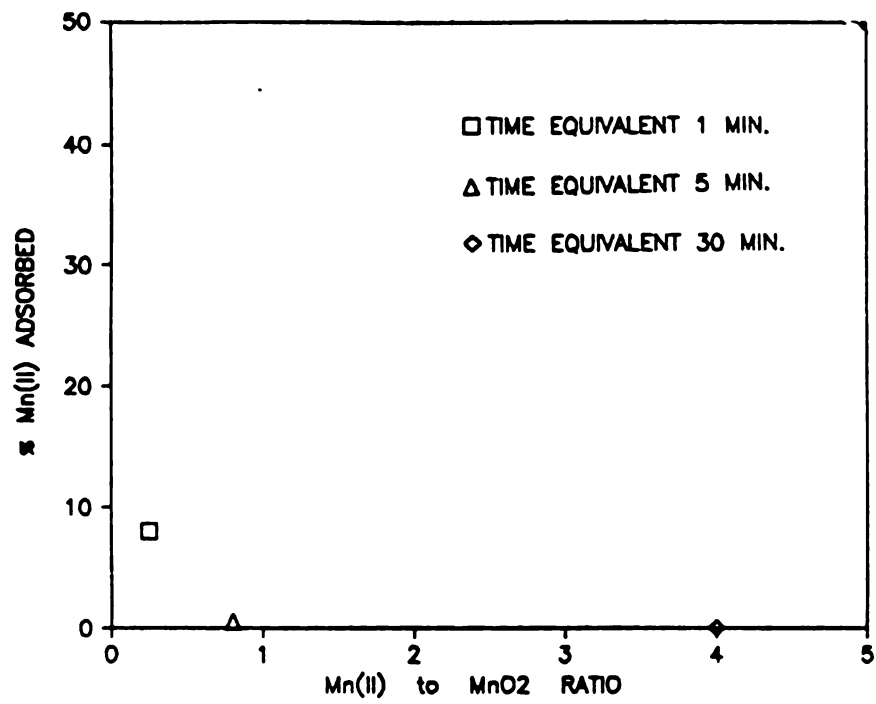
Figure 14. Adsorption of Mn^{2+} by MnO_2 at Selected
Metal/Oxide Ratios

system during the standard oxidation experiment at time intervals 1.0, 5.0, and 30.0 minutes, respectively, based on the amount of Cr that was oxidized. The amount of Mn adsorbed was determined from the amount deleted from solution after 5 minutes. The results are shown on Figure 14. The results indicate that adsorption only occurs at the conditions found very early in the reaction. This small percentage of adsorption could contribute to the low Mn/Cr^{6+} ratios seen early in the oxidation experiments, but is does not appear to be a satisfactory explanation by itself. The experiments show that by the end of the experiment there should be no measurable adsorption of Mn^{2+}, suggesting the final stoichiometric ratio is accurate.

As re-adsorption of solution Mn does not appear to be significant, differential desorption kinetics could be the reason the low Mn/Cr^{6+} ratios. The initial deviation and subsequent adjustment of the Mn/Cr ratio to the predicted stoichiometric value during the reaction could be explained if Cr^{6+} is released to solution faster than Mn^{2+}. During the fast part of the reaction the difference would result in a significant deviation in the ratio. As the reaction slows down and nears completion the Mn^{2+} in solution would have a chance to "catch up" to its stoichiometric equivalent of Cr^{6+}. The unfavorable nature of the MnO_2 surface for Cr^{6+} adsorption (see Appendix I) would likely cause rapid desorption of this species. It does not seem unreasonable that this may be faster than the dissolution of the MnO_2

structure and release of Mn^{2+} to solution following reduction. The surface charge, at least, would be favorable for the attraction of the positively charged Mn^{2+} ions. If the formation of new surface sites for Cr^{3+} adsorption is a required reaction step, the dissolution and release of Mn to solution may be the rate limiting step in the reaction.

As shown on Figure 13, the Mn/Cr^{6+} ratio when the reaction is complete is slightly above the predicted ratio of 1.50 (1.51-1.59). Possible explanations for this include; 1) the average oxidation state of structural Mn in the oxide may be less than 4.0, and some oxidation of Cr by Mn^{3+} may take place, and 2) the total solution Mn may include small amounts of Mn not produced by the REDOX reaction. Based on the iodometric titration the average oxidation state of the Mn in the stock suspension is about 3.9. The predicted reaction stoichiometry, assuming both Mn^{3+} and Mn^{4+} oxidize Cr in proportion to their respective mole fractions, would result in a Mn/Cr^{6+} ratio of 1.54. Thus the experimentally determined ratio may be reflecting the actual reaction stoichiometry. It is also possible that some particulate MnO_2 and/or residual Mn^{2+} released upon oxide dissolution may be included in the total dissolved Mn analysis. The particle size decreases during the reaction which may cause some MnO_2 to pass through the filter. This probably causes some of the variation in the data. Despite these minor variations in the reaction product stoichiometry

with time, the experimental results confirm the predicted reaction stoichiometry, as least with respect to Cr and Mn.

As described earlier, the specific reaction predicted to occur at pH 4.5 is balanced with respect to protons. The change in the proton concentration during the reaction, as measured by a pH electrode, was not adequate to confirm this prediction. The experiments were conducted either open to the atmosphere or in an N_2 purged system. However no measures were taken to ensure the absence of CO_2 species in the system. Without using CO_2 free reagents, an accurate measurement of proton consumption or generation can not be obtained. The pH was monitored in both open air and N_2 systems to measure any pH changes which occurred throughout the reaction so that a qualitative assessment of the role protons in the reaction could be made. The "standard" oxidation experiment could not be used for this purpose, because the addition of the Cr^{3+} aliquot results in a small pH drop (0.1 to 0.2 units) from the acidified Cr^{3+} stock solution. To avoid this problem, several experiments were conducted in which the aliquot of MnO_2 stock suspension was added to the Cr^{3+} solution with the pH pre-set at 4.5. Experiments done in this reverse order did not show any appreciable change in pH upon addition of the MnO_2 or as the reaction proceeded. This would seem to support the hypothesis of a proton neutral reaction at pH 4.5, however this conclusion is tenuous because of the potential buffer effect of the CO_2 system.

1.3 THE EFFECT OF CHANGING REACTANT CONCENTRATIONS

1.31 Introduction

The effect on the reaction rate of sorbent/sorbate ratios was studied by holding either the initial Cr^{3+} or MnO_2 concentration constant, and then varying the other parameter. This was done in systems where 1) the molar concentrations of both reactants was similar, and 2) where one reactant was in a large excess (essentially constant). Most of the data from 2) is presented in the section on reaction kinetics. The purpose of this section is to explore qualitatively, the effects on the oxidation rate of varying either the sorbent (MnO_2) or the sorbate (Cr^{3+}). From this data, the implications with respect to the nature of the reaction were evaluated.

1.32 Results and Discussion

The effect of the MnO_2 loading, when the concentrations of reactants are similar, on the oxidation of 9.6×10^{-6} M (0.50 mg/l) Cr^{3+} is shown on Figure 15. The amount (rate) of Cr oxidized increases as the initial MnO_2 concentration is increased from 4.6×10^{-6} to 2.9×10^{-4} M. This result is confirmed from the measurements of Mn in solution as the reaction proceeds, shown on Figure 16. The dissolved Mn data for the highest MnO_2 loading was not included on this figure because significant adsorption of released Mn^{2+}
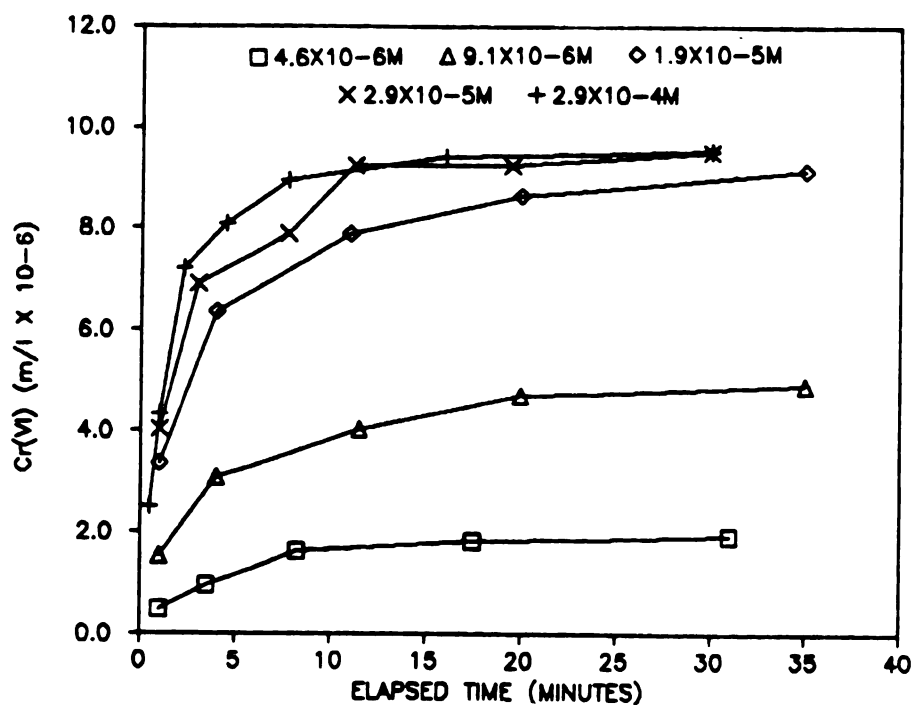
Figure 15.   Effect of MnO$_2$ Loading on Cr Oxidation Rate
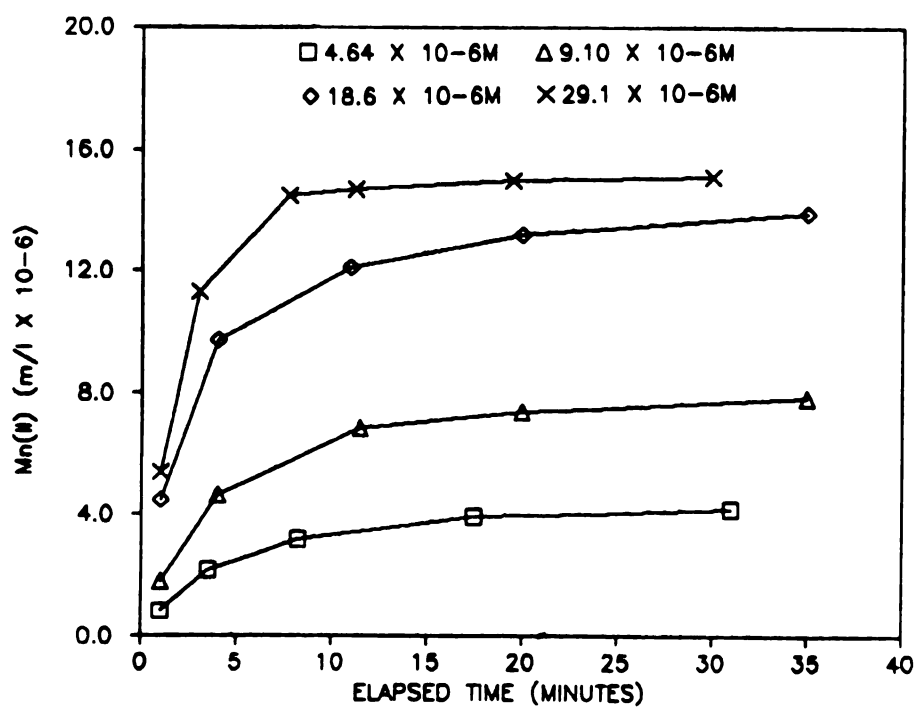
Figure 16.   Effect of MnO$_2$ Loading on MnO$_2$ Dissolution Rate

occurs at this loading. The rate of the oxidation-reduction reaction increases nearly proportionally to MnO_2 loading until the MnO_2 loading exceeds 1.9×10^{-5} M beyond which a further increase in the MnO_2 loading results in a smaller increase in the reaction rate. This relationship is more clearly illustrated in Figures 17 and 18. These graphs show the amount of Cr oxidized and Mn reduced, respectively, at the 1.0 and 4.0 minute time intervals (i.e. the fast part of the reaction) for the various MnO_2 loadings. The graphs show that the amount of Cr oxidized, or Mn reduced, is linearly dependent on the MnO_2 loading up until the initial MnO_2 loading is about 1.9×10^{-5} M, at which time the molar MnO_2 to Cr^{3+} ratio is about 2. Increasing the initial oxide loading further results in an increase in the initial oxidation rate that is not proportional to the increased loading. As shown on Figure 17, after this MnO_2 to Cr^{3+} ratio is attained, an order of magnitude increase in MnO_2 loading results in only a small increase in the amount of Cr oxidized at either time interval.

The distinct change in the linear relationship between reaction rate and MnO_2 is not "solution-like" reaction behavior and provides evidence that the reaction is adsorption controlled. The linear rate dependence at low MnO_2 loadings (below $MnO_2/Cr^{3+} = 2$) suggests the reaction rate in this region is limited by the initially available surface area (and hence the concentration of surface sites). The break in this linear behavior for MnO_2:Cr^{3+} ratios
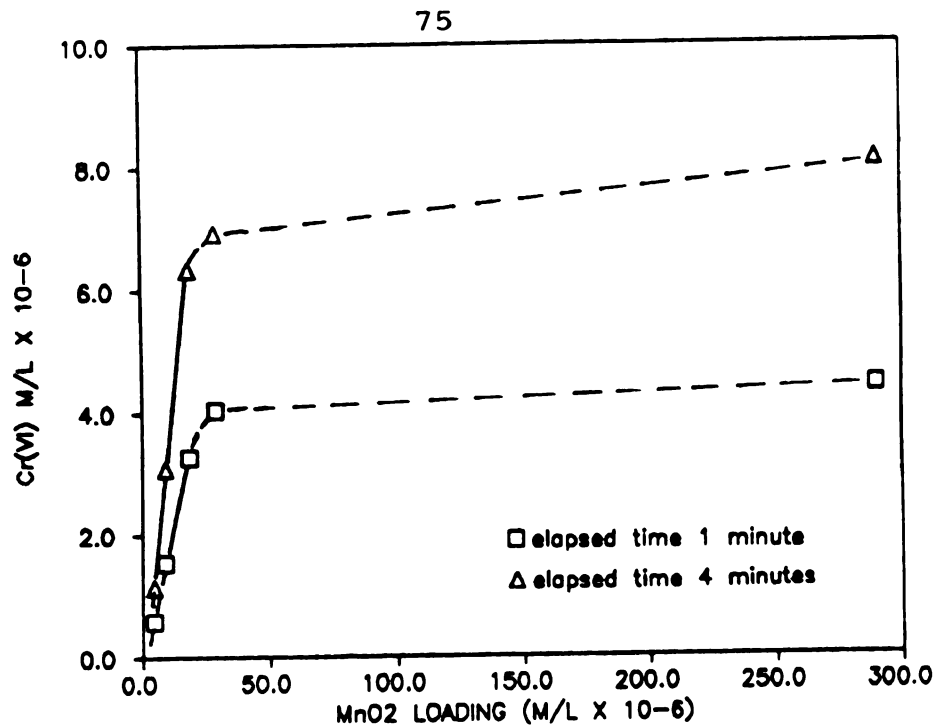
Figure 17. Amount of Cr Oxidized at 1 and 4 Minutes as a Function of MnO_2 Loading
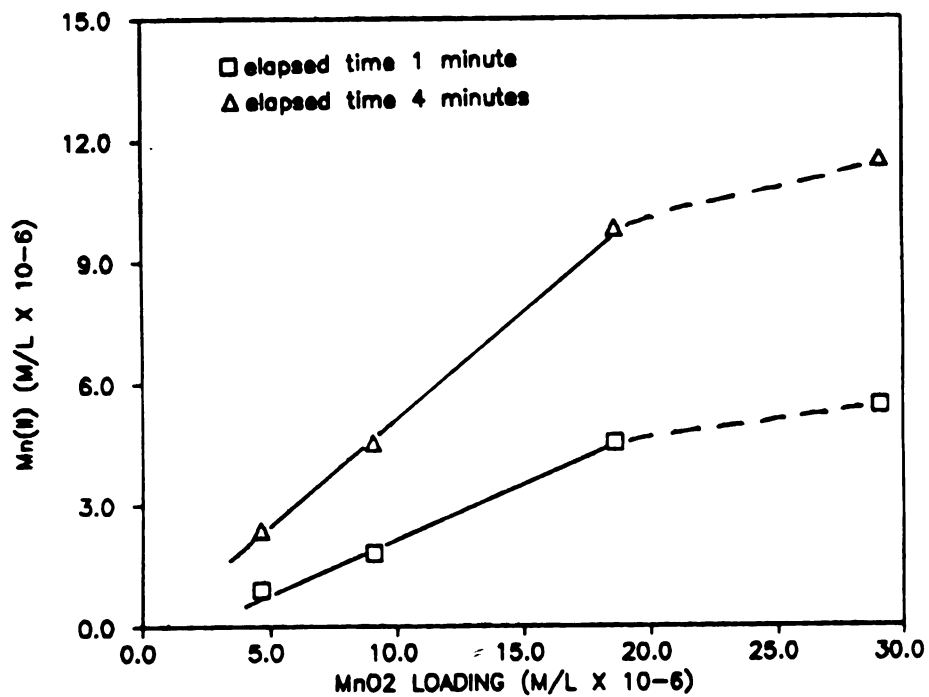
Figure 18. Amount of MnO_2 Reduced at 1 and 4 Minutes as a Function of MnO_2 Loading

greater than two suggests that there may be a relationship to the initial binding capacity of the MnO_2 for Cr. By assuming the reaction is adsorption controlled, the following explanation is proposed. Below the critical oxide loading there are insufficient sites for the adsorption of Cr, at that particular pH. So increasing the oxide loading in this range causes an increase in adsorption (and thus oxidation rate) proportional with the increase in binding sites. As the oxide loading is increased, there reaches a point where the fraction of initial Cr^{3+} which can be adsorbed at pH 4.5 becomes a maximum. Increasing the MnO_2 loading beyond this point would then result in very little increased oxidation, as there is already enough oxide to adsorb the maximum amount of Cr at this pH. Therefore, even large increases in the MnO_2 loading will result in very little change in the oxidation rate.

There are some difficulties with this interpretation. A molar MnO_2 to Cr^{3+} ratio of 2.0 as the condition necessary for maximum fractional adsorption would suggest that the binding capacity of MnO_2 for Cr^{3+} at pH 4.5 is much greater than for other trace metals. However, the kinetics of adsorption, which may be slow as compared to the oxidation reaction, and the formation of new oxidation sites during the reaction may be complicating the actual relationship between the original binding capacity of the oxide suspension and the rate of the oxidation reaction. In other words, the quantitative relationship between maximum

fractional adsorption and the initial oxidation rate is not clear. It is clear however, that the rate dependence is very responsive to the amount of MnO_2 present, and that this rate dependence changes greatly at a critical value, the latter at least suggests the reaction is adsorption controlled.

The experiments described above were conducted with a constant initial Cr^{3+} concentration with the MnO_2 loading varied. Experiments were also conducted to explore the effects of varying the initial Cr^{3+} concentrations, both with MnO_2 in excess and with both reactants in similar concentrations.

The effect of the initial Cr^{3+} loading on the oxidation rate, in the presence of excess MnO_2, is shown on Figure 19. The data demonstrate that rate of oxidation increases with increasing Cr loading. Figure 20 shows a graph of the amount of Cr oxidized in 30 seconds versus initial Cr. There is a linear trend between the Cr loading and the initial oxidation rate. With excess MnO_2, the fraction of adsorption remains at a maximum so the addition of more Cr^{3+} results in an equivalent increase in the amount adsorbed.

When the surface sites are not in great excess, the rate dependence on Cr loading shows a more complicated relationship. Using an initial MnO_2 concentration of 9.1×10^{-6} M, experiments were conducted in which the Cr concentration was varied from 3.8 to 11.5×10^{-6} M. The results are shown on Figures 21 and 22 for the Cr oxidized
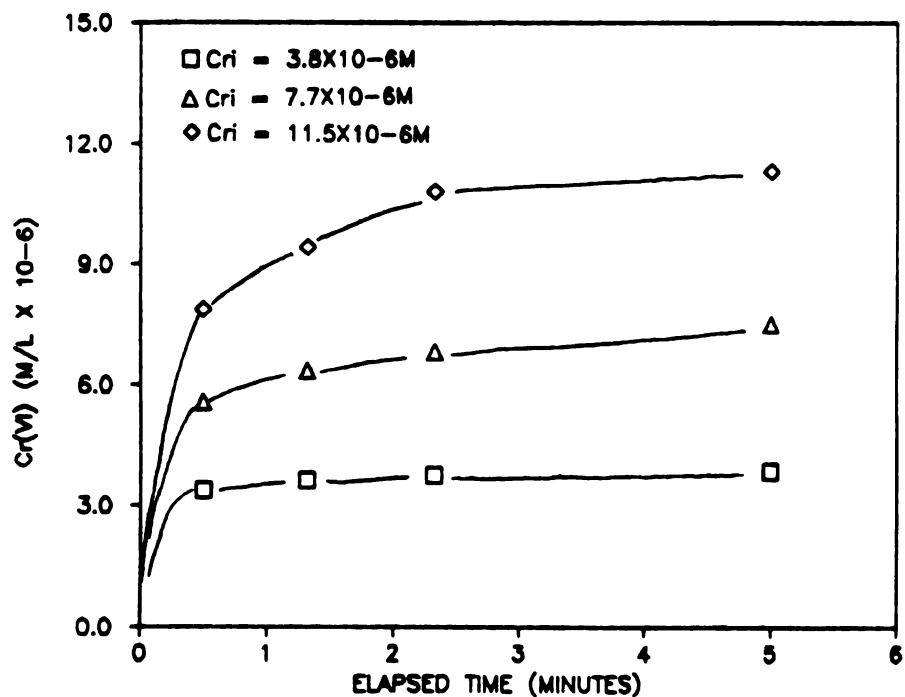
Figure 19. Effect of Cr^{3+} Loading on Cr Oxidation Rate with MnO_2 in Excess
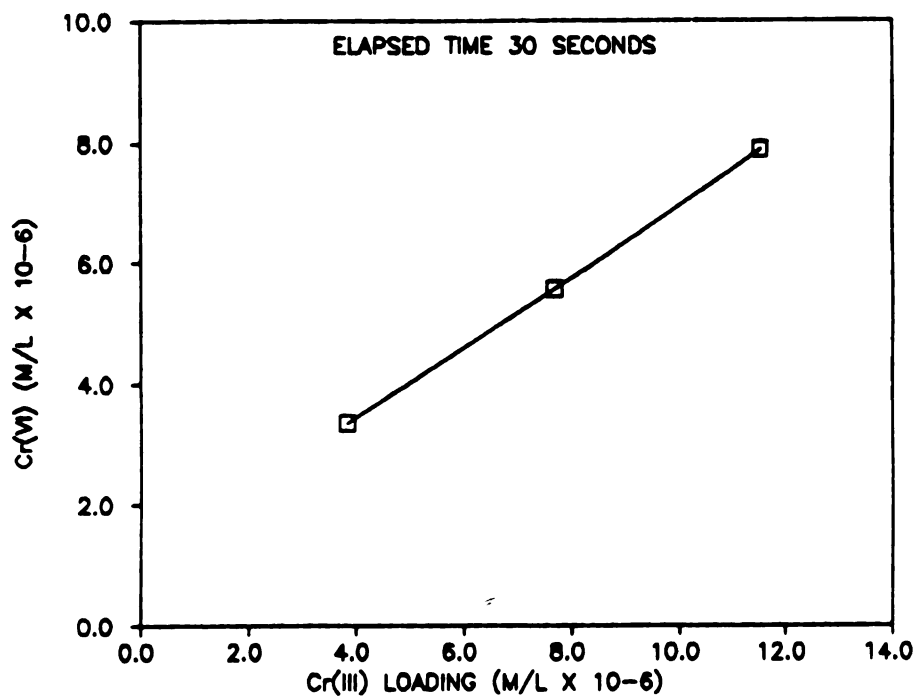
Figure 20. Amount of Cr Oxidized in 30 Seconds as a Function of Cr^{3+} Loading with MnO_2 in Excess
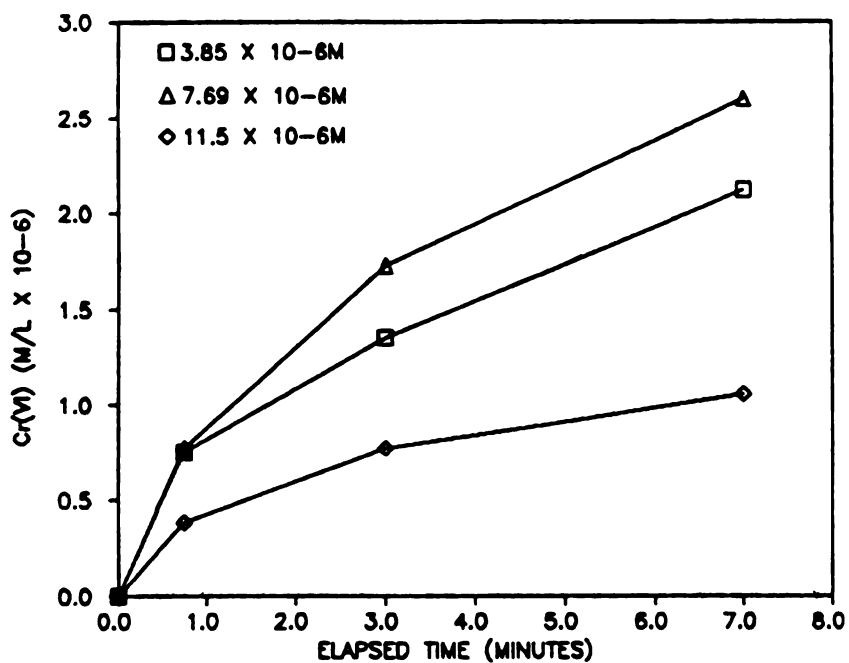
Figure 21.   Effect of Cr^{3+} Loading on Cr Oxidation Rate with Similar Reactant Concentrations
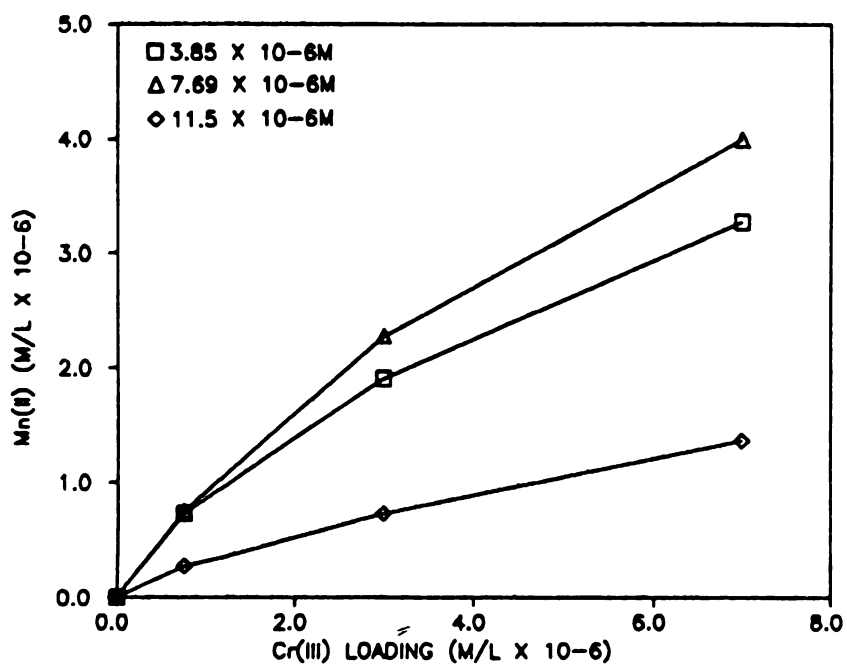
Figure 22.   Effect of Cr^{3+} Loading on MnO$_2$ Dissolution Rate with Similar Reactant Concentrations

and MnO_2 reduced, respectively. Increasing the Cr loading from 3.8 to 7.7 X 10^{-6} M resulted in a small increase in the oxidation rate, although the amount oxidized within the first minute was almost identical. A further increase in the Cr loading to 12.0 X 10^{-6} M resulted in a significant decrease in the oxidation rate.

This decrease in reaction rate with an increase in one of the reactants is in certainly in direct contrast to solute-solute reactions as increasing one of the reactants would drive the reaction forward. The only apparent explanation for this type of behavior is that the reaction is adsorption controlled. At a given pH, the amount of adsorption (fractional adsorption) is controlled by the sorbent/sorbate ratio. As this ratio decreases the fractional adsorption at this pH will decrease (i.e. the adsorption edge shifts to a higher pH), even though the concentration of one of the reactants has increased. This relationship may explain the decreasing rate of oxidation with the decrease in the sorbent/sorbate ratio.

1.4 KINETIC CONSIDERATIONS

1.41 Introduction

It is clear from the preceding discussions that the oxidation-reduction reaction between Cr^{3+} and MnO_2 is not easily described by adsorption theory. Because of the apparent autocatalytic nature of this reaction a

thermodynamic description is not entirely adequate. To attempt to gain further insight into this reaction, a kinetic analysis of some of the rate data was conducted.

1.42 Methods

From the general stoichiometry of the reaction and the irreversible nature of the reaction, the experimental rate law can be written as follows:

(1) $d[MnO_2]/dt = \frac{2}{3}d[Cr^{3+}]/dt = -k[MnO_2]^a[Cr^{3+}]^b$

where; $[MnO_2]$ is the concentration of MnO_2
        $[Cr^{3+}]$ is the concentration of Cr^{3+}
        k is the rate constant
        a,b are exponents reflecting the reaction
                  order of MnO_2 and Cr^{3+}, respectively

An attempt was made to determine k, a and b. The reaction order with respect to MnO_2 (a) was determined by the method of initial rates (Gardiner, 1972). This method requires that all but one reactant remain essentially constant during the reaction so that the initial rate of change of this reactant can be used to determine its reaction order. To determine the reaction order with respect to MnO_2, experiments were conducted in which the initial Cr^{3+} concentrations were in large molar excess to the MnO_2 concentrations. Thus the Cr^{3+} concentration remained essentially constant during the reaction while the MnO_2 was reduced. In this case, the rate law in terms of the dissolution of the MnO_2 can be represented as:

$$(2) \quad d[Mn^{2+}]/dt = -k[MnO_2]_t{}^a$$

where: $[Mn^{2+}]$ is the amount of oxide dissolved
$[MnO_2]_t$ is amount of MnO_2 remaining
at any time, t

The dissolution of MnO_2 was measured in a set of experiments containing 9.6×10^{-5} M Cr^{3+} where the initial MnO_2 concentration was varied from 4.8×10^{-6} to 1.4×10^{-5} M. From this data, the initial rate of the dissolution reaction was determined. The initial rate was estimated by two different methods to ensure accuracy. The first method was to plot the curve of Mn^{2+} measured versus the elapsed time of the reaction and then determine the slope of the line drawn through the linear portion of the reaction. In most cases the first three data points yielded a roughly linear relationship. The data used for determining the initial rates and the calculations of the slope (via linear regression) are shown on pages 224 to 227 in Appendix III.

The second method of estimating the initial rate of dissolution with this data set was to fit a curve to the dissolution versus time data and then to take the 1st derivative of the equation for the curve at time zero. Curve fitting was conducted with the computer program STATGRAPHICS, 1985. Several curve fitting equations were tried but the data were best fit with the formula:

$$(3) \quad [Mn^{2+}] = A - B * EXP(-C * time)$$

The plots of the fitted curves with correlation coefficients, the values of the curve equation coefficients

and the first derivatives at time zero are presented in Appendix III, pages 228 to 233.

The order of the reaction with respect to MnO_2 was determined from these initial rates from the slope of the best-fit line through the plot of the log of the initial rate versus the log of the initial MnO_2 loading. These plots and the regression calculations are presented in Appendix III on pages 234 and 235, for the two methods of determining the initial rates respectively.

The experimental rate constant, k_{ex}, was also determined from the experimental data above, with Cr^{3+} present in excess. This data set will be referred to as data set A in subsequent discussions. Additionally, two other sets of experiments were conducted with Cr^{3+} present in excess. One contained 9.6×10^{-5} M, identical to the experiments described above, the other contained twice as much Cr^{3+}, or 1.9×10^{-4} M. The initial MnO_2 loadings were varied from 4.7×10^{-6} M to 5.0×10^{-5} M in both sets of experiments. These data sets will be referred to as data sets B and C respectively. The reaction order with respect to MnO_2 was also determined for these data sets (via the curve fitting method). The fitted curves and calculations are presented in Appendix III, pages 236 to 241 and 242 to 247, respectively.

The rate constant was determined by the method used by Stone and Morgan (1984) from the integrated form of the rate law. The amount of MnO_2 remaining at any time t ($[MnO_2]_t$),

is simply the initial oxide loading less the amount of Mn^{2+} in solution as the result of reduction, or:

$$(4) \quad [MnO_2]_t = [MnO_2]_i - [Mn^{2+}]$$

Substituting for $[MnO_2]_t$ in the rate law presented in equation (2) and integrating yields the equation:

$$(5) \quad \ln([MnO_2]_i - [Mn^{2+}]) - \ln[MnO_2]_i = -kt$$

If this equation is valid, then a graph of $\ln([MnO_2]_i \quad [Mn^{2+}]) - [MnO_2]_i$ versus time should result in a straight line with a slope equal to the experimental rate constant, k_{ex}. The graphs for all three sets of experimental data are presented in Appendix III, pages 248-250.

The reaction order with respect to Cr^{3+} was more difficult to address. An attempt was made to employ the initial rates approach by conducting experiments with MnO_2 in large excess in order to maintain a constant MnO_2 concentration. Because it must actually be the number of surface sites that are constant, a very large molar excess of MnO_2 is required to use this technique. Under these conditions, the oxidation reaction proceeded too quickly to obtain enough data to determine the initial rate. Because of this result this approach was abandoned.

The reaction order with respect to Cr^{3+} was evaluated using a method similar to that presented in Stone and Morgan (1984), which was a study of the reduction of Mn oxide by the organic molecule hydroquinone. These investigators

determined the reaction order with respect to hydroquinone, which was present in excess in their experiments, by determining the effect on the experimental rate constant of varying the amount of excess hydroquinone. The reaction order with respect to hydroquinone was then determined from the slope of a plot of the log of the rate constant versus the log of the hydroquinone loading.

The reaction order with respect to Cr^{3+} was determined by the change in the log of k_{ex}, divided by the log of the change in the Cr^{3+} loading, using the data from data sets B and C described above.

1.43 Results

The calculated reaction orders with respect to MnO_2 in the presence of excess Cr^{3+} are shown on Table 1. All of the slopes were very close to 1.0 indicating that the reaction is 1st order with respect to MnO_2. The reaction orders determined from data set A, 1.03 and 1.08, show that both methods chosen to determine the initial reaction rate were adequate. A first order rate dependence with respect to the adsorbing substrate has been observed in other investigations of multi-phase oxidation-reduction reactions (Stone and Morgan, 1984; Postma, 1985). This result is expected for simple adsorption controlled reactions as the amount of adsorption is directly proportional to the surface area of the sorbent in the system.

TABLE 1

REACTION ORDER WITH RESPECT TO MnO$_2$

Data Set	[Cr^{3+}]	Range of MnO$_2$ Loading (M)	Reaction Order		Method of Initial Rate Determination
			Slope	r^2	
A	9.6×10^{-5}	4.8×10^{-6} to 1.5×10^{-5}	1.03	0.963	slope of first 3 data points
A	9.6×10^{-5}	4.8×10^{-6} to 1.5×10^{-5}	1.08	0.967	1st derivative of fitted curve
B	9.6×10^{-5}	4.7×10^{-6} to 5.0×10^{-5}	0.90	0.998	1st derivative of fitted curve
C	1.9×10^{-4}	4.7×10^{-6} to 5.0×10^{-5}	0.99	0.996	1st derivative of fitted curve

TABLE 2

EXPERIMENTAL RATE CONSTANTS

Data Set	[Cr^{3+}]	Range of k_{ex}	Average k_{ex}
A	9.6×10^{-5}	0.141-0.195	0.166
B	9.6×10^{-5}	0.143-0.173	0.159
C	1.9×10^{-4}	0.075-0.134	0.111

The plots of $\ln([MnO_2]_i - [Mn^{2+}]) - \ln[MnO_2]$ versus time were only linear for about the first half of the reaction. Thus the experimental rate constant, k_{ex}, was determined from this part of the reaction. A typical plot of this type is shown on Figure 23. The value of k_{ex} was determined from a linear regression of the first part of the reaction as depicted on the Figure. This calculation was conducted for data sets A, B and C. The average value and range of values for k_{ex} determined from each data set are summarized on Table 2. The plotted data and regression calculations are presented in Appendix III, pages 251 to 263. The non-linear behavior exhibited by the data after the reaction had proceeded demonstrates that the rate law is not valid after considerable dissolution of the oxide had taken place. Interestingly, Stone and Morgan (1984) reported very similar results for the reduction of Mn oxide by hydroquinone. It is likely that this result is caused by a change in the surface properties of the Mn oxide after significant dissolution has taken place.

The reaction order with respect to Cr^{3+} was computed by the equation:

$$\text{Reaction Order} = \frac{(\text{change in log } k_{ex})}{(\text{change in log Cr loading})}$$

The values of k_{ex} for the 9.6×10^{-5} M and 1.9×10^{-4} M Cr^{3+} loadings were 0.159 and 0.111, respectively. These result in a reaction order of 0.5 with respect to Cr^{3+}. A reaction order less than 1.0 was also found in the study by Stone and
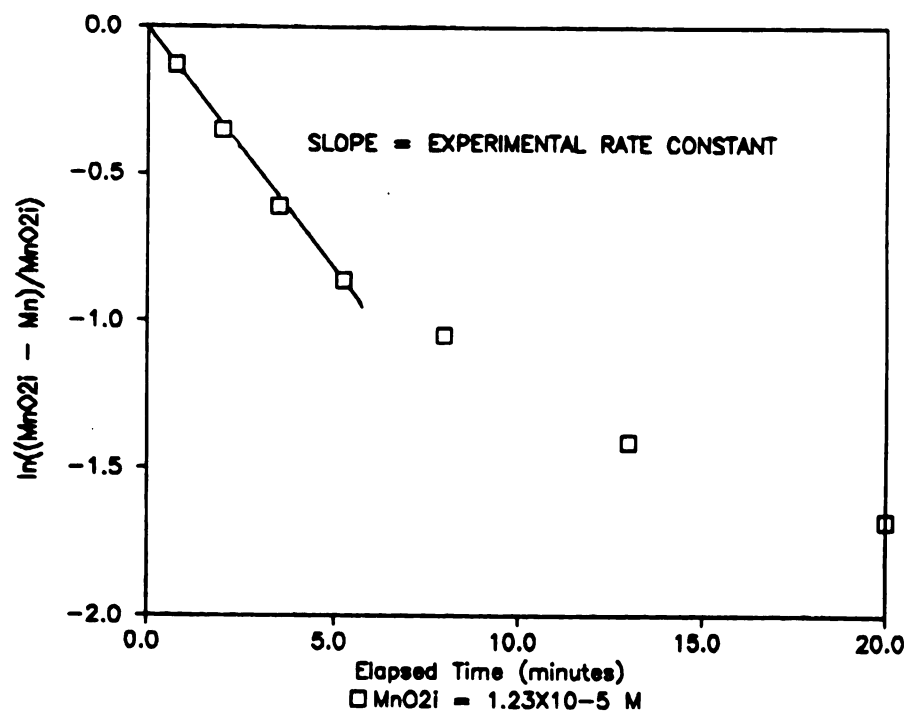
Figure 23. Typical Plot for Determination of Experimental
Rate Constant

Morgan (1984) for systems with hydroquinone in large excess. Based on these results, the experimental rate law for the reduction of MnO_2 by the oxidation of Cr^{3+}, with Cr^{3+} present in large excess, can be written as follows:

$$(6) \quad d[MnO_2]/dt = -k_{ex}[MnO_2]^{1.0}[Cr^{3+}]^{0.5}$$

where: k_{ex} depends on the initial $[Cr^{3+}]$ and has units of $(moles)^{-0.5}(minutes)^{-1.0}$

The 1st order reaction with respect to $[MnO_2]$ is in agreement with other data from adsorption controlled reactions. The square root dependence on the Cr^{3+} concentration presents some interesting implications with respect to the reaction mechanism. It may be related to the fact that each Cr^{3+} ion must lose 3 electrons and each Mn^{4+} can only except 2. This suggests there may be intermediate reaction products and several reaction steps which are not considered in the overall thermodynamic reaction equation. A detailed analysis of reaction mechanisms and rate-controlling steps was outside of the scope of the present research.

1.5 SUMMARY AND CONCLUSIONS

The general nature, stoichiometry and kinetics of the oxidation of Cr^{3+} by MnO_2 has been evaluated by experiments under controlled laboratory conditions. Experiments were conducted to determine the rate and extent of the reaction by measuring the amount of Cr^{6+} formed by oxidation and the

amount of Mn^{2+} solubilized upon reduction for a variety of initial reactant concentrations.

The important results from these experiments are summarized as follows:

1. The oxidation of Cr^{3+} is a relatively fast reaction, with most of an initial 9.6×10^{-6} M Cr^{3+} spike being oxidized within 30 minutes in a 1.9×10^{-5} M MnO_2 suspension.

2. The oxidation of Cr^{3+} occurs even in systems with very low MnO_2 concentrations; which means the reaction occurs when the potential for adsorption (as compared to other metals) should be very low. The reaction proceeds until all of·the Cr is oxidized or nearly all of the MnO_2 has been reduced.

3. The reaction exhibits parabolic kinetics, with much of the reaction occurring at a nearly linear rate within the first several minutes, followed by a decreasing rate of reaction with time.

4. Except for the initial stage of the reaction, the stoichiometry of the reaction products shows that 3 moles of MnO_2 are reduced for every 2 moles of Cr oxidized. This confirms the predicted stoichiometry for the reaction of Cr^{3+} with Mn^{4+} from the oxide surface.

5. The rate of the reaction is dependent on the initial ratio of the reactants. Increasing the concentration of

MnO_2 results in a linear increase in reaction rate up until the initial MnO_2 to Cr^{3+} molar ratio is approximately 2. Further increasing the MnO_2 concentration to higher MnO_2 to Cr^{3+} ratios results in increasingly smaller increases in the reaction rate.

6. With Cr^{3+} present in large molar excess to MnO_2, the reaction exhibits first order rate dependence with respect to MnO_2 and a square root dependence with respect to Cr^{3+}.

From the above results two general conclusions were made. The first is that Cr^{3+} is oxidized by Mn^{4+} ions which are part of the oxide structure. This conclusion is supported by the strong adherence of the reaction products to the predicted reaction stoichiometry. The predicted stoichiometry is maintained throughout the reaction except in the first several minutes when the Mn^{2+} to Cr^{6+} ratio is lower than the predicted 1.5. It is proposed that the release of reduced Mn to solution is slow with respect to the overall reaction causing this deviation from stoichiometry when the reaction is fast.

The second main conclusion drawn from the data was that if the reaction is adsorption controlled, then 1) the affinity of Cr^{3+} for the MnO_2 surface must be very high, and 2) the reaction must be autocatalytic, with new surface sites being generated by the reduction and dissolution of the Mn oxide. This conclusion was drawn from the oxidation

data at low MnO_2 to Cr^{3+} ratios. The adsorption of metals, especially at low pH, is very much dependent on the ratio of the oxide to the metal. The adsorption of metals such as copper and zinc by MnO_2 at low pH's is minimal, or even undetectable when the oxide concentrations are less than or equal to the metal concentration. However, the oxidation of Cr proceeded strongly under these conditions. This suggests that the affinity of Cr^{3+} for the MnO_2 surface is much higher than for other metals.

Even if the affinity of Cr^{3+} for the MnO_2 surface were high, an adsorption controlled reaction could not proceed to the extent shown by the experimental data unless new surface sites were generated by the reaction. Conceptually, this result is consistent with the predicted reaction mechanism. As an Mn^{4+} ion in the oxide structure is reduced, it becomes unstable within the mineral structure and is released to solution. Effectively, the oxide particulate begins to dissolve. The loss of a coordinated Mn ion must result in a vacancy within the mineral lattice, which is essentially just another surface site. From a thermodynamic standpoint, the Cr^{3+} ions in solution are not only reactive with respect to the binding sites initially present on the oxide surface, but also with respect to all of the potential surface sites which can be generated during the reaction.

An alternative hypothesis to the second conclusion above, which explains the apparent discrepancies between the experimental data and available data on adsorption

equilibria was also investigated and rejected. The alternative hypothesis was that the reaction was not adsorption controlled and the reaction was comparable to a solute-solute, or metal-ligand type interaction. This hypothesis was rejected based on the influence of the initial MnO_2 to Cr^{3+} ratio on the reaction rate. The reaction rate slowed down with an increased Cr^{3+} concentration when MnO_2 was not present in a large excess. This result is consistent with adsorption equilibria and in direct contrast to solute-solute interactions.

Investigation of the experimental rate law showed that the reaction is first order with respect to MnO_2 and has a square root dependence with respect to Cr^{3+}. The 1st order rate dependence with respect to MnO_2 is consistent with other surface controlled reactions with MnO_2. The square root dependence with respect to Cr suggests the reaction may be complex, with several elementary steps.

PART 2.0   THE EFFECT OF SOLUTION CHEMISTRY ON THE OXIDATION
          OF CR(III) BY MN OXIDE

2.1   INTRODUCTION

This part of the report describes the effects of the solution chemistry on the rate and extent of the oxidation/reduction reaction between Cr^{3+} and the MnO_2 surface.   Experiments were conducted to explore the role of solution composition which may influence the rate and extent of this reaction in natural aqueous systems.   In particular, the effects of pH, dissolved oxygen (presence or absence), ionic strength, nature of the swamping electrolyte and a competing adsorbed trace metal (copper) were examined.   This part of the project was designed to provide further insight into the potential importance of this redox reaction in the environment, as well as to further define the fundamental nature of the reaction.

2.2   THE EFFECTS OF SOLUTION pH

2.21 Introduction

The potential effects of hydrogen ion activity (pH) on the adsorption-oxidation-desorption of Cr at the MnO_2 surface are numerous.   The potential effects on the system upon a change in pH include: 1) changes in the speciation of the oxide surface sites (i.e. surface hydrolysis), 2) a change in the electrostatic properties of the oxide surface, 3) changes in the speciation of the dissolved metal species,

4) the decrease in Cr^{3+} solubility with increasing pH and 5) the instability of the MnO_2 at low pH. With the Cr concentrations used in the experiments in this research, effects 1-3 above could only be studied in the pH range of approximately 3.0 to 5.0, as the formation of Cr hydroxide at higher pH's overwhelms all other pH effects. This narrow working range presents some difficulty in determining whether there is a pH dependence in the oxidation rate. The effects of 4 and 5 above were studied outside of this pH range at pH's less than 3.0 and greater than 5.0.

From past work on the adsorption of other trace metals on MnO_2 (McKenzie, 1980; Gadde and Laitinen, 1974), it has been shown that the quantity of metals adsorbed per unit weight of oxide generally increases within the pH interval of 3.0 to 5.0. This suggests there are more sites available with increasing pH and/or the energetics are becoming more favorable for adsorption. If Cr^{3+} adsorbs similarly to these other metals, it might be expected that the oxidation rate of adsorbed Cr would increase as the pH increased. However, given that the oxidation reaction exhibits characteristics considered atypical compared to the adsorption of other metals, it is not clear whether a pH dependence should be detected experimentally.

To explore the effect pH on the oxidation rate at low pH's, duplicate experiments were performed at pH's 1.55, 3.00 and 4.50. The concentrations of reagents used were: MnO_2 = 1.9 X 10^{-5} M, Cr^{3+} = 9.6 X 10^{-6} M and the matrix was

0.10 M NaNO$_3$. These experiments were conducted open to the atmosphere. The pH was adjusted to the desired level with 0.10 N HNO$_3$ approximately 10 minutes before the addition of the Cr^{3+} spike. Dissolved Cr^{6+} and Mn^{2+} were then measured in filtered aliquots withdrawn over time.

2.22 Results and Discussion

The amount of Cr oxidized and the amount of Mn solubilized for each experiment are shown on Figures 24 and 25 respectively. The amount of Cr oxidized over the first ten minutes of the reaction at pH 3.0 and 4.5 was nearly the same. The amount oxidized at pH 1.55 was significantly less over this same time period. The similar rates of oxidation at pH 3.0 and 4.5 was supported by the amount of Mn^{2+} formed during the reaction (see Figure 25). However, the quantity of Mn solubilized at pH 1.55 was much greater than that at the higher pH's, inconsistent with the lesser amount of Cr oxidized. This result was not unexpected as MnO$_2$ has been shown to be unstable at pH's lower than 3.5 (Murray, 1974).

To verify the role of oxide dissolution in this apparent discrepancy, another set of identical experiments were performed at pH 1.65 and 4.5. A blank (not spiked with Cr) MnO$_2$ suspension was also set to pH 1.65 and aliquots were withdrawn over the time of the experiment, filtered and measured for Mn^{2+}. From the blank the amount of Mn^{2+} formed from the dissolution of the oxide was subtracted from the total Mn solubilized during the redox reaction with Cr. The
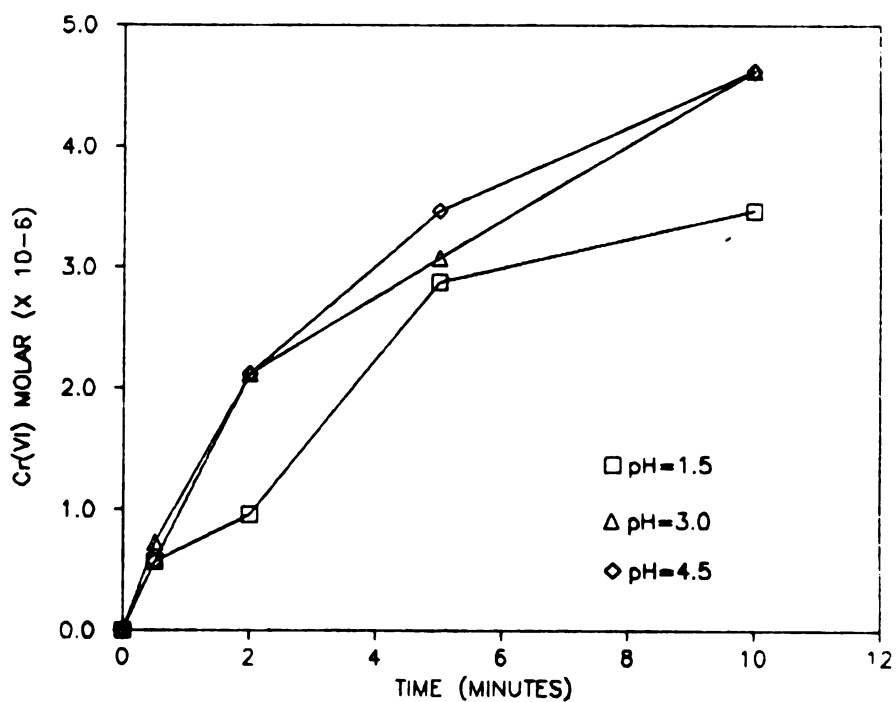
Figure 24. Effect of pH on the Oxidation Rate of Cr^{3+} by MnO_2
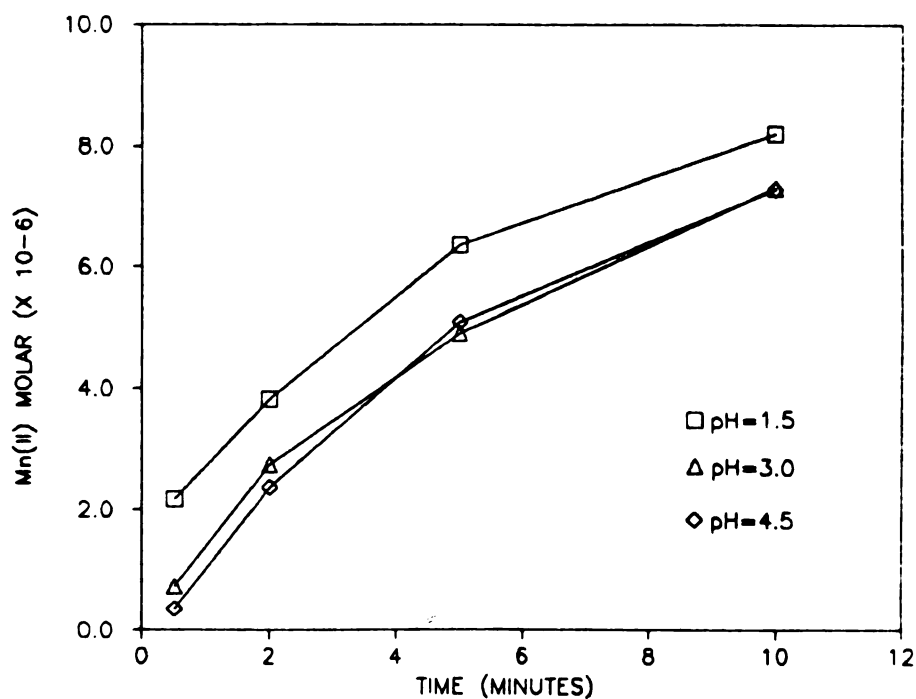
Figure 25. Effect of pH on the Dissolution Rate of MnO_2 During the Oxidation of Cr^{3+}

quantity of Cr oxidized and the corrected values of Mn solubilized are shown on Figures 26 and 27, respectively. In agreement with the previous experiments, the rate of Cr oxidation was significantly less at the lower pH. The corrected rate of Mn^{2+} production (Figure 27) is also lower at pH 1.65 than at pH 4.50. The molar ratio of Mn^{2+} to Cr^{6+} for the reaction products at both pH's is very close to the predicted 1.5. Thus the correction obtained from the blank appears to result in the true rate of reduction caused by Cr oxidation at the low pH. Approximately 20% of the original MnO_2 suspension dissolved in the blank over the time interval of the experiment. This rate of dissolution can probably account for the lower oxidation rate at pH 1.65, especially since the smaller more reactive particles may be the first to dissolve. With the exception of this dissolution effect, there does not appear to be a measurable pH effect on the reaction rate at pH's below 5.

2.3 THE OXIDATION OF SOLID CR-HYDROXIDE

2.31 Introduction

The oxidation of Cr by MnO_2 at higher pH's (i.e. greater than 6.0) will be influenced by the formation of $Cr(OH)_3$ solid. The formation of this species has been ignored in some previous studies of Cr-Mn oxide redox reactions. Studies by Rai et al. (1986), using reagent MnO_2, and James and Bartlett (1983), using Mn oxide bearing soils, have
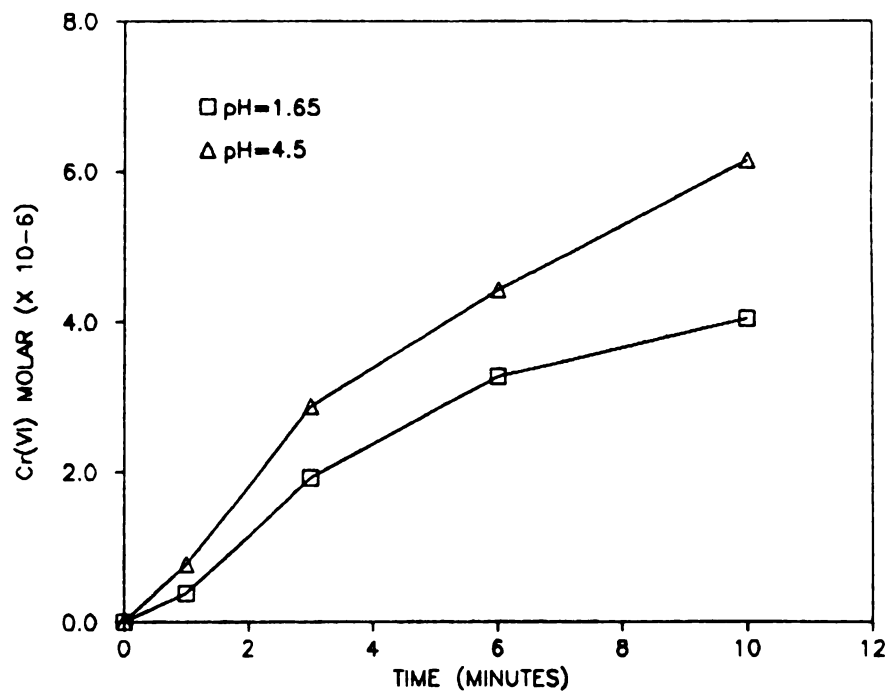
Figure 26. Effect of pH on the Oxidation Rate of Cr^{3+} by MnO_2
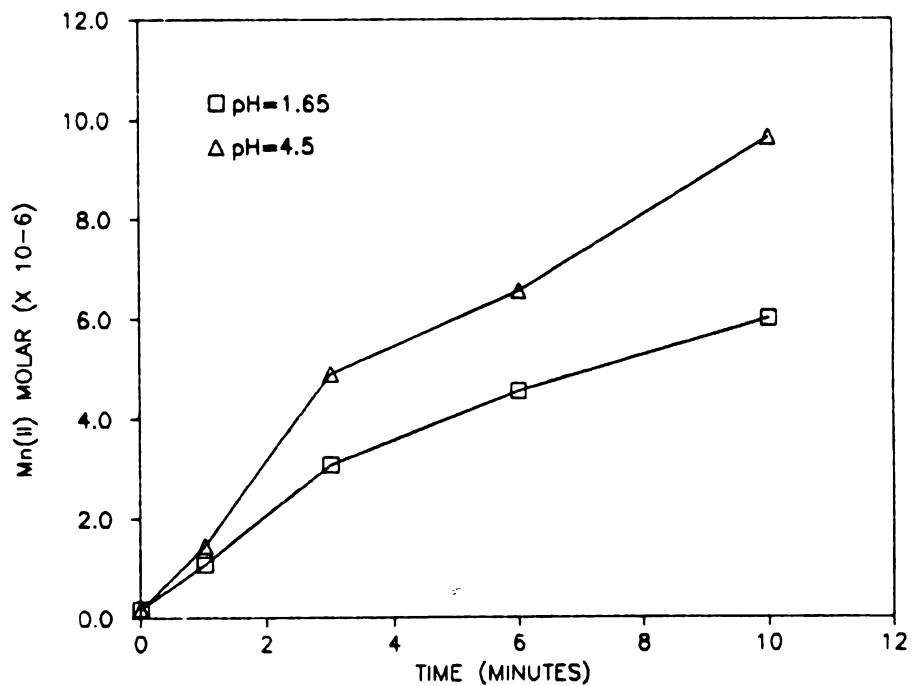
Figure 27. Effect of pH on the Dissolution Rate of MnO_2 During the Oxidation of Cr^{3+} with Blank Corrections

shown that oxidation of chromium hydroxide does occur, but at a much slower rate and reduced extent than dissolved chromium species. As dissolved Cr^{3+} is believed to be the species interacting with the MnO_2, the formation of a solid Cr phase with very low solubility should severely limit the oxidation/reduction reaction. Since Cr solubility should be controlled by hydroxides under the pH conditions of most natural systems, the oxidation by MnO_2 may not be environmentally significant. However, if oxidation by MnO_2 can proceed under these conditions, this reaction may be very environmentally significant.

To determine the extent and rate of the oxidation of Cr hydroxide by the MnO_2 used in the current investigation, a set of long term experiments were conducted. Both aged and freshly precipitated $Cr(OH)_3$ solid were used. For the freshly precipitated hydroxide, one liter of $1.92 \times 10^{-5}M$ $Cr(NO)_3/0.10$ M $NaNO_3$ solution was adjusted to pH 8.2 with NaOH. A light greenish precipitate was seen to form upon adjustment of the pH. This solution was allowed to set for approximately 60 minutes with occasional pH adjustments to maintain the pH above 7.5. After this time, an aliquot of MnO_2 stock solution was added to bring the total Mn concentration to approximately 9×10^{-3} M. The suspension was sampled periodically over the next 48 days and analyzed for Cr^{6+}. The aged $Cr(OH)_3$ was prepared as above but was allowed to set for 48 hours with occasional pH adjustments

before the addition of the MnO_2. The solution was sampled periodically over the next 46 days.

2.32 Results and Discussion

The results of these experiments are shown on Figure 28. As can be seen from this graph, small amounts of Cr were oxidized in both experiments, with a maximum of 10.6 X 10^{-7} and 2.9 X 10^{-7} moles oxidized in the fresh and aged systems, respectively. More oxidation occurred with freshly precipitated $Cr(OH)_3$, similar to the results of James and Bartlett (1983). These investigators interpreted this result as evidence for a residual positive charge on the fresh hydroxide, allowing adsorption onto the Mn oxide surface. Although this cannot be verified by the present results, the fact that the oxidation was not complete until at least 10 days time would suggest that the larger quantity oxidized in the freshly precipitated hydroxide solution was not simply due to incomplete precipitation of Cr hydroxide, as any remaining dissolved Cr species would have likely been oxidized very quickly. It should be noted that only about 5% of the freshly precipitated $Cr(OH)_3$ was oxidized throughout the duration of the experiment. Still, this quantity is almost two orders of magnitude higher than the solubility of Cr^{3+} in this pH range. In summary, the formation of Cr hydroxides greatly reduces the rate and extent of the oxidation reaction. However, the extent of
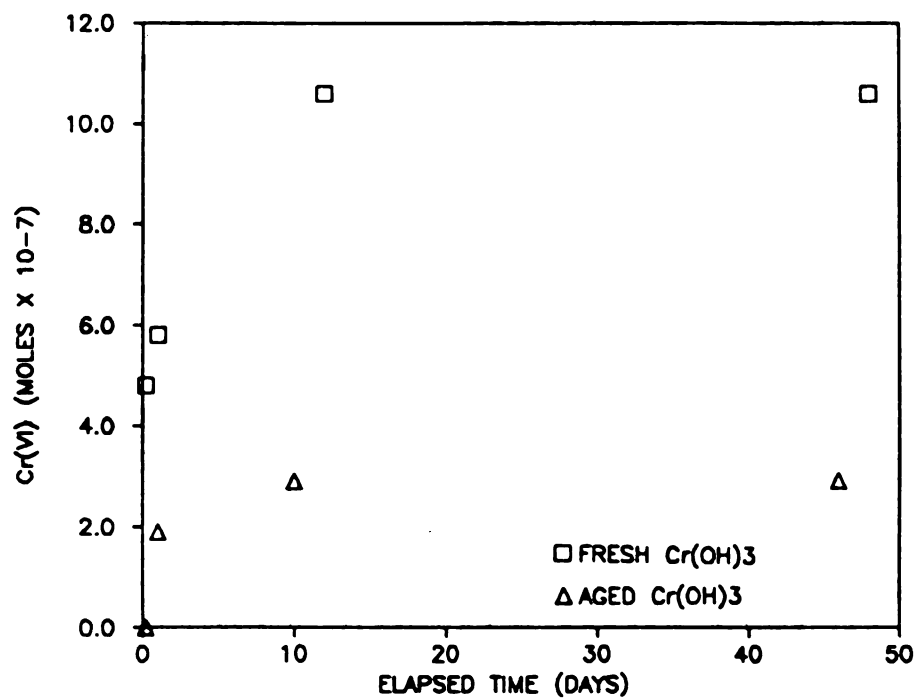
Figure 28. Oxidation of Fresh and Aged Cr(OH)$_3$ by MnO$_2$

the reaction is still sufficient to increase the solubility of Cr significantly.

2.4 THE EFFECT OF DISSOLVED OXYGEN

2.41 Introduction

Research by Nakayama et al. (1981) on the oxidation of Cr^{3+} by a trivalent Mn oxide, MnO(OH), showed that the presence of dissolved oxygen had a large effect on the oxidation rate, with the reaction rate much slower in the absence of oxygen. These investigators did not propose an explanation for this behavior, but termed the role of the Mn oxide as having a "catalytic" effect in the oxidation of Cr. In contrast, Rai et al. (1986) did not find any effect of dissolved oxygen content on the oxidation of Cr by reagent MnO_2.

To determine whether dissolved oxygen would influence the oxidation rate of Cr in the present study, duplicate experiments were performed in open air and in N_2-purged experimental systems. The O_2 deficient conditions were established by bubbling N_2 gas through the solution in the reaction vessel, which itself was contained in an N_2 purged glove box. The dissolved O_2 was measured by an Orion model 97-08-99 dissolved oxygen electrode. The concentration of dissolved oxygen was below 0.10 mg/l during the duration of the experiment. The MnO_2 suspension was shown to be stable under these conditions (see Methods). The concentration of

reactants used were: Cr^{3+} = 9.6 X 10^{-6} M, MnO_2 = 1.9 X 10^{-5} M. The solution matrix was 0.10 M $NaNO_3$.

2.42 Results and Discussion

The rates of Cr oxidized and Mn solubilized for both open-air and N_2-purged systems are shown in Figures 29 and 30, respectively. The oxidation rate of Cr can be seen to be very similar in air and N_2. The rate in the absence of O_2 actually appears to be slightly greater. However, the rate of Mn^{2+} produced is almost identical for both experiments, suggesting the slight difference in the oxidation rates may have been analytical. From these results it is concluded that dissolved oxygen does not play an important role in the redox reaction, at least under the experimental conditions investigated. These results are consistent with the proposed reaction mechanism, which does not include a role for dissolved oxygen.

2.5 THE EFFECT OF IONIC STRENGTH

2.51 Introduction

There are several potential effects of changing ionic the strength with an inert electrolyte on adsorption reactions. These include: 1) changes in the activity of dissolved species, 2) changes in the electrostatic potential at the oxide surface and 3) changes in colloid stability (Swallow et al, 1980 and Morgan and Stumm, 1964). In
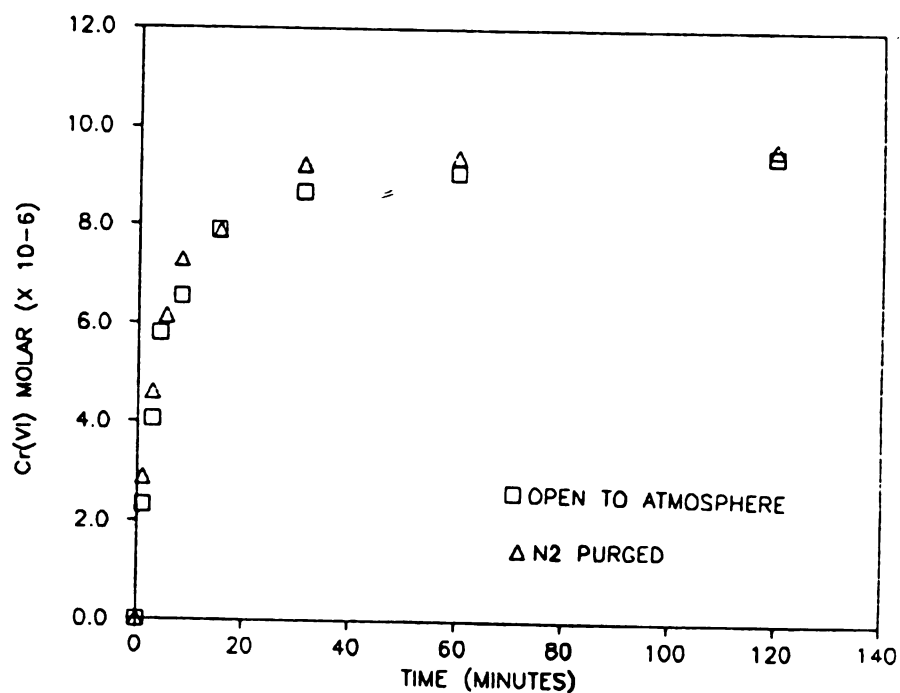
Figure 29. Rate of Cr Oxidation by MnO_2 in Open-Air and N_2 Atmospheres
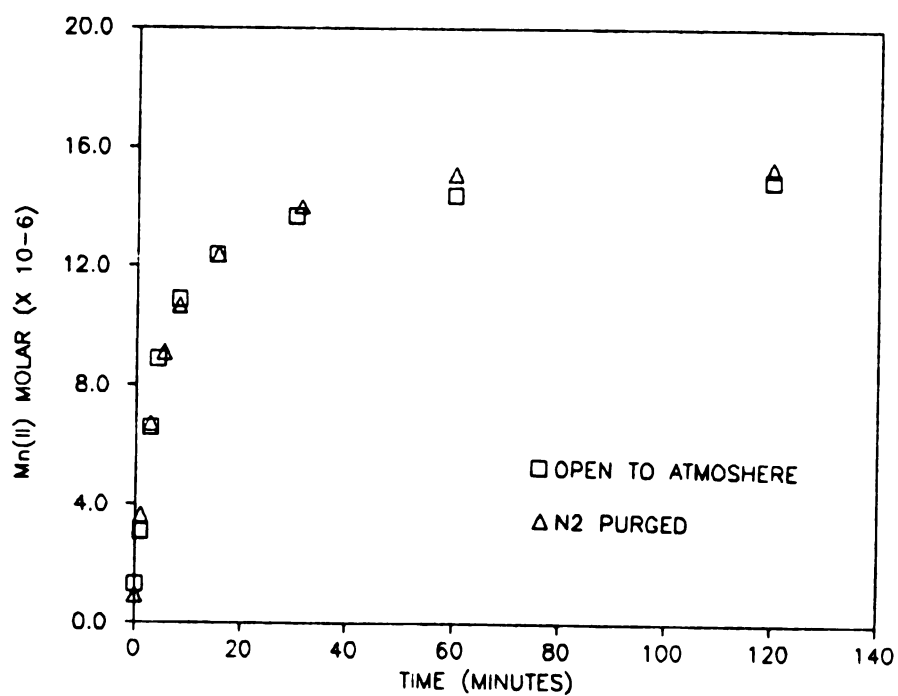
Figure 30. Rate of MnO_2 Reduction by Cr^{3+} in Open-Air and N_2 Atmospheres

general, past studies have shown a general tendency for decreased adsorption with increasing ionic strength (see Appendix I). However, the adsorption of many trace metals on oxide surfaces is apparently unaffected by changes in ionic strength. In particular, there appears to be little competition for surface sites between trace metals and background electrolytes and the changing electrostatic conditions induced by these electrolytes appear to have little influence on specifically adsorbed trace metals (Swallow et al. 1980). Several studies (Morgan and Stumm, 1964; Posselt et al., 1968) have shown that adsorption kinetics on Mn oxide surfaces are controlled by ionic strength. It is believed that the flocculation of the oxide, brought about by the collapse of the diffuse layer with increasing ionic strength, necessitates that ions diffuse through the flocculated suspension to find an available site for adsorption.

To determine whether the rate of oxidation of Cr by MnO_2 is influenced by ionic strength, several sets of duplicate experiments were conducted in which the concentration of the swamping electrolyte was varied over several orders of magnitude. The first set of experiments measured the rate of oxidation of Cr^{3+} and the solubilization of Mn in solutions of 0.005, 0.05 and 0.50 M $NaNO_3$, where in this case the molarity of the electrolyte solution is equivalent to the ionic strength. The concentrations of reactants were 1.9 X 10^{-5} M and 9.6 X 10^{-6}

M for MnO_2 and Cr^{3+}, respectively. Another set of experiments were conducted with 0.01 and 0.10 M $Ca(NO_3)_2$ (ionic strength 0.03 and 0.30, respectively) to set the ionic strength. All experiments were conducted at pH 4.5.

2.52 Results and Discussion

The results for oxidation and reduction rates in the $NaNO_3$ matrices are shown on Figures 31 and 32. The oxidation rate of Cr^{3+} and the corresponding reduction of Mn is significantly slower as ionic strength increases. Similar results are seen for the rate of reaction in the $Ca(NO_3)_2$ matrices (Figures 33 and 34) although the rate difference is not as pronounced and is only apparent during the early stages of the reaction. It should be noted that these two sets of experiments were not conducted close enough together in time to allow direct comparison between the two electrolytes.

Given the data from past research, the most likely cause of the decreasing oxidation rate with increasing ionic strength appears to be the flocculation of the oxide. The flocculation of the MnO_2 suspension was easily visible in the concentrated matrices and the flocs became larger as the ionic strength was increased. This effect was more pronounced for the $NaNO_3$ solutions which is somewhat surprising since divalent ions usually produce a much higher degree of flocculation than monovalent ions (Drever, 1982). A possible explanation for this result is that Ca^{2+} adsorbs
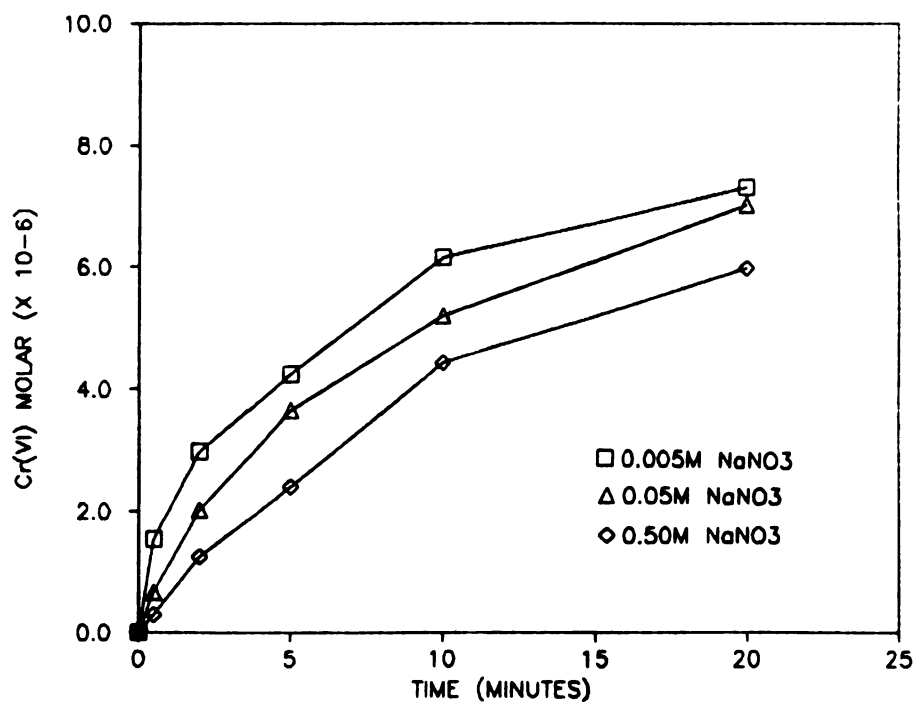
Figure 31. Effect of Ionic Strength on the Oxidation Rate as Set by $NaNO_3$
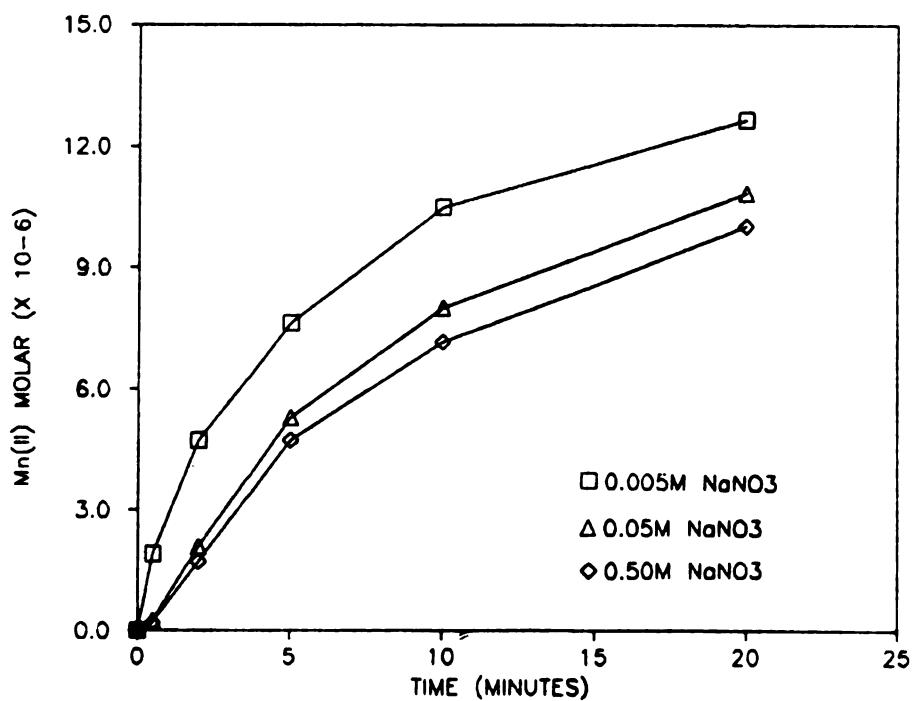
Figure 32. Effect of Ionic Strength on the Reduction Rate as Set by $NaNO_3$
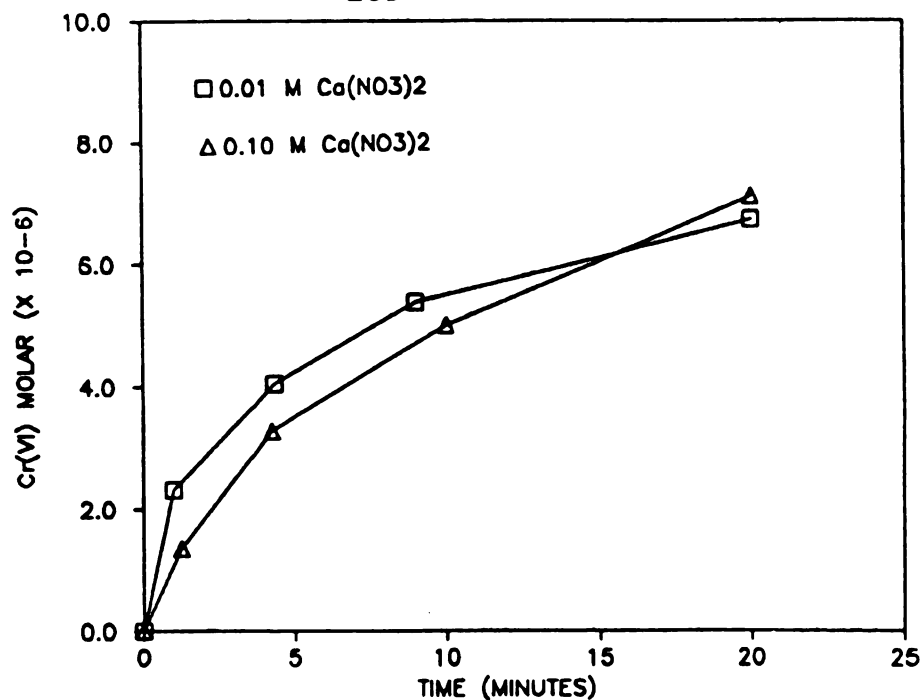
Figure 33. Effect of Ionic Strength on the Oxidation Rate as Set by $Ca(NO_3)_2$
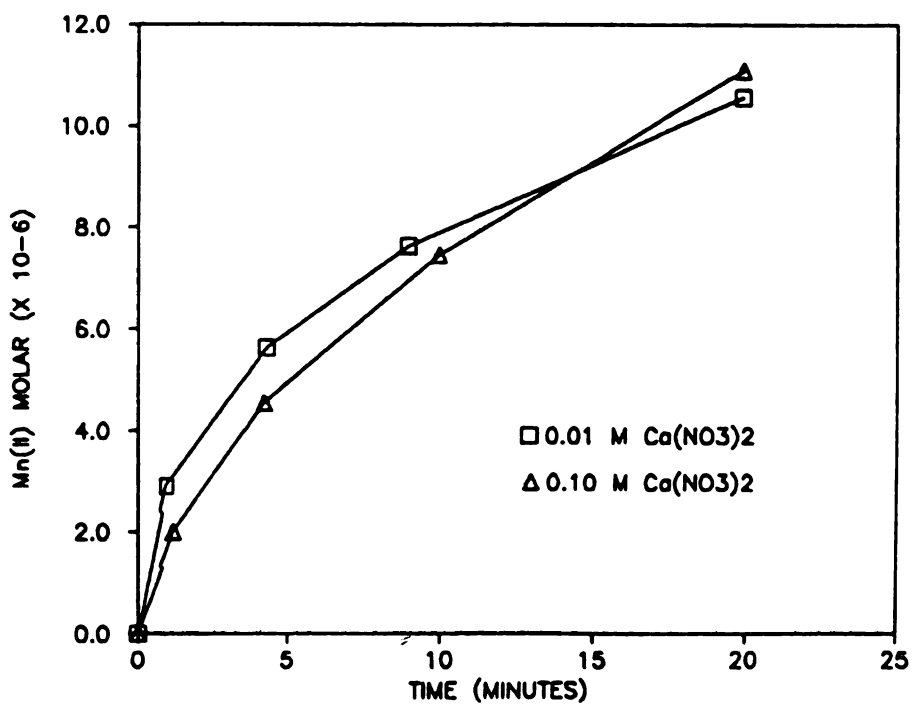
Figure 34. Effect of Ionic Strength on the Reduction Rate as Set by $Ca(NO_3)_2$

on MnO_2 by a different mechanism than Na^+, resulting in different effects on the electrostatic properties. The adsorption capacity of an oxide surface for trace metals is generally unaffected by ionic strength. However, a study by Posselt et al., (1968) demonstrated that the adsorption capacity of MnO_2 for Ca^{2+} was reduced by increasing the ionic strength with $NaClO_4$. The possibility of effects other than the flocculation of the oxide, therefore, cannot be ruled out by the present results.

2.6 EFFECTS OF THE NATURE OF THE ELECTROLYTE

2.61 Introduction

In addition to the effects of ionic strength discussed above, the composition of the matrix solution may influence an adsorption reaction by "specific" effects, which are based on the composition of the solution. These specific effects may include the competition for surface sites on the oxide, and more importantly in the case of trace metals, the complexation of trace metals by dissolved ligands. Complexation of the adsorbing metal can cause an increase or a decrease in adsorption of a trace metal (see Appendix I). Rai et al., (1986) showed that the solubility of $Cr(OH)_3$-solid was unaffected by low concentrations of common ligands such as SO_4^{2-}, NO_3^-, Cl^- and HCO_3^-, which suggests that complexing is unimportant under these conditions. Elderfield (1970), using published stability constants,

concluded that complexing by ligands other than OH^- would be insignificant even under sea water conditions. Although the data is scarce, all indications are that complexing of Cr should be minimal in most aqueous systems. One possible exception may be the complexing of Cr^{3+} with organic ligands. Nakayama et al. (1981) demonstrated that both coprecipitation of Cr^{3+} with Fe oxide and oxidation of Cr^{3+} with Mn oxide could be reduced by the formation of a Cr-citric acid complex.

Based on available data, it was hypothesized that changing the swamping electrolyte solution would not effect rate of the redox reaction between Cr^{3+} and the MnO_2 surface. To test this hypothesis, duplicate experiments were performed in various swamping electrolyte solutions of identical concentrations. The first test compared the rate of MnO_2 dissolution upon addition of a Cr^{3+} spike in 0.05 M solutions of $CaCl_2$, $Ca(NO_3)_2$, $NaNO_3$ and NaCl. The quantity of Cr^{6+} was not measured in most of these experiments due to the problems created by Cl in the Cr^{6+} extraction procedure. The concentration of reactants were that of the "standard" oxidation experiment and the pH was 4.5.

2.62 Results and Discussion

Figure 35 shows the results of these experiments. Only slight differences were found between electrolyte solutions. The reaction appears to be slightly faster in $Ca(NO_3)_2$ than in either sodium salt and slightly slower in $CaCl_2$. The
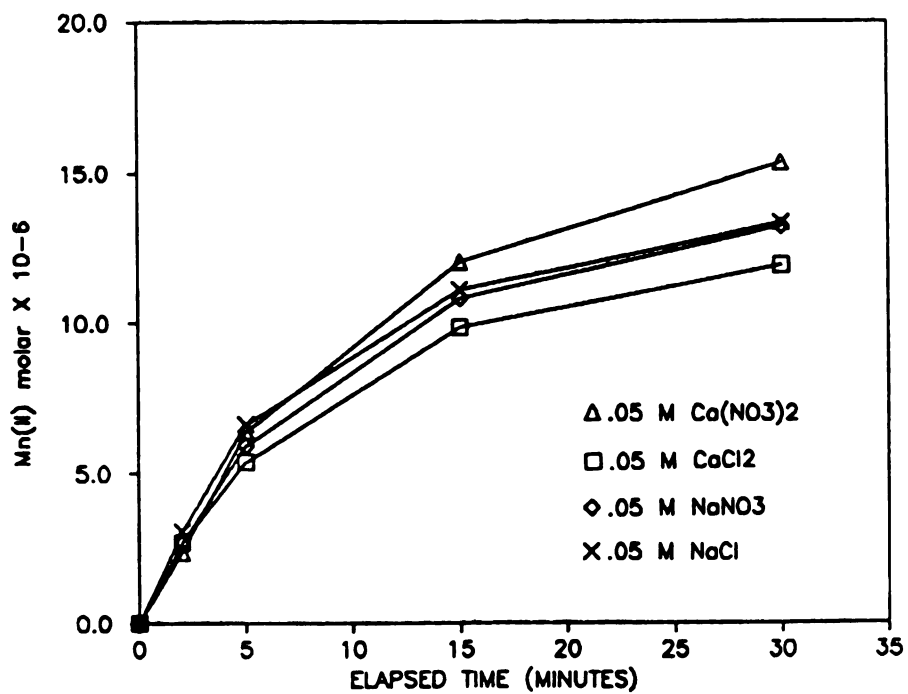
Figure 35.   Reduction Rate of MnO_2 in Various Background
Electrolytes

slightly faster rate of reaction in $Ca(NO_3)_2$ solution is not readily explainable. One possible explanation is the apparent increased degree of flocculation of the MnO_2 which seems to occur in Na salt solutions. The slower rate of reaction in $CaCl_2$ matrix was not anticipated.

To further explore the rate of reaction in $CaCl_2$ solutions, duplicate experiments were performed in 0.005, 0.05 and 0.50 M $CaCl_2$ solutions. The results, in terms of Mn^{2+} solubilized, are shown on Figure 36. There was a slight decrease in the rate of reduction as the concentration of $CaCl_2$ solution was increased from 0.005 to 0.05 M. However, as the concentration was increased to 0.50 M, the rate of oxide dissolution was decreased significantly. The measurement of oxidized Cr confirmed these results for the 0.005 and 0.05 M $CaCl_2$ solutions (Figure 37).

Two possibilities were considered as an explanation for this reduced reaction rate in $CaCl_2$; 1) the competition for binding sites by the high Ca concentrations and 2) the complexing of Cr^{3+} by Cl^-. These possibilities were tested by comparing the reduction rate in 0.50 M $CaCl_2$ to that in 1.0 M NaCl (same Cl concentration, different cation) and in 0.50 M $Ca(NO_3)_2$ (same Ca concentration, different ligand). The results are shown on Figure 38. It can be seen from the graph that only $CaCl_2$ causes this large reduction in the reaction rate. This unique behavior of $CaCl_2$ was further
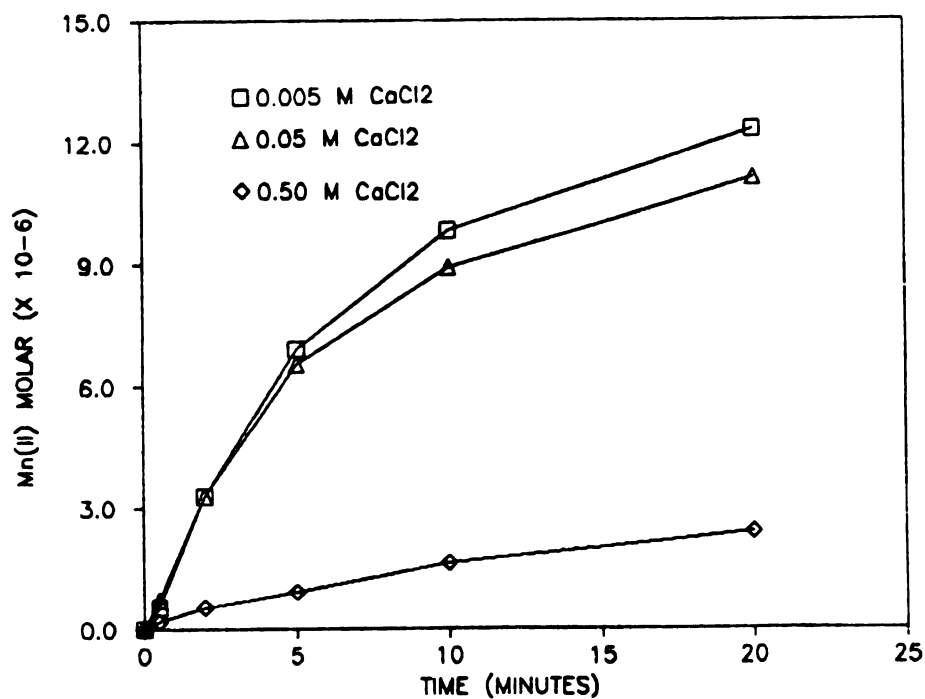
Figure 36. Reduction Rate of MnO_2 in $CaCl_2$ Solutions of Various Concentrations
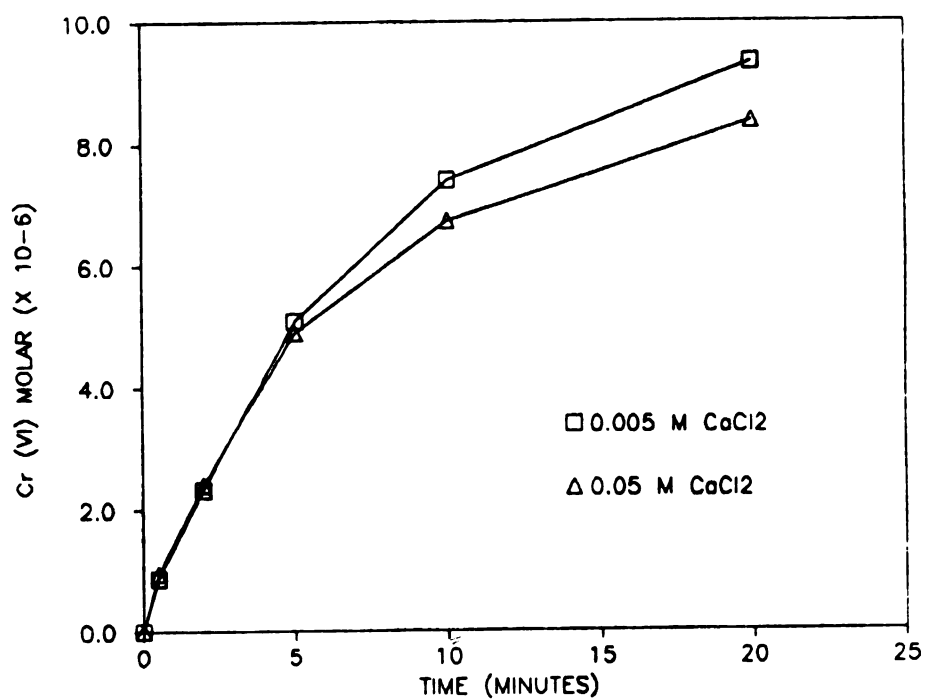
Figure 37. Oxidation Rate of Cr^{3+} in $CaCl_2$ Solutions of Various Concentrations
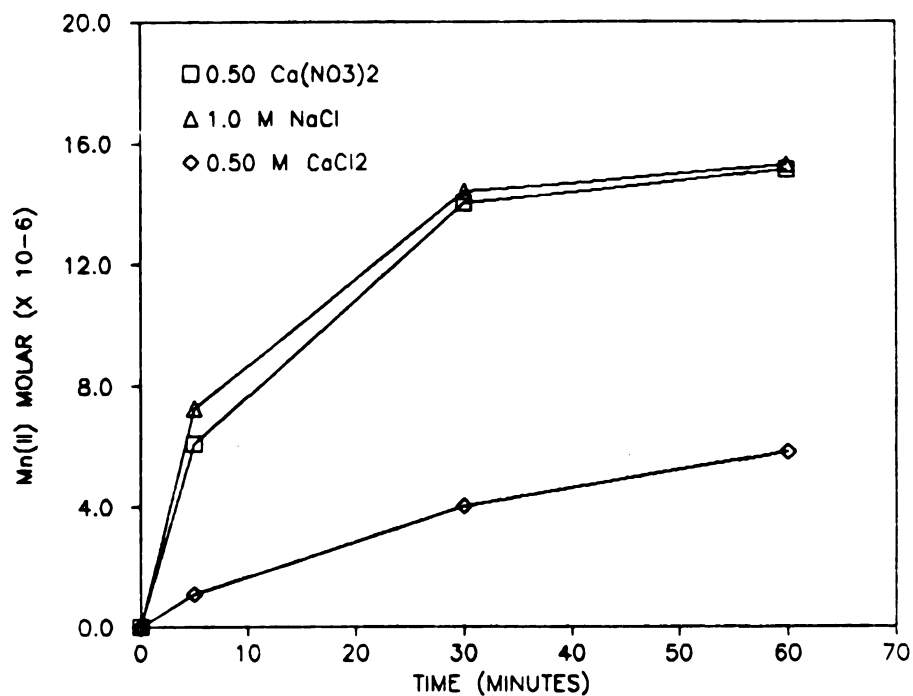
Figure 38. Reduction Rate of MnO_2 in $Ca(CO_3)_2$, NaCl and $CaCl_2$
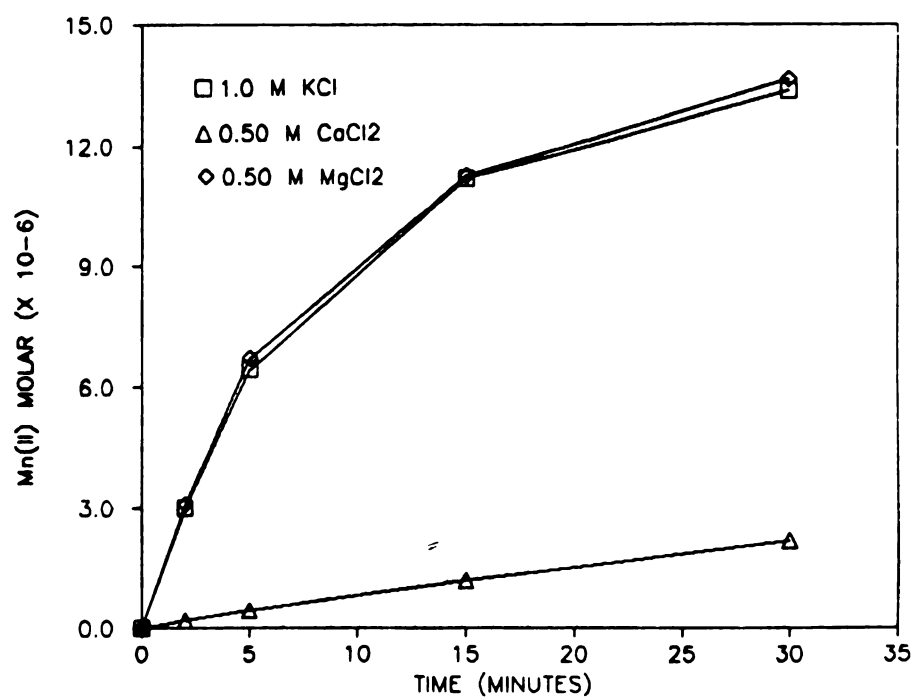
Figure 39. Reduction Rate of MnO_2 in KCl, $CaCl_2$ and $MgCl_2$

verified by comparing reduction rates in 1.0 M KCl and 0.50 M $MgCl_2$ solutions. The results are shown in Figure 39.

From these results it does not appear that either the blocking of surface sites or the complexing of Cr^{3+} by Cl^- can explain the decreased oxidation rate in concentrated $CaCl_2$ solution. The dramatic decrease in the rate of reaction as the $CaCl_2$ concentration is increased from 0.05 to 0.50 M as compared to the minor effect caused by increasing the $CaCl_2$ concentration from 0.005 to 0.05 M would suggest that there is a solubility control. At the present time no explanation is proposed to explain these results.

2.7 THE EFFECT OF ADSORBED COPPER

2.71 Introduction

Past studies have shown that the competition between trace metals for adsorption sites on an oxide surface does not follow a simple relationship (see Appendix I). In some cases, a particular metal may adsorb at the expense of another, while other metals can co-adsorb with no detectable effects on each other. Benjamin and Leckie (1981a) presented evidence that Fe oxides have high energy sites that are specific for each metal, resulting in little competition between metals on this oxide surface. Limited research on metal competition on Mn oxides suggests that some competition may occur (Dempsey and Singer, 1980; Gadde

and Laitinen, 1974). If there is competition between Cr^{3+} and other trace metals for the surface sites on MnO_2, it seems likely that this would influence the rate of oxidation of Cr. There is no reason to pre-suppose, however, that Cr adsorbs at the same surface sites as other metals on Mn oxide.

Although a rigorous treatment of this problem was outside the scope of this research, a preliminary investigation was conducted to determine whether the adsorption of a similar quantity of a competing trace metal would effect the oxidation rate of Cr. The adsorptive behavior of 0.50 mg/l Cu, Zn, Mn and Ni was investigated for a range of MnO_2 concentrations at pH 4.5. The results are shown on Figure 40. From these results it is apparent that Cu adsorbs strongest under these conditions. Based on this result, and the need to maintain reasonably low MnO_2 concentrations, Cu was chosen to study potential competitive effects. It should be noted that an oxide concentration of 1.4×10^{-4} M was required to ensure greater than 90% adsorption of 7.9×10^{-6} M Cu. This is an order of magnitude more MnO_2 than is required to completely oxidize 9.6×10^{-6} M Cr^{3+}.

To study the potential competitive effects of Cu^{2+} adsorption on Cr oxidation, an MnO_2 suspension with Mn = 1.4×10^{-4} M, was allowed to equilibrate with 7.9×10^{-6} M Cu^{2+} at pH 4.5. A sample was withdrawn after an hour, filtered and analyzed for Cu^{2+}. From this
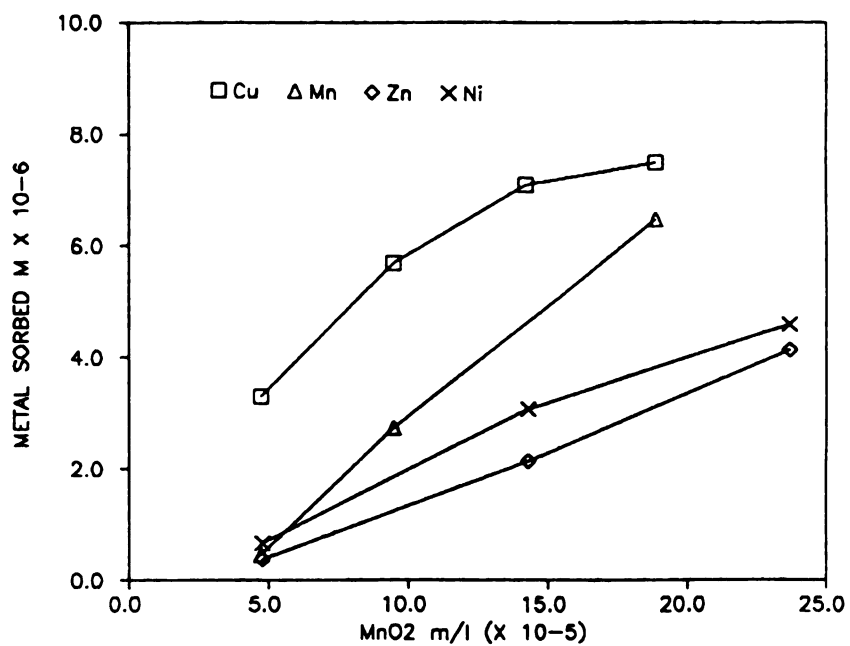
Figure 40. Adsorption of 0.50 mg/l Copper, Manganese, Zinc and Nickel by Various Amounts of MnO_2

measurement the amount of Cu^{2+} adsorbed was calculated. The

system was then spiked with $Cr(NO_3)_3$ to obtain an initial

Cr^{3+} concentration of 9.6 X 10^{-6} M. The system was then

sampled over small time intervals and analyzed for dissolved

Mn^{2+}, Cu^{2+} and Cr^{6+}. A control experiment was also

conducted which was identical to that above except no Cu^{2+}

was added to the system.

2.72 Results and Discussion

The rate of Cr oxidized and Mn reduced for the Cu spiked

experiment are presented on Figure 41. The oxidation of Cr

was almost completed within 15 minutes. The amount of Mn^{2+}

released was less than the predicted stoichiometric amount

due to adsorption by the remaining oxide. As shown on

Figure 41, a considerable amount of Cu was desorbed during

the reaction. The results from the control experiment are

shown on Figure 42. These results show that the rate of

oxidation was very similar to that in the Cu spiked system.

The rate of Mn released, however, was significantly lower.

This relationship is shown more clearly on Figures 43 and

44, which directly compare the results of the control

experiment with the Cu spiked experiment for Cr oxidation

and Mn released, respectively.

The above results seem to indicate that the rate of

oxidation of Cr^{3+} is not effected by the presence of

adsorbed Cu^{2+}. This suggests that the adsorption of Cr^{3+}

does not take place at the expense of Cu^{2+}, unless this
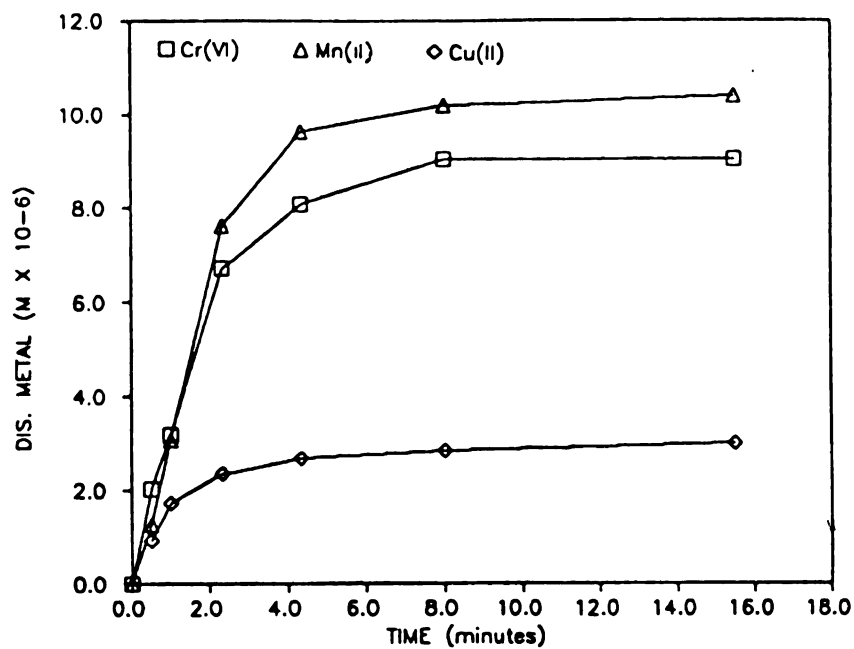
Figure 41. Rate of Oxidation/Reduction with Adsorbed Copper
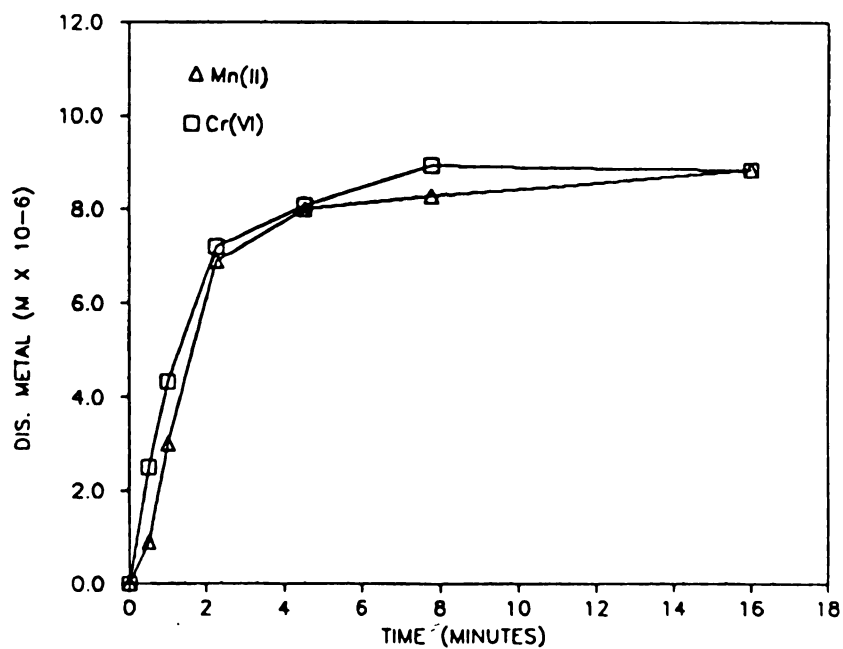
Figure 42. Rate of Oxidation/Reduction in Control
Experiment with No Copper
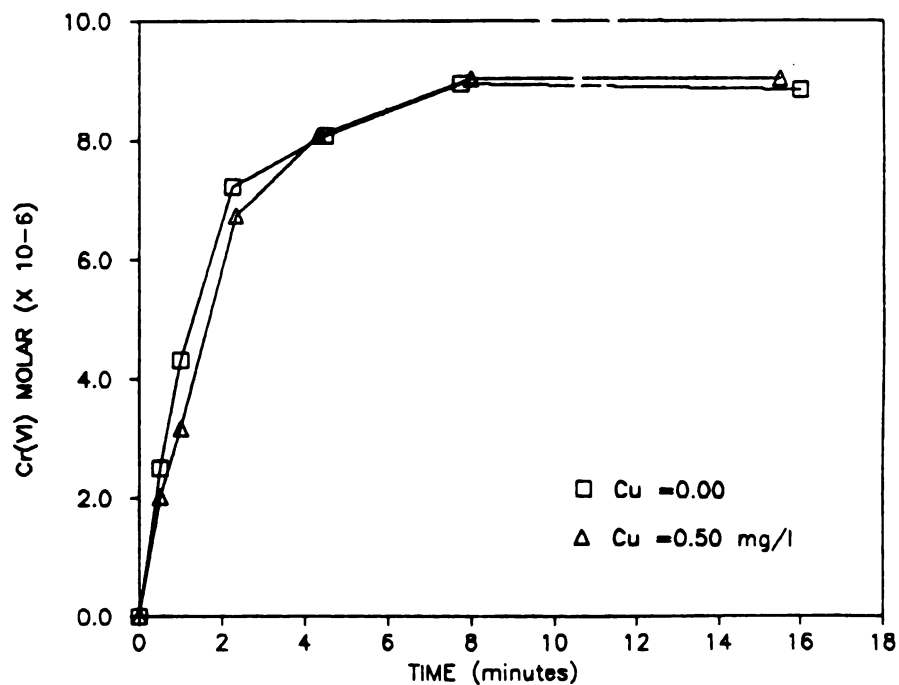
Figure 43. Rates of Cr Oxidation with Adsorbed Copper and
in Control Experiment
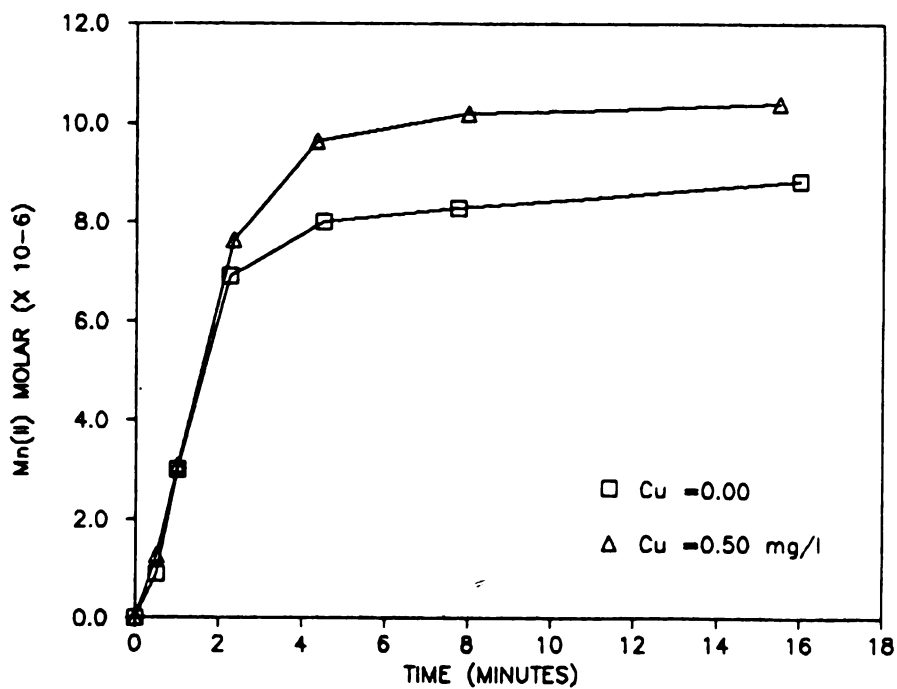
Figure 44. Rate of Mn Solubilization with Adsorbed Copper
and in Control Experiment

competition can occur but not influence the rate of the oxidation reaction. However, significant amounts of Cu were desorbed during the reaction suggesting Cu was somehow displaced from the MnO_2 surface. The desorption of Cu may have been caused, at least in part, by the adsorption of released Mn^{2+}. The competition of Mn^{2+} for surface sites with Cu^{2+} would explain why more Mn remains in solution in the presence of Cu than was found in the control (see Figure 44). It thus appears that these two metals may compete for sites on the MnO_2 surface.

2.8   Summary and Conclusions

The effect of changing solution parameters on the reaction rate has been evaluated by conducting duplicate experiments in which one solution parameter was varied. In particular, the effects on the oxidation rate of Cr of solution pH, dissolved O_2, ionic strength, identity of the swamping electrolyte and the presence of adsorbed copper were investigated. The results of this part of this research can be summarized as follows:

1. There is no measurable pH dependence on the reaction rate over the pH range 3.0 to 5.0.

2. Only small quantities of $Cr(OH)_3$-solid are oxidized by MnO_2, however the amount oxidized exceeds the solubility of Cr at pH's above 7.0.

3. The concentration of dissolved oxygen does not appear to have any measurable effect on the oxidation rate of Cr.

4. The oxidation rate decreases as the ionic strength, as set by a swamping inert electrolyte, increases.

5. Of a variety of swamping electrolyte solutions, only high concentrations of $CaCl_2$ appears to have specific effects on the oxidation rate. The reaction proceeds at a significantly reduced rate in the presence of 0.50 M $CaCl_2$.

6. The presence of adsorbed Cu^{2+} on the MnO_2 suspension does not result in any measurable change in the oxidation rate as compared to a control experiment.

From the above results the following conclusions can be made:

1. The absence of a pH dependence on the oxidation rate is somewhat surprising considering the variety of roles that protons must play in the various steps of the reaction. If the hypothesized adsorption-oxidation-desorption reaction is indeed correct, then it must be concluded that the effects of pH are probably obscured in this relatively fast reaction.

2. The oxidation of solid phase $Cr(OH)_3$ by MnO_2 occurs at a much reduced rate compared to soluble Cr^{3+}. The occurrence of this reaction is significant as this solid

species controls the solubility of Cr in most natural systems. The results suggest that the presence of Mn oxides in soils or sediments may serve to increase the solubility and potential mobility of this trace metal.

3. The dependence of the oxidation rate on ionic strength is interpreted to result from increased oxide flocculation with increasing ionic strength. This suggests the oxidation reaction is surface area controlled, and may be diffusion influenced when the ionic strength is high.

4. In general, only very small effects on the oxidation rate are induced by changing the nature of the swamping electrolyte. The exception is the significant decrease in the oxidation rate induced by high concentrations of $CaCl_2$. It does not appear that the decreased rate is due to the adsorption of Ca^{2+} or the complexing of Cr^{3+} by Cl^-.

5. Although Cu^{2+} is desorbed from the MnO_2 surface during the reaction, there is no effect on the rate of Cr^{3+} oxidation. Unless the competition does not effect the rate, it does not appear that the sites for Cr oxidation are the same as those for Cu adsorption. However, it must be noted that the current experiments do not provide nearly enough information to make any firm conclusions on this issue. Additional experimentation is necessary.

PART 3.0   THE COMPETITION BETWEEN MN AND FE OXIDES FOR CR(III)

3.1 INTRODUCTION

Due to their similar geochemical properties and their tendency to occur together in the natural environment, Mn and Fe oxides are often considered as a single component in metal/sediment partitioning studies. Describing the general adsorptive behavior of most trace metals in natural systems does not require a rigorous evaluation of the partitioning between these two oxides. In the case of chromium however, this is important to consider, as Fe oxides tend to remove Cr from solution while Mn oxides oxidize Cr to the mobile, toxic hexavalent form.   In the few attempts to apply adsorption reactions to chemical modeling (Davies-Colley et al., 1984; Vuceta and Morgan 1978), the presence of two (or more) adsorbing substrates has been handled as a cumulative increase in the adsorption capacity of the solid phase as a whole, with each substrate treated like a ligand with an experimentally determined binding constant. However, there has been little published research which has attempted to experimentally measure the adsorptive properties of a mixture of solid surfaces, or to determine the effect of one additional solid component on the adsorption equilibria of another.

Because Cr which adsorbs to Mn oxides is oxidized while Cr adsorbed to Fe oxides is stable , experiments were

conducted to explore the "competition" between synthetic MnO_2 and $Fe(OH)_3$-am for Cr^{3+}. The experiments were conducted using a suspension containing both MnO_2 and $Fe(OH)_3$-am oxides. The data were interpreted while making one major assumption; that the two solid phases did not chemically react with one another.

A precise measurement of metal partitioning between Fe and Mn oxides is normally very difficult to attain because selective chemical extractions do not adequately distinguish between Mn oxides and amorphous Fe oxides. However in the present study, the contrasting behavior of Cr^{3+} on Mn versus Fe oxides allows a relatively straightforward assessment of Cr partitioning between these two oxides. It has demonstrated that any Cr^{3+} that is adsorbed by MnO_2 will be quickly oxidized and desorbed, while Cr^{3+} adsorbed on Fe oxides is not oxidized. The absence of analytically detectable adsorption on MnO_2, due to the rapid oxidation and desorption of Cr^{6+}, permits the determination of how much Cr has interacted with each oxide, without actually having to chemically separate the oxide phases. In other words, the amount of Cr^{6+} formed is a convenient measurement of the amount of Cr^{3+} that has reacted with MnO_2. Any un-oxidized Cr remaining in the system must be adsorbed by the Fe oxide. Hence, there was no need to rely on selective chemical extractions to determine the amount of Cr adsorbed by each oxide. However, the Cr^{6+} that is formed can be re-adsorbed by $Fe(OH)_3$-am.

Thus procedures were developed to ensure that all Cr^{6+} was selectively desorbed prior to analysis. The amount of Cr^{3+} adsorbed by $Fe(OH)_3$-am could then be assessed indirectly.

Describing the competition of multiple solid phases for trace metals is a very complicated process. Factors which may influence metal partitioning; 1) the binding capacity of each solid phase, 2) the energy of interaction between the adsorbate and the various surface sites (i.e. the relative affinities of each surface for the metal), 3) the kinetics of adsorption onto each surface, and 4), the potential effects of the solid phases on one another (i.e. one solid may tend to "coat" the other). The present experiments were designed to quantitatively measure the competition of MnO_2 and $Fe(OH)_3$-am for Cr^{3+}. The results were interpreted qualitatively in terms of the factors listed above. The specific problems addressed in this part of the study are summarized as follows:

1. The nature of the competition between MnO_2 and $Fe(OH)_3$-am for trivalent Cr. In particular, the relative effectiveness of each oxide to react with Cr^{3+} over a range of reactant concentrations.

2. The ability of MnO_2 to oxidize Cr^{3+} which is adsorbed on $Fe(OH)_3$-am). This area of research provides insight into determining whether adsorptive equilibria will respond to the addition of an additional reacting surface.

3. The effect on the competition for Cr^{3+} of precipitating the iron oxide onto the MnO_2 prior to spiking the suspension with Cr^{3+}. This set of experiments was designed to determine whether Fe oxide may influence the reactivity of MnO_2 when it occurs as a layer, or coating on the MnO_2 surface.

3.2 PROCEDURES

The procedures employed in this part are generally the same as those employed in the rest of the study, except for several modifications and additional techniques. To ensure proper formation of the iron oxide suspension, all of the experiments using multi-sorbent systems were conducted under an N_2 atmosphere. The $Fe(OH)_3$-am was prepared in the glove box in an N_2 atmosphere as described in the Methods section. All other reagents, glassware, etc. were also placed within the glove box before it was sealed and purged. Thus the experiments were all conducted under nitrogen a atmosphere from the synthesis of the Fe oxide through the filtration of the sample aliquots.

Before the multi-sorbent experiments could be conducted, it was necessary to characterize the adsorptive behavior of Cr^{3+} and Cr^{6+} on $Fe(OH)_3$-am. The adsorption of 9.6×10^{-6} M Cr (both III and VI) at pH 4.5 by various concentrations of $Fe(OH)_3$-am was determined by measuring the decrease of Cr concentration in solution after one hour of equilibration.

It was determined that a 1×10^{-3} M $Fe(OH)_3$-am suspension (measured as Fe_T) was sufficient to adsorb nearly 100% of the initial Cr, either as Cr^{3+} or as Cr^{6+} (see Table 3). This oxide concentration could also adsorb all of both oxidation states together, suggesting that the adsorption of one oxidation state did not effect the adsorption of the other under these conditions. This concentration (10^{-3} M) of $Fe(OH)_3$-am was used in all of the multi-sorbent experiments. The Fe oxide to Mn oxide ratios were varied by adjusting the amount of MnO_2.

In order to measure the amount of Cr^{6+} produced by the adsorption onto MnO_2, it was necessary to ensure that any Cr^{6+} adsorbed by the $Fe(OH)_3$-am was desorbed prior to analysis of the sample. This was accomplished by utilizing the contrasting pH dependent adsorption behavior of cations and anions. Anions, in general, tend not to adsorb above the pH_{zpc} of the oxide (see Appendix I). As adsorption is a reversible process, the desorption of Cr^{6+} was accomplished by raising the pH above the pH_{zpc} of the Fe oxide and allowing sufficient time for desorption to proceed. In a system containing 10^{-3} M $Fe(OH)_3$-am and 9.6×10^{-6} M Cr^{6+}, complete desorption was attained by raising the pH of the suspension to 10.0 with 1.0 M NaOH and allowing the system to equilibrate for 45 minutes. This desorption process was shown to be specific for Cr^{6+} by repeating the previous experiment with both oxidation states adsorbed to the Fe oxide. The data from this procedure is presented on

TABLE 3

ADSORPTION OF Cr SPECIES BY $Fe(OH)_3$ AT pH 4.5

Conc. of $Fe(OH)_3$ (M)	% Cr^{3+} Adsorbed*	% Cr^{6+} Adsorbed*
1×10^{-3}	100	96
5×10^{-4}	98	82
1×10^{-4}	49	28
* Initial [Cr] = 9.6×10^{-6} M		

TABLE 4

SELECTIVE DESORPTION OF Cr^{6+} FROM 1×10^{-3} M $Fe(OH)_3$ BY RAISING pH TO 10 FOR 45 MINUTES

Cr Adsorbed (mg/l)	Cr_T Desorbed (mg/l) Replicate		Cr^{6+} Desorbed (mg/l) Replicate	
	1	2	1	2
0.50 Cr^{3+}	0.02	0.00	0.00	0.00
0.25 Cr^{3+}/0.25 Cr^{6+}	0.24	0.27	0.24	0.25
0.50 Cr^{6+}	0.50	0.49	0.50	0.48

Table 4. All of the desorbed Cr was verified to be hexavalent by the Cr^{6+} extraction. Five replicate samples (approximately 20 ml each) of a suspension containing adsorbed Cr^{6+} were also collected, adjusted to pH 10, and analyzed for Cr^{6+} to ensure that this procedure was reproducible and the aliquots were representative of the system. The results, shown on Table 5, show that the technique could be employed with good accuracy and precision.

With a measurement of Cr^{6+} and total Cr it was possible to determine the concentration of all forms of Cr species in an experimental system, including the concentrations of Cr^{3+} and Cr^{6+}, as both dissolved and adsorbed species. For each time interval in which a sample was collected, the following set of procedures were applied in order to determine all forms of Cr in the sample:

1. Immediate filtration (IF). An aliquot system was immediately passed through a 0.22μm filter. This allowed for the measurement of total dissolved Cr (i.e. Cr^{3+} and Cr^{6+} that was not adsorbed).

2. Immediate filtration followed by Cr^{6+} extraction (IFE). A split portion of the (IF) sample was used to determine the concentration of dissolved Cr^{6+}. The Cr^{3+} in solution was then computed as (IF) - (IFE).

3. Immediate Base Addition followed by Cr^{6+} extraction (IBE). 100μl of 1.0 N NaOH was added to an unfiltered aliquot of sample (to pH = 10) and the sample allowed to

TABLE 5

REPLICATE ANALYSIS OF THE DESORPTION
OF Cr^{6+} FROM $Fe(OH)_3$ BY RAISING pH TO 10
$Cr^{6+} = 9.6 \times 10^{-6}$ M; $Fe(OH)_3 = 1 \times 10^{-3}$ M

Replicate	% Cr Desorbed*
1	96
2	98
3	100
4	99
5	97

* Average of two readings on AAS

set for 45 minutes. After this time the sample was filtered and subjected to Cr^{6+} extraction. This procedure caused the desorption of all Cr^{6+} from the Fe oxide and the precipitation and/or adsorption of any Cr^{3+} remaining in solution (as verified by measuring total Cr in solution as well). Thus the Cr^{6+} adsorbed on Fe oxide was computed by (IBE) - (IFE). The Cr^{3+} adsorbed onto Fe oxide was then the initial Cr spike minus the amount of solution Cr and the amount of adsorbed Cr^{6+}, or $Cr^{3+}_{initial}$ - (IF) - (IBE).

This entire sampling scheme was not necessary for every sample taken throughout the experiment. In fact, there was little or no solution Cr present after the first ten minutes of the reaction, after which time the Cr was adsorbed either as Cr^{3+} or Cr^{6+}. At this point in the reaction, Cr^{6+} was measured by the (IB)E procedure and the Cr^{3+} adsorbed was the difference between this and the original Cr concentration.

While Cr^{3+} remained in solution there was the potential for continuing oxidation after the pH was adjusted to 10. The potential for this occurrence was investigated by an oxidation experiment (conducted without iron oxide) in which two replicates were taken; one of which was filtered immediately, the other of which was raised to pH 10 (to precipitate Cr^{3+} hydroxide) and allowed to set for 45 minutes before filtration. A comparison of three sets of replicates taken at different time intervals is shown on

Figure 45. The oxidation reaction clearly did not stop instantaneously when the pH was raised. Thus, until the reaction is essentially complete, the amount of Cr^{6+} measured is probably too high. The presence of iron oxide probably further decreases the discrepancy, as Cr^{3+} may adsorb or precipitate on the oxide surface as well as precipitate as a hydroxide. However, the oxidation versus time curves presented below may not be accurate in the early time intervals. At the completion of the reaction, when no Cr is present in solution, the amount of Cr oxidized accurately reflects the amount of Cr which has interacted with MnO_2.

Because of the complexity of the reaction and the experimental procedures used to obtain the data, the reproducibility of the experimental results were tested. Figure 46 shows the results of two identical multi-sorbent experiments ($Fe_T = 10^{-3}$ M, $MnO_2 = 2.3 \times 10^{-5}$ M, pH = 4.5) conducted exactly one month apart. The amount of Cr^{6+} formed in the multi-sorbent system is highly reproducible. Although complex, the reactions are apparently well defined given a certain set of conditions.

3.3 RESULTS AND DISCUSSION

3.31 The General Nature of the Competition for Cr(III)

The first multi-sorbent experiments conducted were designed to determine the nature of the "competition"
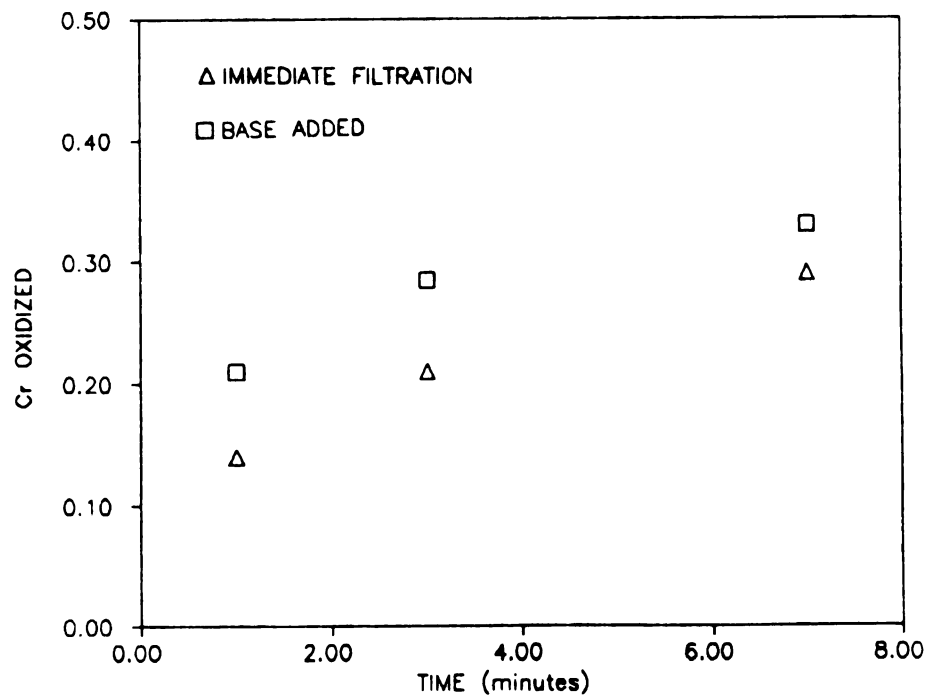
Figure 45. Amount of Cr Oxidized in Filtered Versus pH Stabilized Replicates
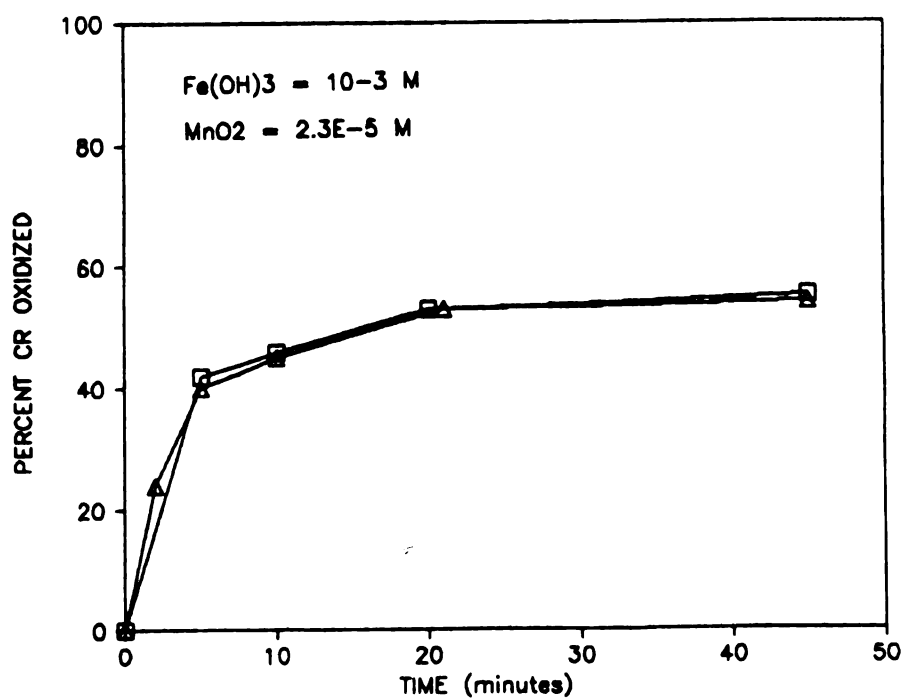
Figure 46. Reproducibilty of Mixed-Oxide Oxidation Rates

between Fe and Mn oxides for Cr^{3+} with as little potential for one oxide affecting the other as possible. In these experiments the 10^{-3} M $Fe(OH)_3$ suspension was precipitated and aged for four hours followed by the addition of an aliquot of MnO_2 suspension. This multi-component suspension was allowed to "equilibrate" for only a few minutes before an aliquot of Cr^{3+} was added to bring the initial Cr^{3+} concentration to 9.6 X 10^{-6} M. As a starting point, the initial MnO_2 concentrations chosen were similar to those studied in single sorbent systems, even though this meant that on a molar basis the Fe oxide would be in much higher concentrations than the MnO_2.

Somewhat unexpectedly, these low levels of MnO_2 (relative to the $Fe(OH)_3$-am) were able to oxidize significant amounts of the Cr spike. The amount of Cr oxidized (as a percentage) versus time for five MnO_2 concentrations, ranging from 1.2 to 9.2 X 10^{-5} M, are shown on Figure 47. As the graph shows, increasing the amount of MnO_2 increases the amount of Cr^{3+} oxidized (and consequently decreases the amount adsorbed onto $Fe(OH)_3$-am). This point is further illustrated in Figure 48 in which the molar amount of Cr oxidized at the end of the experiment is plotted against the initial MnO_2 loading. There is a linear relationship between the amount of MnO_2 and the amount of Cr oxidized.

Even in the presence of a large excess of $Fe(OH)_3$-am, much of the Cr was oxidized, which suggests MnO_2 competes very favorably with $Fe(OH)_3$ for Cr^{3+}. This is further
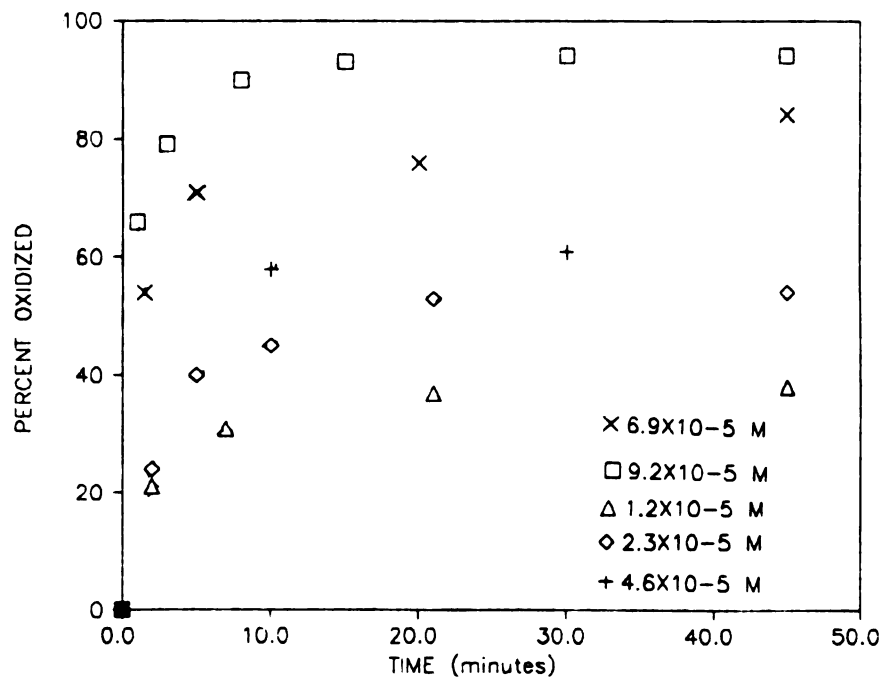
Figure 47. Percent Cr Oxidized in Mixed-Oxide Systems as a
Function of MnO_2 Loading
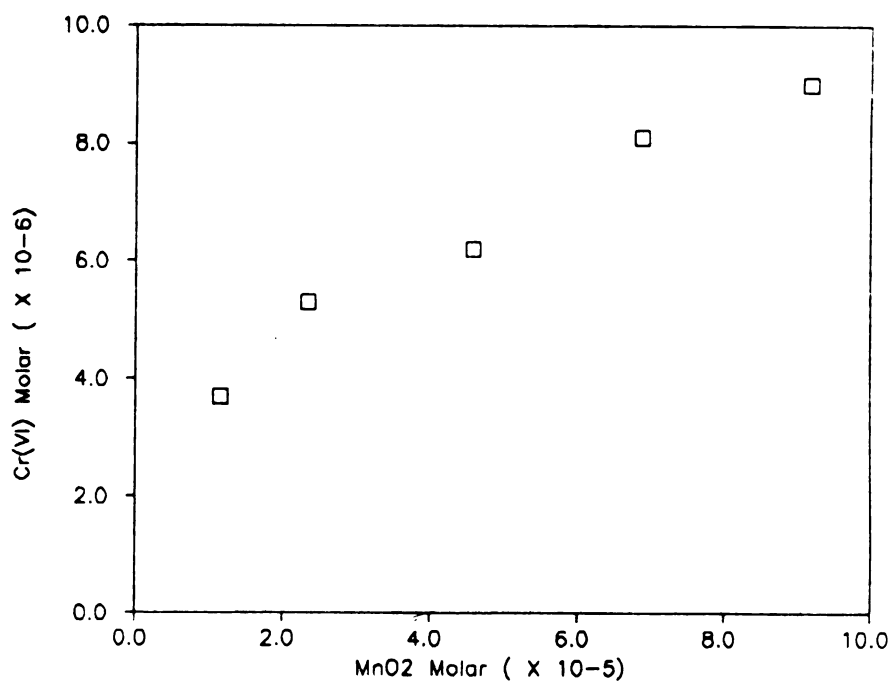
Figure 48. Total Amount of Cr Oxidized in Mixed-Oxide
Systems Versus Initial MnO_2 Concentration

emphasized on Figure 49 which shows the percent Cr oxidized versus the molar ratio of $Fe(OH)_3$-am to MnO_2. Even with an 83-fold excess of $Fe(OH)_3$-am, 38% of the Cr^{3+} was still oxidized by MnO_2 and 62% adsorbed to the Fe oxide. When the $Fe(OH)_3$ excess is reduced to 11 times, 94% of the Cr is oxidized by the MnO_2.

The measurement of solution Cr^{3+} shows that the reaction seems to be nearly complete when Cr^{3+} is depleted from solution, although a small quantity of Cr is oxidized after Cr^{3+} is no longer measurable in solution. This relationship is shown on Figure 50 which is a graph of the percent of the initial Cr oxidized and the percent of Cr remaining in solution. This result suggests that the Cr oxidation occurs primarily through the successful competition for solution Cr by MnO_2, rather than by the oxidation of Cr adsorbed to the $Fe(OH)_3$-am surface. However the potential for oxidation of Cr adsorbed onto the $Fe(OH)_3$ surface was further tested (see below).

The significant oxidation of Cr by MnO_2 in the presence of a nearly two order of magnitude molar excess of $Fe(OH)_3$ presents an interesting problem. Quantitative modeling of adsorption reactions has shown that the binding capacity of an oxide, usually expressed as moles of surface sites per mole of oxide, and not the molar quantity of the oxide, is the correct means of comparing oxide reactivities. The binding capacities of Mn and amorphous Fe oxides reported in other studies (see Appendix I) shows that these two oxides
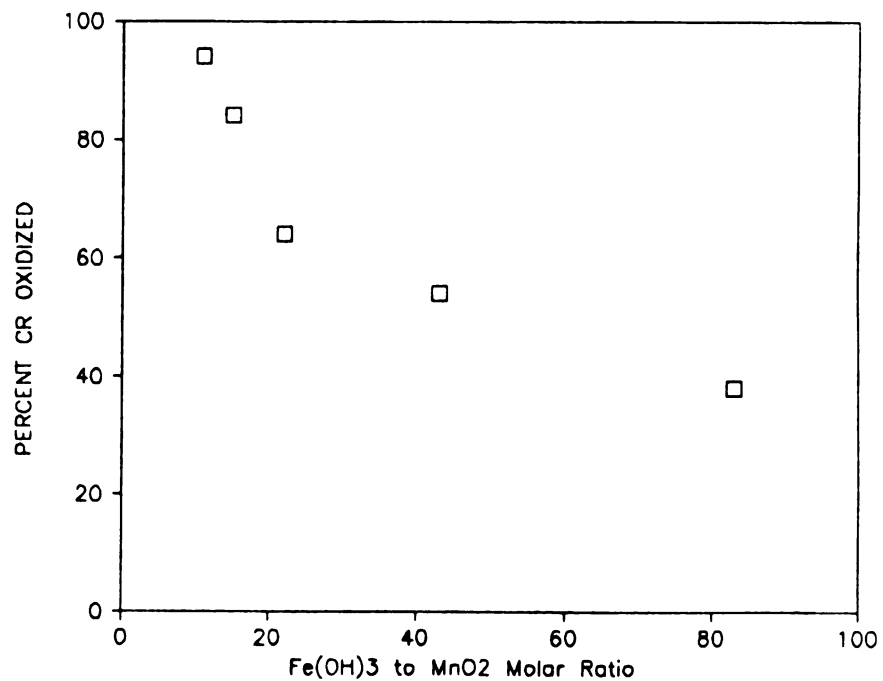
Figure 49. Percent Cr Oxidized Versus the Initial Molar
Ratio of Fe(OH)$_3$ to MnO$_2$
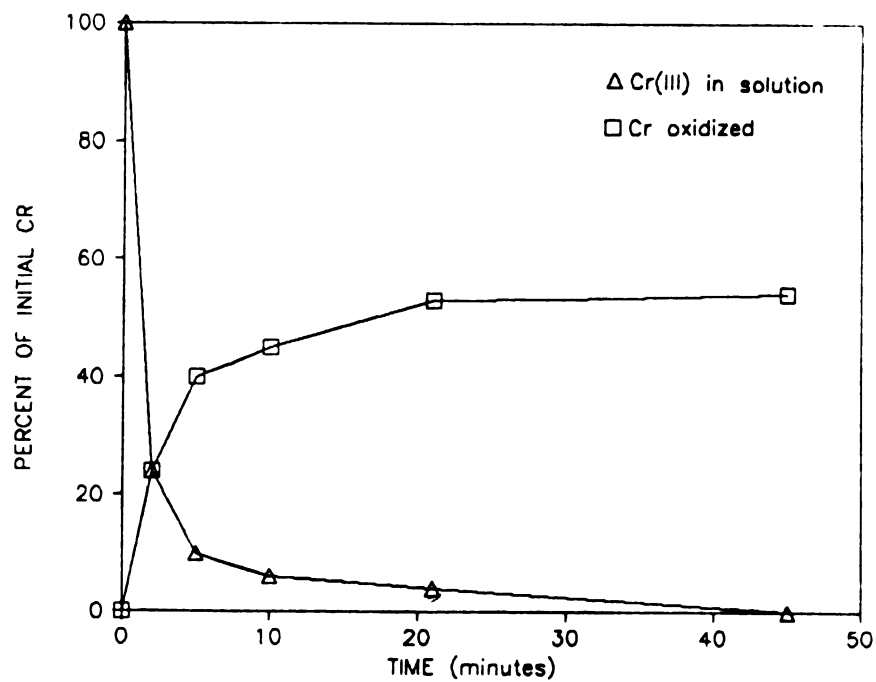
Figure 50. Amount of Cr^{3+} in Solution and Cr Oxidized
Versus Time in a MIxed-Oxide System

have similar binding capacities. However, the adsorption capacity of an oxide is a pH dependent quantity and most binding capacities are determined at higher pH's. Mn oxides have been shown to have a higher adsorption capacity than Fe oxides at low pH's (see Appendix I) so it is conceivable that the molar excess of $Fe(OH)_3$-am is deceiving. The binding capacity of the $Fe(OH)_3$-am used in this study for 9.6×10^{-6} M Cr^{3+} at pH 4.5 was found to be approximately 0.07 moles of Cr per mole of $Fe(OH)_3$-am. The binding capacity of MnO_2 for Cr was not measured as new surface sites are generated during the redox reaction, making this measurement impossible. The binding capacity of MnO_2, even if taken to represent the total of all sites present initially plus those created during the reaction, cannot exceed 0.67 moles Cr/moles MnO_2, as this represents the stoichiometric oxidation equivalent. In other words, only 0.67 moles of Cr can be adsorbed per mole of MnO_2 as all of the MnO_2 would be subsequently reduced and dissolved. This would suggest there can be at most, an order of magnitude difference in the binding capacities of the two oxides for Cr. From this argument it is apparent that the difference in binding capacities alone cannot account for the strong competition by MnO_2, as significant amounts of Cr is oxidized when the Fe oxide is in a nearly two-order of magnitude excess.

Besides the number of surface sites available on each oxide, the energy and rate of the reaction between Cr and

the various surface sites may influence the partitioning between these two sorbents for Cr. If a higher energy bond is formed between Cr and the surface sites on one oxide as compared to the other, it would be expected that this oxide would compete favorably. This is analogous to solution complexes in multi-ligand systems, where metals in solution show a higher degree of coordination with the ligand that forms the higher energy bond. Qualitatively, past research would suggest that the MnO_2-Cr bond should be stronger than the $Fe(OH)_3$-Cr bond at the pH's used in these experiments. This results from the favorable surface charge on MnO_2 at pH 4.5 and the apparent ability of this surface to bond with unhydrolyzed metal species (see Appendix I).

The kinetics of adsorption may also influence the resulting distribution of Cr between the two oxide surfaces. Although adsorption reactions have been included in equilibrium models, it has not been demonstrated that the various surface sites in multi-sorbent systems behave like ligands in solution, where equilibrium speciation is attained based on the concentration of each ligand and coordination energy of each complex. The adsorptive equilibria in these multi-phase systems could be much slower to respond to the addition of new species than metal-ligand equilibria. If this is true, the adsorption kinetics of Cr onto the Fe oxide and Mn oxide surfaces may influence the resulting distribution. If the adsorption of Cr^{3+} onto MnO_2

is faster than the adsorption onto $Fe(OH)_3$, this may explain why MnO_2 can compete so effectively.

To explore this possibility, the kinetics of adsorption of 9.6×10^{-6} M Cr^{3+} on 10^{-3} M $Fe(OH)_3$-am was compared to the oxidation rate of the same amount of Cr^{3+} by 2.3×10^{-5} M MnO_2. In a mixed-oxide system containing the same concentrations of these components, 54% of the initial Cr^{3+} was oxidized and 46% adsorbed by the Fe oxide (see Figure 47). As shown on Figure 51, the adsorption by $Fe(OH)_3$-am was significantly faster than the oxidation by MnO_2. For this set of conditions, the kinetics of the single sorbent systems would predict that more Cr^{3+} should have been adsorbed by $Fe(OH)_3$.

3.32 The Effects of the Order of Addition of the Reagents

In all previously described experiments, the oxide phases were mixed after they were precipitated, and the Cr^{3+} was added last. In the following experiments the competition of these two oxides for Cr was investigated for the following changes in the order of addition of the reagents: 1) the $Fe(OH)_3$ was precipitated on the MnO_2, and 2) the Cr was added to the $Fe(OH)_3$ before the addition of MnO_2.

Since the kinetics suggest that Fe oxide should compete favorably for solution Cr, then either 1) the oxides interact such that the reactivity of one oxide surface (i.e. $Fe(OH)_3$-am) is reduced, or 2) the MnO_2 can simply "out-
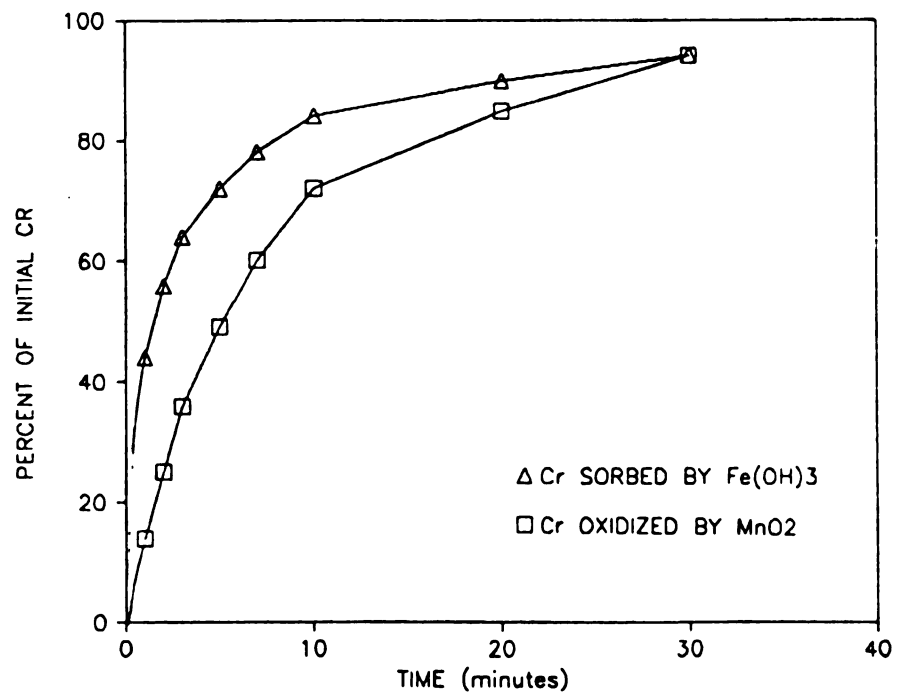
Figure 51. Kinetics of Adsorption by Fe(OH)$_3$ and Oxidation
by MnO$_2$

compete" the $Fe(OH)_3$ due to a higher affinity of Cr for the MnO_2 surface.

If the Mn oxide were to coat the Fe oxide and block binding sites, this could help explain the ability of MnO_2 to compete favorably. This particular situation was not addressed in the present research. However, the potential of Fe oxide to affect the reactivity of MnO_2 was investigated. To explore this problem, the aliquot of the MnO_2 stock suspension was added to the $Fe(NO_3)_3$ solution prior to raising the pH and hydrolyzing the Fe. This, at least theoretically, should have caused some Fe oxide to precipitate on the MnO_2 particles. Multi-substrate suspensions were prepared in this manner for two different MnO_2 loadings. Then, Cr^{3+} was added to the system, samples were collected and analyzed as described above. The data for the amount of Cr oxidized are shown on Figures 52 and 53. Also shown on these graphs is the amount of Cr oxidized for experiments with identical oxide concentrations, in which the MnO_2 was added to the system after the $Fe(OH)_3$-am had been precipitated and aged. There is a significant decrease in the amount of Cr that was oxidized for both MnO_2 loadings when the iron oxide is precipitated on the MnO_2 surface. This clearly demonstrates that there is a potential for one oxide to influence the reactivity of the other. It is still not known whether the addition of MnO_2 to pre-formed $Fe(OH)_3$-am causes a reduction of the reactivity of the Fe oxide, but this possibility cannot be
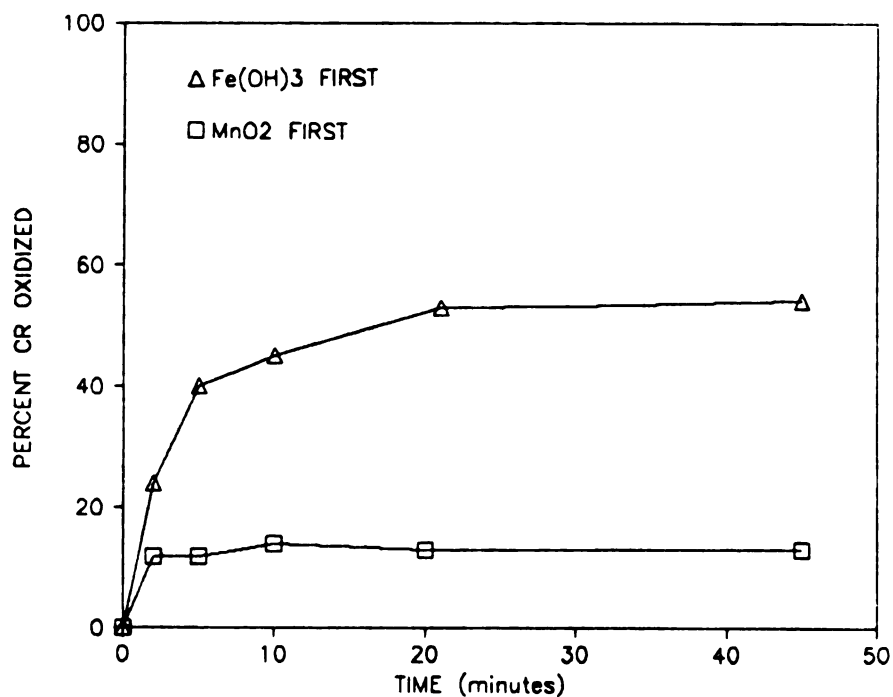
Figure 52.   Percent Cr Oxidized in Mixed-Oxide System When
Fe(OH)$_3$ is Precipitated on 2.3 X 10^{-5} M MnO$_2$
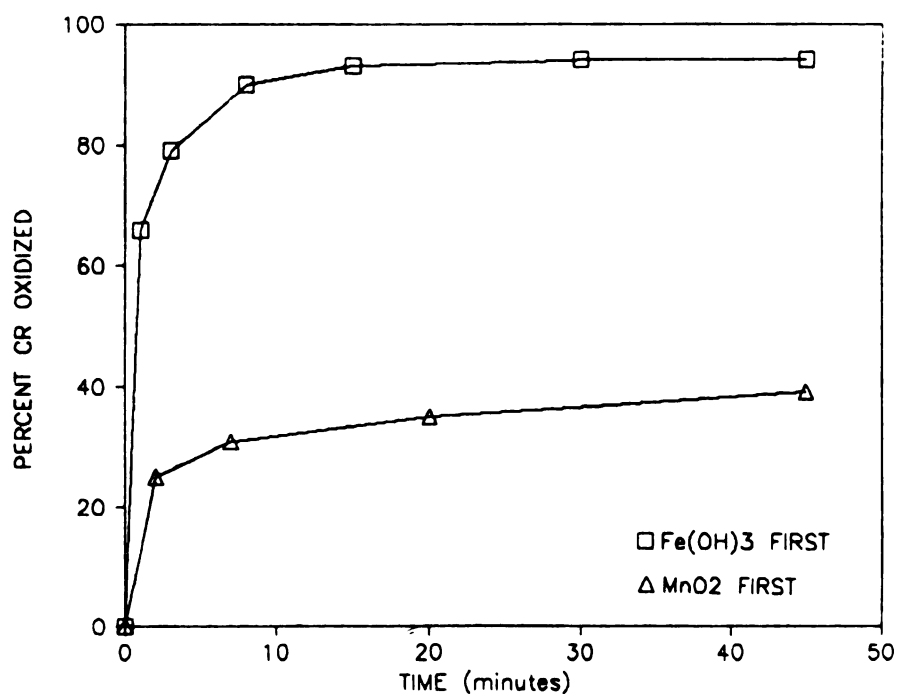
Figure 53.   Percent Cr Oxidized in Mixed-Oxide System When
Fe(OH)$_3$ is Precipitated on 9.2 X 10^{-5} M MnO$_2$

ruled out. If the MnO_2 does not effect the reactivity of the $Fe(OH)_3$, then Cr^{3+} must have a higher affinity for the MnO_2 surface.

As described above, the oxidation of Cr^{3+} by MnO_2 is nearly complete when there is no longer any Cr^{3+} in solution. This suggests (but does not prove) that Cr^{3+} adsorbed onto $Fe(OH)_3$-am is no longer reactive with respect the MnO_2 surface. To determine whether Cr^{3+} adsorbed to the $Fe(OH)_3$ surface can be oxidized by MnO_2, an experiment was conducted in which the initial Cr^{3+} spike (9.6×10^{-6} M) was allowed to adsorb onto the $Fe(OH)_3$-am (10^{-3} M) at pH 4.5, prior to the addition of the MnO_2 suspension (2.3×10^{-5} M). If oxidation occurs under these conditions it would suggest Cr^{3+} adsorbed to $Fe(OH)_3$ becomes desorbed upon the addition of MnO_2. This would strongly suggest that adsorptive equilibria does respond to the addition of a new solid phase.

The results of this experiment are shown on Figure 54. The data show that approximately 6% of the initial Cr spike was oxidized after 1.0 hour. The reaction does not appear to have been completed during this time interval. Also shown on this figure is the oxidation rate in a control experiment containing the same reactant concentrations in which the Cr spike was added to the mixed oxide suspension. Increasing the amount of MnO_2 to 9.2×10^{-5} M and increasing the reaction time to 2.0 hours showed that significant oxidation does occur (see Figure 55) although at a much
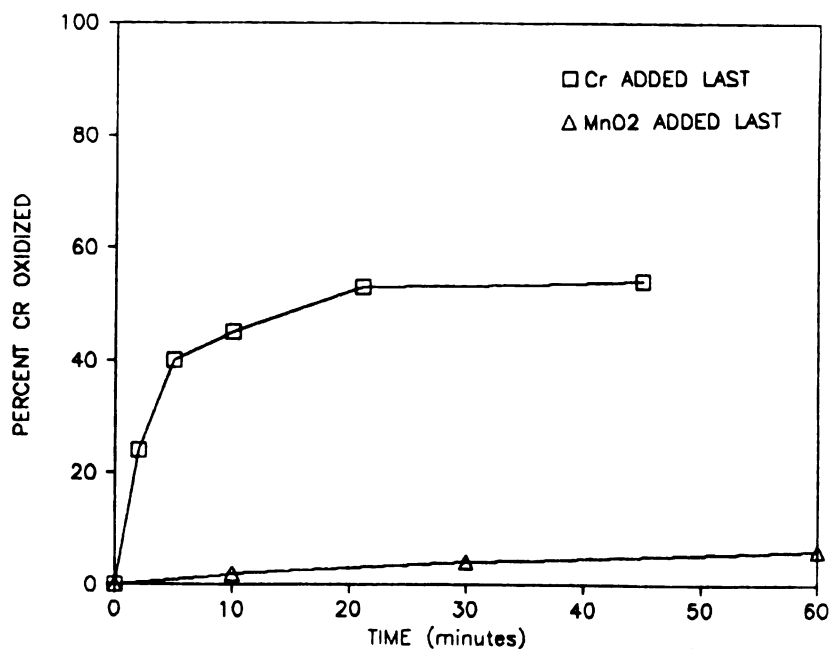
Figure 54. Percent Cr Oxidized in Mixed-Oxide System When Cr^{3+} is Adsorbed to $Fe(OH)_3$ Prior to Addition of 2.3×10^{-5} M MnO_2
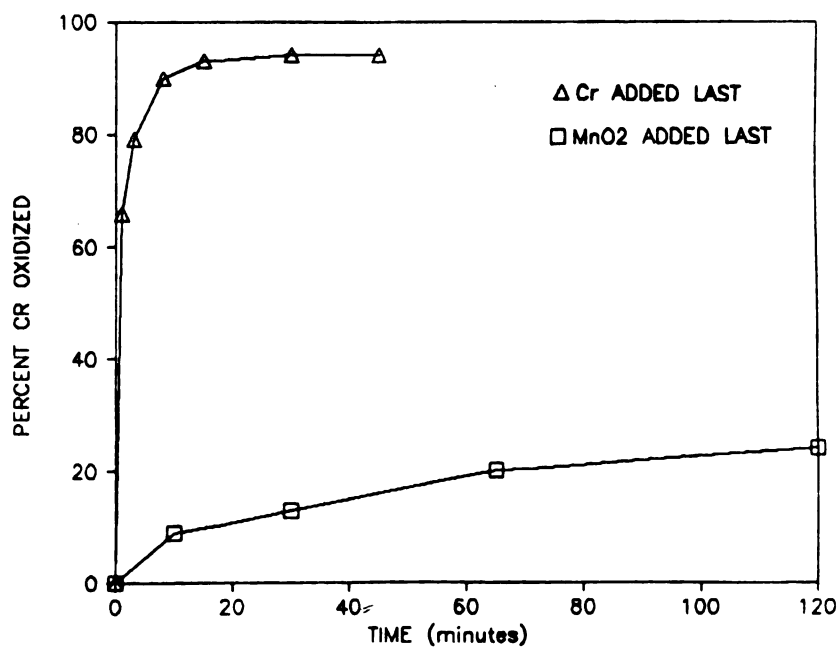
Figure 55. Percent Cr Oxidized in Mixed-Oxide System When Cr^{3+} is Adsorbed to $Fe(OH)_3$ Prior to Addition of 9.2×10^{-5} M MnO_2

slower rate than under than the control. These results demonstrate that MnO_2 can oxidize Cr that was adsorbed to $Fe(OH)_3$.

Since the reaction was apparently incomplete in both of the above experiments, a long term experiment was conducted to see if the amount of Cr oxidized would eventually reach that measured in the experiments where Cr was the last reagent added. An experiment with the same initial concentration of reactants as the one described on Figure 54 was continued for 43 days. The results are shown on Figure 56. The amount of Cr oxidized reached a maximum within 19 days. At this time 50% of the initial Cr spike had become oxidized. This is only slightly less than the 54% oxidized in the identical experiment in which Cr was added as the last reactant.

This result would appear to suggest that the amount of Cr oxidized in the multi-sorbent system is dependent on an equilibrium distribution between the Mn and Fe oxides. When all of the initial Cr is first adsorbed to the $Fe(OH)_3$ the adjustment to equilibrium conditions occurs much slower. This further suggests that the binding energies and binding capacities, rather than the kinetics of adsorption, influence the partitioning of Cr in this multi-sorbent system. If this interpretation is correct, it would suggest that Cr^{3+} has an unusually high affinity for the MnO_2 surface as compared to $Fe(OH)_3$. It would also suggest that
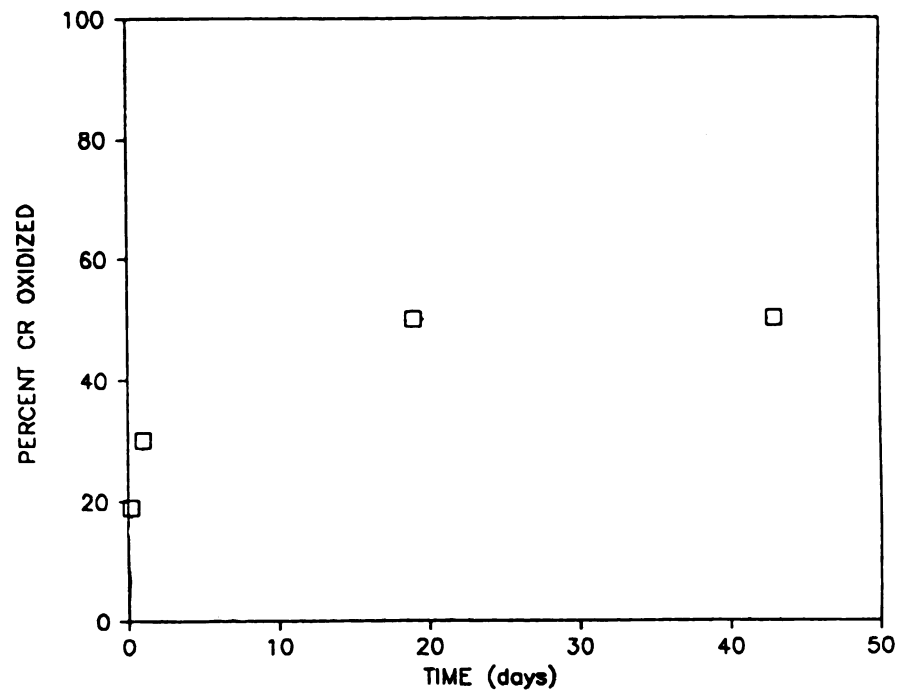
Figure 56. Percent Cr Oxidized in Long Term Mixed-Oxide System When Cr is Adsorbed to Fe(OH)$_3$ Prior to Addition of MnO$_2$

the modeling of multi-sorbent adsorption equilibria can be treated in a similar manner to metal complexation.

3.4 SUMMARY AND CONCLUSIONS

The competition between synthetic MnO_2 and $Fe(OH)_3$-am for Cr^{3+} has been evaluated in multi-sorbent experiments, with the amount of Cr oxidized as a measure of the Cr adsorbed by the MnO_2. The results show that considerable Cr^{3+} was oxidized even in the presence of a large molar excess of $Fe(OH)_3$, suggesting that MnO_2 competes successfully for this trace metal. Reasons for these results were not clear and the following ideas were explored through additional experimentation; 1) the binding capacity of MnO_2 at pH 4.5 is much higher than that of $Fe(OH)_3$, 2) the $Cr-MnO_2$ bond is a higher energy bond and the results reflect the equilibrium speciation between Cr and the various sites, 3) the kinetics of the oxidation reaction are faster than those for adsorption onto $Fe(OH)_3$, and 4) the presence of MnO_2 reduces the reactivity of the $Fe(OH)_3$ surface by blocking surface sites.

Although the surface capacity of MnO_2 is likely to be considerably higher than that of $Fe(OH)_3$ at pH 4.5, especially considering that the oxidation reaction may generate new sites, it does not appear that this difference in binding capacity actually offsets the large molar excess of $Fe(OH)_3$ in these experimental systems. In other words, there was probably more available binding sites on the Fe

oxide than the MnO_2. Furthermore, comparison of single-sorbent kinetics shows that the oxidation reaction is actually slower than the adsorption of Cr onto ($Fe(OH)_3$. This suggests the effective competition by MnO_2 is not simply a result of kinetic considerations.

The strong competition by MnO_2 for Cr^{3+} in mixed sorbent systems is apparently a result of a higher energy of interaction between Cr and MnO_2 surface sites than Cr and $Fe(OH)_3$ surface sites. This is supported by the fact that there is an equilibrium distribution between oxidized Cr and Cr adsorbed on $Fe(OH)_3$, for a given set of experimental conditions, regardless of the order of addition of the reactants. In other words, the same amount of Cr is oxidized whether the Cr spike is added to a mixed oxide suspension or allowed to adsorb to $Fe(OH)_3$ prior to the addition of MnO_2. The potential of one oxide to affect the reactivity of the other was demonstrated, although it seems unlikely that the MnO_2 added as a solid could have a large effect on the $Fe(OH)_3$. This is supported by the fact that MnO_2 competes favorably even when the Cr is adsorbed onto the $Fe(OH)_3$ prior to the addition of the MnO_2.

SUMMARY AND CONCLUSIONS

Research has been conducted to explore the nature and controls of the oxidation of chromium by manganese oxide. This reaction was investigated under controlled laboratory conditions using a synthetic manganese oxide which has similar properties to manganese oxides found in soils and sediments. This section of the report begins with a summary of the principal findings of this investigation. This summary is followed by a brief discussion of these findings in terms of the current knowledge of surface chemistry. Finally, the practical environmental significance of the results are discussed and suggestions for continued areas of research are proposed.

1.0 SUMMARY

The primary findings of this research can be summarized as follows:

1. At low pH's, where Cr^{3+} is soluble, the oxidation of Cr^{3+} by low crystallinity MnO_2 is very rapid and the reaction proceeds to completion or near completion. The completeness of the reaction suggests the reaction is autocatalytic.

2. The reaction stoichiometry, as determined by the measurement of reaction products, confirms the general

hypothesized reaction stoichiometry for pH 4.5 given by
the equation:

$$2 \ Cr(OH)^{2+} + 3 \ MnO_2 = 2 \ HCrO_4^- + 3 \ Mn^{2+}$$
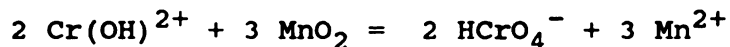
3. The reaction rate is sensitive to changes in the relative
   amounts of MnO_2 and Cr^{3+} present. At low MnO_2 to Cr^{3+}
   ratios the reaction rate increases linearly to increases
   in the MnO_2 concentration. At an oxide to metal molar
   ratio of approximately 2, the change in the reaction
   rate no longer increases in proportion to the increase
   in oxide concentration. At high MnO_2 to Cr^{3+} ratios,
   large increases in the concentration of MnO_2 cause only
   small increases in the oxidation rate.

4. At low MnO_2 to Cr^{3+} ratios, the reaction can be described
   by the following rate equation:

$$d[MnO_2]/dt = -k[MnO_2]^{1.0}[Cr^{3+}]^{0.5}$$

   This rate equation breaks down after considerable MnO_2
   has been dissolved, suggesting the surface properties of
   the oxide or the reaction mechanisms are changing.

5. There is no measurable influence on the reaction rate
   induced by changing the solution pH when the solution is
   below saturation with respect to $Cr(OH)_3$. At higher
   pH's, the formation of $Cr(OH)_3$ causes a large decrease
   in the rate and extent of the reaction. However, the

amount of Cr oxidized exceeds the reported solubility of $Cr(OH)_3$.

6. Increasing the ionic strength with an inert electrolyte causes a decrease in the reaction rate, probably due to the increased flocculation of the oxide particulates.

7. The reaction rate is not sensitive to copper adsorbed on the MnO_2 surface prior to the addition of Cr^{3+}, suggesting that there was either an abundance of sites such that Cu adsorption did not affect the oxidation rate or competition for sites does not influence the oxidation rate.

8. MnO_2 competes effectively for Cr^{3+} with $Fe(OH)_3$ even when the Fe oxide is present in a large molar excess to the MnO_2. The amount of Cr which is oxidized by MnO_2 in a mixed-oxide system does not depend on the order of addition of the reagents, although the rate of reaction is highly dependent on the experimental procedure employed. These preliminary results suggest that the amount of Cr^{3+} oxidized versus the amount adsorbed by $Fe(OH)_3$ is controlled by an equilibrium distribution of the Cr between the two oxides.

2.0 DISCUSSION

Past research (Schroeder and Lee, 1975; Van der Weijden and Reith, 1982) has suggested that the oxidation of Cr by

Mn oxides takes place following the adsorption of this metal on the oxide surface. One of the primary goals of this research was to determine whether the experimental data can be explained in terms of adsorption theory. The results listed above can, in some instances, be adequately explained with surface chemistry models. In other instances, the data are not readily interpretable in terms of an adsorption controlled reaction.

Qualitatively, adsorption models predict the influence of the oxide to metal ratio on the reaction rate which was observed in the present experiments. At low MnO_2 to Cr^{3+} ratios, an increase in the amount of Cr^{3+} was shown to actually cause a decrease in the reaction rate. This behavior is consistent with the prediction for an adsorption controlled reaction, as the fraction of metal which is adsorbed decreases with an increasing metal to oxide ratio. The data from this research also demonstrate that the reaction rate becomes insensitive to increasing MnO_2 concentrations at high MnO_2 to Cr^{3+} ratios. This is also predicted for an adsorption controlled reaction. When enough oxide is present to adsorb the maximum amount of the metal which can be adsorbed at that particular pH, an increase in the oxide concentration would be predicted to result in little increased adsorption. If the reaction is adsorption controlled, it stands to reason that the oxidation rate should also experience only a minor increase.

Another finding which would appear to be consistent with past research on adsorption is the decreasing reaction rate with increasing ionic strength. The rate of adsorption of trace metals, particularly on Mn oxides (Morgan and Stumm, 1964) has been shown to decrease with increasing ionic strength. Although this phenomena has not been adequately investigated, the slower adsorption rate with increasing ionic strength appears to be caused by a decrease in the effective surface area of the oxide due to the increased particle size caused by flocculation. Only the rate of the reaction, not the extent was decreased by increasing the ionic strength.

The finding most difficult to reconcile with adsorption theory is that the reaction proceeds at pH 4.5 with metal to oxide ratios that are insufficient to cause measurable adsorption of other trace metals. However, there are several points to consider which may resolve this question. The first point is that Cr^{3+} may have a much stronger affinity for oxide surfaces than other trace metals. Indeed, Cr^{3+} was found to adsorb the strongest of a series of transition metals on amorphous iron hydroxide (Leckie et al., 1980). This suggests that Cr may inherently adsorb strongly to many surfaces, possibly because this metal has a higher positive charge than most other stable metal species. Thus a comparison of the adsorptive behavior of chromium to other metals on Mn oxide may not be appropriate.

Besides the general tendency for chromium to adsorb more strongly than other metals, there may an intrinsic affinity of Cr for the MnO_2 surface in particular. Both Mn^{4+} and Cr^{3+} are 3d transition metals which have very high crystal field stabilization energies in octahedral coordination. Given that 1) several mechanisms of adsorption, including lattice substitution, have been demonstrated to occur on Mn oxides (see Appendix I) and 2) as many as half of the octahedral sites may be vacant in poorly ordered MnO_2 (Burns and Burns, 1979), it is possible that Cr not only adsorbs to surface sites, but also becomes incorporated within the oxide structure by displacing water or electrolytes from the vacant octahedral sites. This too could contribute to a uniquely high affinity of Cr^{3+} for the MnO_2 surface which may drive the reaction under these experimental conditions.

The extensive oxidation of trace metals at the MnO_2 surface at low pH's and oxide to metal ratios is not unique to this study. Postma (1985) has shown that ferrous iron (Fe^{2+}) is oxidized to ferric iron by MnO_2 at low pH's and low MnO_2 to Fe^{2+} ratios. For instance, at pH 3.0, 100% of the Mn oxide was reduced with initial Fe^{2+} and MnO_2 concentrations of 1×10^{-3} moles and 1.5×10^{-5} moles, respectively. This study did not address the problem from an adsorption perspective, although adsorption was presumed to have preceded oxidation.

Perhaps the reason that these results do not appear to conform to the predictions of an adsorption controlled

oxidation reaction is actually more fundamental. The thermodynamic model of adsorption assumes that the surface sites are a fixed quantity. In the reaction between Cr^{3+} and MnO_2 the amount of surface sites are not fixed as the reduction and release of structural Mn must generate additional adsorption sites. When this autocatalytic nature is considered it becomes apparent only a small fraction of the Cr^{3+} need be adsorbed by the initial MnO_2 surface. After this initial Cr^{3+} is adsorbed, oxidized and desorbed, new sites are available for the next fraction of the initial Cr^{3+}. Thus even if the initial adsorption capacity of the oxide is small, the reaction can proceed until there are not enough sites left to cause adsorption. From a thermodynamic standpoint, the Cr^{3+} in solution may be reacting to the concentration of all potential surface sites, not just the sites initially present.

An oxidation reaction which is proceeded by adsorption imposes certain limitations on the mechanism of the oxidation reaction. Based on the model of the oxide/metal interactions presented in current adsorption theories, electron transfer between the oxide metal and the adsorbed metal would occur after an inner-sphere complex is formed. Zinder, et al., (1986) have shown that reductive dissolution of Fe oxides is facilitated by the coordination of ligands at the oxide surface and that the electron transfer takes place with the hydroxide ions as an electron "bridge". Based on these ideas, a conceptual model of Cr oxidation

following adsorption onto MnO_2 is presented on Figure 57. As Cr^{3+} at pH 4.5 is primarily $Cr(OH)^{2+}$ (Rai et al., 1986), this would suggest that a bidentate bond would be formed between Cr^{3+} and the surface hydroxyls. This model suggests that each Cr^{3+} ion would have to donate electrons to at least 2 adjacent surface Mn^{4+} ions. It is apparent that the adsorption of 2 adjacent Cr ions to reduce three Mn ions, as shown in the figure, is not plausible, as such a restriction would cause surface sites to become limited quickly. More likely, intermediates are formed and the reaction has several steps. Whether or not the conceptual model presented above represents an approximation of the actual reaction mechanism, the overall evidence suggests that the reaction is preceded by adsorption.

3.0 ENVIRONMENTAL SIGNIFICANCE

The ultimate goal of research such as described in this report is to increase our knowledge of the fundamental reactions which may be important in understanding and predicting the fate of trace metals in the environment. The results of this study, which represent only a small step towards this goal, have provided some additional insight on the potential controls of chromium geochemistry in environment.

The findings of this study have demonstrated that the potential for oxidation of Cr to the toxic, mobile hexavalent form by Mn oxides certainly does exist. At pH's
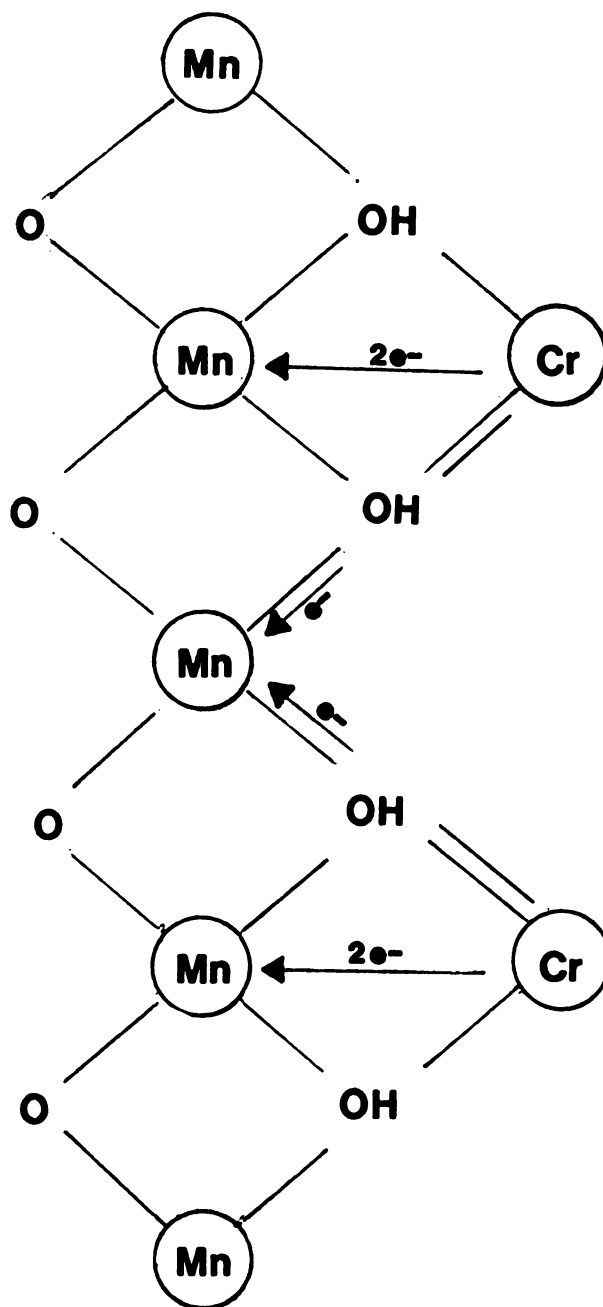
Figure 57. Conceptual Model of the Adsorption
and Oxidation of Cr by Mn Oxide

representing the very low range of natural waters, but which are close to the values found in some in soils, this reaction would appear to be potentially important. Additionally, the reaction could be important in polluted waters with low pH's. The lowering of the pH can solubilize Cr^{3+} which may then be oxidized if sufficient Mn oxides are present.

The preliminary results of this research also suggest that Cr solubility can be increased in the presence of Mn oxides. This may be an important reaction in the soils and sediments of environments with more neutral pH's. The insolubility of the hydroxide species is responsible for the immobility of Cr in many environments. If Mn oxides can cause dissolution of Cr hydroxide by oxidizing the Cr^{3+} in solution, then the mobility of this species may be increased.

The oxidation of Cr adsorbed to iron oxides, followed by the re-adsorption of the Cr^{6+} suggests that this reaction may contribute to the depletion of Cr in Mn rich sediments in the ocean as compared to low Mn sediments. This reaction may also explain the partitioning of chromium in other sediments. Thus, although the rate and extent of the reaction appear to be limited by the formation of the hydroxide species, the reaction may be important in controlling the geochemical behavior of chromium in environments which are enriched in Mn oxides, such as ocean floor sediments. If this reaction is important in these

environments then Mn oxides may exert an influence on the overall global geochemical cycle for chromium.

The preliminary result of the mixed-oxide experiments also suggest that an equilibrium approach to the partitioning of metals based on laboratory determined binding constants may be useful for modeling trace elements in aqueous systems. However, much further research is necessary to establish the feasibility of this approach.

4.0 SUGGESTIONS FOR FURTHER RESEARCH

The continued development of a model of Cr geochemistry in sediment/water systems can be advanced by continued research in several areas, including further study of valence state transformations of this metal, by Mn oxides as well as other oxidizing/reducing agents. The research begun here could be expanded in the following areas:

1. A mechanistic approach to interpreting the reaction rate data.

2. Further efforts to delineate the effects of Mn oxides on the solubility of Cr hydroxides.

3. A study of the role of organic complexes in the geochemistry of chromium. This should include the characterization of such complexes and the effects on the oxidation and adsorption of these complexes by oxides and other adsorbents.

4. Further studies of Cr uptake and valence state
    transformations using naturally occurring sediments and
    soils.

APPENDICES

APPENDIX I

PAST RESEARCH

Since the focus of this research is on adsorption and adsorption controlled oxidation, it was necessary to explore adsorption models, particularly those which have been found useful in describing surface reactions on hydrous oxides. Hence, this section on past research begins with a summary of recent developments in adsorption modeling, including mechanistic interpretations as well as mathematical formulations. This is followed by a summary of previous research on Cr(III) and Cr(VI) adsorption onto solid surfaces and on the oxidation of Cr(III) by surface reactions on various Mn oxides.

ADSORPTION MODELS

Adsorption of metals from solution involves the removal of metal solutes by accumulation at a solid surface. Any solid in solution experiences an imbalance of forces at the solid/solution interface. This imbalance of forces will tend to be reduced by adsorption of ions from solution (Schindler, 1981). At any solid/solution interface there is a surface charge and an electrical potential gradient extending from the surface into the solution phase (Leckie et al. 1980). The origin of this surface charge can be a result of several processes including, 1) chemical reactions

at the solid surface, such as non-stoichiometric dissolution or ionization of surface functional groups, 2) substitution of unlike charged particles in the lattice, or 3) ion adsorption from solution (Stumm and Morgan, 1981). Thus the forces which cause the adsorption of metals may come from chemical interactions, such as the formation of covelant bonds, from electrostatic interactions, such as ion-exchange, and from other forces such as van der Waal's forces or hydrogen bonds (Stumm and Morgan, 1981).

The surfaces of hydrous oxides such as Fe and Mn oxides can be pictured as an amphoteric substance consisting of surface hydroxyls (Schindler, 1981). The charge of the oxide results from a reduced coordination number of the metal ions on the surface layer of the oxide. Thus the surface exhibits acidity (Schindler, 1981). The charge is controlled by the hydration and hydrolysis of this surface and the participation of surface hydroxyl groups in acid-base reactions (Murray, 1974). The dissociation of these surface groups can be represented by the following reactions:

$$SOH_2^+ ==== SOH^O + H^+$$
$$SOH^O ==== SO^- + H^+$$
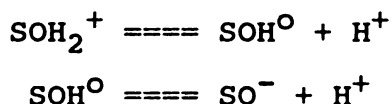
where S represents a surface layer metal ion such as Fe or Mn. It can be seen from these reactions that the surface charge is dependent on the pH of the solution. At equilibrium, the electrical potential of a chemical species must be the same in all phases of the system. Hence the ions

H^+ and OH^- are usually chosen as the potential-determining ions (PDI) for calculating the surface potential (Leckie et al. 1980). Since the surface charge is influenced by the pH of the solution, there is a unique pH for each solid where the surface is uncharged. This pH is commonly termed the pH of zero-point-charge (pH_{zpc}) (Stumm and Morgan, 1981). This pH, which is characterized by the condition:

$$[SOH_2^+] = [SO^-]$$

will depend on the acidity of the metal ion and the electrostatic field strength of the solid (Murray, 1974), and will thus be unique for each oxide. Healy et al.,(1966) demonstrated that the pH_{zpc} for a series of Mn oxides was related to the crystallinity, in that as the atomic packing of the lattice increases the pH_{zpc} increases.

When the pH of the solution environment is above the pH_{zpc} of an oxide surface, the oxide surface will have a negative charge, and conversely a positive charge when the solution pH is less than the pH_{zpc} (Parks, 1965). The pH_{zpc} of Mn oxides (MnO_2 species) are about 1.5-2.7 and for Fe oxides ($Fe(OH)_3$-am; $FeOOH$) are about 7.9-8.5 (Kinniburgh and Jackson, 1981). Thus in many natural waters Fe oxides will have a positive surface charge and Mn oxides a negative charge.

Although the electrostatic attraction/repulsion is important in adsorption energetics, adsorption does take place on surfaces with an unfavorable charge. In other words

a cationic species can adsorb onto an oxide species below
the pH_{zpc} where the net charge on the oxide surface is
positive. This shows that other bonding mechanisms
contribute to the energy of adsorption. The typical pattern
of cation adsorption with variable pH is marked by an abrupt
increase in adsorption from near 0% to near 100% over a
several unit increase in pH. This area of abrupt increase
in adsorption is termed the adsorption edge (Leckie et
al.,1980). Anion adsorption patterns are a mirror image of
cation adsorption with the abrupt adsorption occurring over
a several unit decrease in pH. These patterns of adsorption
have led to analogies of solution processes: hydrolysis of
metals for cation adsorption and protonation of bases for
anion adsorption.

The location of the adsorption edge for various metals
on an oxide surface is a function of the properties of the
metal in solution (i.e. size, pH of hydrolysis) and on the
amount of solid substrate in the system (Kinniburgh and
Jackson, 1981), but is apparently only weakly influenced by
the identity of the solid (Leckie et al. 1980). For cation
adsorption, an increase in the metal/oxide ratio causes the
adsorption edge to shift to a higher pH. In other words,
increasing the amount of metal in solution while keeping pH
and the oxide concentration constant will result in a
decreasing fraction of adsorption, which is the opposite
effect in precipitation reactions (Leckie et al.,1980).
Anion adsorption is affected in the same manner but in a

mirror image, that is, increasing the metal oxide ratio causes the adsorption edge to shift to a lower pH.

While the analogies to solution chemistry are obvious, adsorption is set apart thermodynamically from solute reactions by the electrostatic interactions between surface and solute. The total free energy of adsorption must be broken down into its chemical and electrostatic components:

$$\triangle G_{adsorp} = \triangle G_{chem} + \triangle G_{coul}$$

because the electrostatic term $\triangle G_{coul}$ changes with the reaction of ions with the surface and with the electrostatic interactions of adsorbed species (Morel et al., 1981). The $\triangle G_{chem}$ contains the energy of chemical bonding and other non-electrostatic components. This free energy expression is the basis for all models put forward to explain and predict the adsorption process.

In the last twenty years a variety of adsorption models have been developed to explain experimental adsorption data. The ultimate aim of such models is to be able to predict the adsorption of various species over changing conditions of pH, sorbate/sorbent concentrations, and solution chemistry. Any model that will be useful to model natural systems must also be able to account for the effects of competing cations and ligands.

Early models of the solid-solution interface, such as the model of Guoy and Chapman, considered an entirely electrostatic theory of adsorption based on an electrical

double layer (EDL) model of the interface. The EDL concept defines the area at the interface which has different properties than bulk solution as having two layers or planes each with a distinct surface potential. The Guoy-Chapman model considered ions as point charges that were held to the surface by electrostatic forces in the diffuse, outer layer of the EDL. The Guoy-Chapman model was modified by Stern and later Graham to include non-electrostatic specific adsorption, such that specifically bound ions were bonded to the surface in the compact layer (Stern layer) nearest to the surface (Stumm and Morgan, 1981). This model works well for predicting electrical phenomena at some interfaces but results in anomalies when applied to the metal oxide/solution interface (Leckie et al.,1980).

The evolution of adsorption models which describe adsorption on hydrous oxides has involved the consideration of discreet surface species reacting with solution species. Such models must consider both chemical and electrostatic interactions and are still constrained by the charge-balance and charge-potential relationships of the electrostatic EDL models (James, 1981).

A model described by James and Healy (1972) recognized that the adsorption edge of hydrolyzable metals is strongly dependent on the pH of hydrolysis of the metal. This model does not attempt to demonstrate direct surface-metal bonds but suggests that adsorption is due to the preferential uptake of hydrolyzed metal species. This hydrolysis-

adsorption reaction may take place at pH's below the pH of hydrolysis in solution thus may also be thought of as the surface hydrolysis of adsorbed metals. The free energy of adsorption in this model is then broken down such that:

$$\triangle G_{sorp} = \triangle G_{chem} + \triangle G_{coul} + \triangle G_{solv}$$

where the $\triangle G_{solv}$ term is the energy to replace secondary hydration water of a metal with interfacial water of low dielectric (James and Healy, 1972). Thus this model predicts that the hydrated metal species is adsorbed. The $\triangle G_{chem}$ term is undefined and used to correct for the discrepancy in electrical potential in the EDL caused by considering discreet ions and real surfaces (James and Healy, 1972).

Recent developments in adsorption models have attempted to define this reaction as a chemical rather than physical process, although all such models are defined by a consistent set of stoichiometric and energetic expressions rather than by any proven mechanism (Morel et al.,1981). Models generally applied to adsorption onto hydrous oxides consider the oxide surface as a polyprotic acid (Schindler, 1981) and the adsorption of trace metals as a complexation reaction with the formation of covelant bonds between the surface site and metal ion (Leckie et al., 1980). These models must still consider the electrostatic energy term separately from the other energy components.

The way in which the various models are different from each other has to do with how the chemical and electrical components of the total free energy are formulated. The

species predicted to react at the surface and the location of the adsorbed ions with respect to the EDL can be modeled by a variety of theoretical formulations, any of which can result in the ability to model experimental data. Morel et al., (1981) compared several recent adsorption models and concluded that all were too flexible, and that the models differ from each other in three general areas: 1) the set of surface species and surface reactions considered, 2) the expression of the "mass law", and 3) the calculation of the coulombic term.

These differences can be demonstrated by comparing two recent models of adsorption on hydrous oxides: the model of Stumm et al., (1970) and Schindler et al., (1976) hereafter referred to as the surface-complexation model, and the model of Davis and Leckie (1978) hereafter referred to as the site-binding model. Both are "chemical" rather than "physical" models, each formulating a distinct set of reactions between the solute ions and discreet surface sites.

The set of surface species considered (i.e. SO^-, SOH, SOH_2^+) are the same for both models but there are differences in the surface reactions considered, including both trace metal and electrolyte interactions. The surface-complexation model predicts that the unhydrolyzed free metal is the primary adsorbed species ($SO-Me^+$) while the site-binding model predicts simultaneous adsorption and hydrolysis such that (SO-MeOH) is generally the primary

adsorbed species. By considering different solution species and different degrees of hydrolysis or protonation of the surface species it is possible to write more than one reasonable reaction to describe the observed stoichiometry of experimental data. Many times more than one reaction is required to model the experimental data.

The two models also differ with respect to ionic strength effects. The surface-complexation model does not consider electrolytes to be specifically adsorbed. Hence the adsorption constants generated are conditional constants containing all the effects of the background electrolytes, which are not clearly understood, but may include activity coefficient corrections, compression of the EDL, and those dependent on the particular electrolyte (Morel et al.,1981). The site-binding model allows for the specific adsorption of weakly bound electrolyte ions and thus adsorption constants applicable over varying ionic strength.

Mass law expressions can vary both in units and in the treatment of polydentate species (Morel et al., 1981). The units may be based on the number of surface sites (moles of sites per liter) or on surface area (area of sites per total surface area). If the area of all surface sites are identical then the adsorption constants will be independent of the units chosen. Models may also differ in how polydentate surface reactions are handled. The surface-complexation model considers a bidentate bond as a bond between the solute ion and two identical adjacent surface

sites while the site-binding model considers distinct monodentate and bidentate surface sites analogous to bidentate complexes in solution (Morel et al.,1981 and Leckie et al., 1980). The resultant mass law expressions:

$$K = \frac{[(SO)_2Me]}{[SO]^2[Me]} \quad \text{and} \quad K = \frac{[(SO)_2Me]}{[(SO)_2][Me]}$$

show that there is a square dependence on surface site concentration in the surface-complexation model and not in the site-binding model.

There are many different ways to formulate the coulombic term, $\triangle G_{coul}$, of the adsorption process. Most are a variation of the general expression:

$$lnK_{coul} = (-1/RT)\triangle G_{coul} = -\triangle z(-F/RT)\gamma$$

where γ is the electrical potential at the locus of adsorption and $\triangle z$ is the net change in charge number of the surface species due to adsorption (Morel et al., 1981).

The differences between the various models arises from the different "pictures" of the EDL in terms of where a particular ion (PDI, specifically sorbed ion, electrolytes) is considered to be adsorbed. In other words, the models differ in the assignment of the electrostatic potential experienced by an adsorbed species and hence in the equations used to relate surface potential to surface charge (Westall and Hohl, 1980). For example, the surface-complexation model suggests that the PDI's and specifically

sorbed ions experience the same potential (i.e. both are adsorbed in the compact layer of the EDL) and that electrolytes experience a different potential in the diffuse layer. In contrast, the site-binding model, sometimes referred to as a triple-layer model, pictures the PDI's (H and OH) in an inner compact layer (i.e. essentially part of the solid) and the adsorption of both specifically sorbed species and weakly bound electrolytes to occur in an outer compact layer experiencing a different electrical potential. It must be noted that the formulation of the coulombic term must be consistent with the formulation of the physical picture of the adsorption model (i.e. the predicted surface species).

As stated previously, the purpose of adsorption models is to be able to explain real data over a variety of conditions. Studies comparing the ability of several models to predict experimental data (Westall and Hohl, 1980 and Morel et al., 1981) have shown that there are so many adjustable parameters in these models, that nearly all of them can be made to work quite well. This shows that the models are all too flexible.

The fundamental problem remains to be the inability to separate the $\triangle G_{coul}$ term from the $\triangle G_{chem}$ term in the expression of the free energy of adsorption. The approach has been to isolate the $\triangle G_{chem}$ term by extrapolating measured experimental data to a condition of zero surface potential and surface charge (i.e. $\triangle G_{coul}=0$) (Anderson et

al., 1981; Westall and Hohl, 1980). However, the path chosen for this extrapolation is model dependent, resulting in variations in the $\triangle G_{chem}$ term from model to model. Upon determination of the $\triangle G_{chem}$ term, which is a true thermodynamic constant, the adsorption model attempts to predict adsorption over a range of solution parameters by its theoretical formulations of the electrostatic interactions. To do this the surface charge is calculated based on the requirements of the particular model, and then, by its relationship to capacitance, the surface potential is calculated. However, the capacitance is merely a fitting parameter, and hence the surface potential necessary to fit the experimental data can always be determined. Hence each model can calculate the "correct" free energy of adsorption but with different contributions of $\triangle G_{chem}$ and $\triangle G_{coul}$. So what is lacking for the formation of a single, less general model is independent verification of the true surface speciation of the adsorbed species and of the true surface potential (Anderson et al., 1981; Leckie et al., 1980). Analytical determination of these parameters is very difficult or impossible by present methods.

CHEMICAL CONTROLS OF ADSORPTION BEHAVIOR

Given the nature of the present research there are two topics with respect to adsorption behavior that will be discussed. The first is a summary of research on the competition of sorbate ions for the surface of hydrous

oxides. This discussion of multi-sorbate interactions will be broken down into four sections: 1) comparisons of the relative affinities, or selectivity sequences for a group of ions as determined from single sorbate/sorbent systems, 2) experimental results of the actual competition between metals for surface sites, 3) the effects of ionic strength on metal adsorption, and 4) the effect of complexing ligands on metal adsorption. The second topic of consideration, which is necessary background for mixed sorbent experiments, is the comparison of the adsorptive properties of Mn and Fe oxides. Of special interest are the unique properties of the MnO_2 surface.

There have been many studies that have measured the relative adsorptive properties of a series of ions on a particular oxide surface. By comparing the amount of metal adsorbed at a certain pH and metal/oxide concentration, or by determining the pH required to sorb a certain amount of metal at constant oxide concentration, the selectivity sequence of a group of metals can be determined. The lower the pH that a cationic metal ion adsorbs, the greater affinity that metal has for the surface. Table I.1 summarizes the selectivity sequences for alkali metals, alkali earth metals, and transition metals for oxides of Mn and Fe. It should be noted that comparisons between these groups yields the following relationship: transition metals > alkali earth metals > alkali metals in terms of the affinity for oxide surfaces (Kinniburgh and Jackson, 1981).

TABLE I.1		
SELECTIVITY SEQUENCES OF ADSORBED IONS		

Investigation	Substrate	Selectivity Sequence
Stumm et al, 1970	MnO_2*	Cs > Na
Posselt et al, 1968	MnO_2	Ba > Sr > Ca > Mg
Murray, 1975	MnO_2	Ba > Sr > Ca > Mg
Kinniburgh et al, 1976	$Fe(OH)_3$	Ba > Ca > Sr > Mg
McKenzie, 1980	MnO_2	Pb > Cu > Mn > Co > Zn > Ni
Gadde and Laitinen, 1974	MnO_2	Pb > Zn > Cd
Murray, 1975	MnO_2	Co $\geq$ Mn > Zn > Ni
Loganathon and Burau, 1973	MnO_2	Co > Zn
Kinniburgh, et al, 1976	$Fe(OH)_3$	Pb > Cu > Zn > Ni > Cd > Co
Gadde and Laitinen, 1974	$Fe(OH)_3$	Pb > Zn > Cd
Leckie et al, 1983	$Fe(OH)_3$	Cr > Pb > Cu > Zn > Cd > Ni
Forbes et al, 1976	FeOOH	Cu > Pb > Zn > Co > Cd
McKenzie, 1980	FeOOH	Cu > Pb > Zn > Co > Ni > Mn

* all MnO_2 species are low pH_{zpc} forms

The selectivity sequence for monovalent cations, which are thought to adsorb due primarily to electrostatic forces, is found to vary from surface to surface, apparently due to the acidity and pH_{zpc} of the surface considered (Kinniburgh and Jackson, 1981). The selectivity sequence for the alkali metals on MnO_2 ($Cs^+ >..>Li^+$) is thought to be a size dependent sequence with the larger ions (i.e. Cs) having a smaller hydrated radius. The smaller, more polarizable hydration spheres are also more distortable allowing closer approach to the surface (Kinniburgh and Jackson, 1981). Another factor that may influence the selectivity sequence is the polarity of the surface. Solid surfaces with high polarity (i.e. high pH_{zpc}) tend to have a high degree of structure in the surficial water molecules. The selectivity sequences on these types of solids tends to be opposite that on MnO_2 (i.e. $Li^+ >..> Cs^+$) depending on the tendency of the ion to break up this structured water. This relationship is not, however, unequivocal (Kinniburgh and Jackson, 1981).

The selectivity sequences for the alkali earth metals varies greatly from surface to surface (see Kinniburgh and Jackson, 1981). From Table I.1 it can be seen that the sequence for low pH_{zpc} MnO_2 (Ba > Sr > Ca > Mg) is consistent in different studies and also different from the sequence on amorphous iron oxides (Ba > Ca > Sr > Mg). This suggests there must be some factors involved that are specific to the surface considered. For MnO_2 the sequence follows a size relationship with increasing affinity with

decreasing hydrated radius (Posselt, et. al., 1968). There is also a general relationship with the tendency to hydrolyze (Kinniburgh and Jackson, 1981).

There appears to be a strong dependence on the ability to hydrolyze in the selectivity sequences for the transition metals (Leckie et al., 1983 and others). However, for MnO_2 and amorphous Fe oxides, the order of Pb and Cu is switched compared to crystalline forms of Fe oxides suggesting there are surface specific effects (McKenzie, 1980). There are also discrepancies in the Mn oxide system, probably due to redox reactions with species such as Mn and Co (Hem, 1978; Murray and Dillard, 1979). However, despite these deviations and some pH dependent order changes, there is certainly a strong dependence on the ability to hydrolyze. In general, the greater the electronegativity of the metal ion, the greater the tendency to form covelant bonds with surface oxygen atoms and hence the greater the affinity for the surface (Kinniburgh et al., 1976). This relationship is consistent with the adsorption models discussed previously.

Research in single sorbate systems which has generated selectivity sequences suggests that there are different binding energies for different metals and that some metals should be able to "out-compete" other metals for surface sites. Many studies have documented the adsorption of trace metals in the presence of a large excess of Ca, Mg, or Na which suggests either 1) trace metals bond more strongly to the available surface sites and compete favorably, or 2)

these ions bind to different sites on the oxide surface. In order to determine the nature of "competition" amongst metals and whether adsorption models can be used to predict competition in multi-sorbate systems, several studies have measured adsorption in such experimental systems. Table I.2 summarizes some of these studies.

From these results it does not appear that competition among adsorbates can be easily predicted or that it is simply the case of the more strongly bound species adsorbing at the expense of the weaker binding species. In fact, despite the very different binding energies for various metals, competitive effects are weak or non-existent in some cases. This suggests that metals may not compete for the same binding sites on the oxide surface. Benjamin and Leckie, (1981b) studied the adsorption of Cd onto Fe_2O_3-H_2O am in the presence of other stronger binding metals in a 10-100 times excess. There was only limited competition under these conditions. These authors suggest that this oxide surface consists of a variety of sites, most of which will bind to a many different metals, but with different binding strengths unique for each metal. In other words, a site which is a high energy site for Cu adsorption may be only a weak energy site for Pb.

Evidence for different types of surface sites with different bonding energies has been provided in single sorbate experiments as well (Benjamin and Leckie, 1981a). These investigators showed that the average binding constant

			TABLE I.2	
		SUMMARY OF MULTI-SORBATE ADSORPTION STUDIES		
Investigation	Substrate	Primary Metal	Competing Metal	Results
Dempsey & Singer, 1980	$Fe(OH)_3$	Zn	Ca	No competition
	MnO_2	Zn	Ca	Slight competition at low pH only
Balistrieri & Murray, 1982	FeOOH	Pb, Cu, Zn or Cd	the other three	No competition except when Cd is primary metal
Swallow et al, 1980	$Fe(OH)_3$	Pb,Cu	Cu,Pb	No competition
Gadde & Laitinen, 1974	MnO_2	Cd or Zn	Pb	Decreased sorption of Cd and Zn by Pb
Benjamin & Leckie, 1981	$Fe_2O_3-H_2O$ amorph.	Cd	Cu,Pb or Zn	Slight or absent competitive effect
		Cu	Pb	Weak competition

for Cu, Cd and other metals on $Fe_2O_3-H_2O$ am changed as adsorption density reached a certain level, even though there was still a large excess of unoccupied sites. They argued that electrostatic effects due to EDL or sorbate-sorbate interactions could not be responsible for this phenomena, and suggested the hypothesis of different sites with different binding energies to explain the data. The change in the average binding constant was attributed to the condition where the high energy sites (which preferentially fill up first) become limiting. The "concentration" of these high energy sites appears to be unique for different metals.

This is an important concept in terms of the application of existing adsorption models to real systems, as all of the models described previously consider only one type (energy) of surface site and thus may have limited utility in describing adsorption over a wide range of sorbate/sorbent conditions. It also suggests that adsorption onto Fe oxides may be accurately modeled without considering competition between trace metals which would greatly simplify this task (Benjamin and Leckie, 1981b). However, based on the limited data for competition studies on Mn oxides (see Table I.2) it appears that this may not be the case for all surfaces.

Studies which have explored the effects of the swamping electrolyte (i.e. ionic strength effects) have also resulted in a variety of results (see Table I.3). Although electrolytes have been shown to bind to the surface less strongly than trace metals it is clear that these species

TABLE I.3
SUMMARY OF IONIC STRENGTH EFFECTS ON ADSORPTION

Investigation	Sorbent	Metal	Electrolyte (conc. range M)	Results
Kinniburgh et al, 1975	$Fe(OH)_3$	Ca,Sr	$NaNO_3$ (0.4 - 2.0)	small decrease in adsorption
Posselt et al, 1968	MnO_2	Ca	$NaClO_4$ (.004 - .134)	proportionate decrease in log of sorption capacity with ionic strength
Swallow et al, 1980	$Fe(OH)_3$	Pb,Cu	$NaClO_4$ (.005 - .50)	No effect
			5 NaCl and SOW	Pb adsorption decreased by presence of Cl
Balistrieri and Murray, 1982	FeOOH	Pb,Cu, Zn,Cd	.1 $NaNO_3$ to SOW by stepwise of .53 NaCl, .028 Na_sSO_4, and .054 $MgCl_2$	- increase in Cu adsorption - increase in Pb adsorption at low pH and less at high pH - decrease in Zn and Cd adsorption

must be considered as they are usually present in great excess. The effects of ionic strength on the adsorption of trace metals are unclear but may include, 1) electrostatic effects caused by changes in the charge of the EDL, 2) activity coefficient effects (decreasing metal activity with increasing ionic strength), 3) competition for binding sites on the oxide surface, and 4) competition with the surface via the formation of solution complexes (which may or may not adsorb).

Results from studies employing "inert" electrolytes (such as $NaNO_3$ and $NaClO_4$) to set ionic strength show that these species have only minor effects on the adsorption of trace metals, at least on Fe oxides (Kinniburgh et al.,1975; Swallow et al., 1980). This suggests that the electrostatic EDL effects of ionic strength on adsorption of trace metals are minor, possibly because adsorption of trace metals result in no net change in surface charge (Swallow et al., 1980).

Balistrieri and Murray, (1982) explored the influence of the components of major ion sea water (NaCl, Na_2SO_4 and $MgCl_2$) on the adsorption of trace metals by geothite. Although not explicitly a study of ionic strength, this research demonstrated both electrostatic and competition effects may have been responsible for the difference in adsorptive behavior in 0.10 M $NaNO_3$ compared to synthetic major ion seawater. Apparently Mg and SO_4 caused both increases and decreases in adsorption depending on the

metal. It should be noted that these researchers found no effect by Cl on the adsorption of Pb, while Swallow et al., (1980) found a pronounced decrease in adsorption on amorphous Fe oxide. It may well be that electrolytes may have different effects on different surfaces, or possibly even variable effects on a single surface under different solution conditions.

Another process which must certainly be considered for predicting adsorption in complicated natural systems is solution complexation of metal ions by complexing ligands. The potential effects on adsorption include, competition for metal ions (i.e. the complex does not adsorb), the adsorption of ligands onto the surface resulting in a change in surface charge, and the adsorption of complexes. The latter is indistinguishable from the complexation of a metal by an adsorbed ligand.

Studies by Davis and Leckie (1978b) and Benjamin and Leckie (1981c) have shown that complexing ligands cause only slight effects on the charge of the EDL in the presence of a swamping electrolyte and that complete non-adsorptive behavior of complexes is probably rare. These studies indicate that in general a metal-ligand complex exhibits either "metal-like" or "ligand-like" adsorptive behavior and this can cause either an increase or decrease in adsorption. The effect on adsorption may also be pH dependent and will almost certainly depend on the identity of the solid. The difference between "metal-like" and "ligand-like" complexes

is apparently due to the stereochemical arrangement of the complex at the surface rather than the overall charge on the complex, with "metal-like" complexes adsorbed with the metal closer to the surface (Leckie et al.,1980). In general, simple, soluble ligands like SO_4 and Cl tend to form metal-like complexes which tend to decrease metal adsorption (Leckie et al., 1980). It is certain that surface speciation is vital for the development of an adsorption model that will work well in predicting the behavior of metals in the environment.

ADSORPTION ON MN VS FE OXIDES

From the preceding discussions it is evident that the adsorption of trace metals is somewhat unique for each oxide surface considered. A good case in point are the apparent differences between hydrous iron and manganese oxides. Because some of the experiments in the present research are designed to examine the competition for Cr^{3+} by these two oxide species, it is valuable to summarize the apparent differences based on past research. It must be noted that only a few studies (McKenzie, 1980; Balistrieri and Murray 1982; Gadde and Laitinen, 1974; Dempsey and Singer, 1980) have evaluated adsorption on these two oxides for the purpose of making a comparison. Some apparent differences may be due to widely different experimental parameters, procedures and interpretations. Table I.4 summarizes the main differences in adsorption behavior

TABLE I.4
APPARENT DIFFERENCES IN ADSORPTION BEHAVIOR OF Mn AND Fe OXIDES BASED ON PAST RESEARCH

Component of Behavior	Mn Oxides	Fe Oxides
1. Adsorption of anionic species	Anions do not adsorb	Anions adsorb at most pH's
2. pH dependence of metal adsorption	Adsorption edge is gradual and begins at very low (<2) pH's	Adsorption edge is abrupt with very little or no adsorption at very low pH's.
3. Stoichiometry of the reaction in terms of proton release	Variable but most report near 1 H^+ released per metal adsorbed - May increase with increasing pH	1.2 to 2 H^+ released per metal adsorbed with most studies >1.5
4. Capacity and intensity of adsorption	Higher amount of surface sites per mole of solid and some evidence for higher energy of interaction	Amorphous iron oxides have similar surface site conc. as MnO_2 - Geothite has much lower capacity
5. Type of bonding mechanism	Several have been suggested. More difficult to model by current models maybe due to difficulty in characterizing the surface	Can be modeled by surface-complexation models which suggests that binding to surface hydroxls is dominant
6. Competition amongst adsorbates	Although data is scarce, it appears that some metals may compete for the same sites suggesting that stronger binding metals should sorb at the expense of other species.	Rather extensive study indicates that competition among metals is minimal which suggests metals adsorb mainly to specific sites

between MnO_2 (low pH_{zpc} variety) and Fe oxides (geothite and amorphous iron hydroxide).

The lack of anion adsorption on Mn oxides compared to Fe oxides has been demonstrated by Balistrieri and Murray (1982). This can be explained partly in terms of the vastly different electrostatic conditions at the surfaces of these two oxides. The surface of Mn oxide is negative for most of the pH ranges studied, and electrostatic repulsion of anions would be expected. However, Leckie et al., (1980), have shown that the apparent lack of adsorption of anions above the pH_{zpc} of amorphous iron hydroxide is an experimentally induced condition rather than an indication of complete electrostatic adsorption behavior of anions. This suggests that anion adsorption on Mn oxides is not theoretically impossible under certain experimental conditions, however it is apparently unimportant under most conditions.

The pH dependent adsorption behavior on MnO_2 appears to be unique compared to most other hydrous oxides. This observation is based on the location and shape of the adsorption edge for trace metal adsorption. First of all, significant adsorption takes place on MnO_2 at pH's below 2.0, near the pH_{zpc}, and increases with a gradual slope as pH increases (McKenzie, 1980; Gadde and Laitinen, 1974). This is in contrast to pH dependent adsorption on Fe oxides which follows the classic adsorption edge pattern and rarely begins at pH's lower than 3.0. The adsorption of metals at very low pH by MnO_2 has not been satisfactorily resolved,

but could be related to, 1) the low pH_{zpc} (i.e. the lack of an unfavorable positive surface charge), 2) different mechanisms of bonding (i.e. exchange of metals for structural Mn) and/or 3) the relatively high dielectric constant of this oxide surface. Although the electrostatic term is certainly more favorable for adsorption on MnO_2 at low pH's, Murray (1975) suggested that the pH_{zpc} should not be the major consideration in the adsorption behavior of oxides. MnO_2 was shown to exhibit similar adsorption behavior with TiO_2, which has a high pH_{zpc} and high dielectric, while adsorption on SiO_2, which also has a low pH_{zpc} but a low dielectric, exhibited quite different behavior. This was interpreted to show that the dielectric of the solid influences the adsorption behavior. The MnO_2 surface, which has a relatively high dielectric, would be more favorable for the adsorption of the unhydrolyzed species due to the relatively small change in the solvation energy required to move the ion to the surface.

The exchange of metals for structural Mn has been demonstrated to occur by measuring the Mn released to solution upon the adsorption of metals (Loganathon and Burau, 1973; McKenzie, 1979; Murray, 1975). However, the amount of Mn released does not suggest that this is an important mechanism for metal adsorption.

Many investigators have measured the release of protons upon the adsorption of metals from solution in order to demonstrate the reaction stoichiometry. As with many other

results of adsorption research, there is a wide variety in the experimental results (see Table I.5) many of which reflect the lack of standardized experimental methods. In very general terms, it appears that the release of protons upon adsorption of divalent trace metals (hereafter referred to as H^+/Me^{2+}) is lower for adsorption on Mn oxides (1.0) than for adsorption onto Fe oxides (1.5-2.0).

There are several issues concerning the interpretation of this experimental data that have not been resolved. One very significant problem is whether the release of electrolytes should be included in adsorption stoichiometry. McKenzie (1979), showed that the release of 2 protons per metal adsorbed at low ionic strength could be systematically reduced to 1 by increasing the ionic strength with KNO_3. He suggested that at low ionic strength there was one proton released from the surface by exchange with the metal and that the other proton was released from the diffuse layer to balance the charge. At higher ionic strength the diffuse layer counterions were primarily K^+ which explains the reduction of the H^+/Me^{2+} ratio. It was suggested that the H^+/Me^{2+} ratio of 2 determined by Loganathon and Burau (1973), was due to the use of an acid washed sample which left H^+ as the diffuse layer counterion.

The interpretation of McKenzie (1979) does not consider specific adsorption of electrolytes, which could also be used to explain these results. For instance, the work of

TABLE I.5

PAST STUDIES OF ADSORPTION REACTION STOICHIOMETRY

Investigator	pH	Oxide	Metals	H^+ Released	Comments
Gadde and Laitinen (1974)	6.0	MnO_2	Pb Cd Zn	1.4 1.3 1.1	
Gadde and Laitinen (1973)	5.0-6.0	HFO	Pb	1.2-1.6	Increased with pH
Loganathon and Burau (1973)	4.0	MnO_2	Co	2.0	2 = H-K-Na Oxide was acid washed
McKenzie (1979)	4.0	MnO_2	Pb,Cu Mn,Zn	1.0-2.0	Dependent on ionic strength
Morgan and Stumm (1964)	4.5-8.2	MnO_2	Mn	1.0-1.7	Increased with pH
McKenzie (1980)	4.0	MnO_2	Pb,Cu Mn,Zn	1.0	Several forms of Mn oxide
	5.0	FeOOH	Pb,Cu Mn,Zn	1.3-2.0	
Forbes et al (1976)	4.5-9.4	FeOOH	Cd,Co,Cu Pb,Zn	2.0	Used two methods
Balistrieri and Murray (1982)	3.4-5.3	MnO_2	Ca,Mg	<1.0	However H+Na+K = 2.0
Murray (1975)	3.5-7.0	MnO_2	Co,Mn,Ni	1.0	Increased with pH
Leckie et al (1980)		Fe_2O_3-am	Cu Pb Cd Zn	1.9 1.65 1.8 3.2	pH = 5.47 pH = 5.35 pH = 7.0 pH = 6.75

Balistrieri and Murray (1982) using the site-binding model shows that the ratio of (H + Na + K) released to (Ca + Mg) adsorbed onto MnO_2 equals two, which suggests that these species adsorb to bidentate surface sites ($H^+/Me^{2+} < 1.0$) and that the charge in the inner adsorption plane is conserved. It is not known whether the adsorption of trace metals also results in this behavior, but these authors have suggested that adsorption of Ca and Mg on iron oxide occurs on monodentate sites (Balistrieri and Murray, 1981).

Further evidence for the model of McKenzie (1979) which predicts that the inner layer of the MnO_2 surface should become positively charged with increasing adsorption has been provided by studies which have measured the sign of the surface charge as a function of adsorption. Loganathon and Burau (1973), Morgan and Stumm (1964) and Murray (1974) have demonstrated that the MnO_2 surface becomes less negative and eventually experiences a charge reversal with increasing adsorption of metals. This phenomena could be due to the exchange of a proton for a divalent metal, resulting in an accumulation of positive charge in the inner plane of adsorption. This would strongly suggest that a H^+/Me^{2+} ratio of 1.0 is correct, at least for some experimental conditions.

McKenzie (1980) suggests that the adsorption of metals at low pH's by MnO_2 is due to the adsorption of the free unhydrolyzed metal ion, and thus the release of one proton by the reaction:

$$SOH^O + Me^{2+} = SOMe^+ + H^+$$
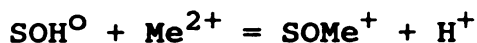
At higher pH's the adsorption of the hydroxo species (or the hydrolysis of the ion at the surface) by the reaction:

$$SOH^O + Me^{2+} + H_2O = SOMeOH + 2H^+$$
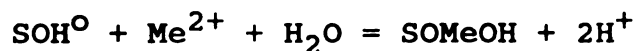
also becomes important, which would cause an increase in the H^+/Me^{2+} ratio. The final reaction at even higher pH's (if the metal concentration is high enough) would be the surface precipitation of the metal species:

$$SO^- + Me^{2+} + 2H_2O = SOMe(OH)_2 + 2H^+$$
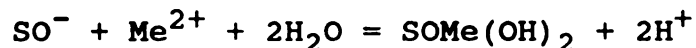
This scenario suggests that the H^+/Me^{2+} should increase with pH to a ratio greater than 1.0. Several investigations have demonstrated this relationship (Morgan and Stumm, 1964; Murray, 1975). Applying a consistent approach to adsorption on Fe oxides would suggest that there is no appreciable adsorption of only the unhydrolyzed species on these oxides. The location of the adsorption edge for various metals on iron oxides does appear to be related to the appearance of the hydroxo metal complex, although the free metal is still commonly in great excess (McKenzie, 1980). This would suggest that the hydrolyzed species may be preferentially adsorbed. The H^+/Me^{2+} ratio for adsorption on iron oxides supports this idea, as this ratio is usually reported to range from 1.5 to 2.0 (Leckie et al.,1980; McKenzie, 1980; Forbes et al., 1976). One could speculate that the lack of adsorption at low pH's (i.e. the unhydrolyzed species) on

iron oxides may be related to the inability to overcome the solvation energy.

On a weight basis, the adsorption capacities of MnO_2 and amorphous Fe oxide are on the same order of magnitude, although the crystalline Fe oxides have a significantly lower capacity (Louma and Davis, 1983). Based on the ability to adsorb at lower pH's, MnO_2 would appear to be a more efficient adsorbent than Fe oxides (Gadde and Laitinen, 1974; McKenzie, 1980). It must be emphasized however, that multi-sorbent experiments have not been reported and the competition between solids for metals will likely be a complicated process.

Based on the above discussion the following points would appear to summarize the pertinent points to consider for the mixed oxide experiments presented in this research:

1. Although the adsorption capacities are similar, MnO_2 should be a more efficient adsorbent than amorphous Fe oxides at lower pH's, such as those used in the present research. This may be due to the ability of MnO_2 to adsorb the unhydrolyzed metal ion.

2. The adsorption of the oxidized, anionic form of Cr by MnO_2 should be negligible; but the adsorption of this species by Fe oxides in multi-sorbent systems will be significant.

3. Although the data is scarce, it appears that adsorption on MnO_2 may be more susceptible to competitive effects

in multi-sorbate systems than Fe oxides. This, however, undoubtedly will be strongly dependent on solution characteristics.

ADSORPTION OF CHROMIUM BY HYDROUS OXIDES

Compared to other hydrolyzable metals there has been relatively little study of the adsorption of Cr^{3+} onto oxide surfaces. This is probably due, in part, to the low solubility of this species in the pH range of natural waters. Some of the previous research on this subject is summarized on Table I.6. A recent study by Leckie et al., (1983) is the most complete study to date of Cr^{3+} adsorption. The important conclusions from this and other studies can be summarized in the following list:

1. The pH dependent adsorption of Cr^{3+} on Fe and Al oxides is typical for hydrolyzable metals, with the adsorption edge occurring at around pH 3-5 for all of the substrates studied. The adsorption edge experiences the normal shift to higher pH's as the concentration of the oxide is decreased.

2. The adsorption edge of Cr^{3+} is at a lower pH than most other metal ions, suggesting a relatively stronger binding interaction (Leckie et al., 1983).

3. Based on the multi-site model of Benjamin and Leckie (1981a), it would appear that there are an abundance of

high energy sites for Cr^{3+} adsorption on $Fe_2O_3 \cdot H_2O$ am, as the adsorption edge does not shift as Cr^{3+} concentrations are increased from 10^{-7} to 10^{-5} M. This is in contrast to the behavior of other metals under the same experimental conditions, and provides further evidence for a strong adsorptive bond.

4. The presence of the complexing ligands SO_4^{2-}, Cl^- and AsO_4^{3-} had little effect on the adsorption of Cr^{3+} on $Fe_2O_3 \cdot H_2O$ am. However, in fly-ash transport water, the adsorption was increased relative to a "clean" system, suggesting that Cr^{3+}-ligand complexes adsorb in a ligand-like manner (Leckie et al., 1983).

5. Cr^{3+} adsorption by clay minerals follows that predicted by the CEC of the mineral at low pH's. However, at pH=4 the CEC was exceeded on montmorillonite. Removal of Cr from solution by clays is high compared to other metals (Griffin et al., 1977).

Due to the strong binding of Cr^{3+} to the substrates that have been studied and the unique adsorption characteristics of MnO_2, it is predicted that adsorption of Cr^{3+} by this oxide would be very strong even at low pH's. The effects of competition on this surface between Cr^{3+} and other metals, however, are difficult to predict.

There has been considerably more research on the adsorption of Cr^{6+} on hydrous oxides, probably because this anionic form is both highly toxic and mobile due to its high

TABLE I.6
PAST RESEARCH ON THE ADSORPTION OF Cr(III)

Investigator	Substrate (conc.)	Cr^{3+} (conc.)	pH (range)	Comments
James and Healy, 1972	SiO_2 ($75m^2$/L)	2×10^{-4} M	3-6	Adsorbed at lower pH's than most other ions
Leckie et al, 1983	$Fe_2O_3 \cdot H_2O$ (4×10^{-4} to 1×10^{-3} M)	5×10^{-5} to 5×10^{-7} M	3-6	Studied ion/ oxide ratios, kinetics and effect of ligands
	Al_2O_3 (2-20g/L)	1×10^{-5} to 1×10^{-7} M	3-10	Adsorption edge similar to that on Fe oxide
Griffin et al, 1977	clays 0.1 g montmor. kaolinite	80ppm	1-5	Uptake related to CEC except for mont. at pH = 4

solubility. Some of the studies of this topic are summarized on Table I.7. As opposed to the trivalent form, hexavalent chromium is a relatively weak binder as compared to other anions. The pertinent aspects of the adsorption behavior of this species are summarized as follows:

1. The adsorption of Cr^{6+} follows the typical pattern for anions; the adsorption edge in a mirror image of cation adsorption.

2. Cr^{6+} also behaves as a typical anion in terms of adsorption capacity. Since anions are generally larger than cations, each adsorbed species covers more surface area, causing the surface to become saturated at a certain solute/solid ratio.

3. There is no evidence for appreciable adsorption of Cr^{6+} above the pH_{zpc} of Fe or Al oxides, which suggests the electrostatic contribution to the adsorptive bond is very important (Leckie et al., 1983; Rai et al., 1986; MacNaughton, 1974). This idea is enhanced by the rather large decrease is adsorption as a function of increasing ionic strength with "inert" electrolytes (Rai et al., 1986; MacNaughton, 1974).

4. The adsorption of Cr^{6+} is greatly reduced by the presence of other anions. The effect has been attributed to both the competition for surface sites and the decrease of the positive surface charge caused by the adsorption of

the anions (Aoki and Munemori, 1982; Rai et al., 1986; Leckie et al., 1983).

5. The adsorption of cations results in only a very small increase in the adsorption of Cr^{6+}. This suggests that these species are not adsorbed on the same sites and that the increase is due to the increase in positive surface charge and/or the adsorption of Cr-metal complexes. If the pH and cation concentrations are high enough to cause the surface precipitation of metal hydroxides, the adsorption of Cr^{6+} is usually enhanced. This is due to the high pH_{zpc} of the metal hydroxide relative to the oxide it has precipitated on (Aoki and Munemori, 1982; Benjamin, 1983).

These results affirm that adsorption of Cr^{6+} by MnO_2 is very unlikely. It also suggests that hexavalent Cr formed by the oxidation of the trivalent species would tend to be removed from solution by Fe oxides, provided more strongly bound anions are not present in significant amounts.

OXIDATION OF CR(III) BY MN OXIDES

The ability of Mn oxides to participate in various redox reactions has been known for some time. Redox reactions between Mn oxides and metals such as Co, Ni, and Pb (Hem, 1978; Crowther et al., 1983), Fe^{2+} (Postma, 1985) and various organic compounds (Stone and Morgan, 1984) have been demonstrated in the laboratory. Several studies have also

TABLE I.7

PAST RESEARCH ON THE ADSORPTION OF Cr(VI)

Investigator	Substrate (conc.)	Cr^{6+} (conc.)	pH (range)	Comments
Davis and Leckie 1980	$Fe(OH)_3$ $(10^{-3}M)$	5×10^{-7} M	5-9	both $HCrO_4^-$ and CrO_4^{2-} adsorbed
MacNaughton 1974	Al_2O_3 12g/L	2×10^{-4} M	3-9	increase conc. of KNO_3 reduces adsorption
Benjamin 1983	$Fe_2O_3 \cdot H_2O$ $10^{-3}-10^{-4}$ M	10^{-5} to 10^{-6} M	4.5-9	effects of trace metals on adsorption
Aoki and Munemori 1982	$Fe(OH)_3$ 5×10^{-3} to 10^{-2} M	10^{-3} M	4-9	effects of both metals and ligands
Mayer and Schick 1981	alumina kaolinite sediment	10^{-6} M	8	effects of salinity
Rai et al, 1986	$Fe_2O_3 \cdot H_2O$ .87 to 17.4	10^{-4} to 5×10^{-6} M	3-10	effects of a wide variety of cations & anions
Leckie et al, 1983	$Fe_2O_3 \cdot H_2O$ 8×10^{-4} to 5×10^{-5} M	10^{-5} to 10^{-6} M	3-11	effects of a wide variety of cations & anions

shown that Mn oxides have the ability to catalyze the oxidation of Cr^{3+} to Cr^{6+} (see Table I.8). It has been suggested that this process is a three step reaction consisting of adsorption, oxidation and desorption (Rai et al., 1986; Bartlett and James, 1979; Schroeder and Lee, 1975). From the following review of this past research it can be seen that some studies are of questionable merit and that there are still many unanswered questions concerning the reaction mechanism and whether this process may be environmentally significant.

Schroeder and Lee (1975) presented some of the earliest work to show that the oxidation of Cr^{3+} is much faster in the presence of Mn oxide than by O_2 gas only. Although these authors reported their oxide only as "MnO_2" (reagent grade?) they demonstrated that in the presence of this oxide, 100% of their initial 0.125mg/L Cr^{3+} became oxidized within seven days, with 89% of the oxidation occurring within the first day. They also showed that the rate of oxidation increased as the concentration of MnO_2 was increased. This reaction was strongly inhibited when natural lake water was used in place of distilled water. The authors attributed this to competition for adsorption sites by cations such as Ca and Mg, and suggested that the oxidation reaction requires adsorption onto surface sites which are few in number. One problem with this study, is, that at a pH of 8.6, the formation of $Cr(OH)_3$-solid may have been overlooked. The solubility of this species is only 7.4 X 10^{-8} M from pH 6.3

TABLE I.8

SUMMARY OF PAST RESEARCH OF THE OXIDATION
OF Cr^{3+} BY Mn OXIDES

Investigator	Mn Oxide (conc.)	Cr(III) (conc.)	pH Range	Solution Matrix
Schroeder and Lee (1975)	unspecified MnO_2 ($2.9x10^{-3}$ to $2.9x10^{-4}$ M)	$2.4x10^{-6}$M	8.6	$KHCO_3$ buffer
Nakayama et al (1982)	MnO(OH) (30mg/L) natural Mn nodules (50mg/L)	$1x10^{-5}$M	8.1	seawater
Van Der Weijden and Reith (1982)	reagent grade and "natural" MnO_2 ($1.15x10^{-3}$)	$1.9x10^{-6}$M	5.5 6.3 8.1	freshwater freshwater seawater
Bartlett and James (1979)	natural soil (2000:1) solution:soil	$1x10^{-6}$M	3.2-9.0	distilled water; pH adjusted with HCl, $KHCO_3$
James and Bartlett (1983)	natural soil (3.0g)	$1x10^{-3}$M	6.7	$Cr(OH)_3$ or Cr-citrate formed in solution
Rai et al., (1986)	MnO_2 ($1.4x10^{-1}$ to $1.4x10^{-3}$ M)	1.9-38.5 x 10^{-5}M	3.0-4.7 6.3,8.3 10.1	distilled water

to 11.0 (Rai et al., 1986), which suggests the formation of this species may have formed to some extent and complicated the reaction process.

Nakayama et al., (1981) studied the oxidation of Cr^{3+} by MnO(OH) (a trivalent Mn oxide) and by powdered, naturally occurring, deep-sea Mn nodules in a natural sea water matrix at pH 8.1. They found small percentages of the original Cr^{3+} spike (1 X 10^{-5} M) became oxidized over several hundred hours. They also demonstrated that the reaction was slower in the absence of O_2 (i.e. N_2 purged system) and that the presence of 10^{-3} M citric acid prevented the reaction from occurring. Again, the use of 10^{-5} M Cr^{3+} at pH 8.1 probably resulted in hydroxide precipitation.

A similar study by Van Der Weijden and Reith (1982) using both reagent grade and "natural" MnO_2 also demonstrated the oxidation of Cr^{3+} in seawater (pH=8.1), although $Cr(OH)_3$-solid probably influenced these experiments as well. Their experiments were run for 1000 hours, but like the other studies, most of the oxidation appeared to occur in the first 10 hours or less. These investigators also ran experiments in fresh water at pH 5.5 and 6.3 and made measurements of the amount of Cr adsorbed during the duration of the experiments. They found the highest rate of oxidation at pH 5.5, with about 80% oxidized at the time of their first measurement (within 1 hour?). There was no detectable adsorption at this pH over the entire duration of the experiment. At pH 6.3 the redox reaction was slightly

slower and a small percentage of the original Cr was found to be adsorbed. This adsorbed fraction decreased as the percent oxidized increased. This could be explained by the very slow oxidation of Cr adsorbed onto the Mn oxide, or possibly the adsorbed Cr is actually $Cr(OH)_3$-solid which oxidizes at a much slower rate. At pH 5.5, the solution was probably undersaturated with respect to the hydroxide, which would explain why there was no "adsorption". The methods used in this study were not explained in detail, making their conclusions difficult to evaluate.

Bartlett and James (1979) demonstrated the oxidation of Cr^{3+} by naturally occurring soils. The evidence provided for this oxidation being caused by oxidized manganese in the soil included; 1) there was no oxidation by low Mn soils, 2) there was no oxidation in acid soil samples where Mn is in its reduced form, 3) the oxidation of Cr was accompanied by an increase in the extractable Mn from the soil, and 4) the oxidation of Cr was proportional to the amount of Mn that could be reduced by hydroquinone. These authors recognized the solubility problem of Cr^{3+} at pH's greater than about 5.5 and studied the reaction at both low and high pH's. They demonstrated that the amount and rate of Cr oxidized decreased with increasing pH and attributed this to the decrease in solubility and the reduced rate of oxidation of the hydroxide precipitate. In a later paper (James and Bartlett, 1983) these authors also showed that small amounts of $Cr(OH)_3$-solid did oxidize in Mn-rich soils and that the

aging of this species before the addition of the soil caused a reduction in the amount oxidized. They speculated that the fresh precipitate may have contained a residual positive charge that caused adsorption onto the Mn oxide surface.

The most complete and experimentally sound description of the oxidation of Cr^{3+} by Mn oxide in a simple system is provided in a recent paper by Rai et al., (1986). Using reagent MnO_2 (pyrolusite), the authors measured the oxidation of Cr as a function of pH, atmospheric composition (O_2 vs. N_2 purged), Cr^{3+} concentration, and surface area of MnO_2. They also measured the Mn released to solution during the redox reaction and were able to gain insight into the reaction mechanism. The conclusions of this report can summarized as follows:

1. The experimental results are consistent with surface Mn^{4+} as the oxidizing agent for Cr^{3+} oxidation.

2. The oxidation of Cr^{3+} by MnO_2 in acidic conditions slows down with time, and follows the average rate law:

$$df_{Cr}/dt = k\ (A/V)\ [Cr_T]^{-1}\ (1-f_{Cr})^{3.2(+-0.08)}$$

where: df_{Cr} = fraction of oxidized Cr to total Cr
(A/V) = surface area of MnO_2 to solution volume
Cr_T = total dissolved Cr concentration

3. The rate of oxidation demonstrates a small (and questionable) decrease as the pH is increased from 3.0 to 4.7.

4. At higher pH's (6.3, 8.3, 10.1) where $Cr(OH)_3$-solid was allowed to form, the amount of oxidation was greatly decreased, but the amount oxidized exceeded Cr^{3+} solubility.

5. There was no difference in the oxidation rate in an O_2 versus an N_2 purged system, suggesting $[O_2]$ does not influence the reaction at low pH's.

6. The amount of Cr^{3+} oxidized is nearly proportional to the surface area of MnO_2 present.

7. The rate of oxidation was independent of the initial Cr concentration from 1.9 to 38.5 X 10^{-5} M. The MnO_2 dissolution rate (Mn released to solution) however, decreased with increasing initial Cr^{3+} concentrations.

8. The ratio of Mn to Cr^{6+} released was always greater than the ratio of 1.5 predicted by the reaction stoichiometry, due to acid dissolution of the MnO_2; and this ratio decreased with increasing Cr^{3+}.

In their mechanistic interpretations, the authors pointed to 7) and 8) above to suggest that the desorption of Cr^{6+} as the rate limiting step. The adsorption of Cr^{6+} on this form of MnO_2 would be expected to take place under acidic conditions because the pH_{zpc} is about 7.3. This adsorption was interpreted to limit the sites available for oxidation and for acidic dissolution. This argument assumes that all of the initial Cr^{3+} concentrations saturate the surface

sites where oxidation takes place. Thus the initial rates are independent of the initial Cr^{3+} concentration, and the rate as the experiment progressed is controlled by the desorption of adsorbed Cr^{6+}. This also suggests that acid dissolution sites are different from Cr oxidation sites.

It is certainly apparent that the adsorption of the reaction product (Cr^{6+}) does have an effect on the overall reaction. This suggests that oxidation of Cr by Mn oxides with a low pH_{zpc} may display a quite different reaction rate and rate-controlling step. In acidic solutions, none of the reaction products would be expected to be adsorbed, and the dissolution of the oxide should result in more active sites for continued oxidation.

Based on all of the above summarized research the following summary describes some of what is known and also what needs to be determined by further research:

1. The oxidation of Cr^{3+} by Mn oxides does occur and it is faster than oxidation by O_2.

2. The rate of reaction follows a trend of decreasing with time in most of the previous experiments described.

3. The rate depends on the amount of Mn oxide present suggesting the reaction is surface area controlled.

4. Much more work is needed where care is taken to remain below $Cr(OH)_3$ saturation in order to unambiguously describe the reaction of the dissolved species. Further

study is also warranted at higher (more realistic) pH's to describe the influence of Mn oxides on Cr solubility.

5. The role of dissolved O_2 gas remains equivocal, as two studies have demonstrated conflicting results.

6. More work is clearly needed to describe the reaction mechanism, effects of solution chemistry and the extent this oxidation reaction would be expected to be important in nature. This includes the need for research using low pH_{zpc}, low crystallinity MnO_2 such as those forms commonly found in nature.

APPENDIX II

EXPERIMENTAL DATA

TABLE OF DATA SHOWN ON FIGURE 3					
2/5/85 Fresh Oxide		6/30/85 No Vibration		6/30/85 Sonic Vibration	
Time (min)	Cr^{6+} (mg/l)	Time (min)	Cr^{6+} (mg/l)	Time (min)	Cr^{6+} (mg/l)
1.50	0.19	1.00	0.10	1.00	0.15
4.75	0.33	2.75	0.17	2.75	0.24
9.25	0.40	5.00	0.25	5.10	0.32
15.50	0.42	8.00	0.29	8.00	0.38
25.00	0.46	15.00	0.37	15.25	0.41
45.00	0.49	30.00	0.45	31.00	0.48
80.00	0.50	60.00	0.48	60.00	0.49
120.00	0.50	125.00	0.50	135.00	0.50

TABLE OF DATA SHOWN ON FIGURE 4					
Volume of MnO_2 Stock Suspension (microliters)	Concentration of Mn in Stock Solution (molar)				
	1/7/85	5/12/85	10/28/85	3/8/86	7/23/86
25	---	---	2.28×10^{-6}	---	---
30	---	---	2.82×10^{-6}	---	---
50	---	4.64×10^{-6}	4.82×10^{-6}	4.82×10^{-6}	4.73×10^{-6}
75	---	---	---	7.28×10^{-6}	---
100	9.28×10^{-6}	9.37×10^{-6}	---	9.73×10^{-6}	9.55×10^{-6}
200	1.85×10^{-5}	1.86×10^{-5}	---	1.84×10^{-5}	1.93×10^{-5}
300	2.86×10^{-5}	2.82×10^{-5}	---	---	---
500	4.67×10^{-5}	4.83×10^{-5}	4.69×10^{-5}	---	4.69×10^{-5}
1000	9.30×10^{-5}	---	9.16×10^{-5}	9.44×10^{-5}	9.16×10^{-5}

TABLE OF DATA SHOWN ON FIGURE 5			
Time (hrs)	Dissolved Mn (mg/l)		
	pH = 1.60	pH = 1.95	pH = 4.50
0.017	0.05	0.02	0.02
0.583	--	0.03	--
0.750	0.10	--	0.01
1.750	0.13	0.04	0.01
3.000	--	--	--
4.000	0.16	0.06	0.02

TABLE OF DATA SHOWN ON FIGURES 7, 8 AND 9			
Cr^{6+} In Spike (mg/l)	Recovery In Unmodified Method (mg/l)	Recovery In Modified Method 2x (mg/l)	Recovery In Modified Method 3x (mg/l)
0.00	0.000	0.000	0.000
0.10	0.075	0.105	0.100
0.20	0.140	0.205	0.198
0.30	0.245	0.287	0.287
0.40	0.325	0.375	0.387
0.50	0.3475	0.468	0.488

TABLE OF DATA SHOWN ON FIGURE 10				
Time (min)	Cr^{6+} (mg/l)		Mn (mg/l)	
	1/17/85	2/5/85	1/17/85	2/5/85
1.00	0.17	---	0.245	---
1.50	--	0.190	---	0.285
4.00	0.32	---	0.535	---
4.75	--	0.330	---	0.560
9.25	--	0.400	---	0.680
11.00	0.41	---	0.670	---
15.50	--	0.425	---	0.730
20.00	0.45	---	0.730	---
25.00	--	0.455	---	0.770
35.00	0.47	---	0.770	---
45.00	--	0.490	---	0.810
55.00	0.48	---	0.800	---
80.00	--	0.495	---	0.820
85.00	0.48	---	0.810	---

TABLE OF DATA SHOWN ON FIGURE 11			
Time (min)	Cr^{6+} (mg/l)	Cr Total (mg/l)	Mn (mg/l)
1	0.180	0.455	0.250
4	0.330	0.480	0.530
11	0.410	0.485	0.660
20	0.460	0.490	0.725
35	0.470	0.490	0.765
55	0.480	0.490	0.795
85	0.480	0.490	0.810
120	0.495	0.490	0.820
150	0.500	0.490	0.820

TABLE OF DATA SHOWN ON FIGURE 12		
Time (min)	Mn (mg/l)	Cr^{6+} (mg/l)
1.00	0.045	0.025
3.50	0.120	0.050
8.25	0.175	0.085
17.50	0.215	0.095
31.00	0.230	0.100
55.00	0.235	0.105
75.00	0.240	0.110

TABLE OF DATA SHOWN ON FIGURE 13	
Time (min)	Mn to Cr^{6+} Molar Ratio
1.0	1.31
4.0	1.52
11.0	1.52
20.0	1.49
35.0	1.54
55.0	1.57
85.0	1.59
120.0	1.57
150.0	1.55

TABLE OF DATA SHOWN ON FIGURE 14	
Time Equivalent (min)	Percent Mn Adsorbed
1.0	8.0
5.0	1.0
30.0	0.0

TABLE OF DATA SHOWN ON FIGURES 15 AND 17					
Time (min)	Initial Mn Oxide Loading (M)				
	4.6×10^{-6}	9.1×10^{-6}	1.9×10^{-5}	2.9×10^{-5}	2.9×10^{-4}
	Cr^{6+} in Solution (mg/l)				
0.50	---	---	---	---	0.130
1.00	0.025	0.080	0.175	0.210	0.225
2.25	---	---	---	---	0.375
3.00	---	---	---	0.360	---
3.50	0.050	---	---	---	---
4.00	---	0.160	0.330	---	---
4.50	---	---	---	---	0.420
7.75	---	---	---	0.410	0.465
8.25	0.085	---	---	---	---
11.00	---	---	0.410	---	---
11.25	---	---	---	0.480	---
11.50	---	0.210	---	---	---
16.00	---	---	---	---	0.490
17.50	0.095	---	---	---	---
19.50	---	---	---	0.480	---
20.00	---	0.245	0.450	---	---
30.00	---	---	---	0.495	---
31.00	0.100	---	---	---	---
35.00	---	0.255	0.475	---	---

TABLE OF DATA SHOWN ON FIGURES 16 AND 18				
Time (min)	Initial Mn Oxide Loading (M)			
	4.6×10^{-6}	9.1×10^{-6}	1.9×10^{-5}	2.9×10^{-5}
	Mn in Solution (mg/l)			
0.50	---	---	---	---
1.00	0.045	0.100	0.245	0.295
2.25	---	---	---	---
3.00	---	---	---	0.620
3.50	0.120	---	---	---
4.00	---	0.255	0.535	---
4.50	---	---	---	---
7.75	---	---	---	0.795
8.25	0.175	---	---	---
11.00	---	---	0.665	---
11.25	---	---	---	0.810
11.50	---	0.375	---	---
16.00	---	---	---	---
17.50	0.215	---	---	---
19.50	---	---	---	0.825
20.00	---	0.405	0.725	---
30.00	---	---	---	0.830
31.00	0.230	---	---	---
35.00	---	0.430	0.765	---

TABLE OF DATA SHOWN ON FIGURES 19 AND 20			
Time (min)	Cr^{6+} (1) (mg/l)	Cr^{6+} (2) (mg/l)	Cr^{6+} (3) (mg/l)
0.50	0.17	0.29	0.41
1.33	0.19	0.33	0.49
2.33	0.19	0.36	0.56
5.00	0.20	0.39	0.59

(1) Cr^{3+} initial = 0.20 mg/l

(2) Cr^{3+} initial = 0.40 mg/l

(3) Cr^{3+} initial = 0.60 mg/l

TABLE OF DATA SHOWN ON FIGURES 21 AND 22						
Time (min)	Cr^{3+} Loading (M)					
	3.85 x 10^{-6}		7.69 x 10^{-6}		11.5 x 10^{-6}	
	Cr^{6+} (mg/l)	Mn (mg/l)	Cr^{6+} (mg/l)	Mn (mg/l)	Cr^{6+} (mg/l)	Mn (mg/l)
0.00	0.00	0.00	0.00	0.00	0.00	0.00
0.75	0.04	0.04	0.04	0.04	0.02	0.015
3.00	0.07	0.105	0.09	0.125	0.04	0.04
7.00	0.11	0.18	0.135	0.22	0.055	0.075

TABLE OF DATA SHOWN ON FIGURES 24 AND 25						
Time (min)	Cr^{6+} In Solution (mg/l)			Mn In Solution (mg/l)		
	pH = 1.5	pH = 3.0	pH = 4.5	pH = 1.5	pH = 3.0	pH = 4.5
0.5	0.03	0.04	0.03	0.12	0.04	0.02
2.0	0.05	0.11	0.11	0.21	0.15	0.13
5.0	0.15	0.16	0.18	0.35	0.27	0.28
10.0	0.18	0.24	0.24	0.45	0.40	0.40

TABLE OF DATA SHOWN ON FIGURES 26 AND 27				
Time (min)	pH = 1.65		pH = 4.50	
	Cr^{6+}	Mn	Cr^{6+}	Mn
1	0.02	0.06	0.04	0.06
3	0.10	0.17	0.15	0.25
6	0.17	0.25	0.23	0.34
10	0.21	0.33	0.32	0.51

TABLE OF DATA SHOWN ON FIGURE 28		
Time (days)	Fresh Cr(OH)$_3$	Aged Cr(OH)$_3$
	Cr^{6+} (mg/l)	Cr^{6+} (mg/l)
0.25	0.025	0.00
1.00	0.030	0.15
10.00	---	0.02
12.00	0.055	--
46.00	---	0.02
48.00	0.060	--

TABLE OF DATA SHOWN ON FIGURES 29 AND 30.					
Open To Atmosphere			N$_2$ Purged		
Time (min)	Cr^{6+} (mg/l)	Mn (mg/l)	Time (min)	Cr^{6+} (mg/l)	Mn (mg/l)
0.00	0.00	0.07	0.00	0.00	0.05
1.00	0.12	0.17	1.00	0.15	0.20
2.75	0.21	0.36	2.75	0.24	0.37
4.00	0.30	0.49	5.17	0.32	0.50
8.00	0.34	0.60	8.00	0.38	0.59
15.00	0.41	0.68	15.25	0.41	0.68
30.00	0.45	0.75	31.00	0.48	0.77
60.00	0.47	0.79	60.00	0.49	0.83
120.00	0.49	0.82	120.00	0.50	0.84

TABLE OF DATA SHOWN ON FIGURES 31 AND 32						
Time (min)	MATRIX					
	0.005 M NaNO$_3$ Solution		0.05 M NaNO$_3$ Solution		0.5 M NaNO$_3$ Solution	
	Cr^{6+} (mg/l)	Mn (mg/l)	Cr^{6+} (mg/l)	Mn (mg/l)	Cr^{6+} (mg/l)	Mn (mg/l)
0.5	0.080	0.105	0.035	0.030	0.015	0.040
2.0	0.155	0.260	0.105	0.130	0.065	0.125
5.0	0.220	0.420	0.190	0.305	0.125	0.290
10.0	0.320	0.575	0.270	0.455	0.230	0.425
20.0	0.380	0.695	0.365	0.610	0.310	0.580

TABLE OF DATA SHOWN ON FIGURES 33 AND 34				
Time (min)	MATRIX			
	0.01 M Ca(NO$_3$)$_2$ Solution		0.10 M Ca(CO$_3$)$_2$ Solution	
	Cr^{6+} (mg/l)	Mn (mg/l)	Cr^{6+} (mg/l)	Mn (mg/l)
0.0	0.000	0.01	0.00	0.05
0.5	0.030	0.02	0.02	0.06
2.0	0.070	0.09	0.06	0.13
5.0	0.134	0.20	0.13	0.25
10.0	0.220	0.36	0.25	0.39
20.0	0.310	0.51	0.33	0.57

TABLE OF DATA SHOWN ON FIGURE 35				
Time (min)	MATRIX			
	0.05 M NaCl	0.05 M NaNO$_3$	0.05 M Ca(NO$_3$)$_2$	0.05 M CaCl$_2$
	Mn (mg/l)	Mn (mg/l)	Mn (mg/l)	Mn (mg/l)
0	0.000	0.050	0.00	0.015
2	0.170	0.150	0.13	0.150
5	0.365	0.325	0.35	0.295
15	0.610	0.595	0.66	0.540
30	0.730	0.725	0.84	0.655

TABLE OF DATA SHOWN ON FIGURES 36 AND 37					
Time (min)	MATRIX				
	0.005 M CaCl$_2$ Solution		0.05 M CaCl$_2$ Solution		0.5 M CaCl$_2$ Solution
	Cr^{6+} (mg/l)	Mn (mg/l)	Cr^{6+} (mg/l)	Mn (mg/l)	Mn (mg/l)
0.5	0.045	0.030	0.050	0.04	0.01
2.0	0.120	0.180	0.125	0.18	0.03
5.0	0.265	0.380	0.255	0.36	0.05
10.0	0.385	0.540	0.350	0.49	0.09
20.0	0.485	0.675	0.435	0.61	0.13

TABLE OF DATA SHOWN ON FIGURE 38			
Time (min)	MATRIX		
	0.5 M Ca(NO$_3$)$_2$	0.5 M CaCl$_2$	1.0 M NaCl
	Mn (mg/l)	Mn (mg/l)	Mn (mg/l)
0	0.040	0.08	0.01
5	0.375	0.14	0.41
30	0.810	0.30	0.80
60	0.870	0.40	0.85

TABLE OF DATA SHOWN ON FIGURE 39			
Time (min)	MATRIX		
	1.0 M KCl	0.5 M CaCl$_2$	0.5 M MgCl$_2$
	Mn (mg/l)	Mn (mg/l)	Mn (mg/l)
0	0.035	0.090	0.00
2	0.200	0.100	0.17
5	0.390	0.115	0.37
15	0.650	0.155	0.62
30	0.770	0.210	0.75

TABLE OF DATA SHOWN ON FIGURE 40				
MnO$_2$ Loading (molar)	Metal Absorbed (molar)			
	Cu	Mn	Zn	Ni
4.73×10^{-5}	3.3×10^{-6}	4.60×10^{-7}	--	--
4.77×10^{-5}	--	--	3.80×10^{-7}	6.80×10^{-7}
9.47×10^{-5}	5.7×10^{-6}	2.73×10^{-6}	--	--
1.42×10^{-4}	7.1×10^{-6}	--	--	--
1.43×10^{-4}	--	--	2.14×10^{-6}	3.07×10^{-6}
1.89×10^{-4}	7.5×10^{-6}	6.46×10^{-6}	--	--
2.37×10^{-4}	--	--	4.13×10^{-6}	4.60×10^{-6}

TABLE OF DATA SHOWN ON FIGURES 41, 43 AND 44			
Time (min)	Metal Released To Solution (mg/l)		
	Cr^{6+}	Mn	Cu
0.50	0.11	0.09	0.06
1.00	0.17	0.19	0.11
2.33	0.35	0.45	0.15
4.50	0.42	0.53	0.17
8.00	0.47	0.56	0.18
15.50	0.47	0.57	0.19

TABLE ON DATA SHOWN ON FIGURES 42, 43 AND 44		
Time (min)	Metal Released To Solution (mg/l)	
	Cr^{6+}	Mn
0.50	0.13	0.06
1.00	0.23	0.16
2.25	0.37	0.38
4.50	0.42	0.44
7.75	0.46	0.46
16.00	0.46	0.46

TABLE OF DATA SHOWN ON FIGURE 45		
Time (min)	Percent Cr Oxidized	
	Immediate Filtration	Base Added
1	0.14	0.21
3	0.21	0.29
7	0.29	0.33

TABLE OF DATA SHOWN ON FIGURE 46		
Time (min)	Duplicate 1 Cr^{6+} (mg/l)	Duplicate 2 Cr^{6+} (mg/l)
2.0	---	0.120
5.0	0.210	0.200
10.0	0.230	0.225
20.0	0.265	0.265
21.0	0.275	0.270
45.0	---	---

Time	Amount of Cr Oxidized (mg/l)				
(min)	MnO$_2$ Loading (M)				
	1.2 x 10^{-5}	2.3 x 10^{-5}	4.6 x 10^{-5}	6.9 x 10^{-5}	9.2 x 10^{-5}
1.0	---	---	---	---	0.330
1.5	---	---	---	0.270	---
2.0	0.105	0.120	---	---	---
3.0	---	---	---	---	0.395
5.0	---	0.200	---	0.355	---
7.0	0.155	---	---	---	---
8.0	---	---	---	---	0.450
10.0	---	0.225	0.290	---	---
15.0	---	---	---	---	0.465
20.0	---	---	---	0.380	---
21.0	0.185	0.265	0.305	---	---
30.0	---	---	---	---	0.470
45.0*	0.190	0.270	---	0.420	0.470

TABLE OF DATA SHOWN ON FIGURES 47, 48 AND 49

* Values used for Figures 48 and 49

TABLE OF DATA SHOWN ON FIGURE 50

Time (min)	Cr Total (mg/l)	Cr^{6+} (mg/l)
2.0	0.12	0.120
5.0	0.05	0.200
10.0	0.03	0.225
21.0	0.02	0.265
45.0	0.00	0.270

TABLE OF DATA SHOWN ON FIGURE 51

Time (min)	Cr Adsorbed (mg/l)	Cr Oxidized (mg/l)
1.0	0.22	0.070
2.0	0.28	0.130
3.0	0.32	0.180
5.0	0.36	0.245
7.0	0.39	0.300
10.0	0.42	0.360
20.0	0.45	0.425
30.0	0.47	0.470

TABLE OF DATA SHOWN ON FIGURES 52 AND 54			
Time (min)	Fe(OH)$_3$ First	MnO$_2$ First	MnO$_2$ Last
	Cr^{6+} (mg/l)	Cr^{6+} (mg/l)	Cr^{6+} (mg/l)
2.0	0.120	0.060	--
5.0	0.200	0.060	--
10.0	0.225	0.070	0.04
20.0	---	0.065	--
21.0	0.265	---	--
30.0	---	---	0.05
45.0	0.270	0.065	--
60.0	---	---	0.06

TABLE OF DATA SHOWN ON FIGURES 53 AND 55			
Time (min)	Fe(OH)$_3$ First	MnO$_2$ First	MnO$_2$ Last
	Cr^{6+} (mg/l)	Cr^{6+} (mg/l)	Cr^{6+} (mg/l)
1.0	0.330	---	---
2.0	---	0.125	---
3.0	0.395	---	---
7.0	---	0.155	---
8.0	0.450	---	---
10.0	---	---	0.055
15.0	0.465	---	---
20.0	---	0.175	---
30.0	0.470	---	0.075
45.0	0.470	0.195	---
60.0	---	---	0.110

TABLE OF DATA SHOWN ON FIGURE 56	
Time (days)	Cr^{6+} (mg/l)
0.2	0.095
1.0	0.150
19.0	0.250
43.0	0.250

APPENDIX III

APPENDIX III

RATE DATA CALCULATIONS
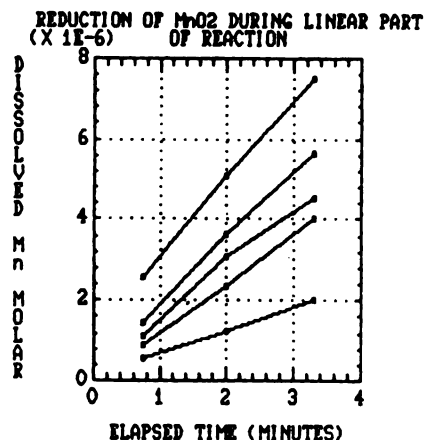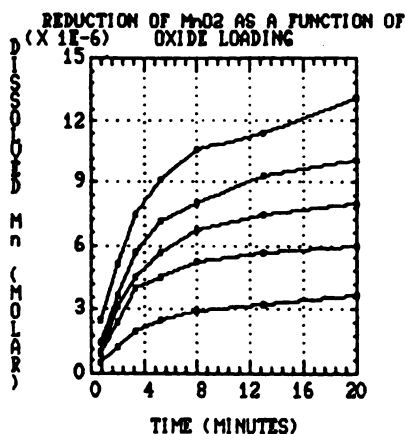
Data Set A. Points used to determine initial rate by linear regression of first three data points. Cr^{3+} = 9.6 X 10^{-5} M.

```
Simple Regression of mn50 on time
                                 Standard          T              Prob.
    Parameter       Estimate      Error          Value           Level
    -----------------------------------------------------------------------
    Intercept      1.13391E-7    1.30764E-8      8.67148         0.0730925
    Slope          5.71046E-7    5.76167E-9      99.1112         6.42307E-3


    -----------------------------------------------------------------------
                        Analysis of Variance
    -----------------------------------------------------------------------
    Source          Sum of Squares    Df   Mean Square    F-Ratio
    Model                .0000         1       .0000       9823.0306
    Error                .0000000      1       .0000000
    -----------------------------------------------------------------------
    Total (Corr.)        .0000000      2

    Correlation Coefficient = 0.999949
    Stnd. Error of Est. = 1.03897E-8

    Do you want to plot the fitted line? (Y/N):



    1HELP    2LABEL   3SAVSC   4RECORD 5        6        7        8
    PRINT        SAT JUN 13   1987 12:11:00 PM   VERSION 1.1
```

Linear Regression MnO_2 initial = 4.8 X 10^{-6} M
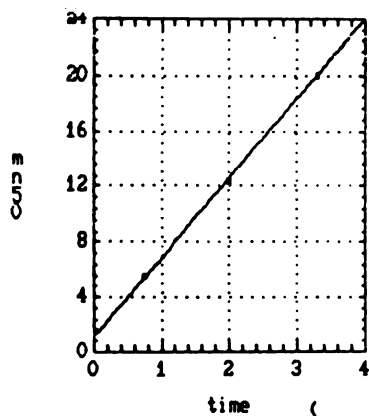
Simple Regression of mn75 on time

Parameter	Estimate	Standard Error	T Value	Prob. Level
Intercept	-2.13119E-8	6.28431E-8	-0.339129	0.791853
Slope	1.21404E-6	2.76897E-8	43.8444	0.0145175

Analysis of Variance

Source	Sum of Squares	Df	Mean Square	F-Ratio
Model	.0000	1	.0000	1922.3293
Error	.0000000	1	.0000000	
Total (Corr.)	.0000000	2		

Correlation Coefficient = 0.99974
Stnd. Error of Est. = 4.99312E-8

Do you want to plot the fitted line? (Y/N):

1HELP   2LABEL   3SAVSC   4RECORD 5   6   7   8
PRINT   SAT JUN 13 1987 12:14:00 PM   VERSION 1.1

Regression of mn75 on time
(X 1E-6)
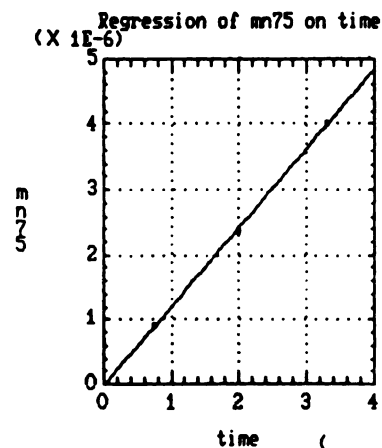
Linear Regression MnO_2 initial = 7.3 X 10^{-6} M

Parameter	Estimate	Error	Value	Level
Intercept	1.79952E-7	3.1486E-7	0.571529	0.669453
Slope	1.3549E-6	1.38733E-7	9.76626	0.0649592

Analysis of Variance

Source	Sum of Squares	Df	Mean Square	F-Ratio
Model	.000000	1	.000000	95.379837
Error	.0000000	1	.0000000	
Total (Corr.)	.0000000	2		

Correlation Coefficient = 0.994799
Stnd. Error of Est. = 2.50168E-7

Do you want to plot the fitted line? (Y/N):

1HELP   2LABEL   3SAVSC   4RECORD 5   6   7   8
PRINT   SAT JUN 13   1987 12:16:00 PM   VERSION 1.1

Regression of mn100 on time
(X 1E-6)
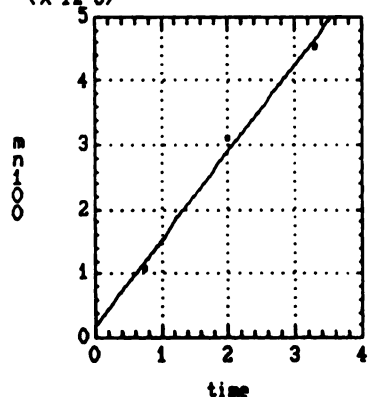
Simple Regression of mn125 on time

Parameter	Estimate	Standard Error	T Value	Prob. Level
Intercept	2.69739E-7	1.35176E-7	1.99546	0.295746
Slope	1.64129E-6	5.95609E-8	27.5564	0.0230923

Analysis of Variance

Source	Sum of Squares	Df	Mean Square	F-Ratio
Model	.00000	1	.00000	759.35788
Error	.0000000	1	.0000000	
Total (Corr.)	.0000000	2		

Correlation Coefficient = 0.999342
Stnd. Error of Est. = 1.07402E-7

Linear Regression MnO_2 initial = 9.7 X 10^{-6} M

(X 1E-6)
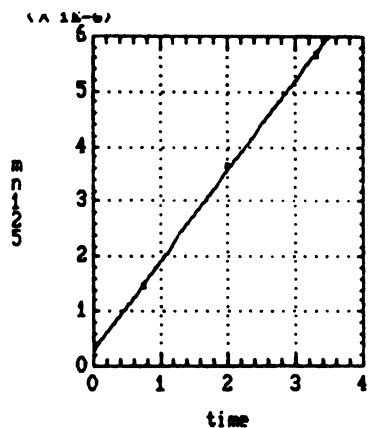
time

Simple Regression of mn150 on time

Parameter	Estimate	Standard Error	T Value	Prob. Level
Intercept	1.15042E-6	1.43538E-7	8.01474	0.0790227
Slope	1.92674E-6	6.32452E-8	30.4645	0.0208896

Analysis of Variance

Source	Sum of Squares	Df	Mean Square	F-Ratio
Model	.00000	1	.00000	928.08860
Error	.0000000	1	.0000000	
Total (Corr.)	.0000000	2		

Correlation Coefficient = 0.999462
Stnd. Error of Est. = 1.14046E-7

Linear Regression MnO_2 initial = 1.2 X 10^{-5} M

1HELP   2LABEL   3SAVSC   4RECORD 5   6   7   8
PRINT   SAT JUN 13 1987 12:21:00 PM VERSION 1.1

Regression of mn150 on time
(X 1E-7)

time
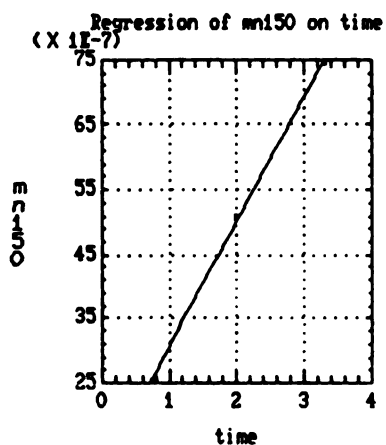
Linear Regression MnO_2 initial = 1.5 X 10^{-5} M

Model Fitting Results

	estimate	stnd.error	ratio
Coefficient 1	.00000356	.00000009	1000000
Coefficient 2	.00000357	.00000011	1000000
Coefficient 3	.23005280	.01821823	1000000

Total iterations = 9   Total function evaluations = 43

Analysis of Variance for the Full Regression

source	sum of squares	df	mean square	ratio
Model	.0000	3	.0000	1476.9650
Error	.0000000	5	.0000000	
Total	.0000000	8		
Total (corr.)	.0000000	7		

R-squared = 0.995835
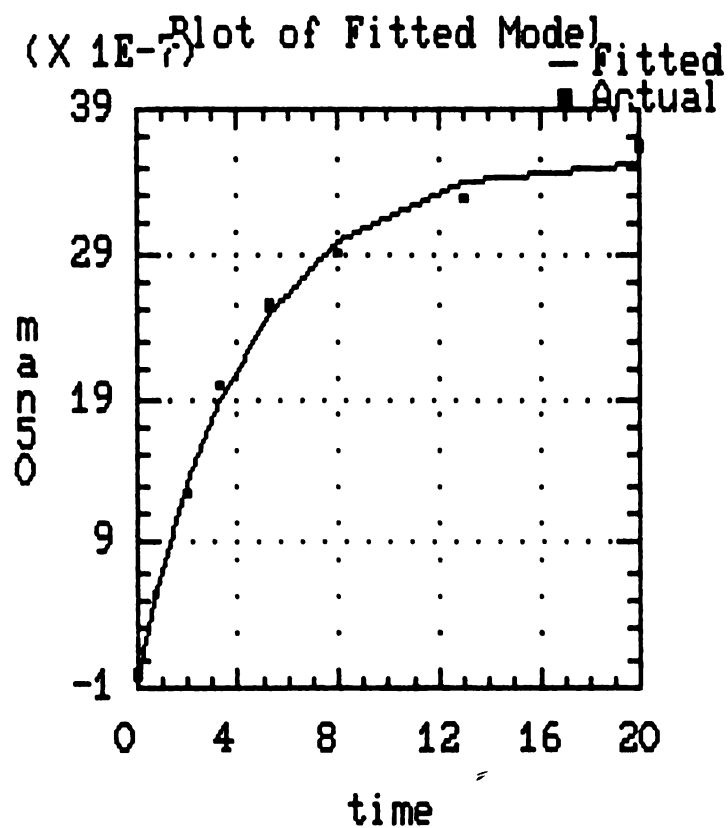
Data Set A. Curve Fitting Results, $MnO_2 = 4.8 \times 10^{-6}$ M

	estimate	stnd. error	ratio
Coefficient 1	.00000590	.00000017	35.0040
Coefficient 2	.00000602	.00000023	25.8496
Coefficient 3	.29502163	.02960444	9.9655

Total iterations = 8   Total function evaluations = 38

Analysis of Variance for the Full Regression

source	sum of squares	df	mean square	ratio
Model	.00000	3	.00000	878.33480
Error	.0000000	5	.0000000	
Total	.0000000	8		
Total (corr.)	.0000000	7		

R-squared = 0.992601
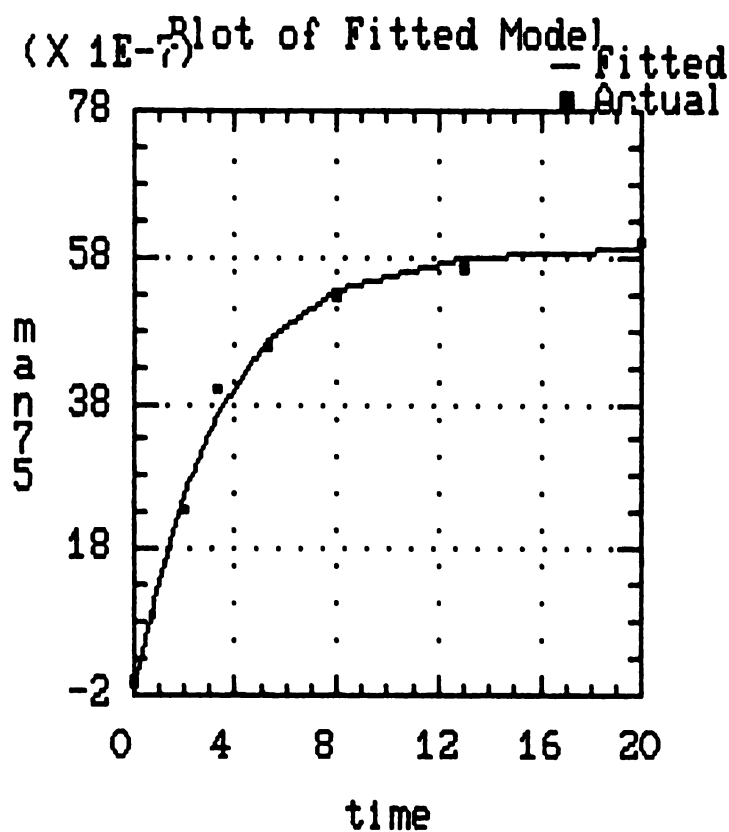
Data Set A. Curve Fitting Results, $MnO_2 = 7.3 \times 10^{-6}$ M

Model Fitting Results

	estimate	stnd.error	ratio
Coefficient 1	.00000786	.00000012	67.7931
Coefficient 2	.00000794	.00000015	53.9750
Coefficient 3	.24945122	.01227581	20.3206

Total iterations = 8   Total function evaluations = 38

Analysis of Variance for the Full Regression

source	sum of squares	df	mean square	ratio
Model	.0000	3	.0000	3721.1481
Error	.0000000	5	.0000000	
Total	.0000000	8		
Total (corr.)	.0000000	7		

R-squared = 0.998322

Plot of Fitted Model
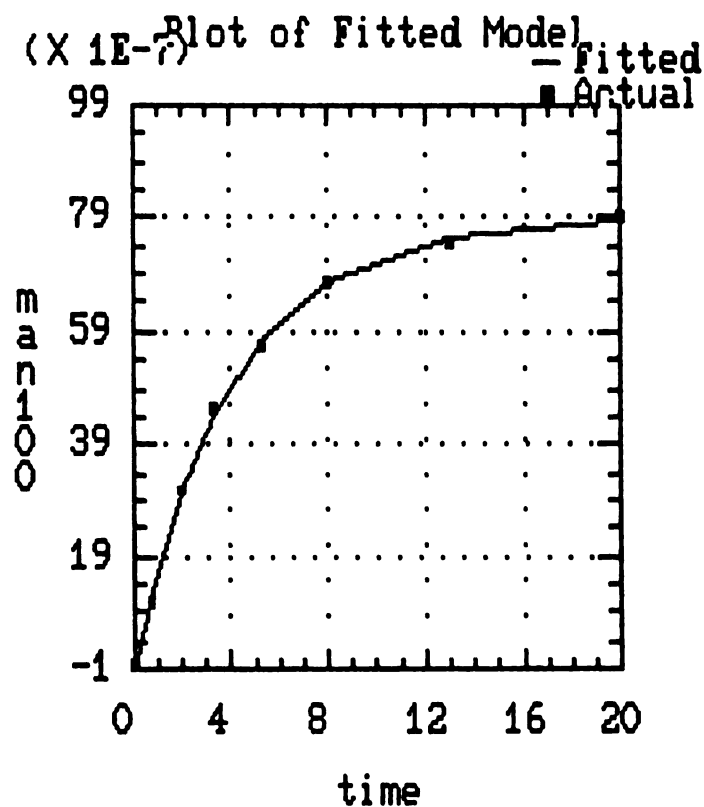
Data Set A. Curve Fitting Results, $MnO_2 = 9.7 \times 10^{-6}$ M

Model Fitting Results

	estimate	stnd.error	ratio
Coefficient 1	.00000986	.00000022	45.6571
Coefficient 2	.00000989	.00000027	37.1122
Coefficient 3	.23665703	.01707132	13.8628

Total iterations = 8   Total function evaluations = 38

Analysis of Variance for the Full Regression

source	sum of squares	df	mean square	ratio
Model	.0000	3	.0000	1768.0200
Error	.0000000	5	.0000000	
Total	.0000000	8		
Total (corr.)	.0000000	7		

R-squared = 0.996491
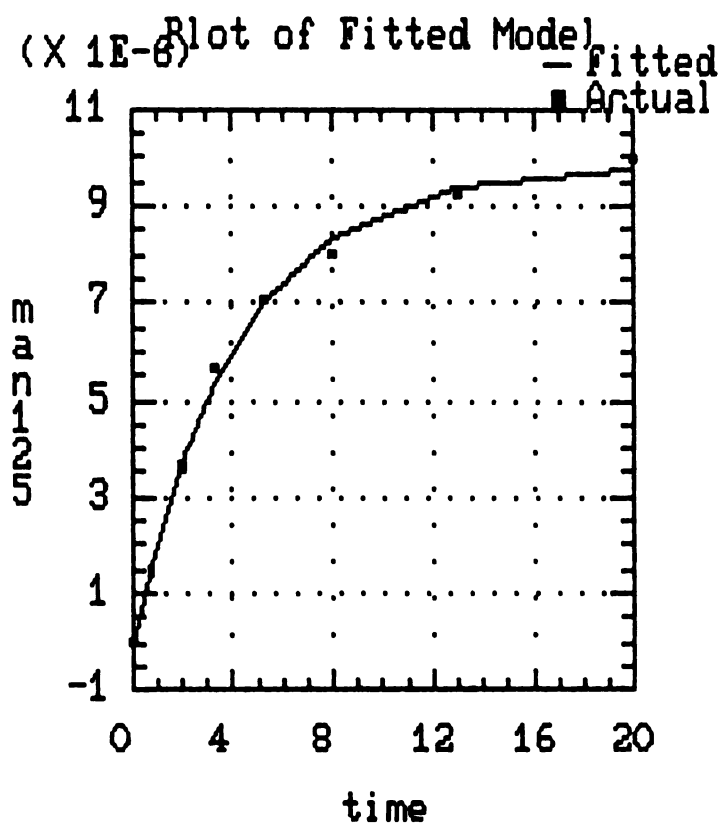
Data Set A. Curve Fitting Results, MnO_2 = 1.2 X 10^{-5} M

Model Fitting Results

	estimate	stnd.error	ratio
Coefficient 1	.00001253	.00000038	32.9308
Coefficient 2	.00001228	.00000048	25.4835
Coefficient 3	.24857830	.02592314	9.5891

Total iterations = 7   Total function evaluations = 33

Analysis of Variance for the Full Regression

source	sum of squares	df	mean square	ratio
Model	.00000	3	.00000	894.47340
Error	.0000000	5	.0000000	
Total	.0000000	8		
Total (corr.)	.0000000	7		

R-squared = 0.992517
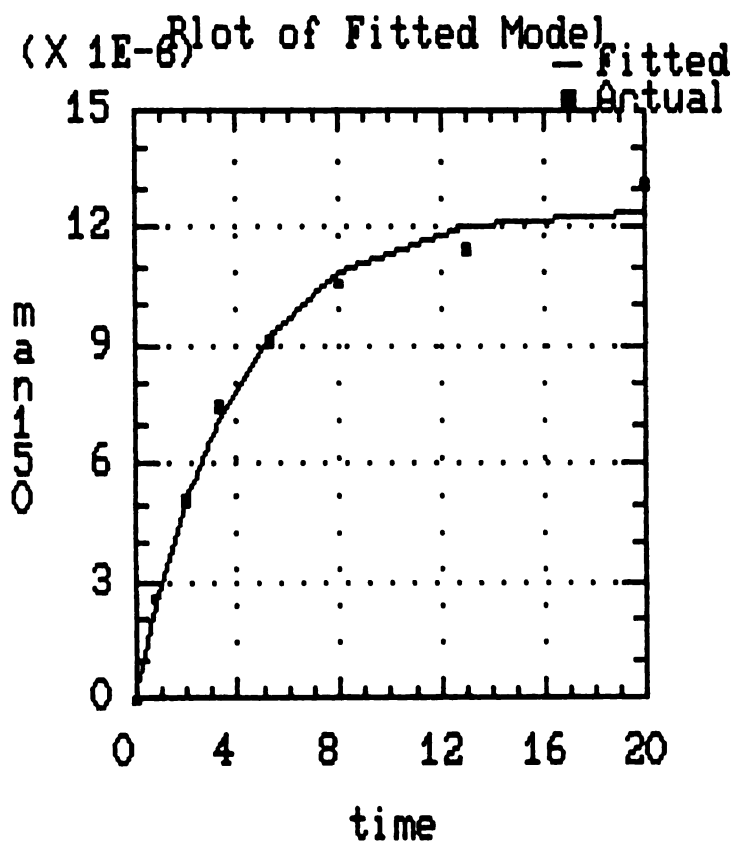
Data Set A. Curve Fitting Results, MnO_2 = 1.5 X 10^{-5} M

Row	deriv100	deriv125	deriv150	deriv50	deriv75	
1	1.98064E-6	2.34054E-6	3.05254E-6	8.21288E-7	1.77603E-6	
2	1.64269E-6	1.95989E-6	2.53335E-6	6.91135E-7	1.42349E-6	
3	1.20264E-6	1.458E-6	1.85673E-6	5.18411E-7	9.84459E-7	
4	8.27242E-7	1.02233E-6	1.27884E-6	3.6712E-7	6.32424E-7	
5	5.34621E-7	6.75658E-7	8.27736E-7	2.45451E-7	3.77387E-7	
6	2.6923E-7	3.5244E-7	4.17842E-7	1.3038E-7	1.67664E-7	
7	7.73477E-8	1.07942E-7	1.20568E-7	4.12722E-8	3.83538E-8	
8	1.34927E-8	2.05939E-8	2.11611E-8	8.24674E-9	4.86323E-9	
9						
10						
11						
12						
13						
14						

Length	8	8	8	8	8	0
Type	N	N	N	N	N	N

Row	1d100	1d125	1d150	1d50	1d75	
1	-13.1321	-12.9651	-12.6995	-14.0124	-13.2411	
2	-13.3192	-13.1426	-12.886	-14.1849	-13.4624	
3	-13.631	-13.4384	-13.1967	-14.4725	-13.8312	
4	-14.0052	-13.7934	-13.5696	-14.8176	-14.2737	
5	-14.4417	-14.2076	-14.0046	-15.2202	-14.79	
6	-15.1277	-14.8584	-14.6882	-15.8528	-15.6013	
7	-16.375	-16.0417	-15.9311	-17.0031	-17.0764	
8	-18.1211	-17.6983	-17.6711	-18.6134	-19.1416	
9						
10						
11						
12						
13						
14						

Length	8	8	8	8	8	0
Type	N	N	N	N	N	N

Data Set A. 1st derivatives and ln of 1st derivatives
for fitted curves. Row 1 = Time 0.00

Simple Regression of rate on loading

Parameter	Estimate	Standard Error	T Value	Prob. Level
Intercept	-1.58573	1.93216	-0.820707	0.471954
Slope	1.03465	0.166327	6.22058	8.37491E-3

Analysis of Variance

Source	Sum of Squares	Df	Mean Square	F-Ratio
Model	.824925	1	.824925	38.695639
Error	.0639549	3	.0213183	
Total (Corr.)	.8888800	4		

Correlation Coefficient = 0.963354
Stnd. Error of Est. = 0.146008

Do you want to plot the fitted line? (Y/N):

1HELP   2LABEL   3SAVSC   4RECORD 5   6   7   8
PRINT   SAT JUN 13   1987 12:54:00 PM   VERSION 1.1

Regression of rate on loading
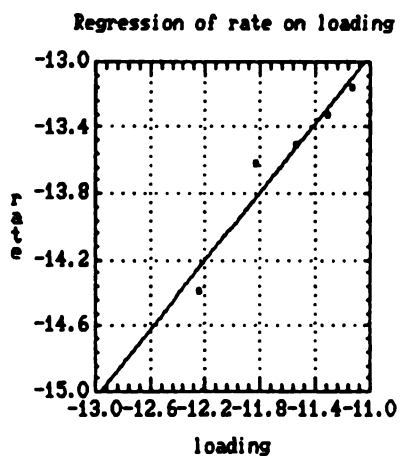
Data Set A. Reaction order with respect to MnO_2 by regression of initial rate (from slope of initial points) on MnO_2 Loading

Regression Analysis - Linear model: Y = a+bX

Dependent variable: irate   Independent variable: KINET3.loading

Parameter	Estimate	Standard Error	T Value	Prob. Level
Intercept	-0.612672	1.91661	-0.319665	0.77019
Slope	1.08487	0.164988	6.57544	7.15595E-3

Analysis of Variance

Source	Sum of Squares	Df	Mean Square	F-Ratio	Prob. Level
Model	.906950	1	.906950	43.236450	.00716
Error	.0629296	3	.0209765		
Total (Corr.)	.9698800	4			

Correlation Coefficient = 0.967014   R-squared = 93.51 percent
Stnd. Error of Est. = 0.144833

Regression of Initial Reduction Rate on Initial MnO2 Loading
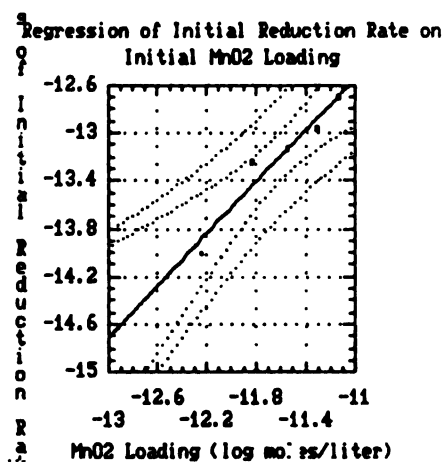
MnO2 Loading (log mo: es/liter)

Data Set A. Reaction order with respect to MnO_2 by regression of initial rate (from curve fitting) on MnO_2 Loading

Model Fitting Results

|	estimate	stnd.error	ratio
Coefficient 1	.00000336	.00000019	17.4729
Coefficient 2	.00000324	.00000019	17.1935
Coefficient 3	.29250717	.05015567	5.8320

Total iterations = 8   Total function evaluations = 37

Analysis of Variance for the Full Regression

source	sum of squares	df	mean square	ratio
Model	.00000	3	.00000	444.09281
Error	.0000000	3	.0000000	
Total	.0000000	6		
Total (corr.)	.0000000	5		

R-squared = 0.993694
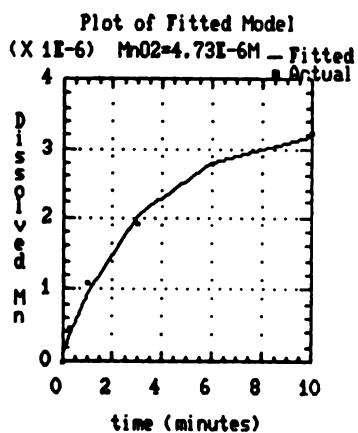
Plot of Fitted Model

Data Set B. Curve Fitting Results, $MnO_2 = 4.7 \times 10^{-6}$ M

Model Fitting Results

	estimate	stnd.error	ratio
Coefficient 1	.00000690	.00000043	16.0566
Coefficient 2	.00000677	.00000041	16.3469
Coefficient 3	.27170512	.04773283	5.6922

Total iterations = 8   Total function evaluations = 37

Analysis of Variance for the Full Regression

source	sum of squares	df	mean square	ratio
Model	.00000	3	.00000	424.28288
Error	.0000000	3	.0000000	
Total	.0000000	6		
Total (corr.)	.0000000	5		

R-squared = 0.993808
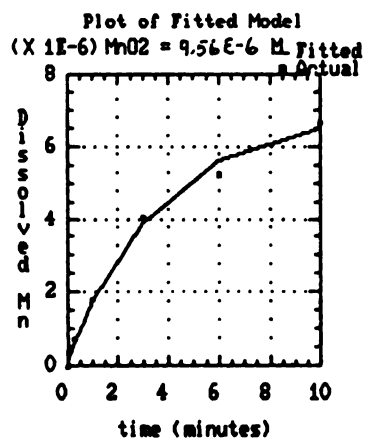
Plot of Fitted Model
(X 1E-6) MnO2 = 9.56E-6 M

Data Set B. Curve Fitting Results, $MnO_2 = 9.6 \times 10^{-6}$ M

Model Fitting Results

	estimate	stnd.error	ratio
Coefficient 1	.00001390	.00000044	31.8949
Coefficient 2	.00001372	.00000042	32.6356
Coefficient 3	.27411479	.02420291	11.3257

Total iterations = 8   Total function evaluations = 37

Analysis of Variance for the Full Regression

source	sum of squares	df	mean square	ratio
Model	.0000	3	.0000	1637.5181
Error	.0000000	3	.0000000	
Total	.0000000	6		
Total (corr.)	.0000000	5		

R-squared = 0.998415
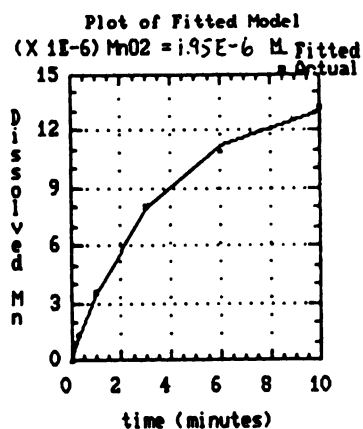
Plot of Fitted Model
(X 1E-6) MnO2 = 1.95E-6 M

Data Set B. Curve Fitting Results, $MnO_2 = 1.9 \times 10^{-5}$ M

Model Fitting Results			
	estimate	stnd.error	ratio
Coefficient 1	.00003949	.00000166	23.7602
Coefficient 2	.00003888	.00000155	25.0105
Coefficient 3	.20213162	.02007746	10.0676

Total iterations = 8   Total function evaluations = 37

Analysis of Variance for the Full Regression				
source	sum of squares	df	mean square	ratio
Model	.0000	3	.0000	1712.9383
Error	.0000000	3	.0000000	
Total	.0000000	6		
Total (corr.)	.0000000	5		

R-squared = 0.998563
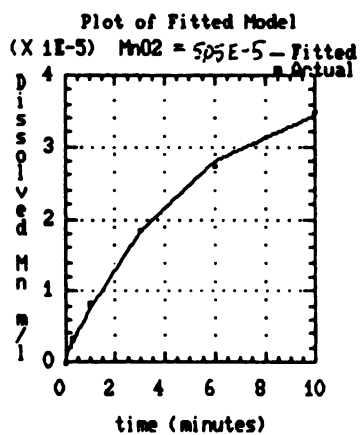
Plot of Fitted Model

(X 1E-5) MnO2 = 5.05E-5 — Fitted

Data Set B. Curve Fitting Results, $MnO_2 = 5.0 \times 10^{-5}$ M

Cursor at Row:	1	Data Editor	Maximum Rows:	6
Column:	1		Number of Cols:	4

Row	1d51	1d52	1d53	1d54		
1	-13.8692	-13.206	-12.4909	-11.7539		
2	-13.957	-13.2876	-12.5731	-11.8145		
3	-14.1617	-13.4778	-12.765	-11.956		
4	-14.7467	-14.0212	-13.3132	-12.3603		
5	-15.6242	-14.8363	-14.1356	-12.9667		
6	-16.7943	-15.9231	-15.232	-13.7752		
7						
8						
9						
10						
11						
12						
13						
14						
Length	6	6	6	6	0	0
Type	N	N	N	N	N	N

Data Set B. ln of 1st derivatives
for fitted curves. Row 1 = Time 0.00

Regression Analysis - Linear model: Y = a+bX

Dependent variable: inrate5 | **Independent variable: lload**

Parameter	Estimate	Standard Error	T Value	Prob. Level
Intercept	-2.81136	0.413184	-6.80413	0.0209245
Slope	0.899377	0.0369774	24.3224	1.68612E-3

Analysis of Variance

Source	Sum of Squares	Df	Mean Square	F-Ratio	Prob. Level
Model	2.48589	1	2.48589	591.57790	.00169
Error	.0084043	2	.0042021		
Total (Corr.)	2.4942927	3			

Correlation Coefficient = 0.998314   R-squared = 99.66 percent
Stnd. Error of Est. = 0.0648239

Regression of initial rate on initial MnO2 Loading

Log initial rate

-13 -12 -11 -10 -9

Log initial MnO2 (Cr=5mg/l)
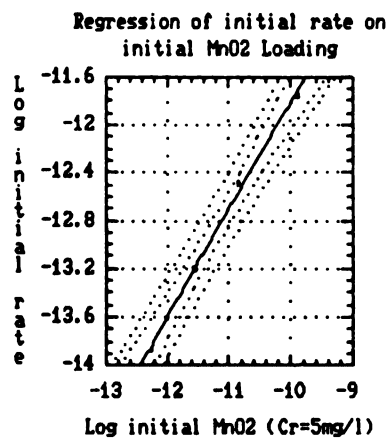
Data Set B. Reaction order with respect to MnO_2 by regression of initial rate (from curve fitting) on MnO_2 Loading

Model Fitting Results			
	estimate	stnd.error	ratio
Coefficient 1	.00000327	.00000043	7.57298
Coefficient 2	.00000311	.00000040	7.69695
Coefficient 3	.21230551	.07042296	3.01472

Total iterations = 9   Total function evaluations = 41

Analysis of Variance for the Full Regression				
source	sum of squares	df	mean square	ratio
Model	.00000	3	.00000	161.66454
Error	.0000000	3	.0000000	
Total	.0000000	6		
Total (corr.)	.0000000	5		

R-squared = 0.983243

Plot of Fitted Model
(X 1E-6) MnO2=4.73E-6M — Fitted

Data Set C. Curve Fitting Results, $MnO_2 = 4.7 \times 10^{-6}$ M

Model Fitting Results			
	estimate	stnd.error	ratio
Coefficient 1	.00000390	.00000024	16.5220
Coefficient 2	.00000372	.00000024	15.6650
Coefficient 3	.32068178	.06193637	5.1776

Total iterations = 7   Total function evaluations = 29

Analysis of Variance for the Full Regression				
source	sum of squares	df	mean square	ratio
Model	.00000	3	.00000	341.22146
Error	.0000000	3	.0000000	
Total	.0000000	6		
Total (corr.)	.0000000	5		

R-squared = 0.991399

Plot of Fitted Model

Data Set C. Curve Fitting Results, $MnO_2 = 9.6 \times 10^{-6}$ M

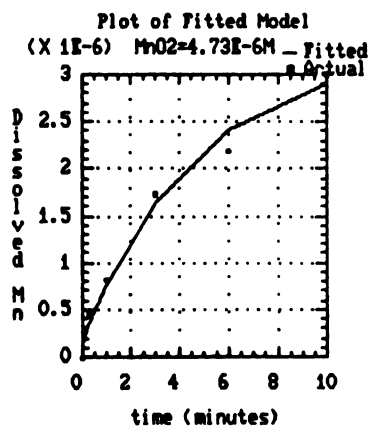| Model Fitting Results	estimate	stnd.error	ratio
Coefficient 1	.00001286	.00000053	24.4652
Coefficient 2	.00001258	.00000050	25.3412
Coefficient 3	.23776309	.02540785	9.3579

Total iterations = 7   Total function evaluations = 33

Analysis of Variance for the Full Regression

source	sum of squares	df	mean square	ratio
Model	.0000	3	.0000	1304.9798
Error	.0000000	3	.0000000	
Total	.0000000	6		
Total (corr.)	.0000000	5		

R-squared = 0.998018
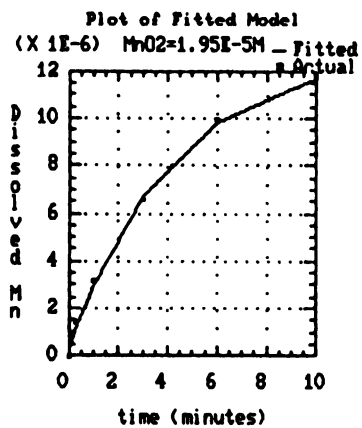
Plot of Fitted Model

(X 1E-6) MnO2=1.95E-5M — Fitted — Actual

Data Set C. Curve Fitting Results, $MnO_2 = 1.9 \times 10^{-5}$ M

Model Fitting Results

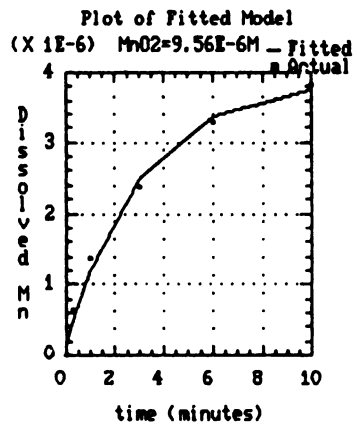|	estimate	stnd.error	ratio
Coefficient 1	.00003344	.00000103	32.4206
Coefficient 2	.00003303	.00000096	34.2507
Coefficient 3	.19696206	.01407699	13.9918

Total iterations = 8   Total function evaluations = 37

Analysis of Variance for the Full Regression

source	sum of squares	df	mean square	ratio
Model	.0000	3	.0000	3366.7497
Error	.0000000	3	.0000000	
Total	.0000000	6		
Total (corr.)	.0000000	5		

R-squared = 0.999279
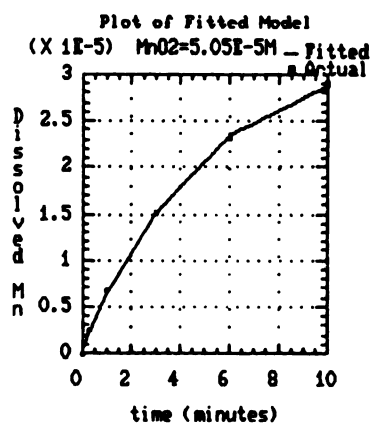
Plot of Fitted Model
(X 1E-5) MnO2=5.05E-5M — Fitted

Data Set C. Curve Fitting Results, $MnO_2 = 5.0 \times 10^{-5}$ M

```
Cursor at Row:      1      Data Editor      Maximum Rows:      6
          Column:   1                       Number of Cols:    4

Row      1d101      1d102      1d103      1d104

  1 |  -14.2306   -13.6391   -12.7199   -11.9428                          |
  2 |  -14.2943   -13.7353   -12.7912   -12.0019                          |
  3 |  -14.4429   -13.9598   -12.9576   -12.1398                          |
  4 |  -14.8675   -14.6011   -13.4332   -12.5337                          |
  5 |  -15.5044   -15.5632   -14.1465   -13.1246                          |
  6 |  -16.3537   -16.8459   -15.0975   -13.9125                          |
  7 |                                                                     |
  8 |                                                                     |
  9 |                                                                     |
 10 |                                                                     |
 11 |                                                                     |
 12 |                                                                     |
 13 |                                                                     |
 14 |                                                                     |

Length   6          6          6          6          0          0
Type     N          N          N          N          N          N
```

**Data Set C. ln of 1st derivatives
for fitted curves. Row 1 = Time 0.00**

Regression Analysis - Linear model: Y = a+bX

Dependent variable: inrate10   Independent variable: lload

Parameter	Estimate	Standard Error	T Value	Prob. Level
Intercept	-2.08535	0.716558	-2.91023	0.100573
Slope	0.99176	0.0641274	15.4655	4.1549E-3

Analysis of Variance

Source	Sum of Squares	Df	Mean Square	F-Ratio	Prob. Level
Model	3.02281	1	3.02281	239.18069	.00415
Error	.0252764	2	.0126382		
Total (Corr.)	3.0480906	3			

Correlation Coefficient = 0.995845   R-squared = 99.17 percent
Stnd. Error of Est. = 0.11242

Regression of Initial Rate on Initial MnO2 Loading
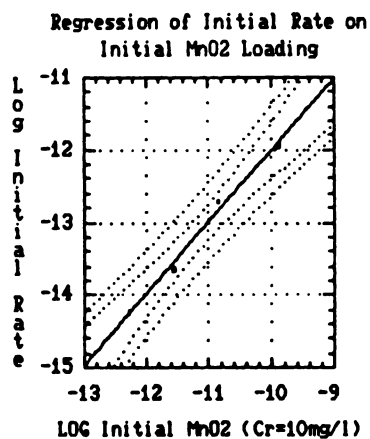
Data Set C. Reaction order with respect to MnO_2 by regression of initial rate (from curve fitting) on MnO_2 Loading
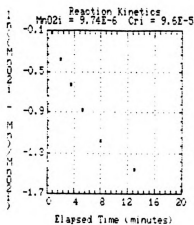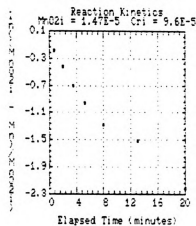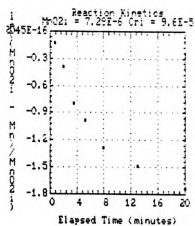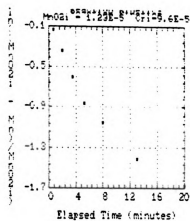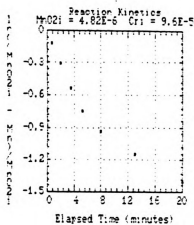
Data Set A.   Plots used to determine K_{ex}

Reaction Kinetics
Mn02i = 4.7E-6 Cri = 9.6E-5

Reaction Kinetics
Mn02i = 9.6E-6 Cri = 9.6E-5

Reaction Kinetics
Mn02i = 1.9E-5 Cri = 9.6E-5

Reaction Kinetics
Mn02i = 5.0E-5 Cri = 9.6E-5

Elapsed Time (minutes)

Elapsed time (minutes)

Elapsed Time (minutes)

Elapsed Time (minutes)
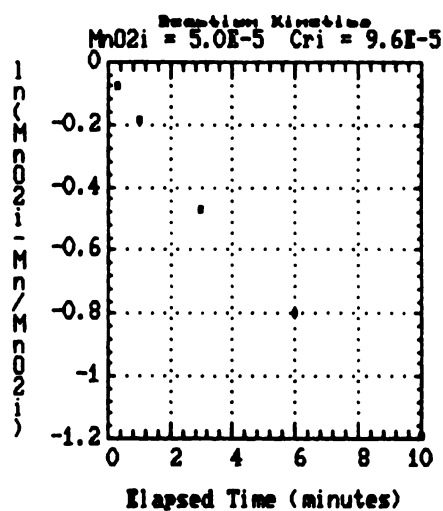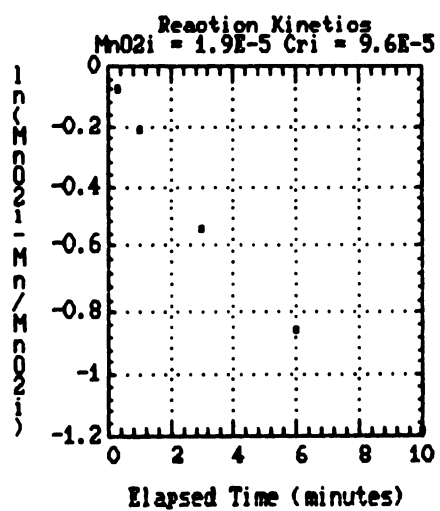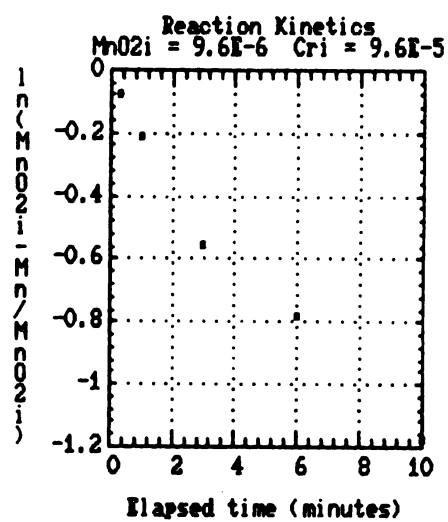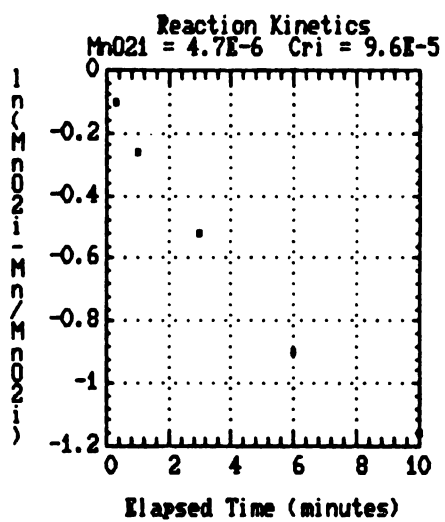
Data Set B.   Plots used to determine K_{ex}
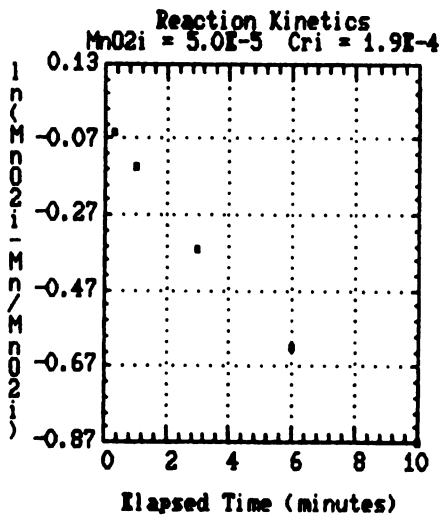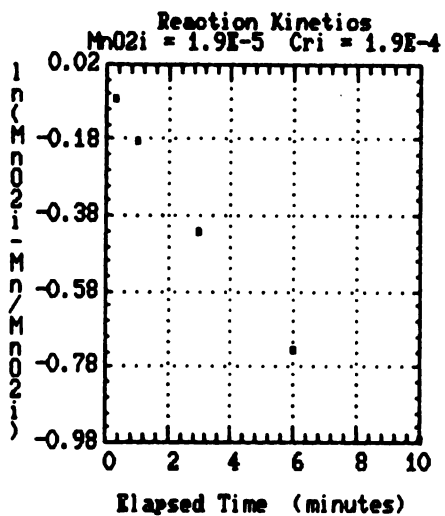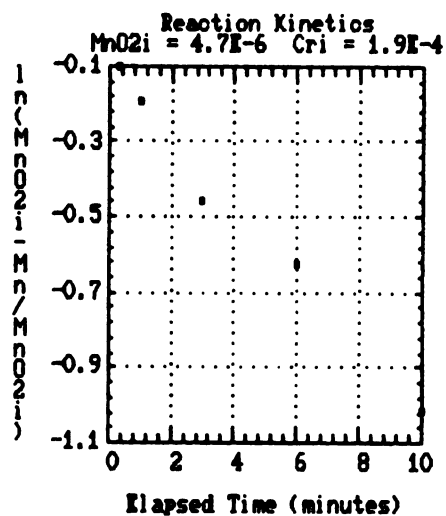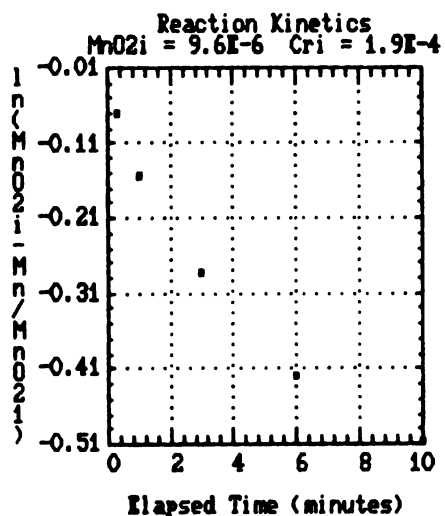
Data Set C. Plots used to determine K_{ex}

Simple Regression of mn48 on time

Parameter	Estimate	Standard Error	T Value	Prob. Level
Intercept	-0.0252762	0.0200301	-1.26191	0.334213
Slope	-0.140773	6.01373E-3	-23.4087	1.81995E-3

Analysis of Variance

Source	Sum of Squares	Df	Mean Square	F-Ratio
Model	.22418	1	.22418	547.96624
Error	.0008182	2	.0004091	

| Total (Corr.) | .2250000 | 3 | | |

Correlation Coefficient = -0.99818
Stnd. Error of Est. = 0.0202256

Do you want to plot the fitted line? (Y/N):

1HELP   2LABEL 3SAVSC 4RECORD 5   6   7   8   9REVIEW 10QUIT
PRINT   SUN MAR 27 1998 03:21:00 PM VERSION 1.1   REC:OFF

Regression of mn48 on time
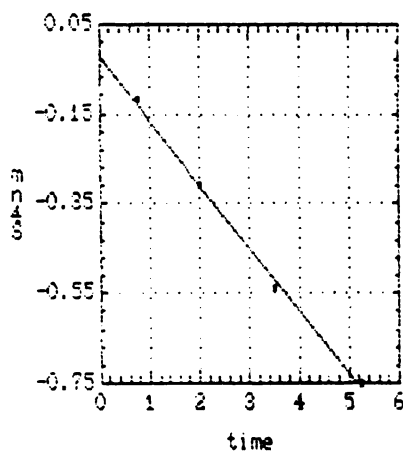
Data Set A. Regression to Determine K_{ex}
MnO_2 = 4.8 X 10^{-6} M

Simple Regression of mn73 on time

Parameter	Estimate	Standard Error	T Value	Prob. Level
Intercept	-0.0133425	0.0862069	-0.154773	0.891208
Slope	-0.195359	0.0258923	-7.54798	0.0171035

Analysis of Variance

Source	Sum of Squares	Df	Mean Square	F-Ratio
Model	.431744	1	.431744	56.971968
Error	.0151564	2	.0075782	
Total (Corr.)	.4469000	3		

Correlation Coefficient = -0.982897
Stnd. Error of Est. = 0.0870527

Do you want to plot the fitted line? (Y/N):

1HELP   2LABEL 3SAVSC 4RECORD 5   6   7   8   9REVIEW 10QUIT
PRINT   SUN MAR 27 1988 03:23:00 PM VERSION 1.1   REC:OFF

Regression of mn73 on time
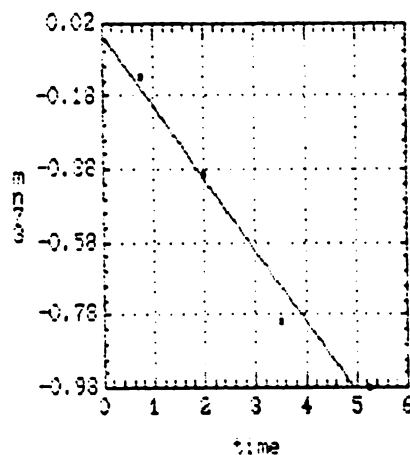
Data Set A. Regression to Determine K_{ex}
MnO_2 = 7.3 X 10^{-6} M

Simple Regression of mn97 on time

Parameter	Estimate	Standard Error	T Value	Prob. Level
Intercept	-0.024116	0.0360788	-0.668426	0.572679
Slope	-0.165525	0.0108321	-15.2909	4.25521E-3

Analysis of Variance

Source	Sum of Squares	Df	Mean Square	F-Ratio
Model	.30995	1	.30995	233.50718
Error	.0026547	2	.0013273	

| Total (Corr.) | .3126000 | 3 | | |

Correlation Coefficient = -0.995745
Stnd. Error of Est. = 0.0364329

Do you want to plot the fitted line? (Y/N):

1HELP   2LABEL 3SAVSC 4RECORD 5   6   7   8   9REVIEW 10QUIT
PRINT   SUN MAR 27 1988 03:25:00 PM VERSION 1.1   REC:OFF

Regression of mn97 on time
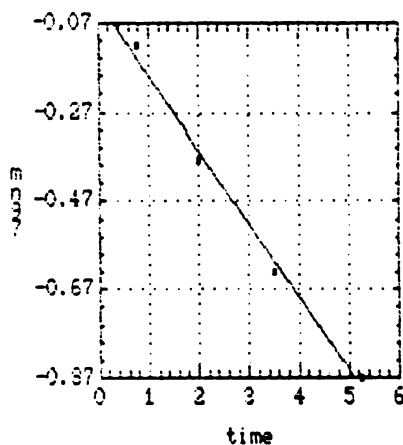
Data Set A.   Regression to Determine K_{ex}
MnO_2 = 9.7 X 10^{-6} M

Simple Regression of mn123 on time

Parameter	Estimate	Standard Error	T Value	Prob. Level
Intercept	-0.019558	0.019665	-0.99456	0.424749
Slope	-0.162762	5.90411E-3	-27.5676	1.31324E-3

Analysis of Variance

Source	Sum of Squares	Df	Mean Square	F-Ratio
Model	.29969	1	.29969	759.97513
Error	.0007887	2	.0003943	
Total (Corr.)	.3004750	3		

Correlation Coefficient = -0.998687
Stnd. Error of Est. = 0.0198579

Do you want to plot the fitted line? (Y/N):

1HELP 2LABEL 3SAVSC 4RECORD 5   6   7   8   9REVIEW 10QUIT
PRINT   SUN MAR 27 1988 03:27:00 PM VERSION 1.1   REC:OFF

Regression of mn123 on time

Data Set A. Regression to Determine K_{ex}
MnO_2 = 1.2 X 10^{-5} M

Simple Regression of mni47 on time

Parameter	Estimate	Standard Error	T Value	Prob. Level
Intercept	-0.0785085	0.0288175	-2.72433	0.112459
Slope	-0.171823	8.65201E-3	-19.8593	2.52594E-3

Analysis of Variance

Source	Sum of Squares	Df	Mean Square	F-Ratio
Model	.33398	1	.33398	394.39325
Error	.0016936	2	.0008468	

| Total (Corr.)	.3356750	3

Correlation Coefficient = -0.997474
Stnd. Error of Est. = 0.0291002

Do you want to plot the fitted line? (Y/N):

1HELP   2LABEL 3SAVSC 4RECORD 5   6   7   8   9REVIEW 10QUIT
PRINT   SUN MAR 27 1998 03:28:00 PM VERSION 1.1   REC:OFF

Regression of mni47 on time

Data Set A. Regression to Determine K_{ex}
$MnO_2 = 1.5 \times 10^{-5}$ M

```
Simple Regression of mn50 on time
                             Standard           T              Prob.
Parameter         Estimate     Error          Value            Level
----------------------------------------------------------------------
Intercept        -0.078455   0.0372117       -2.10834        0.281947
Slope            -0.149915   0.0202906       -7.38841        0.0856442


----------------------------------------------------------------------
                      Analysis of Variance
----------------------------------------------------------------------
Source           Sum of Squares    Df   Mean Square    F-Ratio
Model                  .088250      1      .088250     54.588602
Error                  .0016166     1      .0016166
----------------------------------------------------------------------
Total (Corr.)          .0898667     2

Correlation Coefficient = -0.990965
Stnd. Error of Est. = 0.0402074

Do you want to plot the fitted line? (Y/N):



  1HELP    2LABEL  3SAVSC  4RECORD 5       6       7        8
  PRINT    FRI SEP 4  1987  09:50:00 PM  VERSION 1.1
```
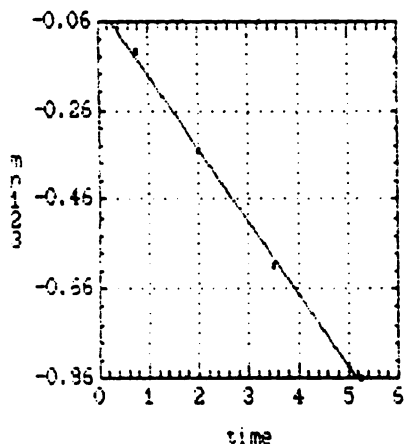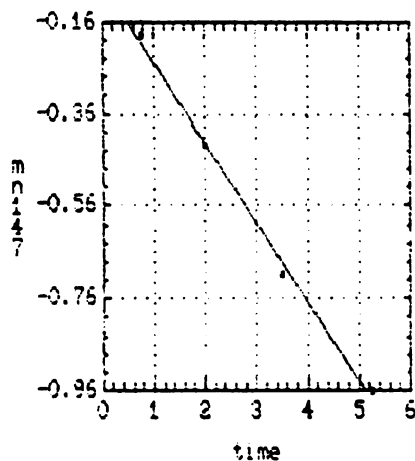
Regression of mn50 on time
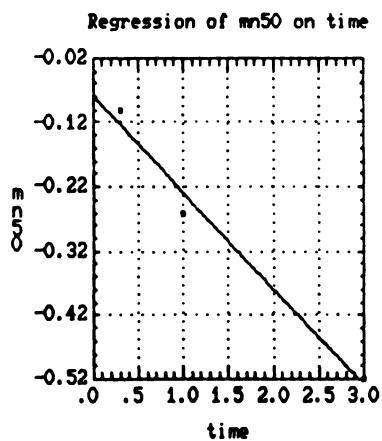
Data Set B.   Regression to Determine K_{ex}
MnO_2 = 4.7 X 10^{-6} M

Simple Regression of mn100 on time

Parameter	Estimate	Standard Error	T Value	Prob. Level
Intercept	-0.0317827	5.9323E-3	-5.35757	0.117475
Slope	-0.173175	3.23473E-3	-53.5361	0.01189

Analysis of Variance

Source	Sum of Squares	Df	Mean Square	F-Ratio
Model	.1178	1	.1178	2866.1157
Error	.0000411	1	.0000411	
Total (Corr.)	.1178000	2		

Correlation Coefficient = -0.999826
Stnd. Error of Est. = 6.40988E-3

Do you want to plot the fitted line? (Y/N):

1HELP   2LABEL 3SAVSC 4RECORD 5   6   7   8
PRINT   FRI SEP 4 1987   09:52:00 PM   VERSION 1.1

Regression of mn100 on time
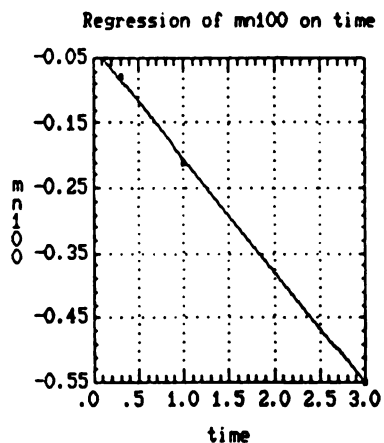
Data Set B. Regression to Determine K_{ex}
$MnO_2 = 9.6 \times 10^{-6}$ M

Simple Regression of mn200 on time

Parameter	Estimate	Standard Error	T Value	Prob. Level
Intercept	-0.0241681	7.81985E-3	-3.09061	0.199217
Slope	-0.169185	4.26396E-3	-39.6779	0.0160413

Analysis of Variance

Source	Sum of Squares	Df	Mean Square	F-Ratio
Model	.1124	1	.1124	1574.3357
Error	.0000714	1	.0000714	
Total (Corr.)	.1124667	2		

Correlation Coefficient = -0.999683
Stnd. Error of Est. = 8.44939E-3

Do you want to plot the fitted line? (Y/N):

```
1HELP    2LABEL  3SAVSC  4RECORD 5        6        7        8
PRINT    FRI SEP 4  1987   09:57:00 PM   VERSION 1.1
```

Regression of mn200 on time
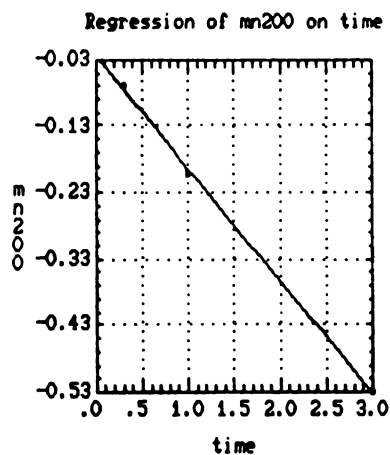
Data Set B. Regression to Determine K_{ex}
$MnO_2 = 1.9 \times 10^{-5}$ M

Simple Regression of mn500 on time

Parameter	Estimate	Standard Error	T Value	Prob. Level
Intercept	-0.0310357	6.4716E-3	-4.79567	0.130874
Slope	-0.143463	3.5288E-3	-40.6551	0.0156559

Analysis of Variance

Source	Sum of Squares	Df	Mean Square	F-Ratio
Model	.0808	1	.0808	1652.8356
Error	.0000489	1	.0000489	
Total (Corr.)	.0808667	2		

Correlation Coefficient = -0.999698
Stnd. Error of Est. = 6.9926E-3

Do you want to plot the fitted line? (Y/N):

```
1HELP    2LABEL  3SAVSC   4RECORD 5        6         7       8
PRINT    FRI SEP 4  1987  10:00:00 PM   VERSION 1.1
```


Regression of mn500 on time
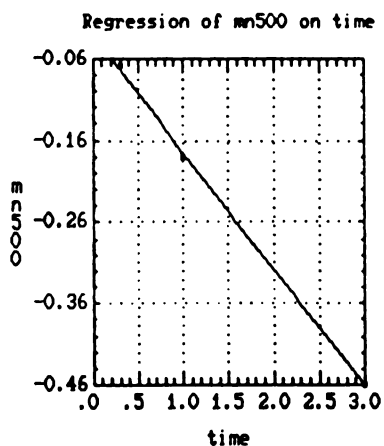
Data Set B. Regression to Determine K_{ex}
$MnO_2 = 5.0 \times 10^{-5}$ M

Parameter	Estimate	Standard Error	Value	Level
Intercept	-0.0583616	2.42685E-3	-24.0483	0.0264573
Slope	-0.133701	1.3233E-3	-101.036	6.3007E-3

Analysis of Variance

Source	Sum of Squares	Df	Mean Square	F-Ratio
Model	.070	1	.070	10208.333
Error	.0000069	1	.0000069	
Total (Corr.)	.0702000	2		

Correlation Coefficient = -0.999951
Stnd. Error of Est. = 2.62222E-3

Do you want to plot the fitted line? (Y/N):

```
1HELP    2LABEL  3SAVSC  4RECORD 5       6       7       8
PRINT    FRI SEP 4  1987  09:39:00 PM  VERSION 1.1
```

Regression of mn47 on time
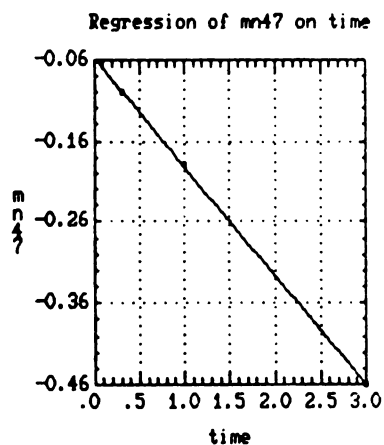
Data Set C. Regression to Determine K_{ex}
$MnO_2 = 4.7 \times 10^{-6}$ M

Simple Regression of mn96 on time

Parameter	Estimate	Standard Error	T Value	Prob. Level
Intercept	-0.0592275	0.0186058	-3.18327	0.193774
Slope	-0.0749576	0.0101453	-7.38841	0.0856442

Analysis of Variance

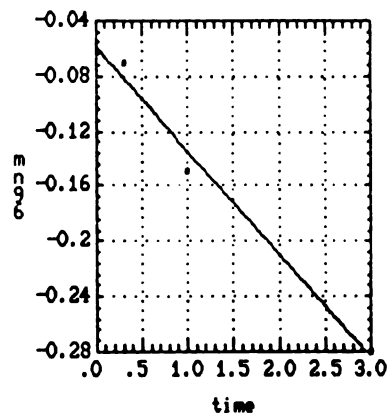| Source	Sum of Squares	Df	Mean Square	F-Ratio
Model	.022063	1	.022063	54.588602
Error	.0004042	1	.0004042	
Total (Corr.)	.0224667	2		

Correlation Coefficient = -0.990965
Stnd. Error of Est. = 0.0201037

Do you want to plot the fitted line? (Y/N):

1HELP   2LABEL   3SAVSC   4RECORD 5   6   7   8
PRINT   FRI SEP 4 1987   09:42:00 PM   VERSION 1.1

Regression of mn96 on time

Data Set C. Regression to Determine K_{ex}
$MnO_2 = 9.6 \times 10^{-6}$ M

Simple Regression of mn195 on time

Parameter	Estimate	Standard Error	T Value	Prob. Level
Intercept	-0.0429626	0.0159093	-2.70047	0.225777
Slope	-0.123514	8.67496E-3	-14.238	0.0446393

Analysis of Variance

Source	Sum of Squares	Df	Mean Square	F-Ratio
Model	.05990	1	.05990	202.72192
Error	.0002955	1	.0002955	
Total (Corr.)	.0602000	2		

Correlation Coefficient = -0.997543
Stnd. Error of Est. = 0.0171901

Do you want to plot the fitted line? (Y/N):

1HELP   2LABEL 3SAVSC   4RECORD 5   6   7   8
PRINT   FRI SEP 4 1987   09:44:00 PM   VERSION 1.1

Regression of mn195 on time
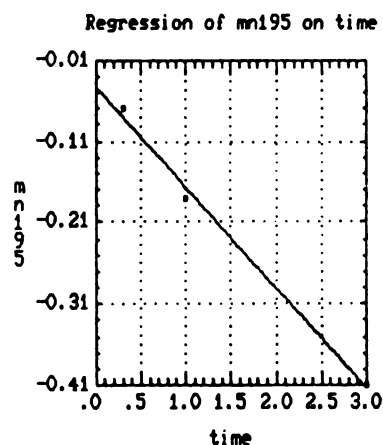
Data Set C.   Regression to Determine K_{ex}
$MnO_2 = 1.9 \times 10^{-5}$ M

Simple Regression of mn505 on time

Parameter	Estimate	Standard Error	T Value	Prob. Level
Intercept	-0.0202886	7.0109E-3	-2.89387	0.211811
Slope	-0.113752	3.82286E-3	-29.7557	0.0213868

Analysis of Variance

Source	Sum of Squares	Df	Mean Square	F-Ratio
Model	.05081	1	.05081	885.40434
Error	.0000574	1	.0000574	
Total (Corr.)	.0508667	2		

Correlation Coefficient = -0.999436
Stnd. Error of Est. = 7.57532E-3

Do you want to plot the fitted line? (Y/N):

```
 1HELP    2LABEL  3SAVSC  4RECORD 5         6        7        8
 PRINT    FRI SEP 4  1987  09:47:00 PM  VERSION 1.1
```


Regression of mn505 on time
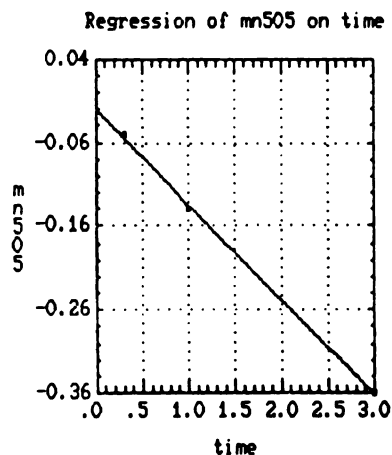
Data Set C. Regression to Determine K_{ex}
$MnO_2 = 5.0 \times 10^{-5}$ M

BIBLIOGRAPHY

BIBLIOGRAPHY

Anderson, M.A., Jenne, E.A. and Chao, T.T. (1973) The sorption of silver by poorly crystallized manganese oxides. Geochim. Cosmochim. Acta, 37, 611-622.

Anderson, M.A., Bauer, C., Hansmann, D., Loux, N. and Stanforth, R. (1981) Expectations and limitations for aqueous adsorption chemistry. In: Adsorption of inorganics at liquid-solid interfaces (Anderson, M.A. and Rubin, A.J., eds.) Ann arbor Science, 327-347.

Aoki, T. and Munemori, M. (1982) Recovery of chromium VI from waste waters with iron III hydroxide. Wat. Res., 16, 793-796.

Balistrieri, L.S. and Murray, J.W. (1982) The surface chemistry of delta-MnO_2 in major ion seawater. Geochim. Cosmochim. Acta, 46, 1041-1052.

Balistrieri, L.S. and Murray, J.W. (1982) The adsorption of Cu, Pb, Zn and Cd on geothite from major ion sea water. Geochim. Cosmochim. Acta, 46, 1253-1265.

Balistrieri, L.S. and Murray, J.W. (1981) The surface chemistry of geothite in major ion seawater. Am. J. Sci., 281, 788-806.

Bartlett, R. and James, B. (1979) Behavior of chromium in soils: III. Oxidation. J. Env. Qual., 8, 31-35.

Beliles, R.P. (1979) The lesser metals. In: The Toxicity of Heavy Metals in the Environment, Pt. 2 (F.W. Oehme, ed.) Marcel Dekker, Inc. NY

Benes, P. and Steinnes, E. (1975) Migration forms of trace elements in natural fresh waters and the effect of water storage. Wat. Res., 9, 741-749.

Benjamin, M.M. and Leckie, J.O. (1981a) Multi-site adsorption of Cd, Cu, Zn and Pb on amorphous iron oxyhydroxide. J. Colloid Interface Sci., 79, 209-221.

264

Benjamin, M.M. and Leckie, J.O. (1981b) Competitive adsorption of Cd, Cu, Zn and Pb on amorphous iron hydroxide. J. Colloid Interface Sci., 83, 410-419.

Benjamin, M.M. and Leckie, J.O. (1981c) Conceptual model of metal-ligand surface interactions during adsorption. Env. Sci. Tech., 15, 1050-1057.

Benjamin, M.M. (1983) Adsorption and surface precipitation of metals on amorphous iron oxyhydroxide. Env. Sci. Tech., 17, 686-692.

Bricker, O.P. (1965) Some stability relations in the system $Mn-O_2-H_2O$ at 25° and one atmosphere total pressure. Amer. Min., 50, 1296-1354.

Burns, R.G and Burns V.M. (1979) Manganese oxides. In: Marine Minerals (R.G. Burns, ed.) Min. Soc. Amer. Short Course Notes Vol. 6, 1-46.

Campbell, J.A. and Yeats, P.A. (1981) Dissolved chromium in the northwest Atlantic Ocean. Earth and Plan. Sci. Letters, 53, 427-433.

Carpenter, R.H. and Hayes, W.B. (1980) Annual accretion of Fe-Mn oxides and certain associated metals in a stream environment. Chem. Geol., 29, 249-259.

Chao, T.T and Theobald, P.K. (1976) The significance of secondary iron and manganese oxides in geochemical exploration. Econ. Geol. 71, 1560-1569.

Cranston, R.E. and Murray, J.W. (1978) The determination of chromium species in natural waters. Anal. Chim. Acta, 49, 275-282.

Cranston, R.E. and Murray, J.W. (1980) Chromium species in the Columbia River and estuary. Limnol. Oceanogr. 25, 1104-1112.

Crerar, D.A., Fischer, A.G., and Plaza, C.L. (1980) Geology and geochemistry of manganese (Varentsov, I.M. and Grassely, G., eds.) Vol. I. E Schweizebart'sche Verlagsbuchhandlung, Stutgart., 89-334.

Crowther, D.L., Dillard, J.G. and Murray, J.W. (1983) The mechanism of Co(II) oxidation on synthetic birnessite. Geochim. Cosmochim. Acta, 47, 1399-1403.

Davis, J.A. and Leckie, J.O. (1978) Surface ionization and complexation at the oxide/water interface. II. Surface properties of amorphous iron oxyhydroxide and adsorption of metal ions. J. Colloid Interface Sci., 67, 90-107.

Davis, J.A. and Leckie, J.O. (1978b) Effect of adsorbed complexing ligands on trace metal uptake by hydrous oxides. Env. Sci. Tech., 12, 1309-1315.

Davis, J.A. and Leckie, J.O. (1980) Surface ionization and complexation at the oxide/water interface. 3. adsorption of anions. J. Colloid Interface Sci., 74, 32-43.

Davies-Colley, R.J., Nelson, P.O. and Williamson, K.J. (1984) Copper and cadmium uptake by estuarine sedimentary phases. Env. Sci. Tech. 18, 491-499.

Dempsey, B.A. and Singer, P.C. (1980) Effects of calcium on the adsorption of zinc by $MnO_x(s)$ and $Fe(OH)_3$ (am). In: Contaminants and Sediments, (R.A. Baker, ed.) Ann Arbor Pub., 333-355.

Douglas, B., McDaniel, D.H. and Alexander, J.J. (1983) Concepts and Methods of Inorganic Chemistry 2nd ed. John Wiley & Sons, New York.

Drever, J.I. (1982) The Geochemistry of Natural Waters. Prentice-Hall, Inc., New Jersey, 388 p.

Elderfield, H. (1970) Chromium speciation in sea water. Earth and Plan. Sci. Letters, 9, 10-16.

Emerson, S., Cranston, R.E. and Liss, P.S. (1979) Redox species in a reducing fjord: equilibrium and kinetic considerations. Deep-Sea Research, 26A, 859-878.

Forbes, E.A., Posner, A.M., and Quirk, J.P. (1976) The specific adsorption of divalent Cd, Co, Cu, Pb and Zn on geothite. J. Soil Sci., 27, 154-166.

Fukai, R. (1967) Valency state of chromium in seawater. Nature, 213, p. 901.

Gadde, R.R. and Laitinen, H.A. (1974) Studies of heavy metal adsorption by hydrous iron and manganese oxides. Anal. Chem., 46, 2022-2026.

Gadde, R.R. and Laitinen, H.A. (1973) Study of sorption of lead by hydrous ferric oxide. Env. Letters, 5, 223-235.

Gardiner, W.C. (1972) Rates and Mechanisms of Chemical
    Reactions W.A. Benjamin, Inc., Menlo Park, CA, 284 p.

Garrels, R.M., McKenzie, F.T. and Hunt, C. (1974) Chemical
    cycles and the global environment: assessing human
    influences. William Kaufmann, Inc. Los Altos, CA.
    206 p.

Gephart, C.J. (1982) The relative importance of iron
    oxides, manganese oxides and organic material on the
    adsorption of chromium in natural water sediment
    systems. Unpublished Master's Thesis, Michigan State
    University.

Griffin, R.A., Au, A.K. and Frost, R.R. (1977) Effect of pH
    on the adsorption of chromium from land-fill leachate
    by clay minerals. J. Env. Sci. Health, A12, 431-449.

Healy, T.W., Herring, A.P., and Fuerstenau, D.W. (1966) The
    effect of crystal structure on the surface properties
    of a series of manganese dioxides. J. Colloid
    Interface Sci., 21, 435-444.

Hem, J.D. (1978) Redox processes at surfaces of manganese
    oxide and their effects on aqueous metal ions. Chem.
    Geol. 21, 199-218.

Holdren, G.R. and Berner, R.A. (1979) Mechanism of feldspar
    weathering --I. Experimental studies. Geochim.
    Cosmochim. Acta, 43, 1161-1171.

James, B.R. and Bartlett, R.J. (1983) Behavior of chromium
    in soils. VI. Interactions between oxidation-reduction
    and organic complexation. J. Env. Qual. 12, 173-176.

James, R.O. (1981) Surface ionization and complexation at
    the colloid/aqueous electrolyte interface. In:
    Adsorption of inorganics at the solid-liquid interface.
    (Anderson, M.A. and Rubin, A.J., eds.) Ann Arbor
    Science, 219-262.

James, R.O. and Healy, T.W. (1972) Adsorption of
    hydrolyzable metal ions at the oxide-water interface.
    J. Colloid Interface Sci., 40, 42-81.

Jenne, E.A. (1968) Controls on Mn, Fe, Co, Ni, Cu, and Zn
    concentrations in soils and water: the significant role
    of hydrous Fe and Mn oxides. Am. Chem. Soc. Adv. in
    Chem. Series 73, 337-383.

Kinniburgh, D.G. and Jackson, M.L. (1981) Cation adsorption
    by hydrous metal oxides and clay. In: Adsorption of
    inorganics at the solid-liquid interface (Anderson,
    M.A. and Rubin, A.J., eds.) Ann Arbor Science, 91-160.

Kinniburgh, D.G., Jackson, M.L. and Syers, J.K. (1976) Adsorption of alkaline earth, transition and heavy metal cations by hydrous oxide gels of iron and aluminum. Soil Sci. Soc. Am. J., 40, 796-799.

Kinniburgh, D.G., Syers, J.K. and Jackson, M.L. (1975) Specific adsorption of trace amounts of calcium and strontium by hydrous oxides of iron and aluminum. Soil Sci. Soc. Am. Proc., 39, 464-470.

Krauskopf, K.B. (1956) Factors controlling the concentrations of thirteen rare metals in sea-water. Geochim. Cosmochim. Acta 9, 1-32.

Leckie, J.O., Benjamin, M.M., Hayes, K.F. Kaufman, G. and Altman, S. (1980) Adsorption/coprecipitation of trace metals from water with iron oxyhydroxide. Electric Power Research Institute, Project 910-1.

Leckie, J.O., Appleton, A.R., Ball, N.B., Hayes, K.F. and Honeyman, B.D. (1983) Adsorptive removal of trace metals from fly-ash effluents onto iron oxyhydroxide. Electric Power Research Institute, Project 910-1.

Lingane, J.J. and Karplus, R. (1946) New method for determination of manganese. Ind. Eng. Chem., 18, 191.

Loganathon, P. and Burau, R.G. (1973) The sorption of heavy metal ions by a hydrous manganese oxide. Geochim. Cosmochim. Acta, 37, 1277-1293.

Loring, D.H. (1979) Geochemistry of Co, Ni, Cr and V in the sediments of the estuary and open Gulf of St. Lawrence. Can. J. Earth Sci., 16, 1197-1209.

Louma, S.N. and Davis, J.A. (1983) Requirements for modeling trace element partitioning in oxidized estuarine sediments. Mar. Chem. 12, 159-181.

MacNaughton, M.G. (1974) The adsorption of chromium (III) at the oxide/water interface. Interim report TR-75-17, Air Force Civil Engineering Center, Tyndall AFB Fl 32401.

Martin, T.D. and Riley, J.K. (1982) Determining dissolved hexavalent chromium in water and wastewater by electrothermal atomization. Atomic Spectroscopy, 3, 174-179.

Mayer, L.M. and Schick, L.L. (1981) Removal of hexavalent chromium from estuarine waters by model substrates and natural sediments. Env. Sci. Tech., 15, 1482-1484.

McKee, J.E. and Wolf, H.W. (1963) Water Quality Criteria, 2nd edition, St. Wat. Qual. Cont. Bd., Sacramento, CA

McKenzie, R.M. (1971) The synthesis of birnessite, cryptomelane and some other oxides and hydroxides of manganese. Min. Mag., 38, 493-502.

McKenzie, R.M. (1980) The adsorption of lead and other heavy metals on oxides of manganese and iron. Aust. J. Soil Res., 18, 61-73.

McKenzie, R.M. (1979) Proton release during adsorption of heavy metal ions by a hydrous manganese dioxide. Geochim. Cosmochim. Acta, 43, 1855-1857.

Mertz, Walter (1971) Chromium: the relation of selected trace elements to health and disease. In: Environmental Geochemistry in Health and Disease, Geol. Soc. Am. Mem. No. 123, Geological Society of America, Boulder CO, 29-35.

Morel, F.M.M., Yeasted, J.C. and Westall, J.C. (1981) Adsorption models: a mathematical analysis in the framework of general equilibrium calculations. In: Adsorption of inorganics at the solid-liquid interface. (Anderson, M.A. and Rubin, A.J., eds.) Ann Arbor Science, 263-294.

Morgan, J.J. and Stumm, W. (1964) Colloid-chemical properties of manganese dioxide. J. Colloid Sci., 19, 347-359.

Murray, J.W., Spell, B. and B. Paul (1983) The contrasting geochemistry of manganese and chromium in the eastern tropical Pacific ocean. From: Trace Metals in Seawater (Wong, C.S. et al., eds.) Plenum Press, 643-669.

Murray, J.W. (1974) The surface chemistry of hydrous manganese dioxide. J. Colloid Interface Sci., 46, 357-371.

Murray J.W. (1975) The interaction of ions at the manganese dioxide-solution interface. Geochim. Cosmochim. Acta., 39, 505-519.

Murray, J.W., Balistrieri, L.S. and Paul, B. (1984) The oxidation state of manganese in marine sediments and ferromanganese nodules. Geochim. Cosmochim. Acta, 48, 1237-1248.

Murray, J.W. and Dillard, J.G. (1979) The oxidation of cobalt(II) adsorbed on manganese dioxide. Geochim. Cosmochim. Acta, 43, 781-787.

Nakayama E., Kuwamoto, T. Tsurubo, S. and Fujinaga, T. (1981) Chemical speciation of chromium in sea water: Part 2. Effects of manganese oxides and reducible organic materials on the redox processes of chromium. Anal. Chim. Acta, 30, 401-404.

Pankow, J.F., Leta, D.P., Lin, J.W., Ohl, S.E, Shum, W.P. and Janaurer, G.E. (1977) Analysis for chromium traces in the aquatic ecosystem. Sci. Tot. Env., 7, 17-26.

Parks, G.A. (1965) The isoelectric points of solid oxides, solid hydroxides and aqueous hydroxo complex systems. Chem. Rev., 65, 177-198.

Posselt, H.S., Anderson, F.J. and Weber, W.J. (1968) Cation adsorption on colloidal hydrous manganese dioxide. Env. Sci. Tech., 2, 1087-1093.

Postma, D. (1985) Concentration of Mn and separation from Fe in sediments--1. Kinetics and stoichiometry of the reaction between birnessite and dissolved Fe(II) at $10^{\circ}C$. Geochim. Cosmochim. Acta, 49, 1023-1033.

Potter, R.M. and Rossman, G.R. (1979) Mineralogy of manganese dendrites and coatings. Amer. Min., 64, 1219-1226.

Rai, D., Zachara, J.M., Eary, L.E., Girvin, D.C., Moore, D.A., Resch, C.T., Sass, B.M. and Schmidt, R.L. (1986) Geochemical Behavior of Chromium Species. Electric Power Research Institute, Project 2485-3.

Robertson, F.N. (1975) Hexavalent chromium in ground water in Paradise Valley, Arizona., 516-527

Ross, S.J., Franzmeier, D.P. and Roth, C.B. (1976) Mineralogy and chemistry of manganese oxides in some Indiana soils. Soil Sci. Soc. Am. J., 40, 137-143.

Schindler, P.W. (1981) Surface complexes at oxide-water interfaces. In: Adsorption of inorganics at solid-liquid interfaces (Anderson, M.A. and Rubin, A.J. eds.) Ann Arbor Science, 1-50.

Schindler, P.W., Walti, E., and Furst, B. (1976) The role of surface hydroxyl groups in the surface chemistry of metal oxides. Chimia, 30, 107-109.

Schroeder, D.C. and Lee, G.F. (1975) Potential transformations of chromium in natural waters. Wat., Air and Soil Poll., 4, 355-365.

Smillie, R.H., Hunter, K., and Loutit, M. (1981) Reduction of chromium (VI) by bacterially produced hydrogen sulfide in a marine environment. Wat. Res., 15, 1351-1354.

Standard Methods (1975) American Public Health Association, 14th Edition, 1193p.

Stone, A.T. and Morgan, J.J. (1984) Reduction and dissolution of manganese (III) and manganese (IV) oxides by organics: I. Reaction with hydroquinone. Env. Sci. Tech., 18, 450-456.

Stumm W. and Morgan J.J. (1981) Aquatic Chemistry 2nd Ed. Wiley, 780 p.

Stumm, W., Huang, C.P. and Jenkins, S.R. (1970) Specific chemical interactions affecting the stability of dispersed systems. Croat. Chem. Acta, 42, 223-245.

Swallow, K.C., Hume, D.N. and Morel, F.M.M. (1980) Sorption of copper and lead by hydrous ferric oxide. Env. Sci. Tech., 14, 1326-1331.

Turekian, K.K., (1978) Chemical Oceanography vol. 2 (J.P Riley and R. Skirrow, eds.) Academic Press, New York.

Van den Berg, C.M.G. and Kramer, J.R. (1979) Determination of complexing capacities and conditional stability constants for copper in natural waters using MnO_2. Anal. Chim. Acta, 106, 113.

Van der Weijden, C.H. and Reith, M. (1982) Chromium (III)-chromium (VI) interconversions in seawater. Mar. Chem. II, 565-572

Vuceta, J. and Morgan, J.J. (1978) Chemical modeling of trace metals in fresh waters: role of complexation and adsorption. Env. Sci. Tech., 12, 1302-1308.

Westall, J.C. and Hohl, H. (1980) A comparison of electrostatic models for the oxide/water interface. Adv. Coll. Interface Sci., 12, 265-294.

Zasoski, R.J. and Burau, R.G. (1979) A technique for studying the kinetics of adsorption in suspensions. Soil Sci. Am. J., 42, 372-374.

Zinder, B., Furrer, G. and Stumm, W. (1986) The coordination chemistry of weathering: II. Dissolution of Fe(III) oxides. Geochim. Cosmochim. Acta, 50, 1861-1869.